Department of Chemical Engineering and Chemical Technology Imperial College London

Generation of Functional Mature Type II Pneumocytes from Human Induced Pluripotent Stem Cells in 3D Dynamic Culture

2018

A thesis submitted for the degree of Doctor of Philosophy in Chemical Engineering

Tamador Fahad Alsobaie

Abstract

Lung diseases have become a more prominent problem worldwide due to smoking and pollution and they are increasingly responsible for elevated mortality and morbidity. Progressive fibrosis followed by a subsequent loss of functional lung tissue and gas-exchange units, are the main causes for chronic lung diseases. In addition, failure to maintain endothelial and epithelial regeneration can also lead to the pathological fibrosis. More research is needed to find an alternative solution for the effective repair of lung tissue (Moodley et al., 2013). For patients with chronic lung disease, lung transplantation is the only option available at present. However, the limited availability of lung donors and possible immunological and surgical complications constrain the wide application of transplantation. Although implantation of ex-*vivo*-produced lung tissue could address the limitations of transplantation, their development has been limited by the lack of models to study the necessary developmental roadmaps for ex-*vivo* production of the required tissues. In this thesis, these issues were addressed through a tissue engineering approach whereby human induced pluripotent stem cells (human IPSCs) were used to produce type-II pneumocyte. This approach offers the promise of cure and regeneration of injured and diseased lungs. Several researchers attempted differentiation of human IPSCs into type-II pneumocytes using 2-Dimensional (2D) cell cultures. The novelty of this work resides in the use of 3-Dimensional (3D) cultures motivated by the ability to mimic the *in-vivo* microenvironment. We show that alginate beads provide a reduced oxygen environment, better cellular expansion, differentiation and functional capacities ideal for the production of Type II pneumocytes. Differentiation was induced by stimulating the signalling pathways involved in alveolar epithelia development, forming human IPSC-derived SFTPC+ cells in 3D cultures without the need for mesenchymal support and xeno-free contamination (i.e. Matrigel™). These cells exhibit the capacity of trans-differentiation of alveolar epithelial type II to type I cells, and show additional functional features such as the lamellar bodies specific of type II pneumocytes, and confirmed by immuno-histology using electron microscopy. Furthermore, the 3D cultures herein developed were comparatively easy to scale up to bioreactors. Overall,

our approach has proved able to promote IPSCs differentiation into Type II pneumocytes in a 3D environment using an engineered scaffold in a scalable manner. In the future, the strategy herein presented can be used for the generation of distal lung tissue for drug screening and disease modelling.

Declaration

Originality

The work described in this thesis was carried out by the author (or in collaboration) in the Department of Chemical Engineering and Chemical Technology of Imperial College London, United Kingdom between May 2013 and December 2016. To the best of my knowledge, it does not contain work by any other person, unless otherwise acknowledged.

Copyright

The copyright of this thesis rests with the author and is made available under a Creative Commons Attribution Non-Commercial No Derivatives licence. Researchers are free to copy, distribute or transmit the thesis on the condition that they attribute it, that they do not use it for commercial purposes and that they do not alter, transform or build upon it. For any reuse or redistribution, researchers must make clear to others the licence terms of this work.

Acknowledgments

The Prophet Muhammad, peace be upon him, said, "He who does not thank people, does not thank Allah". I would like to express my gratitude to those who were part of my PhD journey and whom have generously contributed to the presented work in this thesis.

Special mention goes to my enthusiastic supervisor, Professor. Athanasios Mantalaris for his guidance, support and endless encouragement to throughout my PhD journey.

My sincere thanks also goes to the late Professor Dame Julia Pollak for inspiring me to do my research in “tissue engineering”, you shall always be remembered.

Thanks a lot, to my wonderful colleagues from the Biological System Engineering Lab group, Lia Chon, Michalis, Sophia, Asam, Antoino and Jose for your friendship, support and advise. Finally, my buddy Joana, who is always there for me, thanks for standing by my side through our sleepless nights and for all the fun we have had in the lab.

I would not forget to remember staff in the Department of Chemical Engineering, my guardian angel Mrs. Sarah Payne, Mrs. Susi Underwood, Mr. Keith Walker and Mr. Ben Kistnah for all kinds of support and cooperation with me during my time in Imperial College London.

I am thankful for getting continuous guidance from Mrs. Jane Srivastava from flow cytometry facility for her direction on the flow cytometry, Lorraine Lawrence from the National Heart & Lung Institute for her guidance on the histology techniques and Simone Walker from the National Heart & Lung Institute for her guidance on the western blot which helped me a lot and in successfully finishing my thesis

I have been fluky and very blessed to have real friends in London who are always with me to share my ups and downs. My sincere thankfulness to Dr. Abdulrahman, Dr. Abdelwahab, Malwina and many more friends would not be possible to name them all.

Last but not least, I am deeply grateful to my mother Heila Alhammad and my Father Fahad Alsobaie, who have provided me through moral and emotional support in my life and their

continuous prayers for me which truly were answered. Also, I would like to thank my huge family members, Dr. Mohammed, Abdulaziz, Abdulrahman, Ibrahim, Saad, Nesreen, Saud and Fayz, for supporting me spiritually throughout my PhD. Finally, there aren't enough words or ways to express how grateful I am to my soulmate and the best gift from my God my youngest sister Dr. Sarah for your whole-hearted support.

Table of Contents

Abstract **2**

Declaration **4**

Acknowledgments **5**

Table of Contents **7**

Nomenclature **12**

List of Figures **18**

List of Tables **21**

Chapter 1 ..... **22**

Introduction **22**

Chapter 2 ..... **25**

Literature Review **25**

2.1 The Lung Epithelium **25**

2.1.1 Lung Development **25**

2.1.1.1 The Embryonic Stage (0-4 embryonic weeks) 25

2.1.1.2 The Pseudoglandular Stage (4-16 embryonic weeks) 26

2.1.1.3 The Canalicular Stage (16–25 embryonic weeks) 27

2.1.1.4 The Terminal Saccular stage (26-36 embryonic weeks) 27

2.1.1.5 The Alveolar Stage (36 embryonic weeks to childhood) 27

2.1.2 Creating lung epithelial cells from human ESCs and human IPSCs **29**

2.1.2.1 Early Efforts of Using Stem Cells to Generate Type II Cells 29

2.1.2.2 A revised strategy for Epithelial Differentiation 32

2.1.2.2.1 Endodermal Induction in human ESCs and human IPSCs. 32

2.1.2.2.2 Anterior Foregut Endoderm Induction in human ESCs and human IPSCs 33

2.1.2.2 Generation of Lung Progenitor Cells by leveraging (AFE) 34

2. 2 Cell sources **40**

2.2.1 Human pluripotent stem cells (human PSCs) **40**

2.2.2. Maintain (human PSCs) in *vitro* **43**

2.2.2.1 Growth Medium for (human PSCs) Culture 43

2.2.2.2 Extracellular Matrix (ECM) 44

2.2.2.3 Environmental Indications 44

2.2.2.3.1 Hypoxia 45

2.2.2.4 Addition of anti-apoptotic agents to enhance survival 49

2.3 3D Matrices **50**
2.3.1 ALGINATE HYDROGEL **50**
2.3.2 Cell encapsulation **52**
2.4 Bioreactors for the purpose of tissue engineering **54**
2.5 Tissue engineering of the lung **55**
2.5.1 Tissue engineering of functional unit of the lung **56**
2.5.2 Tissue engineering of whole lung **57**
Chapter 3 ..... **59**
Aim and Objectives **59**
3.1 Overview of experiments **59**
3.2 Aim **59**
3.3 Objectives **60**
3.4 Hypotheses **61**
Chapter 4 ..... **62**
Materials and Methods **62**
4.1 Cell culture **62**
4.1.1 Two-dimensional cell cultures **62**
4.1.2 Culture medium preparation **62**
4.1.3 Preparation of Matrigel™-coated culture plates **63**
4.1.4 3D cultures **63**
4.1.4.3 Alginate bead dissolution 64
4.1.5 Directing the differentiation of human ESCs and IPSCs into alveolar type II pneumocytes **65**
4.3.3 Induction of lung progenitors **65**
4.3.4 Induction of lung/airway epithelial maturation **66**
4.2 Imaging **66**
4.2.1 Phase Constrast and Fluorescence microscopy **66**
4.2.3 Transmission electron microscopy **66**
4.3 Histology **67**
4.3.1 Paraffin embedding **67**
4.3.2 Haematoxylin and eosin stain **67**
4.3.3 Alkaline phosphatase staining **68**
4.3.4 Immunocytochemistry and immunohistochemistry **68**
4.4 Gene Expression Analysis **70**
4.4.1 Ribonucleic acid (RNA) extraction **70**
4.4.2 Reverse Transcriptase and cDNA synthesis **70**

4.4.3 Polymerase chain reaction (PCR) 71
4.5 Viability assays 72
4.5.2 CellTiter-Glo Luminescent Cell Viability Assay Kit 73
4.5.3 3-(4,5-Dimethylthiazol-2-Yl)-2,5-Diphenyltetrazolium Bromide (MTS) Tetrazolium Assay 73
4.6 Flow cytometry 73
4.6.2 Flow cytometry data analysis 74
4.7 Immunoprecipitation and western blotting 74
4.8 Statistics 76
Chapter 5 77
Maintain human IPSCs pluripotency in feeder-free culture and enhance the proliferation of single cells by combining ROCK inhibition and hypoxia 77
5.1 Introduction 77
5.2 Aim and Objectives 78
5.3 Methodology 79
5.4 Results and Discussion 80
5.4.1 Morphological Alkaline Phosphatase AP+ Produced of undifferentiated human IPSCs Cultured on Corning® Matrigel™ Matrix in mTeSR™1 Medium 80
5.4.2 The characterisation of Human IPSCs self-renewal potential over passages 83
5.4.3 Optimised proliferation of human IPSCs when passaged as single-cells and evaluation of pluripotency maintenance under different conditions 87
5.5 CONCLUSION 97
Chapter 6 98
Maintain Human-induced pluripotent stem cells (human IPSCs) Proliferation and Pluripotency in Alginate Beads and Evaluate the Effect of Static and Dynamic Motion 98
6.1 Introduction 98
6.2 Aim and Hypothesis 100
6.2.1 Aim 100
6.2.2 Objectives 100
6.3 Method 100
6.4 Results and Discussion 102
6.4.1 Human IPSCs morphology in alginate hydrogels microbeads 102
6.4.2 Optimization of proliferation of human IPSCs 3D cultures 105

6.4.3 The gene expression profiles of self-renewal of human IPSCs and spontaneous differentiation markers 109
6.4.4 The effect of hypoxia on prolonged adaption 114
6.4.5 Evaluate the ECM secretion by human IPSCs cultured in 3D environment 119
6.5 Conclusion 123
Chapter 7 124
Optimizing the Differentiation of Human IPSCs towards Endoderm in 3D Dynamic Culture. 124
7.1 Introduction 125
7.2 Aims and Objectives 126
7.3 Methodology 127
7.4 RESULTS and DISCUSSION 128
7.4.1 Evaluating the effect of Wnt3a on endoderm differentiation by using qRT-PCR in both 2D and 3D dynamic cultures 128
7.4.2 The effect of CHIR99021 on endoderm differentiation in 2D and 3D dynamic cultures 129
7.4.3 Wnt3a vs CHIR99021 towards endoderm induction in 3D dynamic culture 131
7.4.4 Presence of serum promotes proliferation throughout 3D cultures 134
7.4.5 Effect of RPMI 1640 medium on the stability of alginate beads in 3D dynamic culture 135
7.5 Conclusion 136
Chapter 8 138
8.1 Introduction 138
8.2 Aims and Objectives 140
8.3 Methodology 140
8.4 RESULTS and DISCUSSION 142
8.4.1 Cell proliferation and viability in static and dynamic 3D cultures 142
8.4.2 Induction of human IPSCs differentiation into type II alveolar cells 145
8.4.3 Differentiated lung epithelium cells produced in 3D cultures are functional 150
8.4.4 The interaction of the microenvironment and the encapsulated cells. 154
8.4.5 Extracellular matrix production in 3D dynamic enhancing cells proliferation and differentiation 157
8.5 Conclusion 158
Chapter 9 - Conclusion 160
9.1 General conclusion 160

9.2 Future work **163**
9.2.1 2D culture **163**
9.2.2 3D culture **163**
9.2.3 Further assays to validate type II pneumocytes maturation **164**
Bibliography **135**
Appendices **157**

Nomenclature

2D	2-Dimensional
3D	3-Dimensional
AETI	Alveolar epithelial type I
AETII	Alveolar epithelial type II
AFE	Anterior Foregut Endoderm
AIDS	Acquired immunodeficiency virus
AP	Alkaline phosphatase
AP	Alkaline phosphatase
AQP5	Aquaporin 5
ATCC	American Type Culture Collection
BE	Biochemical Engineering
bFGF	Basic fibroblast growth factor
BMP	Bone morphogenic protein
BMPs	Bone morphogenetic proteins
BSA	Bovine serum albumin
Calcein AM	Calcein acetoxymethylester
cAMP	3'-5'-cyclic adenosine monophosphate
CC10	Clara cell 10
CCSP	Clara cell secreting protein

cDNA	Complementary deoxyribonucleic acid
Cdna	Complementary DNA
CE	Chemical Engineering
CM	Conditioned medium
COPD	Chronic Obstructive Pulmonary Disease
COPD	Chronic obstructive pulmonary disease
DAPI	4',6 diamidino-2-phenylindole
DE	Definitive Endoderm
DMEM	Dulbecco's modified Eagle's medium
DMSO	Dimethylsulfoxide
DNA	Deoxyribonucleic acid
EB	Embryoid body
EB	Embryoid body
EC cells	Embryonal carcinoma cells
EDTA	Ethylenediaminetetraacetic acid
Egf	Epidermal growth factor
EGF	Epidermal growth factor
EMT	Epithelial-to-mesenchymal transition
ES	Embryonic stem
Es	Embryonic stem
ES cells	Embryonic stem cells

EthD-1	Ethidium homodimer-1
FACS	Fluorescence-activated cell sorting
FBS	Fetal bovine serum
FBS	Foetal Bovine Serum
FGF	Fibroblast growth factor
FGF	Fibroblast growth factors
FoxA2	Fork head transcription factor 2
FSC	Forward scatter
GAPDH	Glyceraldehyde-3-phosphate dehydrogenase
GAPDH	Glyceraldehyde-3-phosphate dehydrogenase
GH	Growth hormone
GIT	Gastro-intestinal tract
Gli2/gli3	GLI-kruppel family
GLU	Glutamate
Gluc	Glucose
GMP	Good manufacturing practice
GOI	Gene of interest
H&E	Haematoxylin and eosin
HARV	High Aspect Ratio Vessel
HARV	High Aspect Ratio Vessel bioreactor
HEPES	N-(2-hydroxyethyl) piperazine-N-(2-ethane sulfonic acid)
Human ES	Human Embryonic Stem

Hh	Hedgehog
HNF	Hepatocyte nuclear factor
hTERT	Human telomerase reverse transcriptase
Human	induced pluripotent stem cells
ICM	Inner cell mass
IGFs	insulin-like growth factors
IgG	Immunoglobulin G
IgM	Immunoglobulin M
IPA	Isopropyl alcohol
iPS	Induced pluripotent stem cells
Kgf	keratinocyte growth factor
KOSR	Knock out serum replacement
Lac	Lactate
LIF	Leukaemia inhibitory factor
MEF	Murine embryonic fibroblast
MEF	Mouse embryonic fibroblast
MHC	Major histocompatibility complex
mmHg	Millimetres of mercury
mRNA	Messenger ribonucleic acid
MSCs	Mesenchymal stem cells
Muc5ac+	Mucin secreting cells
NASA	National Aeronautics and Space Administration
NASA	National Aeronautics and Space Administration
NEAA	Non-essential amino acids
NKX2.1	Nk2 homoeobox

OCT	Optimal cutting temperature
Oct-4	Octamer binding factor 4 also known as Oct-3 / Oct-3/4, Pou5f1
Osm	Osmolarity
PBS	Phosphate-buffered saline
pCO2	Partial pressure of carbon dioxide
PCR	Polymerase chain reaction
PCR	Polymerase Chain Reaction
PDGF	Platelet derived growth factor
PFA	Paraformaldehyde
PFE	Posterior forgot endoderm
PI	Propidium iodide
pO2	Partial pressure of oxygen
qRT-PCR	qualitatively Reverse transcription PCR
RA	Retinoic acid
RNA	Ribonucleic acid
RNA	Ribonucleic Acid
ROCK	Rho-associated, coiled-coil containing protein kinase
RT	Room Temperature
RWV	Rotating Wall Vessel
SABM	Small Airway Basal Medium
SAGM	Small Airway Growth Medium
SD	Standard deviation
SEM	Scanning electron microscopy
SHH	Sonic Hedgehog
SP	Surfactant proteins

SPA	Surfactant protein A
SPB	Surfactant protein B
SPC	Surfactant protein C
SPD	Surfactant protein D
SSC	Side scatter
SSEA-1	Stage-specific embryonic antigen-1
SSEA-4	Stage-specific embryonic antigen-4
TE	Trypsin-ethylenediaminetetraacetic acid
TEM	Transmission electron microscopy
TEM	Transmission electron microscopy
TEMED	N, N, N', N'-tetramethylethylenediamine
TGF-α	Transforming growth factor
TGFß	Transforming growth factor-beta
TGFα	Transforming growth factor-alpha
TGFβ	Transforming growth factor β3
TH	Thyroid hormones
Tra 1-60	Trafalgar 1 60
Tra 1-81	Trafalgar 1 81
TRITC	Tetramethyl rhodamine iso-thiocyanate
TTF-1	Thyroid transcription factor-1
UV	Ultraviolet
VEGF	Vascular endothelial growth factor

List of Figures

Figure2.1 Representation of the five phases involved in lung development..... 28

Figure 2.2 Stepwise differentiation strategy relating to pulmonary epithelial cell derivation from pluripotent stem cells. 31

Figure 2.3 Isolation/differentiation of stem cells for the purpose of tissue engineering and regenerative medicine. 42

Figure 2.4.The role of HIF-2 in pluripotency. 48

Figure 2.5. Alginate is a polysaccharide co-polymer comprised of guluronic as well as mannuronic acid groups. 51

Figure 2.6 HARV bioreactor..... 53

Figure 3. 1. Diagrammatic representation of the integrated bioprocessing approach to differentiating stem cells to pulmonary epithelium adopted in this study. 60

Figure 5.1: Morphology of Human IPS Cell Line IMR-90 Cultured on Corning® Matrigel™ Matrix in mTeSR™1 Medium. 82

Figure 5.2: Immunofluorescence staining of pluripotency-associated nuclear and surface proteins in human IPSCs. 85

Figure 5.3: Negative Controls for non-specific immunocytochemistry staining of pluripotency-specific primary antibodies for human IPSCs..... 86

Figure 5.4: Flow cytometric analysis of pluripotency markers over 5 passages..... 87

Figure 5.5 Comparing the passaging of human IPSCs as clusters vs single cells. 88

Figure 5.6. Cells proliferation of single human IPSCs in different conditions and different time points. 91

Figure 5. 7 Single human IPSCs after 12 of plating. 92

Figure 5. 8 Flow Cytometry Analysis of Pluripotency Marker Expression of human IPSCs dissociated to single cell suspensions in in different conditions at 96 hours. 95

Figure 5. 9 Comparing cellular proliferation of human IPSCs and ESCs. 96

Figure 6.1: Summary of the experimental scheme used to culture cells in 3D platforms..... 102

Figure 6.2: IPSCs morphology before and after encapsulation..... 104

Figure 6.3 Comparison of cells proliferation between static and dynamic cultures of human induced pluripotent stem cells..... 106

Figure 6.4 Comparison of cell proliferation of hIPSCs encapsulated in hydrogels of (alginate/gelatin - 3DD G) or (alginate/Matrigel™ - 3DD M) in 3D dynamic cultures. 107

Figure 6.5 Comparison of cells proliferation of hIPSCs encapsulated within alginate hydrogel + gelatin and cultured with mTeSR™ medium with ROCK inhibitor (3DD RI) or without ROCK inhibitor (3DD W/O RI) in 3D dynamic culture. 109

Figure 6.6: Comparing the expression of pluripotency markers OCT3/4 and Nanog in static condition vs dynamic at day 5 and 20. 111

Figure 6.7 Comparing the expression of pluripotency markers OCT3/4 and Nanog in dynamic conditions at day 5 vs 20. 112

Figure 6.8 Comparing the expression of pluripotency markers OCT3/4 and Nanog in static condition day 5 vs 20. 113

Figure 6.9 Comparing the expression of spontaneous differentiation marker PAX6 in static condition vs dynamic at day 5 and 20. 114

Figure 6.10 Comparing the expression of acute hypoxia associated marker HIFα in both dynamic and static 3D-conditions at different time points. 116

Figure 6.11 Comparing the expression of chronic hypoxia adaption associated marker HIF2α in both 3D conditions at different time points. 118

Figure 6.12 Comparing the expression of LAMA5 and FN1 genes in static vs dynamic condictions at days 5 and 20. 120

Figure 6.13 Comparing the gene expression of LAMA5 and FN1 in dynamic conditions at day 5 vs day 20. 121

Figure 6.14 Comparing the gene expression of LAMA5 and FN1 in static conditions at days 5 vs 20. 123

Figure 7.1: Schematic diagram of the direct differentiation of human IPSCs towards the endoderm lineage under 3D dynamic culture. 127

Figure7.2: Gene expression of CFCR4 and Foxa2. 129

Figure 7.3: CHIR99021 effect on endoderm differentiation in 2D vs 3D dynamic. 130

Figure 7.4: Wnta3 vs CHIR99021 effect on endoderm differentiation in 3D dynamic cultures. 133

Figure 7.5: Human IPSCs proliferation within encapsulated alginate beads. 135

Figure 7.6: Calcium alginate beads were cultured in RPMI 1640 leading to membrane rupture. 136

Figure 8.1 Differentiation protocol followed for the induction of lung epithelium from human IPSCs. After 24 in static cultures, cells were differentiated in 4 stages during the 20 days of culture. 141

Figure 8.5 Comparison of static and dynamic 3D cultures in cells proliferation. 144

Figure 8.6 Characterization of endoderm induction at day 4 . 145

Figure 8.7 Gene expression and immunohistochemistry analyses conducted on day 6. 146

Figure 8.10 Gene expression conducted on day 15. 147

Figure 8.6 Immunohistochemistry analyses conducted on day 15. 147

Figure 8.11 Gene expression conducted on day 20. 149

Figure 8.12 Immunohistochemistry analyses conducted on day 20. 150

Figure 8.13 Western blot for Pro C of day 15 for 3D dynamic, static and 2D 150

***Figure 8.14 TEM of a dynamic culture at day 15.* 151**

Figure 8.15 TEM of a static culture at day 15. 152

Figure 8.16 Representative TEM microscopy images of day 20 dynamic. 153

Figure 8.17 Representative TEM microscopy images of day 20 static. 153

Figure 8.18 The impact of hypoxia in cells differentiation. 156

Figure 8.19 ECM gene expression in static and rotary environment. 158

List of Tables

Table 1.1 List of the Critical Analytical Procedures used for the Assessments the self-renewal and differentiated in 2D and 3D of the Human IPSCs. 24

Table 2.1. Summary of published step-wise differentiation protocols for lung epithelial cells from iPSC. 39

Table 4.1.List of Primary and Secondary Antibodies for Immunocytochemistry Staining. 69

Table 4.2. The lists of qRT-PCR primer sequences. 71

Table 4.3. List of Primary Antibodies for Immunoprecipitation and western blotting 75

Chapter 1

Introduction

The main aim of tissue engineering is to replicate a material that closely matches and delivers the functionality of the original substance (Darling and Athanasiou, 2003). However, the selection of human cell sources that can provide sufficient cell numbers for tissue development to repair the defects caused by injury or disease presents a huge challenge in tissue construction for clinical application. It is, therefore, important to maintain huge quantities of undifferentiated cells to supply an adequate starting material for indefinite quantities of progenitor and differentiated cells (Chai and Leong, 2007). To achieve this, it becomes necessary to combine fundamental engineering and biological knowledge by fabricating a feasible bioreactor that provides a reproducible platform for the production of the required cell numbers to meet the clinical requirements.

Lung epithelial cells that are derived from induced pluripotent stem cells (human IPSCs) can potentially be a robust patient-specific source of cells (Ghaedi and Williams, 2015). These can reduce the level of graft rejection while removing the need for administration of strong immunosuppressive drugs after transplantation (Ghaedi and Williams, 2015). However, significant improvements are required in terms of optimising the cell source as well as the scaffolds used to differentiate them before engineered lungs are translated into the clinical setting (Calle et al., 2014). These limitations have been preventing patient access to bioengineered lungs which is not anticipated in the near future.

Although successfully performed before, generation of lung progenitors from human IPSCs has yet to be performed in a scalable way, which would fulfil the need to obtain large numbers of fully differentiated cells (Ghaedi and Williams, 2015). In tissue engineering, the use of 3D culture systems such as scaffolds or bioreactors allows for the production of the required cell numbers, something that traditional 2D flask cultures fail to provide (Tomoshi 2014).Provision of a suitable matrix is necessary to enable culture of anchorage-dependent

cells under 3D conditions (Dye et al., 2016). Among the different matrices used for this purpose, encapsulation in alginate beads has been proven to be a suitable material mainly due to its semi-permeability, allowing for the diffusion of oxygen and nutrients to the cells and the elimination of waste products (Miranda 2010). Furthermore, the HARV bioreactor, which mimics a state of microgravity without exposing cells to turbulence and high shear stress, improves cell-to-cell interaction while providing the required agitation to promote gases and nutrients diffusion (Hammond 2001).

The lung is a complex three-dimensional structure that expresses major differences in the composition of the epithelium along the proximodistal axis. The proper organisation and proliferation along proximodistal axis is crucial for lung development. The most distal region of the lung is organized into a complex system of alveoli that are lined by two primary epithelial cells types: type I and type II pneumocytes. Type I cells contribute to the majority of the alveoli tissue in the lung (covering up to 95% of the alveolar surface area) and are primarily responsible for gas-exchange, while type II pneumocytes secrete alveolar surfactants (such has protein C) and organise in a cube-like shape (Rawlins 2006).

Lung epithelia remains one of the least studied lineages derived from embryonic stem cells *in-vitro* (Siti-Ismail 2012) and to the best of our knowledge, to date, no study has been performed for the direct differentiation of human IPSCs towards lung epithelium using alginate encapsulation and a HARV bioreactor. This technique promises to differentiate and expand high numbers of mature lung progenitors as a future autologous therapy for diseases incurring damage to the lung alveolar epithelium.

In this thesis, a literature review addressing the issues and the clinical need for an alternative treatment for terminal lung illnesses is provided Chapter 2 with an emphasis on the restrictions and disadvantages of the existing platforms, the state-of-art in lung epithelium generation, studies using 3D cultures and bioreactor platforms. Chapter 3 will outline the necessities of human IPSCs differentiation towards type II pneumocytes lung epithelium cells in 3D dynamic cultures and set the overall aim and objectives of this thesis. Chapter 4 describes the materials and methods used for human IPSCs maintenance culture, the differentiation protocols applied, 3D culture preparation and the bioreactor used. Chapter 5

shows the maintenance of human IPSCs in culture and the approaches employed to characterize the pluripotency. To this goal, a study on the effect of several culture conditions on viability and proliferation of single cells will be considered. The optimization of human IPSCs proliferation and self-renewal in both 3D static and dynamic cultures is described in chapter 6. Chapter 7 shows differentiation of human IPSCs into Type II pneumocytes in 3D cultures and how this method compares to two previously established protocols in 2D (Green, 2011; Naujok 2014). The platform presented in chapter 7 has been optimised Chapter 8. Conclusion and critical discussion of the findings of this work are summarized in Chapter 9 where future plans will also be outlined.

Table 1.1 List of the Critical Analytical Procedures used for the Assessments the self-renewal and differentiated in 2D and 3D of the Human IPSCs.

THE ASSESSMENTS	*ANALYTICAL PROCEDURES*
• **MORPHOLOGY**	1. Light microscope 2. TEM
• **CELLULAR MARKERS**	Flow cytometry
• **PROTEIN ANALYSIS**	1. Immunostaining 2. western blot
• **GENE EXPRESSION**	qRT-PCR
• **CELLS PROLIFERATION**	1. CellTiter-Glo 2. MTS
• **FUNCTIONAL ASSAY**	TEM
• **VIABILITY**	LIVE/DEAD Staining

Chapter 2

Literature Review

In this chapter we present the most relevant contributions and the state-of-the-art of lung tissue engineering with an emphasis on type II pneumocyte differentiation, cell sources and 3D cultures. First, the basics of lung development *in-vivo* are described, followed by an overview of the early attempts to derive lung epithelial lineages from pluripotent stem cells. Second, we focus on the latest strategies for epithelial differentiation. Third, the cell lines used in this study and the corresponding maintenance strategies are reviewed. Finally, the scaffolds used for 3D cultures and bioreactors are discussed.

2.1 The Lung Epithelium

2.1.1 Lung Development

The human lung's development entails five stages, namely: embryonic, pseudoglandular, canalicular, saccular and alveolar, as depicted in shown in (Figure 2.1.) (Schittny, 2017).

2.1.1.1 The Embryonic Stage (0-4 embryonic weeks)

An embryo begins as a single layer that subsequently transforms into a trilaminar structure called the gastrula (Cardoso 2001). The gastrula's three layers are termed mesoderm, ectoderm and endoderm. The outermost ectodermal layer leads to the development of the skin and the nervous system; the mesodermal layer leads to the formation of the muscular and cardiac systems; and the endodermal layer results in the formation of gastro-intestinal (GIT) and respiratory tracts (Schwarz et al. 2000). This endodermal layer is further subcategorised into two segments: the anterior foregut endoderm (AFE) and the posterior forgot endoderm (PFE). The AFE creates the respiratory system whereas PFE differentiates into the GIT and the liver. Previous studies have elucidated the essential genes and transcription factors in lung development. The most primitive genes which initiate endoderm development include Nodal/Activin A and Wnt-β-catenin (Cardoso and Williams 2001).

These genes interact with each other to induce Sox17, FoxA2 and GATA6 transcription factors in order to produce downstream signalling that establishes the foundation of the endodermal layer.

2.1.1.2 The Pseudoglandular Stage (4-16 embryonic weeks)

The lung produced from AFE is situated in close proximity to the cardiac mesoderm. More significantly, the cardiac mesoderm unleashes fibroblast growth factors (FGFs) that play a key role in regulating the formation of lung as well as the GIT. High FGF2 levels result in lung development, whereas a lower level of FGF2 results in GIT formation (Schwarz et al. 2000). Sonic hedgehog (Shh) is another major contributory in the lung development signalling pathway. Shh encodes for a vertebrate homolog belonging to the Hedgehog (Hh) family (van Tuyl and Post 2000). Shh is additionally significant in developing the tracheoesophageal as well as lung-bud septation (Mukasa et al. 1996; Grindley et al. 1997; Lei et al. 1998). Moreover, the retinoic acid (RA) and the RA transcriptional factor receptors induce the formation of lung bud and laryngo-tracheal groove.

During lung morphogenesis, NK2 home box 1 (NKX2.1/TTF-1) gets induced by HNF-3β as well as GATA-6 proteins (Price et al. 1990; Bruno et al. 1999; Jones et al. 2011). The NKX2.1 expression however, is also traced in epithelial cells sourced from the thyroid, lungs, pituitary and foetal brain arising out of AFE (Price et al. 1990) and is therefore, insufficient to indicate differentiation into respiratory tract cells conclusively.

In addition, the interaction of branching lung with the mesenchyme offers additional signals for the pulmonary developmental branching. One such interaction takes place during lung bud development. FGF10 attracts the epithelium into the mesenchyme resulting in early bud formation. Shh, along with transforming growth factor-β (TGF- β) prevents the production of FGF-10 during the bud's shaping. This not only inhibits bud proliferation (Cardoso 2001), but also leads to cleft formation, which are basically sites that constitute the lung's sub-lobar and lobular branches (Cardoso 2001). Branching morphogenesis is a key facet of lung development and is tightly controlled by numerous genes and cell signal-

ling pathways including the epidermal growth factor (EGF), the TGF, the FGF and the insulin-like growth factors (ILGFs) families. Together, they assume significance in the migration, proliferation and segregation of cells (Mendelsohn et al. 2000).

2.1.1.3 The Canalicular Stage (16–25 embryonic weeks)

In this stage, the respiratory tract begins to grow in length as well as diameter through the expansion of capillaries, blood vessels and lymphatic ducts. The vascularisation process gets controlled by multiple signalling pathways such as vascular endothelial growth factor (VEGF), which also promotes endothelial cell survival and differentiation, while EGF) regulates ATII cell proliferation and platelet-derived growth factors (PDGFs) are important for epithelial and vascular development (Nexo et al. 1992).

2.1.1.4 The Terminal Saccular stage (26-36 embryonic weeks)

In the saccular stage, the mesenchymal cells begin initiating apoptosis and differentiation, leading to thinning of the interstitium (Nakano et al. 2002). The alveolar epithelial cells differentiate into squamous type-I pneumocytes (ATI cells) and rounded secretory type II pneumocytes (ATII cells) that contain lamellar bodies. In addition, the capillaries develop within the surrounding saccules and create a complex network that represents the nascent stages of the gas-exchange interface. The lymphatic network develops a parallel network to the capillaries (Warburton *et al.*, 2010).

2.1.1.5 The Alveolar Stage (36 embryonic weeks to childhood)

Alveolarisation denotes the last stage in the process of lung development with a major proportion of the gaseous exchange surface developing in the final few weeks of a pregnancy. After the formation of new saccules, the first alveoli are formed. Between the saccules lies the parenchyma, which comprises of a two-fold layer of capillaries that create the primary septa. Tiny protrusions begin to form along the primary septa, which subdivide the saccules into smaller-sized subunits, the alveoli. Each alveolus gets nestled by elastic fibres that constitute the interstitial septa between the two capillary nets. This alveolarisation process continues until the first year and a half (Schittny, 2017).

The alveolar duct has a close proximity to the pulmonary capillaries, containing the surfactant that is produced by ATII cells. They also contain pores (known as the pores of Kohn) that link them to the adjacent alveoli. The broad organisation of these different components allows the interstitial capillaries exposure to two alveoli at the same time. The air/blood interface, made out of ATI cells, comprises of an extremely thin basement membrane and pulmonary capillary endothelium.

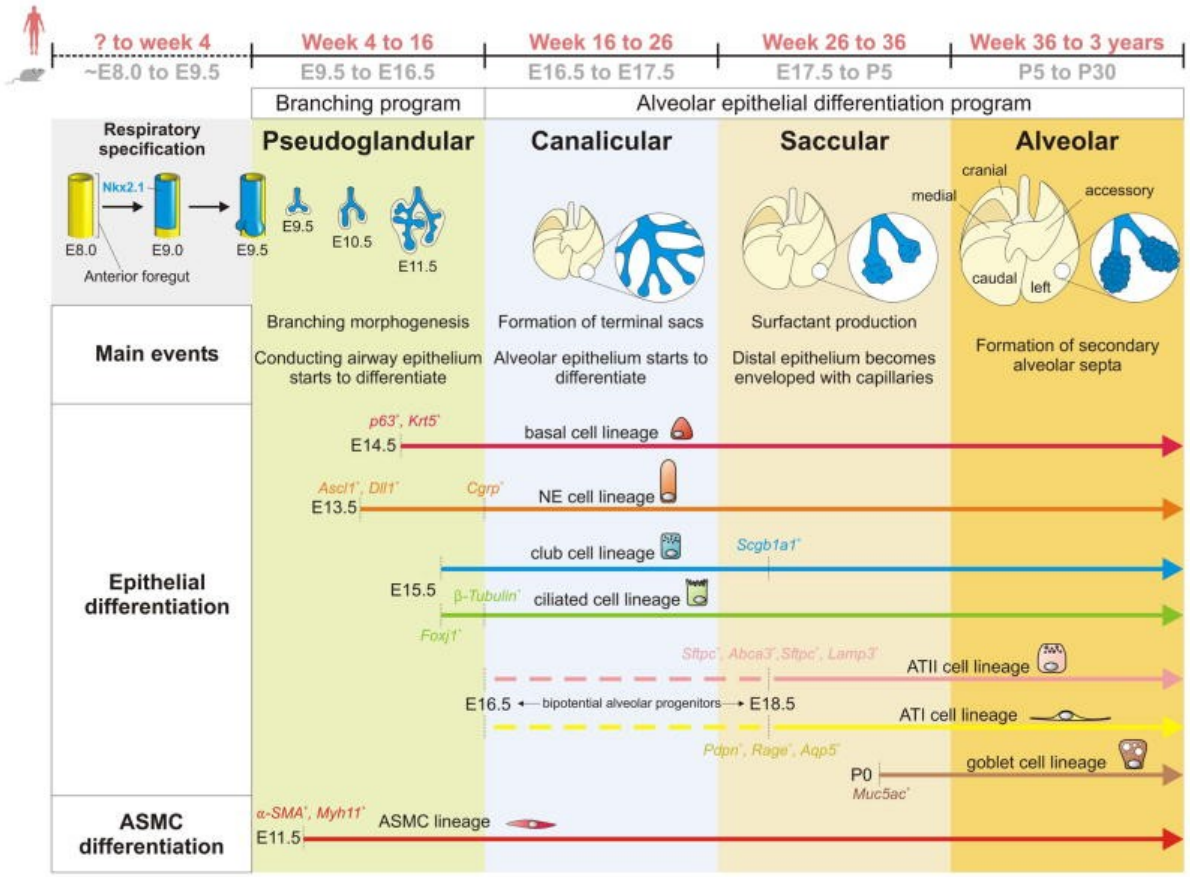


Figure2.1 Representation of the five phases involved in lung development.
Firstly, the embryonic period where lung buds are formed with differentiation into trachea and bronchi. Afterwards, the foetal period begins from embryonic week 7 until 36. In this interval the formation of lung periphery, appropriate vascularisation, type 1 pneumocyte maturation, and the air-blood interface are achieved. The process of lung maturation progresses from week 36 until 3 years of age where maturation of alveoli, proliferation and expansion are completed. Adapted from (Volckaert and Langhe, 2015).

2.1.2 Creating lung epithelial cells from human ESCs and human IPSCs

2.1.2.1 Early Efforts of Using Stem Cells to Generate Type II Cells

In studies conducted over approximately the last seven years, many laboratories have demonstrated that human and mouse IPSCs and human ESCs are capable of differentiating towards ATII cells and proximal airway cells. Owing to the significant physiological function of AT2 cells *in vivo* coupled with the feasibility of quantifying this function by measuring the secretion and expression of surfactant, many investigators have decided to focus on generating AT2 cells from human IPSCs (Ali et al., 2002; Wang et al., 2007; Van Haute et al., 2009; Banerjee et al., 2012b; Longmire et al., 2012). The generation of additional proximal airway epithelial cells like Clara, basal and ciliated cells from human IPSCs or ESCs has proven to be a bigger challenge. Therefore, fewer studies have demonstrated differentiation into airway epithelial cells, in spite of the fact that diseases affecting the upper airways are more common than those affecting distal and alveolar cells. The generation of cells using airway epithelial cell phenotypic markers follows the culture of the ESCs in air–liquid interface conditions (Mou et al., 2012; Longmire et al., 2012; Wong et al., 2012; Firth et al., 2014).

Initially, lung lineage differentiation protocols were geared to culturing human ESCs in conditions commonly used for the growth of freshly isolated airway and alveolar human cells (Banerjee et al., 2012a). The pulmonary orientated media was expected to promote differentiation and survival towards ATI and ATII cells. The protocols detected the expression of surfactant protein, which suggested the presence of AT2 cells. However, the cells were typically present at low levels. In order to circumvent the reduced efficiency as well as heterogeneity, human ESCs were transduced using selection markers like the surfactant protein C (SPC) promoter, providing the ability to choose the derived epithelial population, and yield a purer population of cells. With a novel approach, Wang et al. correlated the SPC promoter to the neomycin resistance gene while using the puromycin selection for the purpose of yielding a >99% pure population of SPC-expressing and ESC-derived cells (Ali et al., 2002; Wang et al., 2007). Van Haute et al. expanded on these results by developing a 20 day air-liquid interface culture for the purpose of sourcing cells expressing SPC, CC10 and

surfactant protein A (SPA) (Van Haute et al., 2009). Although the early attempts marked a key advancement in the field, protocols that were guided by surrendering AT2-like cells from ESCs have given more specific and consistent results since then. The stepwise differentiation protocols source cells from pluripotent stem cells to anterior foregut endoderm and definitive endoderm into a lung-progenitor cell and subsequently via pathways to form cells expressing markers of AT2 cells or other forms of epithelium (Figure 2.2). By making use of these differentiation approaches, many research groups have highlighted the differentiation of human IPSCs and ESCs towards a range of pulmonary epithelium, including AT2 and an additional airway epithelium (Ghaedi et al., 2014; Huang et al., 2013; Longmire et al., 2012).

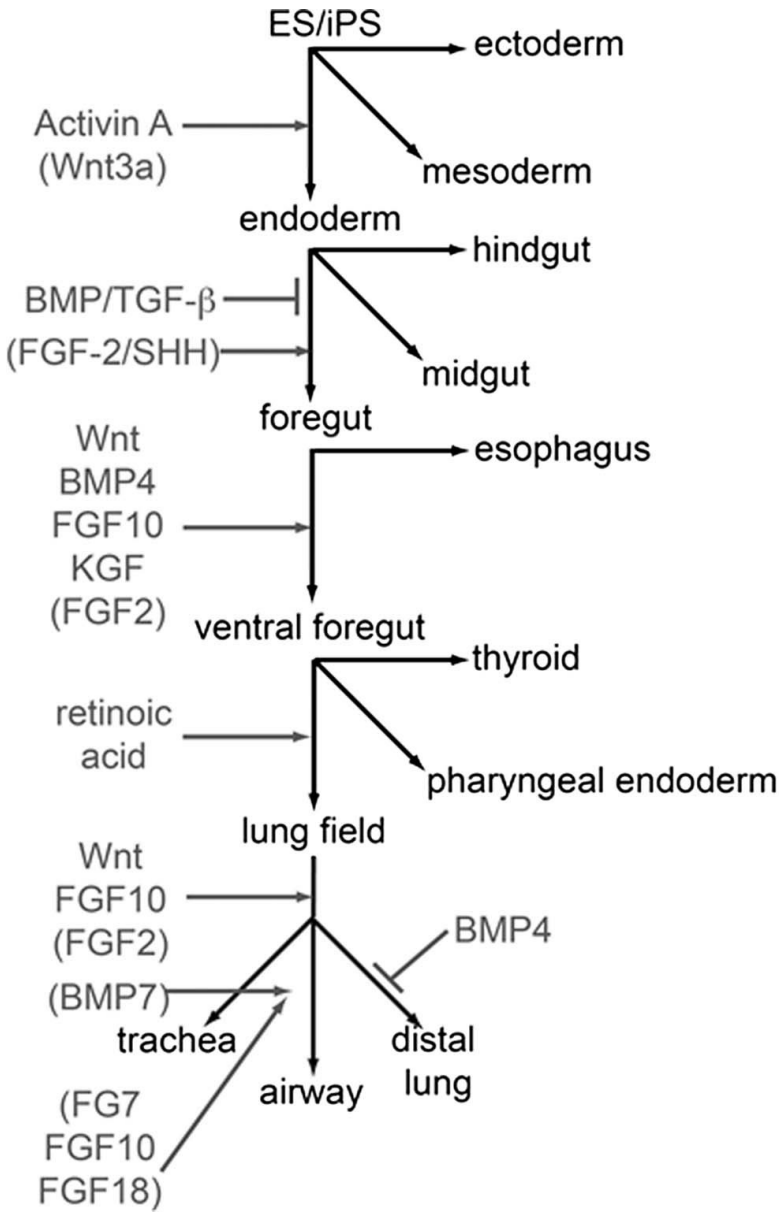


Figure 2.2 Stepwise differentiation strategy relating to pulmonary epithelial cell derivation from pluripotent stem cells.

Depicted vertically is the series of developmental progenitor fates that human pluripotent stem cells must pass through to differentiate into respiratory epithelium. The left-hand side of the figure demonstrates the critical signalling pathways required for the conversion between developmental progenitors. Parentheses indicate a compound that is used only in some differentiation schemes. The right-hand side gives alternative lineages that could arise from a given patterning step. Adapted from (Green, Huang, and Snoeck, 2013).

2.1.2.2 A revised strategy for Epithelial Differentiation

As noted previously, the embryonic lung is formed by definitive endoderm, which means that the appearance of markers linked with this germ layer is a key indicator of pulmonary determination. However, in initial stages of ESC research, it became fairly apparent that it is significantly more difficult to obtain endodermal lineages compared to mesodermal and ectodermal ones. Thus, the focus turned towards developing the means through which endodermal differentiation could be enhanced (Kubo et al., 2004; D'Amour et al., 2005; Grapin-Botton, 2008) .

2.1.2.2.1 Endodermal Induction in human ESCs and human IPSCs.

Endodermal and mesodermal fates are influenced by the expression levels of the nodal signalling pathway (Thisse, Wright and Thisse, 2000). Mouse studies indicated that endoderm specification is determined by TGF-β family signalling, particularly the secretory protein Nodal. Studies on zebra fish demonstrated that nodal signalling specifies endoderm and mesoderm in a concentration-dependent manner (Hagos and Dougan, 2007). Among the signals that activate the nodal pathway is Wnt signalling. Mouse embryos that lacked nodal or beta-catenin (β-catenin) could not form the primitive streak (Funa et al., 2015). This indicates that the nodal as well the Wnt signalling pathways work in a synergistic manner for endoderm formation (Huelsken et al., 2000; Ben-Haim et al., 2006).

Many research groups have used the knowledge of these pathways to promote endoderm differentiation from stem cells in-*vitro*. However, owing to the restricted availability as well as high price of the nodal protein, most groups presently utilise Activin A instead. Activin A is a signalling protein involved downstream in the nodal signalling cascade responsible for inducing a definitive endoderm phenotype in ESCs. As per initial experiments conducted with murine ESCs (Kubo et al., 2004a; Yasunaga et al., 2005) and in human ESCs (D'Amour et al., 2005). Differentiated endoderm can be produced from ESCs with high levels of Activin A under low-serum conditions. The low-serum environment has been suggested to restrict phosphatidylinositol-3-kinase (PI3k) activity, a requirement for definitive endoderm formation (McLean et al., 2007). By leveraging this specific model, numerous laboratories have been able to generate protocols pertaining to endoderm induction (Kubo et al.,

2004; Amour et al., 2005) . Efficacies however, have been shown to be highly variable and dependent on the cell lines that were used. The analysis of a number of transcription factors that are expressed downstream of Nodal/Wnt signalling has been used to gauge the success of endoderm specification in the above protocols. Forkhead transcription factors that belong to the FoxA family as well as GATA factors are the key factors of the endodermal network. Many family members of these transcription factors are expressed in mesoderm or endoderm across a number of species. GATA factors are expressed in mesendoderm (is a state that precedes DE further specification) and are required for endodermal differentiation. In vertebrates, other important players of the Nodal network downstream include MIX, SOX17, and many allied genes such as C-KIT, CXCR4, GATA4, GATA6, and EpCAM. These are expressed in endoderm and can be used as markers to assess appropriate differentiation (Green et al., 2011; Longmire et al., 2012; Ghaedi et al., 2013).

2.1.2.2.2 Anterior Foregut Endoderm Induction in human ESCs and human IPSCs

Following the formation of definitive endoderm within the embryo, the endoderm gets folded into a primitive gut tube from which many organs eventually bud following anterior-posterior patterning (Green et al., 2011) . Studies that examine in *vitro* germ layers characterise the signals entailed in developmental specification, and have demonstrated that endodermal differentiation into varying organs is triggered by signals arising from the adjacent ectoderm and mesoderm (Teo et al., 2011). The primary step in the context of lung formation happens to be the appearance of basic lung buds from the ventral-lateral component of the foregut. The lung buds express NKX2.1 (a transcription factor containing homeodomain) at high levels. This is earliest known marker linked with pulmonary lineage commitment (Cardoso and Lü, 2006). However, NKX2.1 is also linked with the commitment to thyroid lineage and does is not expressed in lung until the lung progenitor differentiation stage (Constam and Robertson, 2000; Green et al., 2011).

As per the report from Green on human ESCs or human IPSCs (Green et al., 2011), as well as that of Longmire relating to mouse ESCs (Longmire et al., 2012), the inhibition of TGF-β/BMP signalling resulted in increased formation of AFE. In their studies they used high levels of Noggin to inhibit bone morphogenetic protein (BMP) signalling and SB141524 to

inhibit TGF-β. This AFE may subsequently be differentiated into the cells that express markers of lung, thymus and thyroid (Mou et al., 2012; Ghaedi et al., 2013; Longmire et al., 2012) .

2.1.2.2 Generation of Lung Progenitor Cells by leveraging (AFE)

Numerous signalling pathways are entailed in differentiating AFE into lung progenitor cells during the process of their development. Signalling molecules as well as pathways that include Nodal, TGF-β, FGF, BMP, Notch, RA and Wnt play important roles in differentiating the AFE into the lung (Kaza et al., 2002; Goss et al., 2009). Expression gradients in signalling molecules result in dose-dependent responses on the foregut's anterior-posterior axis (Ghaedi, Niklason and Williams, 2015). The role of these signalling pathways and molecules is described in further details in (Figure 2.2).

2.1.2.2.1 BMP

BMPs refer to a family of molecules. Their signalling remains active within the foregut endoderm's ventral region *in vivo*, resulting in a rise in NKX2.1 during the process of anteriorisation by suppressing SOX2. During the course of lung development, BMP4 is expressed distally whereas BMP7 is expressed in closer proximity to the airway. BMP7 promote the formation of respiratory structures, such as the trachea and proximal epithelium (Mou et al., 2012;l Morrisey & Hogan, 2010; Mou et al., 2012; Ninomiya et al., 2013).

2.1.2.2.2 Wnt Signalling

According to a number of studies, Wnt signalling plays a key role in patterning anterior endoderm and is important to induce NKX2.1 expression in *vivo* (Shu et al., 2005; Goss et al., 2009). The Wnt pathway is effective in promoting endoderm specification within mammals by stimulating the Nodal pathway during the course of embryogenesis. Both Wnt and BMP unite to regulate the endodermal formation and lung specification. A sequential positive feedback loop develops between Wnt signalling and BMP, with each being capable of activating the other. Both Wnt signalling and BMP are activated by Nodal (Huelsken et al., 2000; Grapin-Botton, 2008).

2.1.2.2.3 FGF

Different FGF family members (like FGF-2, FGF-10 and FGF-7) influence the lung's patterning in addition to the proximal-distal axis from their locations within the mesenchyme (Kaza *et al.*, 2002). FGF signalling, in addition to BMP4 and Wnt signalling, is needed for specifying lung endoderm from the anterior foregut. FGF signalling is concentrated at the distal branching tips. FGF-10 signalling is crucial for growth induction in the lung bud, while FGF-7 is important in the context of proximal airway formation (Ameri *et al.*, 2009; Mou *et al.*, 2012).

2.1.2.2.4 RA

This metabolite assumes significance for adequate lung morphogenesis as well as the segregation of lung epithelium. RA signalling plays an important role in early lung bud formation as well as subsequent branching (Malpel, Mendelsohn and Cardoso, 2000; Desai *et al.*, 2006).

During the process of lung development, the timing and concentration of all factors will undergo changes at numerous stages. Distal FGF-2 and FGF-10 get substituted by proximal keratinocyte growth factors (KGF or FGF-7), during the course of proximal-distal specification whereas Wnt signalling gets inhibited within the proximal stalk progenitors and not in the distal tip (Huelsken et al., 2000; Shu et al., 2005). RA is another important factor for the development of lung bud, with RA concentration being comparatively higher in the proximal stalk region when compared to the distal tip region (Ameri et al., 2009). High RA signalling stymies the development of distal lung and promotes proximal airway development (Morrisey and Hogan, 2010)

Finally, by applying all above mentioned signalling pathways that are known to play a role in in-*vivo* lung development, researchers are now attempting to implement the same signalling pathways in-*vitro* to differentiate pluripotent stem cells into lung epithelium, with a reasonable degree of conformity (Mauck et al., 2000; Green et al., 2011; Mou et al., 2012; Longmire et al., 2012; Ghaedi et al., 2013). A method to pattern anterior foregut endoderm-like cells that were derived from human ESCs or human IPSCs to AT2 cells has been developed by combining Wnt3a, BMP4, EGF, FGF-10 and RA in human PSCs culture (Michael D

Green et al., 2011). A method for generating lung progenitor cells expressing NKX2.1 through the combined activation of BMP, FGF and the Wnt signalling pathways in mouse IPSCs has been described and optimised (Longmire et al., 2012). By making use of the growth factors cocktail that contain FGF10, Wnt, KGF, EGF and RA, could be generated a comparatively homogeneous population of ATII-like cells derived from human IPSC (Ghaedi et al., 2013, 2014; Huang et al., 2013). In addition, the exposure of ATII-like cells to IWR-1, which is a small molecule inhibitor of Wnt/β-catenin/ Creb-binding protein (CPB) transcription altered the ATII-like phenotype into a primarily ATI-like phenotype (Ghaedi et al., 2013, 2014).

While a large part of research has focused on differentiating human IPSCs as well as human ESCs into distal epithelium, a few protocols to differentiate human IPSCs and human ESCs into airway epithelial cells have also been applied. FGF-2, BMP4 and Wnt were shown to be important for the maturation of NKX2.1+ lung progenitors matured into NKX2.1+SOX2+ proximal progenitor cells as well as NKX2.1+P63+basal-like cells in *vitro*. This was induced by a cocktail of growth factors containing BMP7, KGF and high concentrations of RA (Mou et al., 2012). It has also been demonstrated that human pluripotent stem cells are capable of differentiating into CFTR-functional conducting airway epithelium through the combination of FGF, Wnt, and BMP signalling pathways (Wong et al., 2012) (Table 2.1).

Cell line	Before definitive endoderm induction	Definitive endoderm induction	Anterior foregut endoderm induction	Lung progenitor induction	Further Maturation	Airway Specification	Type II specification	Method of verification	Reference
W4/129S6 with a knock-in GFP re-porter gene for NKx2.1	--	Suspension of EBs. With 50 ng/ml Activin in 75% IMDM/ 25% Ham's Modified F12 medium. 5 Days	Adherent culture on gelatin-coated plate with 100 ng/ml Noggin (R&D) and 10 μM SB431542 in cSFDM. 1 Day	100 ng/ml mWnt3a, 10 ng/ml mKGF, 10 ng/ml hFGF10, 10 ng/ml mBMP4, 20 ng/ml hEGF, 500 ng/ml mFGF2 and 100 ng/ml Heparin in cSFDM. Days 7–15. mFGF2 (500 ng/ml), hFGF10 (100 ng/ml), and 100 ng/ml Heparin. 6 days	15 mM HEPES (pH 7.4) +0.8 mM $CaCl_2$ +0.25 % BSA + 5 μg/ml insulin + 5 μg/ml transferrin + 5 ng/ml Na selenite + 50 nM Dexamethas one + 0.1 mM 8-Br-cAMP + 0.1 mM IBMX + 10 ng/ml KGF in Ham's F12 me-dia. 3 days.	--	--	SPC, CC10, Ctfr, Foxj1	Longmire, et al., 2012
CA1, CA2, H9	PSCs were har-vested, gently triturated into single-cell sus-pensions and seeded onto transwells	100 ng/ml activin A in DMEM/F12 + 20% KoOR for 5 Days. Serum concentrations varied, 0.5% most effective. Adapted from D'Amour, K.A. *et al.*	500 ng/ml FGF2 and 50 ng/ml SHH in Endoderm Dif-ferentiation me-dium. 5 Days.	50 ng/ml FGF10, 50 ng/ml KGF (FGF7) and 5 ng/ml BMP4. 5 Days	10 ng/ml FGF10, 10 ng/ml FGF7 and 10 ng/ml FGF18. 5 Days	FGF18 (10 ng/ml) in BEGM. 10 Days. Cells air-lifted and bronchial air -liquid inter-face media added to bottom of transwells. ≥15 Days	--	Functional CTFR expres-sion	Wong, et al., 2012
C1, C2	--	100 ng/ml activin A in RPMI medium for 2 Days. 100 ng/ml activin A, 1×B27 supplement, 0.5 mM sodium butyr-ate, and 0.1% FBS in RPMI. 4 Days	200 ng/ml NOG-GIN, and 10 mM SB-431542 in IMDM +5% FBS for 2 days.	--	--	--	--	--	Ghaedi, et al., 2013a.
RUES2, Sendai Vi-rus and modified mRNA	Cells tryp-sinized to form EBs on low-at-tachment plates.	Y-27632, 10 μM, BMP4, 0.5 ng/ml, bFGF, 2.5 ng/ml, Activin A, in	EBs dissociated to single cells. 1.5 μM Dorsomorp hin di-hydrochl oride, 10 μM SB431542. 2	CHIR99021, 3 μM FGF10, 10 ng/ml, FGF7, 10 ng/ml, BMP4, 10 ng/ml, +/− EGF, 20	*CHIR99021, 3 μM, FGF10, 10 ng/ml, FGF7, 10 ng/ml, BMP4, 10 ng/ml, and ATRA, 50 nM or CHIR99021, 3 μM,	*Same as previ-ous +/− 50 nM dexamethasone, 0.1 mM 8-bromo-cAMP	--	MUC1, MUC2, EPCAM, p63, ABCA3, CC10, MUC5B, SPB, HOPX, proSPC,	Huang, et al., 2014

generated human dermal fibroblasts iPSC lines	Y-27632, BMP4 (3 ng/ml) added. 24 h.	DMEM/F12– B27. 3–5 Days	Days or 1 Day and.10 μM SB431542 and 1 μM IWP2. 1 Day	ng/ml, ATRA 0–1 μM in SFD for 8–10 days	human FGF10, 10 ng/ml, human FGF7, 10 ng/ml Days 15–25	and 0.1 mM IBMX		PDN, FOXJ1, AQP5	
C1, C2	--	100 ng/ml activin A in RPMI medium for 2 Days. 100 ng/ml activin A, 1×B27 supplement, 0.5 mM sodium butyrate, and 0.1% FBS in RPMI. 4 Days	100 ng/ml NOGGIN, and 10 mM SB-431542 in IMDM +5% FBS for 2 days.	Retinoic acid (0.5 μM), FGF-10 (10 ng/ml), EGF (10 ng/ml), Wnt3a (100 ng/ml), and KGF (10 ng/ml) in IMDM +10% FBSfor 10–14 days	Maintained and differentiated to Type II cells in Celprogen's complete Human type II media until use.	--	(Type II to Type I) Cells cultured in rotating bioreactor simulating an air-liquid interface in DMEM-10% FBS. 7 Days. Or IWR-1 (100mM) or ICG-001 (5mM) in DMEM + 10% FBS. 7 Days.	qRT-PCR for SPC, SPB and SPA Flow cytometry or ICC for Nkx2.1, proSPB, proSPC, SPA, SPC, T1α, AQ5, caveolin-1, CD54-PE	Ghaedi, et al., 2013b.
Patient fibroblasts reprogrammed with lentivirus and CRE excision	EBs generated in ultra-low attachment flasks in IMDM + 15% FBS. 6–10 Days.	Single cell suspension of iPSCs in coated transwell insert with ROCK inhibitor for 24 hours. Activin A (100ng/mL) and Wnt3a (25ng/mL) in RPMI medium. Day 1. Activin A (100ng/mL) in RPMI +1% FBS. Days 2–3.	SB431542 (500nM) and Noggin (20ng/ml) in Ultra MEM-ITES +2% FBS. Day 4. SB431542 (500nM) and BMP4 (5ng/ml) in Ultra MEM-ITES +2% FBS. Days 5–9.	BMP4 (5ng/ml), FGF2 (10ng/ml), FGF10 (10ng/ml), and KGF (10ng/ml), in Ultra MEM-ITES +2% FBS. Days 9–17.	--	Epinephourine (1.5 μM), RA (10nM), transferrin (2.5 μg/ml) and hydrocortisone (20nM) in DMEM-F12. Day 17+.	--	Patch-clamp electrophysiology for CTFR. qPCR, IHC, ICC for CTFR, CC10, ZO-1, NKx2.1, MUC5A/C, SPD, ECAD	Firth, et al, 2014
mESC, human CF induced-pluripotent cell lines	EB formation	Advanced DMEM medium, 2% B-27minus vitamin A, 0.05% Albumax II Glutamax, 10 M Y-27632 for 5 days	Advanced DMEM, 0.5–10μM A8301 for 2 days	Advanced DMEM, 50ng/ml BMP4, 100ng/ml FGF2, 50–10 nM GSK3iXV for 2–3 days	Advanced DMEM, RA supplemented B27, 50ng/ml BMP7, 50ng/ml FGF7, 100nM IWR-1, 1–2 μ	--	--	$NK2.1^{+}$, $SOX2^{+}$	Mou, et al 2012

and embryonic cell lines (HUES-3 and HUES-9)					M PD98059 for 2 days PD98059 for				

Table 2.1. Summary of published step-wise differentiation protocols for lung epithelial cells from iPSC.
Adapted from (Ghaedi, Niklason and Williams, 2015).

2. 2 Cell sources

2.2.1 Human pluripotent stem cells (human PSCs)

Stem cell research is not new. In 1963, Ernest McCulloch and James Till, "with Andy Becker and Lou Siminovitch, reported on the presence of self-renewing cells within the bone marrow of mice and postulated that these cells were regenerative stem cells (BECKER, McCULLOCH and TILL, 1963). Based on this work, stem cell research grew and by the end of the decade patients suffering from severe immunodeficiency "were treated using bone marrow transplants" (BECKER, McCULLOCH and TILL, 1963). In 1974, Evans and co-workers showed that embryonic carcinoma cells could differentiate into cells from each of the three embryonic germ layers; ectoderm, mesoderm and endoderm. In 1981, these researchers generated pluripotent murine ES cells from normal tissues which when combined with the development of human ES cells by Thomson in 1998 (Thomson et al., 1998) represented major advances in tissue engineering. ES cells became a new source of cells for tissue engineering leading to the development of several ES cell differentiation approaches. Previous research had already suggested that individual transcription factors, when deleted or overexpressed, could induce cell fate alterations in somatic cells. For instance, an overexpression of the transcription factor MyoD (protein that plays a major role in regulating muscle differentiation) has been shown to facilitate the conversion of fibroblasts to myogenic cells (Davis, Weintraub and Lassar, 1987). It was also demonstrated that mouse B-cells were reprogrammed into progenitors, resulting in a hematopoietic lineage following the removal of Pax5 (Busslinger et al., 1999). In the case of ESCs, transcription factors can lead to segregation into a certain lineage. Takahashi et al. were able to produce human IPSCs directly from human dermal fibroblasts (HDFs) in 2007 (Takahashi et al., 2007). These HDFs were then transduced with retroviruses that contained human SOX2, OCT4, KLF4 as well as c-MYC. However Yu et al. was keen to evade the usage of oncogene c-Myc, they attempted to trace other factors for the purposes of reprogramming human cells (Yu et al., 2007). At day 30, human ES-like colonies became disaggregated and expanded onto SNL feeder cells, causing the establishment of flat colonies of cells that had a morphology similar to that of human ESCs. Many similarities have been found between human ESCs and human IPSCs, such as ESC-specific promoter activity, surface marker expression, in *vitro* differentiation, telomerase activity and pro-

liferation, as along with teratoma formation. However, DNA microarray analyses have indicated that while gene expression profiles are similar, they are not exactly the same for human ESCs and IPSCs (Takahashi, Tanabe et al. 2007).

Based on the prmise that human ESCs are capable of reprogramming myeloid precursors via cell fusion (Yu et al., 2006), a list of genes was prepared that constituted a component of pluripotency, enriching expression in human ESCs as opposed to the expression observed in myeloid precursors. Four genes - SOX2, OCT4, NANOG 18 and LIN28 - from the original set of 14 genes were identified as candidates to reprogram human somatic cells into human IPSCs (Yu et al., 2007). The removal of either SOX2 or OCT4 from this set did not lead to the emergence of any ES-like colonies, while the elimination of LIN28 or NANOG was not seen to be important in the formation of ES-like colonies, although it did manage to improve the efficacy of the entire reprogramming process. These human IPSCs created by the transduction of foetal and new-born foreskin fibroblasts through this particular set of transcription factors featured telomerase activity, normal karyotypes, expression of ESC surface markers, as well as genes characterising ESCs, exhibiting a comparable methylation pattern to human ESCs and formation of all three germ layers in teratomas (Guenther et al., 2010).

Due to their importance as a great source of cell properties, human pluripotent stem cells (PSCs) are very promising for cell-based therapies, drug discovery, disease modelling, and pharmaceutical applications (Daley, 2012; Engle and Puppala, 2013) (Figure 2.3).

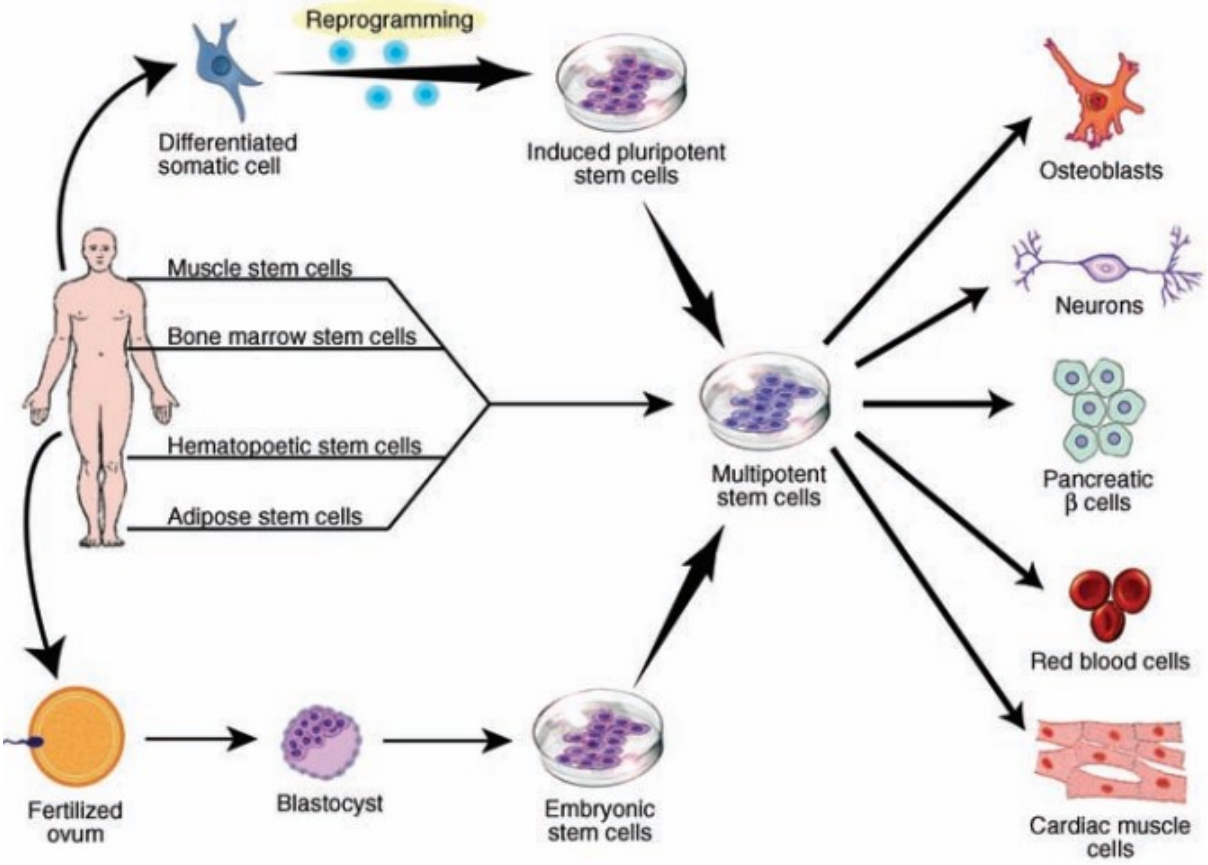


Figure 2.3 Isolation/differentiation of stem cells for the purpose of tissue engineering and regenerative medicine.
It is possible to derive multipotent stem cells directly from numerous human tissues, including, blood, bone marrow, muscle as well as adipose tissue. Meanwhile pluripotent stem cells can also be obtained from the blastocyst's inner cell mass or reprogramming cells that were previously segregated to a pluripotent state by utilising specific factors (such as induced pluripotent stem cells). Multipotent stem cells can be differentiated into many different types of cells and only a few are displayed here (source :Bean & Tuan, 2013).

There have been many attempts to develop new methods for cultivating human PSC cultures to meet the growing demands in regenerative medicine and drug discovery, since maintaining a high-quality of human PSCs is critical for their subsequent applications. However, in spite of the rapid progress made in developing new human PSC culture methods, there are still many challenges which need to be addressed in future application processes. These challenges include: (1) a lack of standardized protocols for specific applications; (2) an absence of efficient assays to monitor cellular stress induced by suboptimal

growth conditions and excessive apoptotic and spontaneous differentiation signals during cell processing; and (3) the impurity or heterogeneity of propagated cells (Serra et al., 2012; Stewart et al., 2006).

2.2.2. Maintain (human PSCs) in vitro

Research has already shown that unlike mouse embryonic stem cells (mouse ESCs), which rely on BMP-4 and Stat3 in the presence of leukemia inhibitory factor (LIF) for self-renewal (Ying et al., 2003), both human ESCs and IPSCs depend on cooperation between different signalling pathways that are related to basic fibroblast growth factor (FGF-2), Noggin, Activin/Nodal, and TGF-β pathways (James et al., 2005; Vallier et al., 2005; Wang et al., 2005; Xiao et al., 2006; Xu et al., 2005). Thus, the pluripotent state of mouse ESCs and human PSCs are quite different, with mouse ESCs and human PSCs being described as representing naive and primed pluripotent states, respectively (Nichols and Smith, 2009; Ying et al., 2008). Generally, mouse ESCs can passage and grow as single cells, whereas human PSCs when detached as single cells experience a drastic loss of viability (Claassen, Desler and Rizzino, 2009). Thus, human PSCs are normally cultured as clusters and grow as colonies and aggregates. Therefore, different culture methods are required to support the growth of murine ESCs and human PSCs *in-vitro* (Schnerch, Cerdan and Bhatia, 2010).

2.2.2.1 Growth Medium for (human PSCs) Culture

The culture medium formulation is one of the most critical components of human PSC cultures, and it has undergone significant evolution since the first used of those cells (Thomson et al., 1998). The goal for the therapeutic use of human PSC is to develop a serum-free, xeno-free, and chemically defined medium, suitable for growing almost all types of human PSC lines. The first attempts to culture human ESC relied on media formulations containing fetal bovine serum (FBS) and undefined/conditioned secretory components from mouse embryonic fibroblasts (MEFs). Since then, scientists have established more standardized and better-defined formulations to replace xenogeneic elements (Genbacev et al., 2005; Li et al., 2005). A chemically defined medium with Activin A, Nodal, and FGF-2 was used to propagate human ESCs (Vallier et al., 2005). The Knockout Serum Replacement (KSR) medium supplemented with FGF-2 is also widely used

with to support feeder-based human PSC culture, and the TeSR1 defined culture medium containing FGF-2, lithium chloride (LiCl), γ-aminobutyric acid (GABA), TGF-β, pipeolic acid, serum albumin and β-mercaptoethanol was developed by Thomson and colleagues for use in feeder-free conditions (Levenstein, et al., 2006). More recently, Thomson and co-workers developed the chemically defined E8 medium, a derivative of TeSR1 containing eight components apart from serum albumin and β-mercaptoethanol. The uses of E8 medium has improved the culturing of human IPSC and human ESC lines, leading to greater improvement in episomal vector-based reprogramming effectiveness and experimental consistency in human IPSCs (Xu et al., 2002; Chen et al., 2010).

2.2.2.2 Extracellular Matrix (ECM)

Various extracellular matrix (ECM) proteins regulate and support human PSC self-renewal or lineage commitment (Bram et al., 2008c; Rodin et al., 2010; Xu et al., 2001). Vitronectin; an ECM protein, has been identified as an important substrate to sustain the self-renewal of human ESCs via adhesion of αVβ5 integrin (Braam et al., 2008c). Substantial evidence exists in support of the impact of specific laminin isoforms on sustaining long-term human PSCs growth. Through plating human PSCs cell clumps on coated human recombinant laminin-511 cell culture dishes, researchers found that single laminin isoform maintains self-renewal of human PSCs for more than 20 passages. This protocol uses a single undefined component and is free from animal products and feeder cells. This protocol can also produce unified human PSCs that potentially suit future therapeutic use (Domogatskaya, Rodin and Tryggvason, 2012). However, the use of laminin for human PSCs maintenance and expansion is, unfortunately, limited at the current state due to the high cost of obtaining it at a high purity. New methods are in development to stimulate the impact of ECM proteins on the growth of human PSCs.

2.2.2.3 Environmental Indications

There are a number of environmental factors that promote human PSCs growth, such as temperature, humidity, rigidity of growth surfaces, cell density, oxygen tension, and modes of multicellular associations (Chen et al., 2014).

For instance, the development of human embryos occurs in a hypoxic environment (Sharp and McKay, 2013a). Therefore, mimicking these conditions is a promising approach in culturing human ESCs. It has been shown that low O_2 tension (~2%–3% O_2) plays a crucial role in maintaining cells self-renewal and differentiation states (Catherine E Forristal *et al.*, 2010a) . However, conventional human ESCs culture has traditionally been done under normoxia (i.e., 21% O_2).

2.2.2.3.1 Hypoxia

Molecular oxygen serves as a metabolic substrate as well as a signalling molecule for cells both *in-vitro* and *in-vivo*. Tissues and cells respond to low O_2 concentrations, known as hypoxia, through the hypoxic response (Raval et al., 2005). Its impact on stem cell differentiation, self-renewal, and ultimately function in-*vitro* is not entirely understood, however, primarily because of the fact that this signal differential effects are cell type and oxygen concentrations-dependent.

In the case of mammals, this hypoxic response signalling pathway is activated by hypoxia-inducible factors (HIFs), which catalyse a series of transcriptional events that result in increased protein levels, as seen for VEGF and erythropoietin (Semenza and Wang, 1992; Levy et al., 1995). Hypoxia-responsive gene products improve survival rates in low O_2 conditions by stimulating O_2 diffusion into the cell and modifying the pathways of intracellular metabolism. The regulation of the hypoxic response happens to be a heavily regulated process. The HIFs include HIF-α (HIF-1α, HIF-2 α or HIF-3 α) and HIF- β (ARNT [HIF-1β], ARNT2 [HIF-2β], or ARNT3 [HIF-3 β]) subunits. Though HIF-1α is believed to feature mainly in the adaptation of cells to hypoxia during the initial stages of hypoxia, both HIF-2α and HIF-3α are known to be linked to stabilise longer responses (Forristal et al., 2010a). Under normal physiological conditions, these HIF subunits are degraded in an O_2-dependent process (Foxler et al., 2012). Furthermore, under hypoxic conditions, HIF-□ becomes stabilised and is capable of translocating into the nucleus where it activates downstream targets that contain singular or multiple hypoxic response element (HRE) within their promoter regions of HIF1 target. HIF-1□ is ubiquitously expressed and is regarded as the most frequent signal transducer of acute hypoxic responses (Raval et al., 2005). Both HIF-2α and HIF-3α are expressed in a tissue-specific manner whereby they outcompete HIF-1α in binding to HIF-1α, either by activating alternative downstream targets (HIF-2α) (Raval et al., 2005) or splaying the role of splice variants with

dominant-negative characteristics (HIF-3 α) (Heikkilä et al., 2011). While mammalian cell culture O_2 levels are approximately 21%, physiological O_2 concentrations are tissue-specific and lie within the range of 3 to 5% (Csete, 2005). Over the past decade, low oxygen levels (typically < 5%) have been found to correlate with stem cell niches in embryos and adult organs. A reduction in oxygen concentration causes slow cycling and self-renewal of cells while preventing long-term DNA damage induced by reactive oxygen species (ROS). Another evidence of the adaptation of stem cells to hypoxic environments is their less abundant and less active mitochondria compared to differentiated cells (Romero-Moya et al., 2013).

2.2.2.3.1.1 Hypoxia role in pluripotency:

Research on the role of hypoxia in the context of embryogenesis has pronounced implications for the manner in which pluripotent stem cells are maintained undifferentiated *in vitro* (Forristal et al., 2010b). Pluripotent stem cells include human ESCs and the recently derived human IPSCs. Based on culture conditions, these cells will either maintain pluripotency or be segregated into various cell types from all the three germ layers mentioned before (Thomson et al., 1998). Thus, pluripotent stem cells hold the promise of being utilised in cell-based therapeutic strategies.

There is also increasing evidence that environmental O_2 concentrations are suboptimal in the context of human ESC cultures. Human ESCs have been observed to expand at a faster rate when they are cultured in low O_2 conditions – thus mimicking in utero conditions (5% O_2) – as opposed normoxic conditions (Forristal et al., 2010a). Additionally, significant hikes in expression of OCT4, SOX-2, and NANOG have been found at the mRNA as well as protein levels as O_2 concentrations are lowered. Mechanistically, both HIF-2α and HIF-3α, but not HIF-1α, were demonstrated to upregulate the expression of the above genes (Forristal et al., 2010b) (Figure 2.4). HIF-2 α has been additionally observed to impact the cellular morphology, with a loss of HIF-2 α resulting in huge areas of differentiation within ESCs colonies (C. E Forristal et al., 2010a). Analogously, Ezashi et al. showed that differentiation introduced by knockout of OCT-4 and SSEA-4, was reduced under O_2 concentrations of 5% (or lower) versus 21% (Ezashi, Das and Roberts, 2005).

The positive effect of hypoxia on pluripotency, as seen in numerous studies, is best explained by showing that SOX-2, OCT-4 and NANOG regulation by HIF-2 (Ji et al., 2009;

Moreno-Manzano et al., 2010; Forristal et al., 2013). HIF-2α binds the promoter of OCT-4 directly via chromatin immunoprecipitation, induced its expression at lower than 1.5% O_2 in renal clear cell carcinoma cells as well as 293T human embryonic kidney cells (Covello et al., 2006). In a similar manner, Moreno-Manzano et al. identified a HIF-2 binding site within the Sox-2 promoter, demonstrating that the element of binding rises after being exposed to 1% O_2 (Moreno-Manzano et al., 2010). Additionally, the expression of NANOG was demonstrated to be much lower after HIF-2α inhibition (Forristal et al., 2013), thereby demonstrating that hypoxia does support pluripotency through numerous mechanisms (Figure 2.4).

Mouse ESCs on the other hand, have been observed to lose pluripotency after being exposed to 1% O_2 (Jeong et al., 2007), apart from experiencing reduced proliferation and cell viability upon exposure to 2% O_2 (Fernandes et al., 2010). This disparity could be interpreted through the involvement of different signalling pathways for maintaining pluripotency between these two species. This hypothesis is corroborated by HIF-1α -induced LIF receptor downregulation (Jeong et al., 2007). Human ESCs are not thought to be impacted by this as LIF signalling has been found to be non-essential for human ESC pluripotency.

Despite the many advances with IPSCs reprogramming technology over the past few years, the rates of derivation continue to be not efficient. Thus, certain research groups are exploring the role of hypoxia in enhancing the reprogramming process. Within this area, initial findings have merited much promise. For instance, four days of hypoxic treatment led to a fourfold increase in the number of NANOG–GFP-positive cells and hypoxia-treated human IPSCs met all of the pluripotent cell criteria while possessing a normal karyotype (Yoshida et al., 2009a). Hypoxia exposure has also expedited the reprogramming of stem cells derived from adipose tissue thereby obtaining stable pluripotent iPSC lines (Shimada et al., 2012). Not much is known about the mechanisms through which hypoxia improves iPSC reprogramming efficiency (Yoshida et al., 2009b). That being said, similar mechanisms are expected to explain pluripotency support in human ESCs (Yoshida et al., 2009b). The transition from somatic mitochondrial oxidative metabolism into anaerobic glycolysis is needed for successfully reprogramming as it is known that pluripotent stem cells utilise anaerobic glycolysis as an alternative to oxidative phosphorylation (Folmes et al., 2011; Folmes et al., 2012; Prigione et al., 2010).

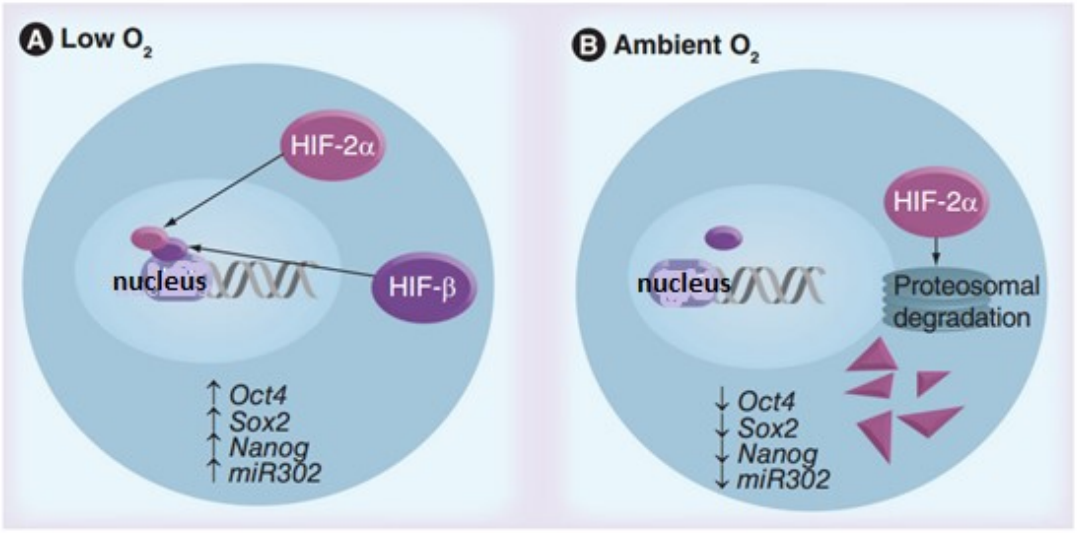


Figure 2.4. The role of HIF-2α in pluripotency.
(A) Under low O_2 conditions, HIF-2α translocates into the nucleus and heterodimerises with HIF-1α thus upregulating pluripotency-associated gene expression. (B) Under ambient O_2 conditions, HIF-2α undergoes proteosomal degradation, therefore preventing it from upregulating pluripotency-associated factors (adapted from Alvarez-Tejado et al., 2001).

2. 2.2.3.1.2 Stem cell differentiation under hypoxic conditions

Hypoxia plays an additional important role in cell-fate specification. Embryoid bodies are three-dimensional aggregates of pluripotent stem cells developed in *vitro*. Interestingly, a higher number of these structures could be generated under low O_2 conditions. The embryoid bodies formed in these conditions showed a heightened potential for outgrowth and attachment (Ezashi, Das and Roberts, 2005). In addition, low O_2 tensions have been demonstrated to promulgate differentiation into specific cell lineages, thereby indicating that O_2 levels could be manipulated to induce differentiation in cell-orientated therapeutic strategies. Meanwhile low O_2 tensions (<5%) have promoted mouse ESC differentiation into the vascular (Lee et al., 2012) and endothelial (Ramírez-Bergeron et al., 2004) lineages, as well as human ESC differentiation into cardiomyocytes (Niebruegge et al., 2009), endothelial cells (Prado-Lopez et al., 2010), retinal progenitor cells (Yoshida et al., 2009a) and chondrocytes (Koay and Athanasiou, 2008). Similar phenomena are expected to take place *in vivo*. For instance, the formation of the cardiovascular system occurs under hypoxic conditions (Simon et al., 2008). The exposure to 10% O_2 (or lower) has been demonstrated to promote the expansion of neural stem cells (Zhao et al., 2008; Rodrigues et al., 2010) as well as neural differentiation in mouse (Fernandes et al., 2010) and human (Francis and Wei, 2010b) ESCs. Additionally, many studies have shown that

culture under 3% oxygen leads to a rise in the number of dopaminergic neurons derived from neural progenitor cells (Studer et al., 2000; Kim et al., 2008). A more recent study has shown that using human ESCs and IPSCs cultured under 5% oxygen concentration lead to better formation of embryoid bodies and enhance the capacity to differentiate into mature lung epithelial cells as human IPSCs are more affected by oxygen variations (Francis and Wei, 2010a). It has been recently confirmed that oxygen plays a positive role in promoting stem cell differentiation towards lung phenotypes (Studer et al., 2000), these results highlight the importance of considering the effect of factors such as O_2 concentrations on cell fate. Although hypoxia showed a positive impact on the differentiation into some lineages, for others it was shown to have a negative impact: for example, adipocyte differentiation has been hindered by reduced O_2 concentrations (0.1–2%) in the case of 3T3 L1 preadipocytes (Yun et al., 2002).

2.2.2.4 Addition of anti-apoptotic agents to enhance survival

Human PSCs are subject to apoptosis upon cellular subculture and dissociation (K Watanabe et al., 2007). Complete dissociation of human PSCs leads to significant cell death and poor cloning efficiency (Zhang et al., 2011). Thus, it is infeasible to use human PSCs in differentiation induction and scalable suspension culture.

A strong inhibitor of ROCK1 and ROCK2 (Y27632, known as ROCKi) was used to enhance survival of dissociated human PSCs into single cells (Watanabe et al., 2007). ROCK signalling was initially discovered as a downstream target of the small GTP-binding protein Rho (Watanabe et al., 2007; Yoshida et al., 2009a) which is involved in the regulation of cellular growth, adhesion, migration, metabolism, and apoptosis through control of the actin cytoskeletal assembly and cell contraction (Watanabe et al., 2007; Yoshida et al., 2009a). ROCK mediates membrane blebbing, develops actin–myosin contraction and triggers caspase signalling cascades and, hence, cellular apoptosis. (Shi and Wei, 2007)

ROCKi is utilised in many survival pathways in *vitro* as well as in-*vivo*. In addition, ROCKi reported to preserve the integrity of both unfrozen and frozen human ESCs (Emre et al., 2010). It has also been demonstrated that ROCKi promotes the recovery of frozen-thawed human ESCs as well as human IPSCs. Another recent study also highlighted the influence

of this inhibitor on increasing cell numbers while promulgating cell survival after dissociation into single cells, and also playing a key role in maintaining the pluripotency of human ESCs (Watanabe et al., 2007).

2.3 3D Matrices

Challenges pertaining to the cellular facets of an engineered tissue include cell sourcing, expansion and differentiation, production and regulatory issues, such as safety, sterility, shipping, storage, quality control and scale-up (Naughton, 2001). Other challenges are related to the biomaterial used for scaffolds used to produce these cells and support both differentiation and tissue growth. These biomaterials are required to fulfil numerous criteria in order to maximise the possibility of a successful repair, including biocompatibility and biodegradability, promotion of tissue growth and appropriate biomechanical properties (Freed and Vunjak-Novakovic, 1995).

2.3.1 ALGINATE HYDROGEL

Numerous researchers have tested the alginate and agarose hydrogels as scaffolds for chondrocytes for the purpose of regenerating cartilage tissue (Buschmann et al., 1995; Paige et al., 1996; Fragonas et al., 2000; Mauck et al., 2000; Chang et al., 2001). Within the hydrogel biomaterials, alginate and agarose are usually considered to be inert as they experience a dearth of native ligands that may allow for the engagement with mammalian cells (Chang et al., 2001).

Hydrogels have been increasingly studied as matrices for the purpose of tissue engineering (Lee and Mooney, 2012). Hydrogels are typically designed to feature pores that are big enough to house living cells or releasing growth factors. A key advantage of hydrogels in the context of tissue engineering matrices is their ability of establishing covalent or hydrophobic bonds to cell membrane peptide ligands so as to stimulate adhesion and cell growth in the hydrogel matrix. Their drawback is the lack of low mechanical strength, which leads to handling difficulties (Lee and Mooney, 2001). Alginate refers to a collective term denoting a family of polysaccharides that are produced by brown algae as well as bacteria (Govan, Fyfe and Jarman, 1981). They denote (linear) co-polymers of 4-linked L-guluronic acid (G) and β-D-mannuronic acid (M) – arranged in a specific block-wise pattern in addition to a chain of homopolymeric regions of G (G blocks) and M (M blocks) and residues which are interspersed within the areas of alternating structure (MG blocks)

(Figure 2.5). Along its biosynthetic pathway, alginate gets produced through a post-polymerization reaction that involves a C-5 inversion on the mannuronan M residues. The reaction gets facilitated by mannuronan C-5 epimerases. As all natural alginates get produced from homopolymeric mannuronate through the basic C-5 inversion from G, the variability in composition and sequence traced in the polysaccharide is primarily due to the diverse catalytic properties of the numerous epimerases (Høidal et al., 1999; Strand et al., 2003). Arguably, the most pertinent deployment of alginate in the field of biotechnology field is linked with its ability to generate stable gels upon contact with divalent cations like calcium. Alginate's ionotropic gelation has been illustrated on the basis of X-ray fibre-diffraction data that is sourced from dehydrated specimens (Atkins,1973a; Atkins, 1973b) by leveraging the "egg-box" model (Figure 2.5) (Grant et al., 1973; Morris et al., 1978). This model states that chain-chain associations get induced through the presence of calcium, leading to the formation of junction zones between the 2/1 helical chains of G sequences which present cavities suitable enough for the purpose of accommodating divalent cations.

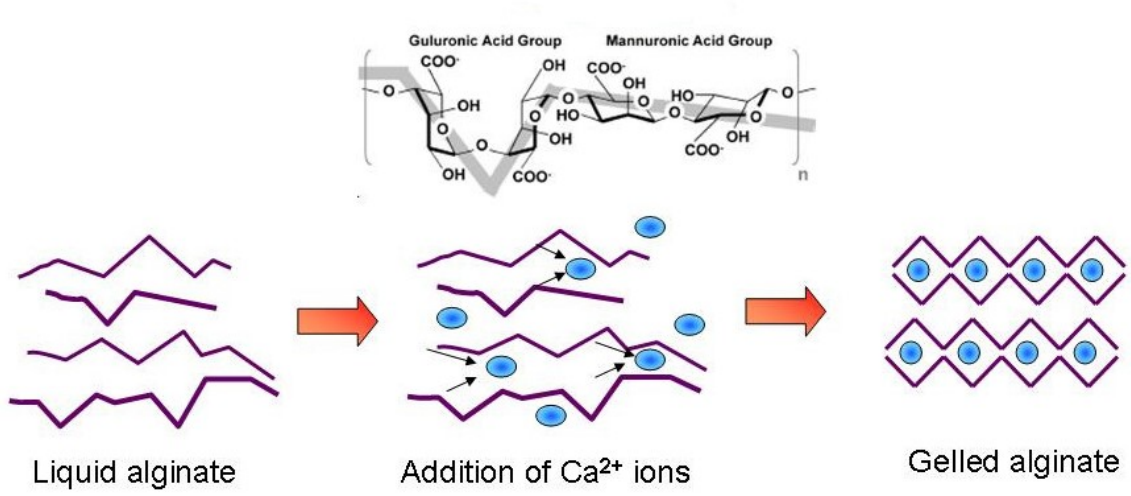


Figure 2.5. Alginate is a polysaccharide co-polymer comprised of guluronic as well as mannuronic acid groups.
The calcium is ionically substituted at the carboxylic site in the presence of divalent calcium ions. A second alginate strand is also capable of connecting the calcium ion, generating a link whereby the calcium ion attaches to two alginate strands. The result is in the form of a chain of calcium-linked alginate strands forming a solid gel (egg-box model) (Modife Bienaimé, Barbotin, and Nava-Saucedo, 2003).

2.3.2 Cell encapsulation

Encapsulation of animal cells in alginate hydrogels has been attempted for a range of cell types (Tyler, 1990; Sun, 1997; Chang et al., 2001). The immobilization of ES cell into these gels coupled with their proliferation should lead to the formation of a number of isolated ES cell aggregates and subsequently, embryoid bodies (EBs) which can then potentially differentiate into the cells of all the three germ layers. The number of EBs that can be generated via this technology cannot be attained using any other existing method. These encapsulated ES cells are capable of growing as small colonies in the beads and pave the way for morula- and blastula-like structures. The ability of generating huge numbers of EBs by means of encapsulation makes EBs a potential *in-vitro* source of organs in the context of tissue engineering approaches. The differentiated EBs can get released easily from the beads under Ca2+ depletion (Magyar et al., 2001). Murine ESC colonies can be differentiated into cystic EBs using cardiomyocytes upon release from 1.6% alginate microbeads (Magyar et al. 2001). Production human EBs in dynamic culture by leveraging a rotating cell-culture system has also been achieved using alginate hydrogels Gerecht-Nir et al., (2004a). The STLV (slow turning lateral vessel) of a specific bioreactor boosts the formation as well as differentiation of human EBs significantly, as against traditional Petri dishes. The studies demonstrated that controlling cell aggregation through the manipulation of human EBs turned out to be a more efficacious and higher-yield strategy for expanding human EBs with improved differentiation capabilities (Gerecht-Nir et al., 2004). The authors subsequently demonstrated the setting up of human EBs in 3D porous alginate scaffolds Gerecht-Nir et al., 2004b. The restricted environments of alginate scaffold pores allowed for an effective formation of EBs using a comparatively high degree of cell proliferation as well as differentiation and induced vasculogenesis in the EBs to a more significant extent than rotating or static cultures capabilities (Gerecht-Nir et al., 2004) . Alginate scaffolds feature macromolecular structures that resemble the extracellular matrix. Their hydrogel nature allows for efficient cell seeding as well as tissue engineering (Shapiro and Cohen, 1997; Leor et al., 2000; Zmora, Glicklis and Cohen, 2002). The alginate scaffolds' porosity can then be controlled during the course of fabrication, resulting in sponge-like material at > 90% porosity. This connected the pore structures as well as sizes ranging between 50 and 200 μm in diameter (Zmora, Glicklis and Cohen, 2002). Encapsulation of high numbers of human as well as mouse ESCs is a pragmatic

method to control cell-aggregation in *vitro* (Dang et al., 2004). The authors suggested that the encapsulation of ES cells was important for efficacious cell proliferation, EB formation as well as segregation in the case of stirred-suspension bioreactors. The ability of accurately measuring and controlling culture conditions in stirred-suspension bioreactors will prove to be a valuable tool in optimizing the delivery profiles of exogenous factors impacting ESC differentiation (Dang et al., 2004). Although alginate encapsulation has been described over 20 years ago (Lim and Sun, 1980), the existing study accounts for the initial application of this technology to human ES cells as well as the derivation of distal epithelial lung cells through a bioreactor for the purpose of less labour-augmenting.

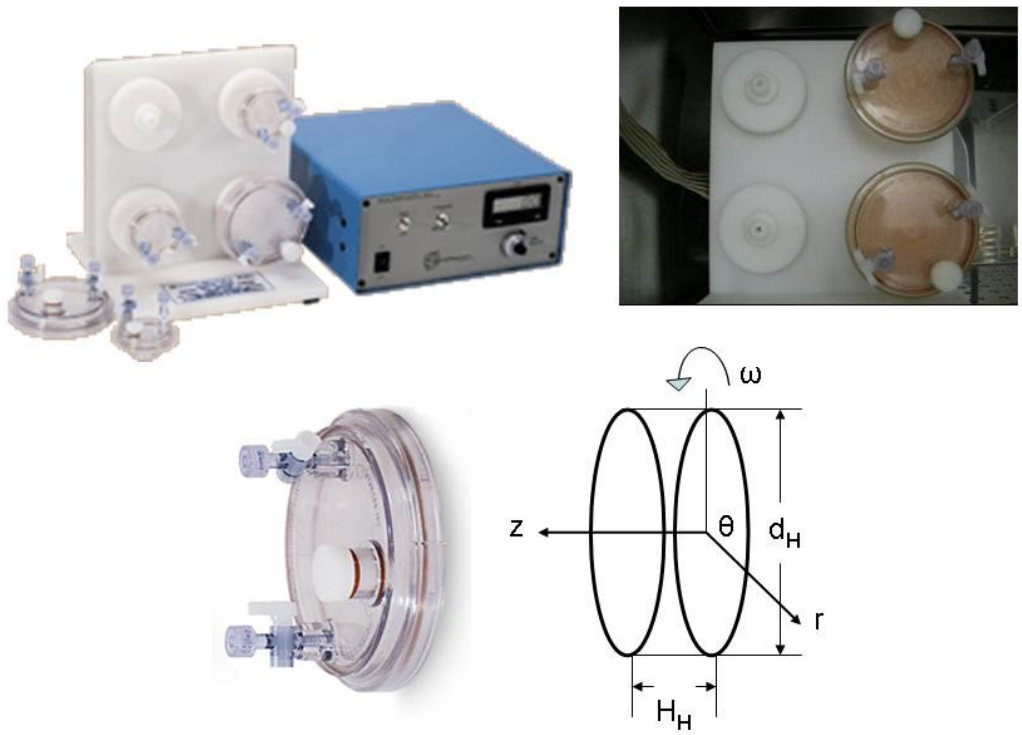


Figure 2.6 HARV bioreactor.
A scheme showing the co-ordinated system of the HARV. A 50ml vessel rotated at its horizontal Z axis at w rpm. The HARV is a vessel of diameter dH ~ 10cm and height H_H ~ 0.64 cm and w filled with 50ml solution (Source: Gao, Ayyaswamy, Ducheyne, and Radin, 2001).

2.4 Bioreactors for the purpose of tissue engineering

Culturing cells in static conditions has some limitations, one of which is mass transfer which is limited to passive diffusion of the soluble factors throughout the culture media (Placzek et al., 2009). An examination of the oxygen levels in the gas and liquid phases of murine hybridoma cultures showed that due to microscale mixing, the O_2 transfer through the liquid under standard laboratory conditions had exceed what was predicted by passive diffusion. However, they also found that the level of O_2 at the bottom of the flasks had reached zero (Randers-Eichhorn et al., 1996), suggesting that the use of static vessels in culturing PSCs was no longer suitable, especially in a 3D cultured system due to the fast rate of cell growth. Additionally, the development of heterogeneous cultures may lead to cell differentiation or gain of an anomalous karyotype as a result of low mass transport of nutrient and oxygen in static culture (Azarin and Palecek, 2010). Consequently, to reduce these limitations, while simultaneously scale-up cell cultures, there is a need to create a dynamic environment that can overcome the limitations of traditional culture.

To improve mass transport and gas exchange, many bioreactor designs have been developed for industrial human PSC cultures. For example, the stirred suspension and rotating wall vessel (RWV) bioreactor configurations are the most widely used. There have been some successes in the use of RWV bioreactors vessels to culture embryoid bodies; and in the use of hydrogels or aggregates to culture Human PSCs cells in 3D environment. Stirred suspension bioreactors normally operate at 30-60 rpm, resulting in high levels of shear stress in suspended PSCs cultures (Rodrigues et al., 2011; Placzek et al., 2009). In contrast to RWV, bioreactors which have higher aspect ratios (HARV) or slow turning lateral vessel (STLV) geometries reduce the level of shear stress in PSC suspension cultures (Placzek et al., 2009; Hwang et al., 2009).

The potential effects of different hydrodynamic and other bioreactor conditions on stem cell cultures were analysed and it has been found that bioreactor hydrodynamics negatively impacts the scaling up of human PSC cultures due to changes in the size, yield, kinetics and homogeneity of spheroids (Kinney et al., 2011). Consequently, PSCs cultures have shown variable rates of expansion, viability, and metabolic activity (Kinney et al., 2011). Additionally, at greater speeds, there appears to be some differentiation in human

ESC IMR 90 phenotype lines when rotated at 100-120 rpm due mainly to the effects of shear stress. Although, sheer stress was reduced, this did not affect spontaneous differentiation as it was later found that the forceful movement of the culture vessel affected the distribution of soluble factors (Leung et al., 2011).

Furthermore, it has been suggested that mouse ESC differentiates along the hematopoietic lineage while being cultured on polymeric scaffolds (Roy et al., 2011). In comparison with a 3D static system, ECM production, cellular adhesion and elevation in gene transcription increased in dynamic cultures (Roy et al., 2011). The above findings are further supported by the occurrence of BMP-4 expression only in the case of dynamic cultures (Roy et al., 2011). The aforementioned results are in support of the dynamic simulation of a microenvironment that induces hematopoietic lineage by hydrodynamics of spinner flask cultures (Liu et al., 2006). Further investigations of mouse ESC in bioreactors with distinctive hydrodynamic properties suggest Sca-1+ cells increase. Hence, this suggests presence of stem and progenitor cell types while the production of c-Kit+ endothelial cells in rotator flask cultures. This is consistent with the literature suggesting that hydrodynamics of a cell culture has the ability of manipulating the fate of PSCs (Fridley et al., 2010).

2.5 Tissue engineering of the lung

Most of the studies regarding tissue regulation and cell biology are tested in 2D cell-culture models. Though 2D-cell culture models are valuable in providing inputs that address certain scientific questions, they are not suitable for the replication of in-*vivo* cellular microenvironments. Hence, 3D cell cultures became more appropriate for depicting realistic organ-specific micro-architecture. 3D cell-culture models proved to be useful in drug screening and treating patient-specific diseases (Xu et al., 2013).

Strategies for tissue engineering require the use of specific scaffolds with suitable cell sources, cell signals and culture systems that promote the integration of proper tissues and vascularization in order to create functional transplantable organs. Lung tissue engineering comes with the aim of generating constructs that are able to provide gas ex-

change for restoring and at times replacing dysfunctional lungs. In this context, many attempts have been made for reconstructing structures that resemble the alveolus, known as the lung's unit of function as well as complete lung replacement (Petersen et al., 2010).

2.5.1 Tissue engineering of functional unit of the lung

In-vitro reconstruction has been applied to alveolar like cystic structures when a mixture of fetal lung cells (FLCs) were cultivated with 3D matrixes such as gelatin gel, collagen gel, Gelfoam and Matrigel™. 3D cultures of rat FLCs on gelatin sponge discs with the correct supplementation of growth factors has been proved to drive re-aggregation of previously disaggregated cells and form alveolar-like cystic structures with in *vitro* extended maintenance of epithelial cell differentiation (Douglas, Moorman and Teel, 1976). Furthermore, porous collagen type I chondroitin-6-sulfate scaffolds were proved to support the formation of alveolar-like structures by rat FLCs in-*vitro* (Chen et al., 2005). Mondrinos et al. (2006) suggested that the formation of lumen containing cystic epithelial structures by mouse FLCs were supported by Matrigel™ in combination with serum-free medium with no need of any exogenous factors (Mondrinos et al., 2006). Furthermore, the formation of alveolar-like cystic structures has been demonstrated by 3D culture of rat FLCs in Gelfoam, a gelatin based porous sponge (Andrade et al., 2006; Mondrinos et al., 2006).

The engraftment of the alveolar-like structures in lung parenchyma of adult rate has been observed. Low levels of local inflammatory response have been reported alongside the presence of graft derived epithelial and endothelial cells, in addition to neovascularization within Gelfoam. However, no causality has established between the effect of 3D cultures of adult lung cells and the formation of alveolar-like cystic structures. Alveolar-like constructs have the potential for regeneration in-*vivo* which is relevant since adult lung cells are insufficient for tissue re-engineering (Andrade et al. 2006). The formation of terminal airways cystic structures has been demonstrated by these studies (Andrade et al., 2006; Mondrinos et al., 2006). However, no branching morphogenesis, which is an essential key developmental stage during lung development, had occurred. The reconstruction of branching epithelial structures resembling early saccular stage has been documented in lung development when seeded 3D hydrogel scaffold FLCs were stimulated with FGFs 10, 7 and 2. Stimulation of branching morphogenesis occurred through Matrigel™ supplemented with FDFs 10, 7 and 2 in serum-free media (Mondrinos et al., 2006). This is

indicative of the budding and sacculation of epithelial structures by FLCs of mice. Consequently, simple collagen type 1 hydrogels in conjunction with the exact combination of FDFs supports extensive epithelial budding, sacculation and the formation of robust endothelial network (Mondrinos et al., 2006). Another observation from their studies shows interfacing between epithelial alveolar forming units with capillary-like tubes and continuous lumens.

In addition, with the use of the Matrigel™ model, in-*vivo* generation of vascularized lung tissues has been demonstrated (Mondrinos et al., 2008). Graft-derived endothelial cells were found to contribute to the formation of perfused vessels had anastomosed with the host vasculature in *vivo* when FLCs seeded on Matrigel™ were grafted subcutaneously (Mondrinos et al., 2008). Here, we can note that only a mixture of fetal lung cells is feasible for the engineering and regeneration of lung tissue. Nonetheless, FLCs utilization is considered as a significant limitation of this strategy. Hence, a more sophisticated approach taking lung epithelial cells instead of fetal cells is required. A 3D co-culture model where basal-like airway epithelial cell line (VA10) and endothelial cells in Matrigel™ were co-cultured for conceptual proof has been tested providing cells with a phenotype similar to airway epithelial-basal cells where self-renewal and generation of daughter cells is possible (Franzdóttir et al., 2010). Hence, these are suggested as candidate stem cells of airway epithelium (Franzdóttir et al., 2010). In elegance, the authors reported the complex formation of epithelial branching structures reminiscent of those of an early saccular stage of lung development. Nevertheless, these studies do not demonstrate functionality of ventilation and gas exchange in engineered lung constructs. In order to address this issue, a complete replication of the lung is needed.

2.5.2 Tissue engineering of whole lung

A novel paradigm in lung tissue engineering emerged with use of a decellularized lung produced using methods which effectively remove the native cell population while preserving the 3D complex geometric structure and extracellular matrix composition of the lung tissue. In the first study conducted using these techniques, decellularized rat lungs were repopulated with neonatal rat lung cells and microvascular endothelial cells of the lung. Upon implantation, the recellularized lungs displayed gas exchange and vascular perfusion but only for short periods of time (<120 minutes) (Petersen et al., 2010). Im-

provements of the *in-vivo* function of tissue-engineered lungs were obtained when decellularized rat lungs were later recellularized with rat FLCs and human endothelial cells (Song et al., 2011). Constructs were cultured under dynamic conditions in biomimetic bioreactors for a period of 7 days prior to implantation (Song et al., 2011). Gas exchange could be observed in the engineered lungs for up to 2 weeks post-implantation. Many studies utilize neonatal or fetal lung cells in recellularization. However, this approach is not suitable for clinical use due to incompatibility or immunological complication. Hence, recellularization of decellularized lungs has been attempted with PSCs. The pre-differentiation of murine ESCs with surfactant protein C, produced AEII like cells that were seeded into decellularized mouse lungs (Jensen et al., 2012). Differentiated AEII cells maintained proSPC expressing phenotype as well as vascularization has been observed when the constructs were engrafted subcutaneously (Jensen et al., 2012).

A similar experiment has been conducted where decellularized mouse lungs were seeded with lung progenitor cells derived from several-stage differentiation of mouse ESCs (Longmire et al., 2012). First, the authors differentiated mouse ESCs into the definitive endodermal lineage and later into TTF1 expressing lung progenitor cells. During decellularized lung scaffolds seeding, lung progenitor cells repopulated alveolar regions of the lung and adopted morphologies and protein expressions that indicate type I and type II alveolar epithelial cell differentiation. Such studies illustrate a proof of concept for the potential use of PSCs for recellularization of decellularized lungs. Until now, the representation of 'state of the art' lung tissue engineering is evident by the approach combining decellularized lung scaffolds with ES derived lung epithelial cells. Various protocols were established in order to derive long epithelial lineages from ES cells (Longmire et al., 2012).

Nonetheless, such protocols showed no success in differentiating lung epithelial cells in an efficient manner. Hence, differentiated cells can be contaminated with pluripotent cells. For the feasibility of lung tissue engineering, a sufficient number of lung lineage specific cells has to be obtained in-*vitro* in order to regenerate and reconstruct tissues. The aim of this thesis is to address this need by identifying alternative regulatory factors that are able of improving ES cell differentiation into definitive endoderm and lung epithelial lineages.

Chapter 3

Aim and Objectives

3.1 Overview of experiments

The aim of this study is to apply a multidisciplinary approach, integrating cell biology and engineering to address the need to lung tissue engineering advances. Human IPSCs were chosen based on their pluripotency, differentiation potential, and generation directly from adult cells. Using alginate hydrogels as a substrate to encapsulate these cells, and grow them in three dimensional cultures, a commercially available HARV bioreactor was used to improve and scale-up IPSCs differentiation into lung epithelial cells, namely type II pneumocytes. Cell proliferation was quantified by ATP measurements using the CellTiter Glo® assay. Cell viability was quantified using fluroscence-based live/dead assay. The quality of the cells produced was evaluated by morphology and cell ultrastructure analysis by fluroscence microscopy and transmission electron microscopy (TEM). The latter was also used to analyse features of the functional structure of the cells. Protein and gene expressions were measured using immunocytochemistry and quantitative real-time polymerase chain reaction (qRT-PCR), respectively.

3.2 Aim

The general aim of this thesis is to achieve efficient and reproducible differentiation of human IPSCs into type II cells of the airway epithelium, by developing appropriate bioprocessing technology. Specifically, to develop and establish a novel culture method allowing for maintaining human IPSCs pluripotency in 3D cultures and to enhance their differentiation into endoderm and, subsequently, into type II pneumocytes. Additionally, this work aims to create a basis for the automation of the process using a bioreactor as a means to scale-up the differentiation and expansion of 3D alveolar type 2 epithelial cells in-*vitro*, resulting in large scale production of alveolar type 2 epithelial cells for tissue engineering and other applications (Figure 3. 1).

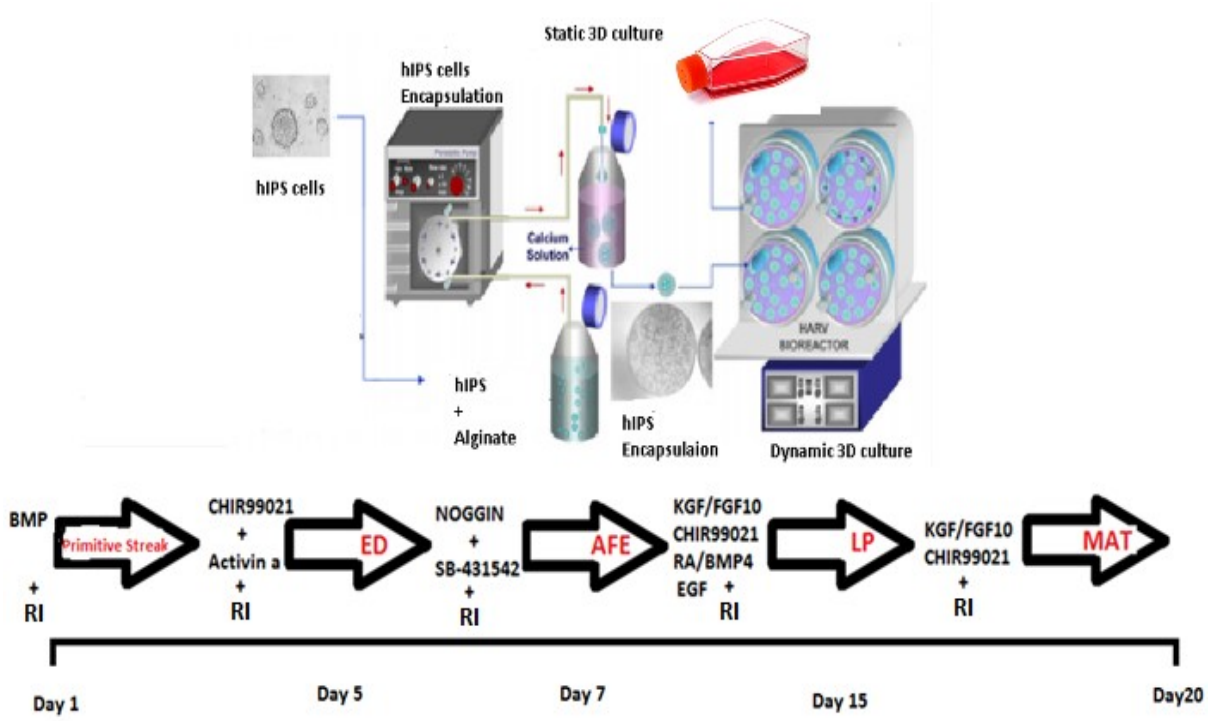


Figure 3. 1. Diagrammatic representation of the integrated bioprocessing approach to differentiating stem cells to pulmonary epithelium adopted in this study. Lineage tracing experimental design is as indicated, (ED) Endoderm, (AFE)Anterior Foregut Endoderm, (LP) Lung Progenitor, (MAT) Maturation and (RI) Rock Inhibitor y-27632 (Modify Teo, Mantalaris and Lim, 2014).

3.3 Objectives

1: Maintenance of pluripotency of human IPSCs in feeder free system and improve the viability of human IPSCs single cell-inoculated to move to 3D culture by inhibiting the ROCK signalling and using hypoxia.

2: Optimization of cell self-renewal and proliferation capabilities of human IPSCs single cells inoculated in 3D alginate beads by increasing mass transport within HARV bioreactor and adding Rock inhibitor (RI) throughout the culture.

3: Optimization of differentiation protocols to produce type II lung epithelium cells in 3D cultures and characterise the produced cells using molecular and functional assays.

3.4 Hypotheses

Several reports have demonstrated that directed differentiation of human PSCs, which includes human ESCs and IPSCs, is one of the most efficient approaches to achieve differentiation of a cell or tissue of interest (Lewandowski and Kurpisz, 2016). Based on this knowledge, the differentiation of human PSCs into lung lineages on monolayer cultures has been achieved using different methodologies with varying degrees of success. It is also known that differentiation would be stimulated under hypoxic three-dimensional environments which would better mimic the physiologic environment where these processes take place. It is hypothesized, therefore, that it is possible to develop strategies to culture human IPSCs in three-dimensional dynamic cultures in porous scaffolds. This technique has been shown to provide sufficient nutrient and oxygen transport and removal of waste products from the cells at the core of the scaffold. Consequently, increased proliferation and differentiation are expected as is a homogeneous distribution of cells in the center of the scaffold.

Specifically, the hypotheses examined in this study were:

1. The combination of hypoxia and ROCK inhibitor (RI) has a positive effect on the proliferation of human IPS single cells.
2. Encapsulation of human IPSCs in alginate hydrogel beads and subsequent use of HARV bioreactors to enhance mass transfer maintains their undifferentiated state and pluripotency in prolonged culture.
3. The addition of ROCK inhibitor (RI) to mTeSR™1 and differentiation medium for 3D culture will provide a significant improvement of cell proliferation in both states (undifferentiated and differentiated towards type II cells lung epithelium).
4. Induced human IPSCs differentiation towards DE in 3D culture using CHIR99021 then Wnta3.
5. Encapsulation and differentiation of human IPSCs under dynamic motion can be a scalable and efficient strategy produce high numbers of type 2 cells.

Chapter 4

Materials and Methods

This chapter describes the experimental methods used to achieve the objectives of the present work, as introduced in Chapter 3. The methodology described in this chapter was used to conduct two- and three-dimensional cell cultures and to characterize and analyse the cells obtained in terms of for self-renewal, maintenance and generation of the desired type II pneumocytes.

4.1 Cell culture

In this work, an embryonic stem cell line (H9) and an induced pluripotent stem cell line (IMR90-1) were used. The latter was produced by lentiviral transfection of isolated fetal human lung fibroblasts with four genes OCT4, SOX2, Nanong and lin28. Both cell lines were obtained from the WiCell Research Institute Inc., Madison, WI, United States of America.

4.1.1 Two-dimensional cell cultures

Both cell-lines were cultured in Matrigel™-coated 6-well plates with 2 mL of complete mTeSR™1 medium (see below for preparation) per well incubated at 37°C, 5% CO_2 in a humidified incubator (Nuaire 5500E). Cultures were examined under the microscope and the culture medium was replaced by fresh medium every day for 4 to 5 five days depending on colony size. After this time, colonies were dissociated with 1 U/mL dispase (a protease suitable for cell dissociation) in (DMEM/F-12 Stem Cell Technology, Canada) and transferred onto newly coated culture plates with fresh medium.

4.1.2 Culture medium preparation

The final culture medium formulation was composed of 400mL mTeSR™1 medium and 100mL mTeSR™1 5X supplement (both from Stem Cell Technology, Canada). The supplement was thawed overnight at 2 - 8°C and added the basal medium for a total volume of

500mL. The complete mTeSR™ medium was aliquoted and stored at -20°C for up to 6 months prior to use. Thawed aliquots were stored at 4°C and used within two weeks.

4.1.3 Preparation of Matrigel™-coated culture plates

The Matrigel™ matrix (BD) was thawed overnight at 4°C on ice. Once thawed, the contents of the vial were mixed by vortexing to ensure a homogeneous mixture. Working aliquots (160µL) were prepared and stored at -80°C for up to 6 months prior to use. The Matrigel™ was kept on ice at all times while handling, aliquoted as quickly as possible using pre-cooled tips and refrozen immediately to prevent gelification. Multi freeze-thaw was avoided. According to the dilution factor provided on the certificate of analysis, each aliquot can be used to coat two 6-well plates.

At the time of use, one Matrigel™ aliquot was thawed on ice and mixed with 13mL of DMEM/F-12 (Sigma-Aldrich) at 4°C and coating was performed immediately using 1mL/ well. The plates were incubated at room temperature for at least 1 hour before use or sealed with parafilm to prevent evaporation of the Matrigel™ solution and stored at 4°C for up to 7 days prior to use. Stored coated plates were kept at room temperature for 30 minutes before use. Just before plating human IPSCs, the Matrigel™ solution was carefully removed using a pipette without scratching the coated surface and 2mL of complete mTeSR™1 medium were immediately added.

4.1.4 3D cultures

Two configurations of 3D cultures were attempted in this work, namely T-flasks and a high aspect ratio vessel (HARV) bioreactor, both using alginate hydrogels.

4.1.4.1 Encapsulation technique

The alginate hydrogels used in this work were prepared from a phosphate buffer saline (PBS) solution of low viscosity alginic acid (1.1% w/v) and bovine gelatine (0.1% v/v), both from Sigma-Aldrich, at pH 7.4.

Monolayer cells were cultured in 6 well plates were incubated in 10 µM of Y-27632 (Tocris BioScience) for two hours. The cells were subsequently rinsed carefully with

PBS and incubated in Accutase (Innovative Cell Technologies) for 10 minutes at 37°C. Single-cell counts were performed using the trypan blue exclusion method (reagent purchased from Sigma-Aldrich). An appropriate volume of suspension was taken based on a requirement of 20,000 cells per alginate bead. This volume was centrifuged at 1000 rpm for 5 min, the supernatant was removed and cell pellets were then re-suspended together in the alginate solution. To get a uniform bead size, a peristaltic pump (model P-1; Amersham Biosciences) was used. The cell-gel solution was pumped at 20 rpm and a drop height of 3 cm using a 25-gauge needle (Becton Dickinson). The tubing was autoclaved and then further sterilized with 1M NaOH for 30 minutes and washed three times with sterile PBS. Beads were dropped into a sterile 100mM calcium chloride ($CaCl_2$) and 10 mM HEPES solution at pH 7.4 prepared in distilled water at room temperature (all chemicals from Sigma-Aldrich). The cell-gel solution discharged from the pump gelled immediately in contact with the $CaCl_2$ solution, forming spherical beads (2.3-2.5 mm in diameter after swelling). The beads were kept in gently stirred $CaCl_2$ solution for 6-8 minutes at room temperature. The beads were cultured in T72 flasks (3D static cultures) and in a HARV bioreactor (dynamic 3D cultures, see below).

4.1.4.2 High Aspect Ratio Vessel (HARV) bioreactor

The High Aspect Ratio Vessel (HARV) (Synthecon Ltd.), also known as a rotating wall bioreactor, was specially developed to study tissue and cellular engineering in a low-shear, non-turbulent environments. It has a large radius-to-depth ratio (40 mm x 10 mm) providing a substantial surface area on the rear face for gas exchange thorough a gas-permeable membrane. The average bioreactor volume is 50 mL. The culture vessel is a disposable, sterile, clear plastic cylinder with two sampling/injection Luer lock ports and a half-inch drain/fill port. Feeding of media/beads was performed thorough the fill port and air bubble were removed thorough the Luer valves daily. The HARV units were attached to a rotator base and incubated under the same conditions described above for two-dimensional cultures.

4.1.4.3 Alginate bead dissolution

A sterile solution of 50mM tri-sodium citrate di-hydrate (Fluka), 77 mM sodium chloride (BDH Laboratory supplies) and 10 mM HEPES (Sigma-Aldrich) prepared in PBS was used for Ca^{2+} depletion and depolymerization. The beads with medium were washed twice before adding the dissolving solution. Later, the beads were incubated at 37°C for about 5

minutes while stirring gently. The solution that contained dissolved beads was centrifuged at 1250 rpm for 5 minutes and the pellet washed once with PBS and centrifuged again, at 1000 for 3 minutes.

4.1.5 Directing the differentiation of human ESCs and IPSCs into alveolar type II pneumocytes

4.1.5.1 Induction of endoderm

ESCs cultures (both 2D and two 3D configurations) were incubated at 37°C overnight with mTeSR™1 medium supplemented with 10 μM of Y-27632. Human PSCs were incubated in 10 μM of Y-27632 for two hours when 70% confluence was reached. In all cases, cells were subsequently rinsed carefully with PBS and incubated in Accutase (Innovative Cell Technologies) for 10 minutes at 37°C.

Endoderm induction was performed during 3-4 days in low serum differentiation media DMEM/F12D (Life Technologies) supplemented with N2 (Life Technologies), B27 (Gibco), ascorbic acid (50 μg/ml, Sigma), Glutamax (2 mM, Life Technologies), monothioglycerol (0.4 μM, Sigma), 2 % fetal bovine serum (FBS,) (Life Technologies), 1% penicillin-streptomycin (Thermo Fisher Scientific). For the formation of the primitive streak, 10μM of Y-27632, and 3ng/mL of human BMP4 were added to the medium for 24 hours. In the case of 3D cultures, alginate beads were then resuspended in endoderm induction media containing 10μM Y-27632, 100ng/mL, human activin A, (Tocris Bioscience) and 3 μM of CHIR99021 (Tocris Bioscience)Tocris for 96 hours. Cells were fed every 48 hours (depending on the density) by replacing half of the exhaust medium by fresh medium.

4.1.5.2 Induction of anterior foregut endoderm

From day 4 to 6, the medium was changed to basal medium, supplemented with 100 ng/ml of human recombinant Noggin and 10 μM of SB-431542 (both from Tocris BioScience) which are known to induce anterior foregut endoderm (AFE) formation (Huang et al., 2013)

4.1.5.3 Induction of lung progenitors

From day 8 to day 17, lung progenitor induction was conducted. AFE cells obtained were treated with a 'ventralization' cocktail containing 3μM CHIR99021 (WNT signalling agonist), 10 ng/mL human FGF10, 10ng/mL human FGF7, 10 ng/mL human BMP4, 20 ng/mL

murine EGF (optional) and 1μM all-trans retinoic acid (ATRA) in SFD medium. All supplements were purchased from Tocris Bioscience except ATRA, obtained from Sigma-Aldrich.

4.1.5.4 Induction of lung/airway epithelial maturation

From day 18/19 to day 25, lung field progenitor cells were exposed to basal medium containing a combination of three factors (3μM CHIR99021, 10ng/mL human FGF10, 10 ng/ml, human FGF7,). With the addition of maturation components, namely 50 nM dexamethasone (Sigma) , 0.1 mM 8-Bromo-cAMP (Sigma), and 0.1 mM IBMX (3,7-Dihydro-1-methyl-3-(2-methylpro(pyl)-1H-purine-2,6-dione) (Sigma).

4.2 Imaging

4.2.1 Phase Contrast and Fluorescence microscopy

Phase contrast and fluorescence microscopy images were acquired on one of two microscopes: a IX70 inverted microscope (Olympus) equipped with a colour Cool Pix 950 digital camera (Nikon) and a black and white, high resolution charge coupled device (CCD)-Camera (Soft Imaging Systems) and results analysis performed in analySISB and analySISD softwares; or a BX60 upright microscope (Olympus) equipped with an Axiocam digital camera (ImageJ) and results analysis performed using the KS-300 software. For fluorescence imaging, the excitation wavelengths were 490nm for FITC (fluorescein isothiocyanate) and GFP (green fluorescent protein), 570nm for TRITC (tetramethyl rhodamine iso- thiocyanate) and Texas Red and finally 360nm for nuclear counterstain, DAPI (4'-6-Diamidino-2-phenylindole).

4.2.3 Transmission electron microscopy

Transmission electron microscopy (TEM) samples, in the form of cell suspension of beads, were washed in buffer containing 0.1M phosphate and 0.1M sucrose, rinsed in PBS twice and then fixed in 3% (v/v) glutaraldehyde in 0.1M cacodylate buffer (pH 7.2) for 30 min. Cells were then post-fixed in 1% (v/v) osmium tetroxide in 0.1M cacodylate buffer, transferred to 50% (v/v) ethanol aqueous solution, centrifuged 500 rpm/5 minutes and the resultant cell pellets were encased in molten agar. The agar blocks were dehydrated and infiltrated with Araldite epoxy resin (Taab Laboratories Ltd,) and embedded in

moulds. The resin was polymerized at 60°C for 24 hours and semi-thin (1µm) and ultra-thin (60-80nm) sections were cut using a Reichert-Jung Ultracut E ultramicrotome (Leica Microsystems) .The semi-thin sections, for selection of areas of interest on light microscopy, were stained using a solution of 0.8% (v/v) toluidine blue (Agar Scientific) in 0.8% (w/v) borax and 0.16% (w/v) pyronin Y. The ultra-thin sections were stained in a saturated solution of uranyl acetate in 50% (v/v) ethanol, followed by Reynold's lead citrate. Ultrathin sections were observed in a Philips CM10 transmission electron microscope (Amsterdam).

4.3 Histology

Beads for histology analysis were fixed in 4% (w/v) paraformaldehyde (PFA) for 30 minutes at room temperature and then placed in PBS for 15 minutes prior to dehydration.

4.3.1 Paraffin embedding

Fixed beads were taken thorough a series of increasing ethanol concentrations (50%, 70%, 95% and 100% (v/v)) for 30 minutes and three changes for each concentration to remove all the water. The ethanol was then completely replaced with neat xylene which was then replaced with paraffin-saturated xylene, at room temperature, overnight. The beads in paraffin-saturated xylene were placed in an oven (60°C) for 20 minutes and the xylene completely replaced by liquid paraffin. The samples were then embedded, sectioned (5 µm) and left at room temperature, overnight, to adhere to glass slides coated with Vectabond™ (Vector Laboratories).

4.3.2 Haematoxylin and eosin stain

For haematoxylin and eosin staining ***(H&E)***, the paraffin was removed from the sections by immersion in xylene, decreasing ethanol concentrations and then water. Sections were then dipped in haematoxylin (Harris' solution; VWR) for 30 seconds, washed in running tap water for 2-3 minutes and examined for sufficient staining. Excess stain was removed by decolouring in 0.5-1% (v/v) HCl (Sigma Aldrich) in 70% (v/v) ethanol (Thermo Fisher Scientific) for a few seconds and then washed in tap water for 5 minutes. Sections were finally dipped in 1% (v/v) eosin (VWR) for 2 minutes and washed briefly in tap water to remove excess stain. The tissue was dehydrated by submersion in 70% [v/v] Ethanol,

once, 100% [v/v] wice), cleared in xylene (VWR) and mounted in DPX mounting solution (VWR).

4.3.3 Alkaline phosphatase staining

Alkaline phosphatase (AP) activity in the human IPSCs was analysed after five days in culture. Cells were fixed in 4% Paraformaldehyde in PBS for 1-2 minutes maximum as fixing for longer periods leads to alkaline phosphatase inactivation. Fixed colonies were washed with 1 X wash Buffer (20mM Tris-HCL, pH 7.4, 0.15 NaCl, 0.05% Tween-20) (Life-Tecnhnology). The colonies were then treated with Fast Red Violet, Naphtol AS-BI phosphate solution (sigma) and distilled water in a 2:1:1 ratio and incubated in the dark at room temperature for 15 minutes, after which the staining solution was removed and the colonies were washed again with 1 X wash buffer. The cells were covered with 1 X PBS to prevent drying and observed under light microscope for AP expression. AP is a hydrolase enzyme responsible for dephosphorylating molecules such as nucleotides, proteins, and alkaloids under alkaline conditions. Undifferentiated cells appear blue, whereas differentiated cells appear colorless.

4.3.4 Immunocytochemistry and immunohistochemistry

For immunocytochemistry of paraffin-embedded samples, de-waxed sections were autoclaved in a tri-sodium citrate, dihydrate buffer (10 mM, pH6.0) (all from Sigma Aldrich) and allowed to cool and dry in order to increase immunogenicity.

Immunocytochemistry was performed throughout cells culture in slide chamber according to the following protocol. Live samples were cultured in 4 or 8 well chamber slides (VWR), washed once with phosphate-buffered saline (PBS) (Invitrogen) and then fixed with 4% (v/v) paraformaldehyde (Sigma-Aldrich) for 30 minutes. Fixed samples and paraffin embedded sections were washed three times with PBS (Invitrogen, UK), followed by permeabilisation with 0.1% (v/v) Triton X-100 (Sigma-Aldrich). After washing twice in PBS, non-specific binding was blocked by incubation with 10% (v/v) rabbit, goat or mouse serum (Vector Laboratories, USA) according to the origin of the primary antibodies. The primary antibodies were diluted according to the manufacturer's protocol with 0.1% (w/v) bovine serum albumin (BSA) (Sigma-Aldrich) and 0.01% (w/v) sodium azide (Sigma-Aldrich) in PBS. Sections were incubated with primary antibodies overnight at

4°C. On the following day, sections were washed three times with PBS and secondary antibodies conjugated with fluorescent dyes and incubated in 0.1% bovine serum albumin (BSA) in PBS, for 1 hour at room temperature. If an enzyme-linked secondary antibody is used, a further incubation in substrate will be required. The host organism of the secondary antibodies were selected according to the origin of primary antibodies used. Lastly, the samples were counterstained with 4,6-diamidino-2-phenylindole (DAPI) or propidium iodide (PI) (Vector Laboratories, USA) to stain cell nuclei.

Table 4.1. List of Primary and Secondary Antibodies for Immunocytochemistry Staining.

Secondary antibodies were*Goat-anti-mouse (Alexa Fluor 594), **Goat-anti-rabbit (Alexa Fluor 594), (Human ESCs/IPSCs Characterization kit (Applied StemCell, Inc)).

ANTIGEN	*PRIMARY ANTIBODY*	*COMPANY*	*DILUTION*
C(PROSP-C)	Polyclonal antibody Rabbit	AB3786-Millpore	1:1000-1:2000
B(PROSP-B)	Polyclonal antibody Rabbit	AB3430-Millpore	1:4000-1:8000
GBDH	goat polyclonal IgG	sc-9890 Santa Cruz	1:50-1:500
HNF-3Î	goat polyclonal IgG	sc-6554 Santa Cruz	1:50-1:500
ANTI-TTF	Rabbit monoclonal IgG	AB76013-Abcam	1:100-1:1000
OCT4	Anti-Oct4**	Applied StemCell, Inc	As described in company protocol
SOX2	Anti- Sox2**	Applied StemCell, Inc	As described in company protocol
NANOG	Anti- Nanog**	Applied StemCell, Inc	As described in company protocol
SSEA-4	Anti- SSEA-4*	Applied StemCell, Inc	As described in company protocol
TRA-1-81	Anti- TRA-1-81*	Applied StemCell, Inc	As described in company protocol
TRA-1-60	Anti- TRA-1-60*	Applied StemCell, Inc	As described in company protocol

4.4 Gene Expression Analysis

4.4.1 Ribonucleic acid (RNA) extraction

RNA was extracted from the sample or cell culture using the total RNA isolation kit (Qiagen) according to the manufacturer's protocol. Briefly, attached cells were trypsinized and spun down to get a cell pellet which was re-suspended in RNA protect reagent (Qiagen). The pellet was then dissolved in 350 to 600 µL lysis buffer (depending on cell numbers) which contained 10 µL/mL β-mercaptoethanol. The lysis buffer that contains the cell lysate can be stored at -80°C for long-term storage before proceeding with the RNA extraction protocol. Cell lysates were re-suspended gently a few times until there was no visible sign of cell clumps and transferred to the QIAshredder spin-columns (Qiagen) to homogenize the cell lysates. The columns were centrifuged at 13300g for 2 minutes. To purify the RNA, 70% (v/v) ethanol was added to the samples at the same volume of lysis buffer used. The samples were gently mixed and then transferred to RNeasy mini spin-columns (Qiagen). Following centrifugation, at 15000 rpm for 15 seconds, the flow-through was discarded (the RNAs were attached to the spin-column membrane). The membrane was washed with 700µl of kit washing buffer and centrifuged at 13300g for 15 seconds discarding the flow-through. The spin-columns were transferred to new 2ml collection tubes and elution was prepared with and 500 µL RPE buffer and the columns were centrifuged at 13300g for 2 min. Lastly, the column was transferred to a new tube and 30 µL of RNAse-free water were added at the centre of the membrane for elution. The columns were centrifuged at 13300g for 1 min. The RNA concentrations were measured using aNanoDrop® ND-1000 spectrophotometer (NanoDrop Technologies). The machine was set-up and calibrated according to the manufacturer's instructions. The ratio of sample absorbance at 230nm, 260nm and 280nm was used to measure the purity of RNA. The purified RNA should be free of DNA, proteins, or other contaminants for which a ratio of ~2.0 for the 260/280 ratio and 1.8-2.2 for the 260/230 ratio should be expected. Samples were stored at -80°C for long-term storage until further use.

4.4.2 Reverse Transcriptase and cDNA synthesis

To prepare the purified RNA for the production of cDNA, 1 - 2 µg of total RNA from each sample was diluted in Diethyl pyrocarbonate (DEPC) (Thermo Fisher) treated water to a final volume of 12.7µL and incubated for five minutes at 65°C to remove the secondary

structure. The reaction mixture containing: 4µL 5X Moloney Murine Leukaemia Virus Reverse Transcriptase (M-MLV RT) buffer (Promega), 2µL 4mM dNTPs (Promega), 1µL of 50µM Oligo dT16 primers (Applied Biosystems) and 0.3µl M-MLV RT enzyme (Promega) was added to the RNA and incubated for 1 hour at 37°C. Reverse transcription was terminated by incubating at 95°C for 5 min. Resultant cDNA was either used immediately or stored at −20°C.

The sense and anti-sense primers were designed using primer express 2 software (Applied Biosystems). The oligonucleotides were purchased from Invitrogen and are listed in Table 4.2

Table 4.2. The lists of qRT-PCR primer sequences.

Genes	Forward primer (5′−3′)	Reverse primer (5′−3′)
GAPDH	GACAACAGCCTCAAGATCATCAG	ATGGCATGGACTGTGGTCATGAG
NKX2.1	TCGCTCCAGCTCGTACACC	GGACGTGAGCAAGAACATG
OCT3/4	CCTCACTTCACTGCACTGTA	CAGGTTTTCTTTCCCTAGCT
CXCR4	CACCGCATCTGGAGAACCA	GCCCATTTCCTCGGTGTAGTT
FOXA2	GGGAGCGGTGAAGATGGA	TCATGTTGCTCACGGAGGAGTA
AQ5a	ACTGGGTTTTCTGGGTAGGG	ATGGTCTTCTTCCGCTCTTC
Beta ac-	CATGTACGTTGCTATCCAGGC	CTCCTTAATGTCACGCACGAT
CFTTR	CTATGACCCGGATAACAAGGAGG	CAAAAATGGCTGGGTGTAGGA
NANOG	TTTGGAAGCTGCTGGGGAAG	GATGGGAGGAGGGGAGAGGA
HIFA2	GGACTTACACAGGTGGAGCTA	TCTCACGAATCTCCTCATGGT
SFTPC	CACCTGAAACGCCTTCTTATCG	TGGCTCATGTGGAGACCCAT
HIFA1	CCAGCAGACTCAAATACAAGAACC	TGTATGTGGGTAGGAGATGGAGAT
LAMA5	CCTCGTCCTCCAATGACAC	GCGCTGCAGTCACAATTC
FN1	AGGAAGCCGAGGTTTTAACTG	AGGACGCTCATAAGTGTCACC
PAX6	TGTCCAACGGATGTGTGAT	TTTCCCAAGCAAAGATGGAC

4.4.3 Polymerase chain reaction (PCR)

Amplification quantitative PCR (qPCR) analysis of cDNA was performed in a StepOne Real-Time PCR System (Applied Biosystems) by using the SYBR green detection system (SensiFAST™ SYBR® Hi-ROX Kit,Thermo Fisher) Reactions were performed in an optical 96-well plate containing 9µL of reaction mixture + 1µL of cDNA in each well. The reaction

plate was sealed with a transparent adhesive cover and centrifuged briefly at 1000rcf for 1 minute to spin down the contents and eliminate any air bubbles from the solutions. The samples undergone the following PCR temperature stages: 95°C for 2 minutes, 40 cycles of 95°C for 5 seconds and 60°C for 30 seconds. The reaction was finished with a dissociation step which consisted of 15 seconds at 95°C, 15 seconds at 60°C and 15 seconds at 95°C. A single peak in the resultant dissociation plot represented a single specific product. Each sample was analysed in triplicates, and negative control reactions without cDNA were included in each experiment. Glyceraldehyde-3-phosphate dehydrogenase (GAPDH) and β-actin were used as a housekeeping gene to normalise expression. Data were analysed using ABI 7900 HT SDS 2.3 software (Applied Biosystems).

4.5 Viability assays

4.5.1 Live/Dead assay

In situ live and dead cells can be visualized using the LIVE/DEAD® Viability/Cytotoxicity Assay Kit (Invitrogen) that provides a two-colour fluorescence cell viability assay based on the simultaneous determination of live and dead cells with two probes that measure two recognized parameters of cell viability, intracellular esterase activity and plasma membrane integrity. Live cells are distinguished by the presence of ubiquitous intracellular esterase activity, determined by the enzymatic conversion of the virtually non-fluorescent, cell-permeant calcein AM to the intensely fluorescent calcein. The polyanionic dye calcein is well retained within live cells, producing an intense uniform green fluorescence (EX/EM ~495 nm/~515 nm). Ethdium homodimer-1 (EthD-1) enters cells with damaged membranes and undergoes a 40-fold enhancement of fluorescence upon binding to nucleic acids, thereby producing a bright red fluorescence in dead cells (EX/EM ~495 nm/~635 nm). EthD-1 is excluded by the intact plasma membrane of live cells. The determination of cell viability depends on these physical and biochemical properties of cells. A 4 mM EthD-1 and 2 mM calcein AM solution (Invitrogen) diluted in 10 ml PBS (Life Technology) was added to live cells or alginate beads and incubated at room temperature for 30 minutes, in the dark. After incubation, the solution was aspirated and a small amount of PBS was added to the cells to prevent dehydration. The cells and beads

were then photographed within 30 minutes using an IX70 inverted fluorescent microscope (Olympus) to assess the ammounts of live and dead cells.

4.5.2 CellTiter-Glo Luminescent Cell Viability Assay Kit

The CellTiter-Glo Luminescent Cell Viability Assay (Promega), is a method to determine the number of viable cells in culture based on quantification of the ATP present, which signals the presence of metabolically active cells. The assay procedure involves adding a single reagent directly to cells which results in cell lysis and generation of a luminescent signal proportional to the amount of ATP present. The amount of ATP is considered to be directly proportional to the number of viable cells present in culture.

4.5.3 3-(4,5-dimethylthiazol-2-yl)-5-(3-carboxymethoxyphenyl)-2-(4-sulfophenyl)-2H-tetrazolium, inner salt (MTS) assay

The MTS substrate is prepared in a cell culture medium, added to cells in culture, usually at a final concentration of 0.2 - 0.5mg/mL in culture medium, and incubated for 1 to 4 hours. The quantity of formazan (directly proportional to the number of viable cells) is measured by recording changes in absorbance at 570 nm using a plate spectrophotometer. Viable cells with active metabolism convert MTS into a purple coloured formazan product with an absorbance maximum near 570 nm. When cells die, they lose the ability to convert MTS into formazan, and thus colour formation serves as a useful and convenient marker of only the viable cells. The exact cellular mechanism of MTS reduction into formazan is not well understood, but it likely involves reaction with NADH or similar reducing molecules that transfer electrons to MTS.

4.6 Flow cytometry

Flow cytometry was used to quantify cells expressing a pluripotency marker of human ESCs and IPSCs. Flow cytometry was performed using the human embryonic stem cell kit (BD), which was applied as per manufacturers's instructions. In short, cells were washed twice in PBS and harvested with a cell scraper (Corning), vortexed to obtain single cells and re-suspended in 0.5 mL of fixation/permeabilization buffer and incubated at 2-8°C

for 30 minutes. The cells were centrifuged and re-suspended in 100 µL of a permeabilization/wash buffer (saponin-mediated cell permeabilization) (BD, Bioscince). The cells were incubated for 30-45 minutes at room temperature after adding 10 µL of the conjugated antibodies Nanog PE (Phycoerytrin)(Clone 245610; mouse IgG2A), SSEA-4 APC (Allophycocyanin)(Clone 240408; rat IgG2B) and Oct-3/4 PerCP (Peridinin-chlorophyll-protein complex)(Clone MC-480; mouse IgM) .Simultaneously, the corresponding isotype controls were used. Next, cells were washed with 2 mL of permeabilization/wash buffer and re-suspended in 200-400 µL of stain buffer for flow cytometric analysis. Analysis was conducted in a BD LSR Fortessa (4 laser) cytometer featuring blue (488nm), yellow/green (561nm), violet (405) and red (640nm) lasers.

Before running any samples, routine alignment and calibration is essential. For the calibration procedure, Calibrite™3 beads (Becton Dickinson, UK) were used prior to analysis and are suitable for PE, PerCP and APC calibration. The beads were used to adjust instrument settings, set the fluorescence compensation and check the instrument sensitivity before analysis. Unstained cells and cells stained with isotype were used as controls to ensure no background fluorescence/nonspecific binding was accounted for in these analyses.

4.6.2 Flow cytometry data analysis

Data were further processed using Flowjo. A single parameter histogram shows the number of events (cell counts) on the y-axis over the measurement parameter (relative fluorescence intensity) on the x-axis. Finally, data from the samples were analyzed over the negative control to determine the percentage of the total population formed by the positive phenotype.

4.7 Immunoprecipitation and western blotting

Cells were washed two times with PBS on ice and scraped in 1 mL of RIPA extraction buffer (1% NP-40 lysis buffer, 150 mM NaCl,50 mM Tris pH 7.5,1% Nonidet P-40,2 mM EDTA,50 µg/mL leupeptin,10µg/mL aprotinin,200µM sodium orthovanadate,4mg/mL p-nitrophenyl phosphate) (Thermo Fisher).The scraped cells were briefly vortexed and then incubated on ice for 10 min. The extracts were then centrifuged at 14000 rpm in a 4°C cold microcentrifuge for 15 minutes and the cell extract supernatants were collected.

Protein contents were determined using the Bradford microassay. The samples were prepared to be at 10 µg (5-15µg range) per tube in LDS sample buffer (4X solution, ref 0007, Invitrogen) and reducing agent (mercaptoethanol 10%) all samples had the same final volume (adjusted with distilled water). The tubes were warmed for 5 minutes at 90°C to denature the proteins. Samples were loaded on to BioRad Precast gels Bio-Rad – Criterion XT Precast Gels 10% Bis-Tris-12+2 well comb –ref 345-0111 –45µL max per well. 1L of running buffer diluted to 1X in water was added to the tank containing the gels (MOPS SDS Running Buffer 20X, ref NP0001, Invitrogen). 5µL of a protein ladder was also loaded (Precision plus Protein Standards – Dual Color, ref 161-0374, Bio-Rad) and the samples were run for approximately 90 minutes at 110 V (constant voltage). When the ladder run was complete, the current was stopped. The proteins were transferred to a PVDF membrane which was the size of gel. The membrane was blocked with PBS + 0.1% Tween-20 + 5% milk (Dried Skimmed Milk, less than 1% fat) with gentle agitation. Primary antibody (AF) was added and diluted 1:1000 in blocking buffer for 1 hour at room temperature. The membrane was then washed with for 3 x 5 min with PBS + 0.1% Tween 20 with gentle agitation. After 1h incubation with secondary antibody from Tocris Bioscience -polyclonal goat anti-rabbit Ig/HOURP – working dilution 1/1000 – HAF109. The membrane was washed 3 x 5 min with PBS + 0.1% Tween 20 with gentle agitation and was incubated with chemiluminescent substrate (e.g. ELC 2 from Pierce) according to the manufacturer's instructions. Densitometric analysis of the films was performed using the Quantity One 1-D Analysis Software, 2003 version (BioRad,).

Table 4.3. List of Primary Antibodies for Immunoprecipitation and western blotting

ANTIGEN	*PRIMARY ANTIBODY*	*COMPANY*	*DILUTION*
C(PROSP-C)	Polyclonal antibody Rabbit	AB3786-Millpore	1:1000-1:2000
B(PROSP-B)	Polyclonal antibody Rabbit	AB3430-Millpore	1:4000-1:8000
GBDH	goat polyclonal IgG	sc-9890 Santa Cruz	1:50-1:500

4.8 Statistics

Data are presented as means ± standard error of the mean (SEM). Comparison of two treatment groups was performed using the unpaired two-tailed Student's T-test. Comparisons between several groups were analyzed by one way analysis of variance (ANOVA). The statistical analyses were done using GraphPad software to determine significant differences. P-values lower than 0.05 were considered to show statistical significance. For all experiments, a minimum of 3 independent experimental runs was performed.

Chapter 5

Maintain human IPSCs pluripotency in feeder-free culture and enhance the proliferation of single cells by combining ROCK inhibition and hypoxia

5.1 Introduction

Although human ESCs/IPSCs culture methods have been undergoing many advancements, certain issues require resolution prior to applying such methods clinically. These issues include: the lack of standardization in maintenance and differentiation protocols in the context of serum-free and xeno-free conditions; inadequacy of analysis in monitoring cellular stress and signaling, poor growth conditions, spontaneous differentiation, and apoptosis while undergoing cell processing; and the issue of heterogeneous cell populations (Chen et al., 2014).

Pluripotency and differentiation capabilities of human IPSCs within the body has attracted the attention of researchers in the regenerative medicine field. To reduce heterogeneity and differentiation efficiencies, human IPSCs require maintenance of high pluripotency states initially (Chen et al., 2014). To maintain human ESCs cells culturing ex-*vivo* focused on uses of mouse or human feeder cell layers however, MEFs are undefined xeno-derived resources.

Despite the progress made in feeder-free products that support long-term culture of human ESCs/IPSCs such as Matrigel™ and serum-free medium such as, mTeSR™1 which include some animal proteins, alternative animal-free formulations exist and do support human ESCs/IPSCs cultures as well. They have the potential to support future therapeutic use (Braam et al., 2008). An example of this is recombinant vitronectin (Braam et al., 2008) and Laminin-511 (Braam et al., 2008) yet such formulations are known to be costly and therefore, their use is minimal (Chen et al., 2014). Emphasis has been put on certain technical issues which constrain the utilization of human ESCs in research and clinical applications. Paradoxically, human IPSCs are ideally maintained in colonies, however, for

differentiation protocols to be efficient and robust, they require processing through single cell cultures (Ludwig et al., 2006; Levenstein, et al., 2006; Watanabe et al., 2007).

In spite of being conducted under conditions leading to stem cell maintenance, single cells in suspension cultures of human PSCs, face apoptosis (Amit et al., 2000; Hasegawa et al., 2006). A possibility of turning this issue, is the inhibition of ROCK (Rho-associated protein kinase), a serine-threonine kinase that phosphorylates and activates the myosin II pathway (Baharvand, Salekdeh and Mollamohammadi, 2010; Chambers et al., 2009; Olson, 2008; Watanabe et al., 2007; Wataya et al., 2008). This results in the maintenance of the differentiation potential for up to 72 hours, through the inhibition of an E-cadherin-dependent apoptotic pathway (The Y-2763221, ROCK inhibitor) (Chen et al., 2010; Emre et al., 2010; Ohgushi et al., 2010; Walker et al., 2010). This inhibitor is the most effective inhibitor. Treatment of human ESCs and Human IPSCs is done with 10 μM of Y-27632 before disassociating the colonies into single cells (Mollamohammadi et al., 2009; Miyazaki et al., 2012; Sahara et al., 2014).

Oxygen is an effective signalling molecule due to its impact on fundamental characteristics of different stem cell types (CSETE, 2005). Earlier results suggest that low-oxygen tension (2%) in culture is crucial for robustness of human embryonic stem cell (ESC) self-renewal(Forsyth et al., 2006). Furthermore, under those conditions' cells are capable of reducing the chromosome mutations. For instance, when cultured under 5-7% oxygen, human PSCs showed increased blastocyst development, rates cell numbers and were able to improve quality of human IPSCs cultured in serum-free and xeno-free conditions (Yoshida et al., 2009b; Forristal et al., 2010a).

5.2 Aim and Objectives

This chapter presents the initial work carried out towards the encapsulation of human IPSCs in alginate beads. Here, a strategy to overcome the main problem with obtaining a successful 3D culture system for Human IPSCs is presented as a means to avoid the apoptosis and pluripotency losses during culture previously mentioned in literature (Watanabe et al., 2007). Initially, a study of the effect of combining a feeder- and serum-free culture on the human IPSC cell line IMR90-1 on the maintenance of cellular pluripotency between passages has been conducted. In the course of this study, pluripotency

markers have been measured by immunocytochemistry and flow cytometry. Furthermore, hypoxic environments (5% oxygen) combined with 10 μM of Y-27632 ROCK inhibitor has been attempted as a strategy to maintain viable, highly pluripotent single cell suspensions of human IPSCs.

5.3 Methodology

The human IPSCs cell line IMR-90 was cultured in feeder- and serum-free conditions following manufacturer's instructions. The cells were cultured on Matrigel™-coated 6-well plates in mTeSR™1 culture medium supplemented with TGF-β and FGF-2. In order to maintain the pluripotency and viability of the cells, media exchanges were performed daily. Cells were passaged after reaching 70% confluence with the use of a cell-scrapper, in order to produce small slumps instead of single cells at this point.

To confirm the maintenance of pluripotency for over 5 passages (34-39), cells were assayed for the presence of the pluripotency-associated proteins Oct3/4, Sox2, Nanog, TRA-1-60, TRA-1-80 and SSEA4 by immunofluorescence microscopy; for the presence of alkaline phosphatase activity by light microscopy and for the expression of intracellular protein Nanog and surface protein SSEA4 by flow cytometry, as these are widely used markers of pluripotency (Abujarour et al., 2013).

As encapsulation requires the cells to be in a single-cell suspension, the first step of this project was to optimise the dissociation method, as this commonly leads to dissociation-induced apoptosis (Watanabe et al., 2007) . For this reason, several conditions were tested to overcome this problem. Watanabe shows that for human ESCs, 10 μM of Y-27632 ROCK inhibitor should be added to the culture media two hours before the use of Accutase (contains proteolytic and collagenolytic enzymes) to dissociate cells into a single cell suspension. Cells can then be recovered from the suspension by centrifugation, washed with PBS, gently homogenised with a pipette and passed through a 40 micron cell strainer. The dissociated cells should be seeded onto Matrigel™ ® coated flat-bottomed 96-well plates at low density (50000 cells/ well, 0.32 cm2; three wells for one condition).

In addition to the effect of ROCK-inhibitor in culture, its effects were studied along with the influence of the oxygen concentration in culture, as the cells were cultured at 37°C and in a humidified atmosphere of 5% CO_2 and 5% or 21% O_2, since it has been proven that hypoxia plays an important role in stem cells by maintaining their pluripotent state,

enhancing proliferation and reprogramming somatic cells into pluripotent cells (Yoshida et al., 2009b; Forristal et al., 2010a). For this, 4 study groups were created: no inhibitor/normoxia, inhibitor/normoxia, no inhibitor/hypoxia and inhibitor/hypoxia. To study the effect of each condition on the viability and proliferation of the cells, the MTS Cell Proliferation assay was used at 4 time points - 12h, 48h, 72h, and 96h. A calibration curve was generated for the MTS assay, where the data shows a linear correlation between the absorbance signal and the cell number within the range where the assay was applied, allowing for the use of the equation that defines this relationship to calculate the number of viable cells in culture (Appendix I).

5.4 Results and Discussion

5.4.1 Morphology of undifferentiated human IPSCs Cultured on Corning® Matrigel™ Matrix in mTeSR™1 Medium and the expression of Alkaline Phosphatase AP+

Human IPSCs grown in mTeSR™1 Medium and on Matrigel™ matrix substrate were observed under light microscopy (Figure 5.1). At day 5, the images showed the typical morphology of the round pluripotent colonies, consisting of dense, flat and smooth colonies with a clear border detected under light microscopy (Figure 5.1 A and B). Undifferentiated human IPSCs usually expand as healthy condensed and round multicellular colonies with distinct edges (Courtot et al., 2014). Upon further inspection, the human IPSCs showed larger sized nuclei in comparison to the cytoplasm and prominent nucleoli, indicative of exponential proliferation (Figure 5.1 C). It is also possible to observe the cells closely packed inside the colonies, which indicates, in pair with the previously described morphology, the meeting of criteria that confirms the capability of the in-*vitro* culture to sustain self-renewal. The observed characteristics differ notably from other cells, such as parental human dermal and mouse embryonic fibroblasts. Similar morphology has been described for other IPSCs in several studies (Thomson et al., 1998; Takahashi et al., 2007). Spontaneous differentiation within the colonies that are beginning to differentiate was characterized by a compact central core, loss of defined edges and areas of irregular cellular morphology as shown in Figure 5.1 D) indicated by the arrows. Mechanical passaging was used to save this colony by scrapping out the differentiated cells at the edges.

Research has focused greatly on improving the reproducibility of human IPSCs culture in simple, defined feeder-free methods from all aspects of the culture system, such as media, coating matrix, and passaging method (Totonchi et al., 2010). However, some studies reported an elevated expression of lineage-specific genes in human ESCs/IPSCs cultured under feeder-free conditions, which may affect any consequent attempt to differentiate these cells towards different lineages (Badger et al., 2012). Additionally, changes in the karyotype of human ESCSs/IPSCs cultured under feeder-free conditions have also been reported (Badger et al., 2012). Another concern when adapting human ESCs/IPSCs to feeder-free culture methods is the decrease in the proliferation rate as cells are exposed to fewer growth factors that would originally be released from MEFs in-*vivo.* The ability of different human ESCs/IPSCs lines to attach to feeder-free matrix varies, as a result of their different integrin content as these are important cell attachment proteins (Badger et al., 2012). However, the use of feeder-free conditions eliminates the undefined biological variability component of the feeder layer from the culture system (Nakagawa et al., 2014). For this reason, Matrigel™ has been used as a matrix to culture human IPSCs, particularly as it is reproducible and easy to use (Lam and Longaker, 2012).

Additionally, a complete elimination of serum and animal-derived materials is essential for clinical applications. Thus, it is significant to move towards a feeder-free and serum-free culture system for the medically relevant maintenance, expansion and differentiation of human IPSCs. Hence, ensuring the quality of pluripotent cells is important for their differentiation efficiency. Recent publications showed the feasibility of using a defined serum-free and feeder-free media such as mTeSR™1 for a high quality maintenance of human ESCs and IPS Cs (Bergendahl, et al., 2006; Lannon et al., 2008).

It has been demonstrated that human ESCs and IPSCs show alkaline phosphatase (AP) activity when in their undifferentiated state, so a colorimetric assay was used as functional confirmation of maintenance of pluripotency. This is a widely used, simple, sensitive, rapid, and quantitative functional assay for pluripotent cells (Hoffman and Carpenter, 2005). AP expression was also analysed using enzymatic immunohistochemistry and it has been correlated with other self-renewal assays (Shamblott et al., 1998; Takahashi et al., 2007; Thomson et al., 1995). Therefore, at day 5 of culture, AP activity staining was made on confluent cultured human IPSCs at passage 39. All cells within the colony indicated extraordinary AP activity, as shown in (Figure 5.1) F. Accordingly, it has

been previously shown that the loss of AP occurs before the loss of OCT4 or SSEA3 expression, proving this to be a more sensitive indicator of the undifferentiated stem cell state of human ESCs than any of the previously shown markers (O'Connor et al., 2008). The cell morphology however, does not indicate underlying molecular changes, which should be concluded based on a transcriptional profile and protein expressions.

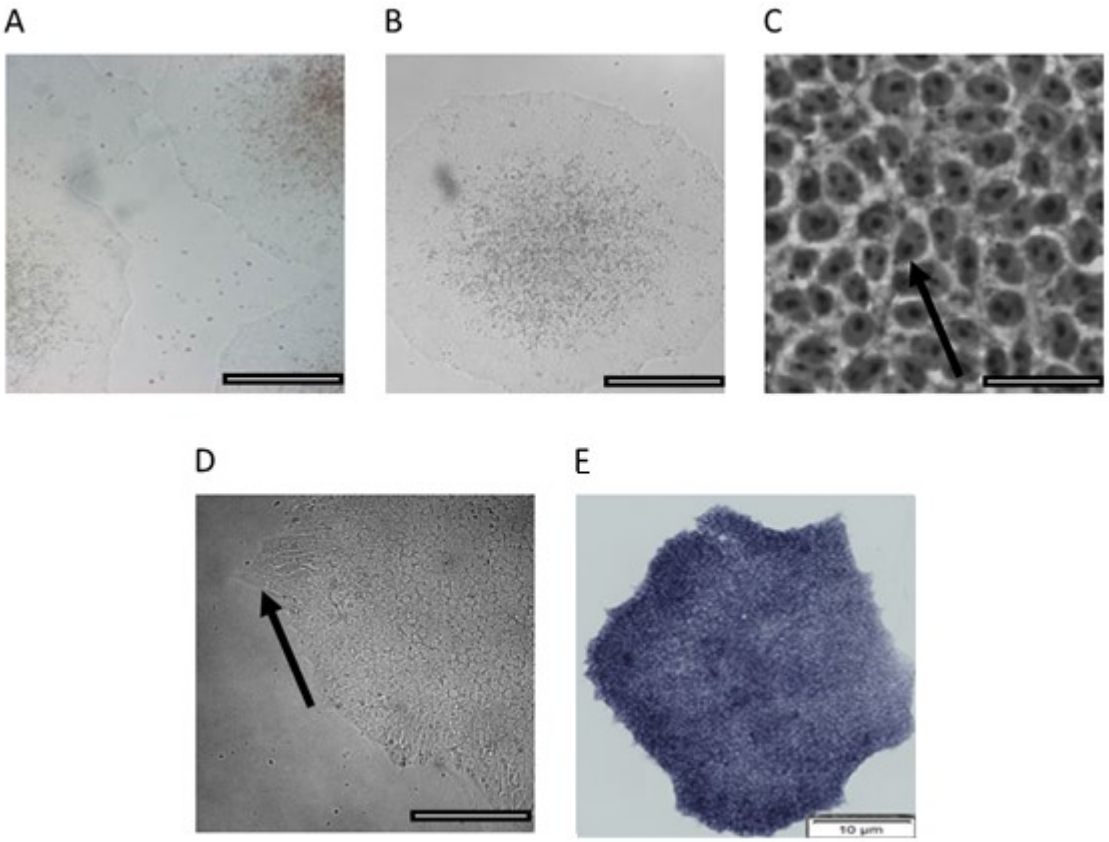


Figure 5.1: Morphology of Human IPS Cell Line IMR-90 Cultured on Corning® Matrigel™ Matrix in mTeSR™1 Medium.

A) Image of Day 5 from the maintenance culture showing Human IPSCs colonies covering a large area of the well. B) The morphology of Human IPSCs colony is dense, flat, and presents smooth edges). C) Human IPSCs are more condensed with a high nucleus/ cytoplasm ratio and prominent nucleoli, as indicated by the arrows. D) Image showed an undifferentiated human IPSCs colony that has begun to spontaneously differentiate around the edges, as indicated by the arrows. E) Human IPSCs stained positive for Alkaline Phosphatase activity. (A, B, and D Scales for each image: 200µm) (E Scales for each image: 10µm) (C Scales for each image: 20µm).

5.4.2 The characterisation of Human IPSCs self-renewal potential over passages

Several assay should be conducted on ES and IPS cells to confirm and characterise their self-renewal capacity (Peppo and Marolt, 2012). These assays characterise cell phenotypes in terms of morphology by measuring cell surface and intracellular markers. Furthermore, pluripotency of cells can also be assessed by their ability to differentiate into cells of all three germ layers. These very features of stem cells make them valuable tools for the study of physiological and pathological development (Evans and Kaufman, 1981; Thomson et al., 1998). However, in *vitro* culture conditions for stem cell growth demand a balance between a number of variables to create the optimal environment which would enable cell survival, growth and maintenance of pluripotency. For example, culture temperature, oxygen tension, appropriate growth media and adhesion matrix can drastically affect cell quality.

To confirm the pluripotency of human IPSCs, immunoreactivity with pluripotency markers was detected at passage 39 at the fifth day of culture in mTeSR™1 medium and Matrigel™ coating (Figure 5.2). Cells showed high expression of the common pluripotency proteins: (A) nuclear markers, Octamer-binding transcription factor 4 (Oct4), SRY (sex determining region Y)-box 2 (Sox2), and Nanog (Figure 5.2), in addition to (B) surface markers, SSEA4, TRA-1-81, and TRA-1-60 (Figure 5.2). Negative controls were created at the same time from the same batch of cells by incubating them only with the secondary antibody, to detect and account for non-specific fluorescence. Oct4, Sox2, and Nanog are transcription factors associated with stemness and known to be highly expressed in undifferentiated human ESCs and IPSCs cells, as well as directly correlated with cellular self-renewal potential (Loh et al, 2006). Stage-specific embryonic antigen 4 (SSEA-4), Tumour Rejection Antigen TRA-1-60, and TRA-1-81 are antigens present on the surface of human ESC (Aoki et al, 2010). The majority of human IPSCs colonies showed highly positive expression of Oct4, Sox2 and Nanog. This result is extremely important because Oct4 is highly associated with cells from the ICM (inner cell mass) and it has been shown that knocking out this gene induces trophoblast development (Nichols et al., 1998; Rosner et al., 1990; Scholer et al., 1990a; Scholer et al., 1989; Scholer et al., 1990b). Both Sox2 and Oct4 are transcription factors which belong to the SRY family. In spite of Sox2 expression in ICM, it can be expressed in later development stage such as germ cells and epiblast.

Additionally, Sox2 plays a central role in ectoderm and nervous system development (Avilion et al., 2003; Gubbay et al., 1990).

At this point, it is important to realise that the expression of Oct4, Sox2 and Nanog does not necessarily indicate early cell differentiation. Nanog is a homebox protein and a protein of early development where Nanog down-regulation is associated with loss of self-renewal potential. Furthermore, both Nanog and Otc4 are considered responsible for the central regulation of stem cell transcription associated genes (Rizzino, 2009). In addition, it has been shown that in spite of Oct4, Sox2 and Nanog being positively expressed, self-renewal can be associated with several other factors (Avilion et al., 2003; Chambers et al., 2003; Lee et al., 2004; Nichols et al., 1998; Scholer et al., 1990b). Such factors include surface marker glycoproteins such as Tra1-60, Tra-1-81, SSEA3 and SSEA4 which are highly associated with self-renewal and therefore their down-regulation is associated with differentiation (Andrews et al., 1982; Damjanov et al., 1982; Reubinoff et al., 2000, Shevinsky et al., 1982; Thomson et al., 1998).

Following the high expression of the pluripotency proteins showed by the immunocytochemical analysis, flow cytometry analysis was used to quantify the expression of the pluripotency associated markers, as opposed to the previous technique, which is merely a qualitative analysis. After passaging cells over 5 times, flow cytometry results show 86% Nanog+SSEA4+, a solid result for the co-expression of an intracellular and a surface marker, as a very high percentage of cells was positive for both markers at the same time (Figure 5.4 A). Typically, the specification test to pass and meet the certificate of analysis for any human IPSCs cell line the cells population should be more than 80% pluripotent (Maherali and Hochedlinger, 2008). At this point, human IPSC culture in mTeSR™1 accumulated undifferentiated cells over passages by showing no difference in the percentage of pluripotency cells co-expressing these two markers between passages 34 and 39 (Figure 5. 4 B). Unstained human IPSCs cells and the manufacturer recommended isotype controls were used as controls to set the exclusion gates that generated these results please review the plot at (Appendix II).

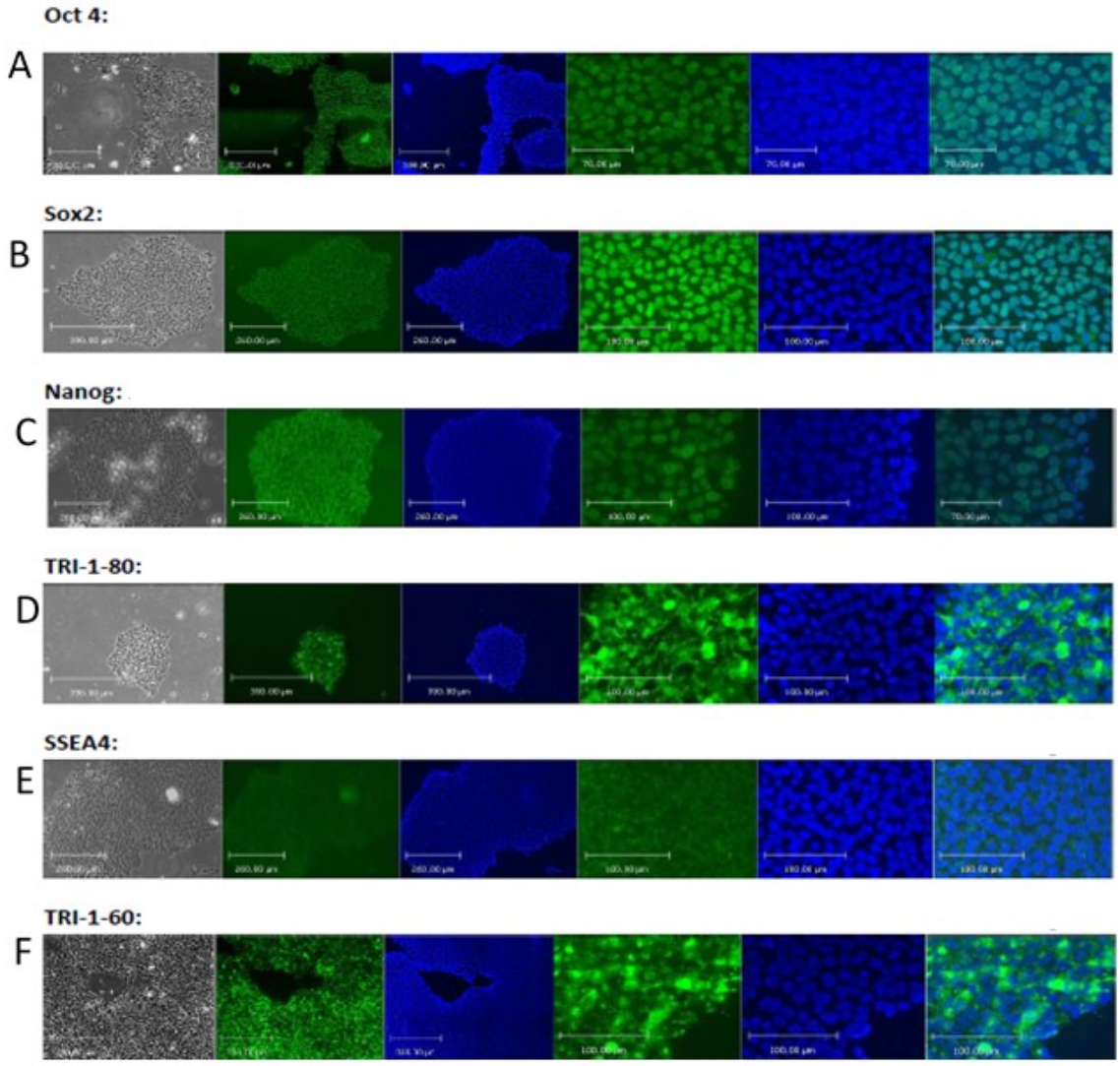


Figure 5.2: Immunofluorescence staining of pluripotency-associated nuclear and surface proteins in human IPSCs.

Expression of pluripotency associated nuclear markers at day 5: (A) Oct4 (Alexa Fluor® 488-FITC-green), (B) Sox2 (Alexa Fluor® 488-FITC-green), and (C) Nanog (Alexa Fluor® 488-FITC-green); Expression of pluripotency surface markers (D) TRA-1-81 (Alexa Fluor® 488-FITC-green), (F) SSEA4 (Alexa Fluor® 488-FITC-green), and (E) TRA-1-60 (Alexa Fluor® 488-FITC-green). The first column shows the bright field images; the second column shows the expression of the nuclear or surface markers in green; the third column shows nuclear counter staining with DAPI and finally the sixth column shows the composite images. Images were captured at 10x magnification. Scale for images, 100 µm and 40x. Scale for images, 200µm magnification, as indicated in the figures, under the appropriate fluorescent filters.

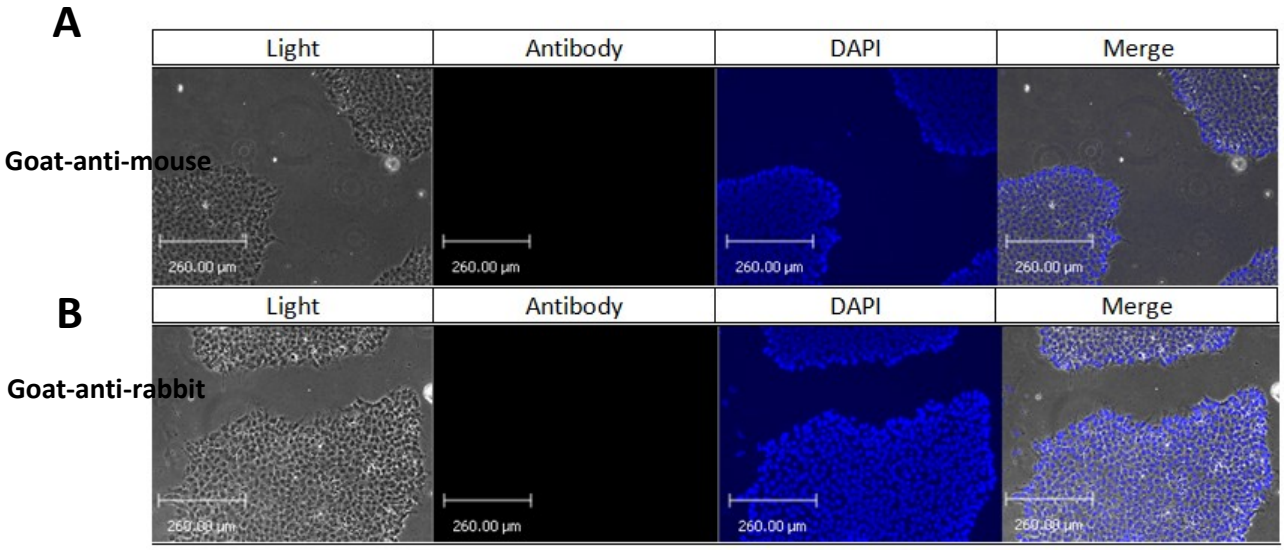


Figure 5.3: Negative Controls for non-specific immunocytochemistry staining of pluripotency-specific primary antibodies for human IPSCs.

A) Human IPSCs stained only with the secondary antibody Alexa Fluor® 488 goat anti-rabbit (FITC-green); (B) Goat-anti-rabbit (Alexa Fluor® 488-FITC-green) and Goat-anti-mouse (Alexa Fluor® 488-FITC-green). The first column shows the bright field images. The second column shows any non-specific binding either in green. The third column shows the nuclear staining with DAPI, as indicated in the figure. The forth column shows the composite images. Images were captured at 40x. Scale for images, 260µm.

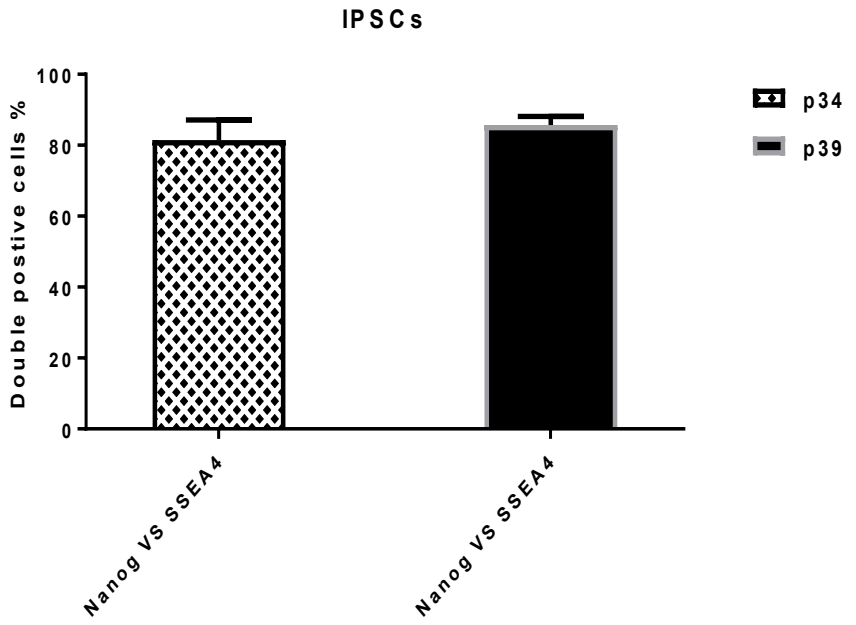


Figure 5.4: Flow cytometric analysis of pluripotency markers over passages.
The plot shows the percentage of double positive cells stained with internal protein Nanog-PE and cell surface protein SSEA4-APC at passages 34 and 39.

5.4.3 Optimised proliferation of human IPSCs when passaged as single-cells and evaluation of pluripotency maintenance under different conditions

In the previous sections, the successful production of human IPSCs in a naïve undifferentiated state has been described. Colonies were producing following feeder-free protocol previously reported (Lannon et al., 2008; Ludwig et al., 2006). Consequently, it was clear that the method employed to passage the cells needed to be optimized before moving on to 3D culture, as encapsulation requires the cells to be suspended as single cells, which often leads to dissociation-induced apoptosis (Watanabe 2007) (Figure 5.5). Based on the literature, 10 μM of the Y-27632 inhibitor were added to the culture media 2 hours before passaging the cells and then for 4 days after passaging. Moreover, in this section, the stimulus of the oxygen tension was also evaluated, because it has been confirmed that hypoxia has a role in maintaining cells in a pluripotent state (Yoshida 2009; Forristal 2010). Thus, four study groups were created: no inhibitor/normoxia, inhibitor/normoxia, no inhibitor/hypoxia and inhibitor/hypoxia.

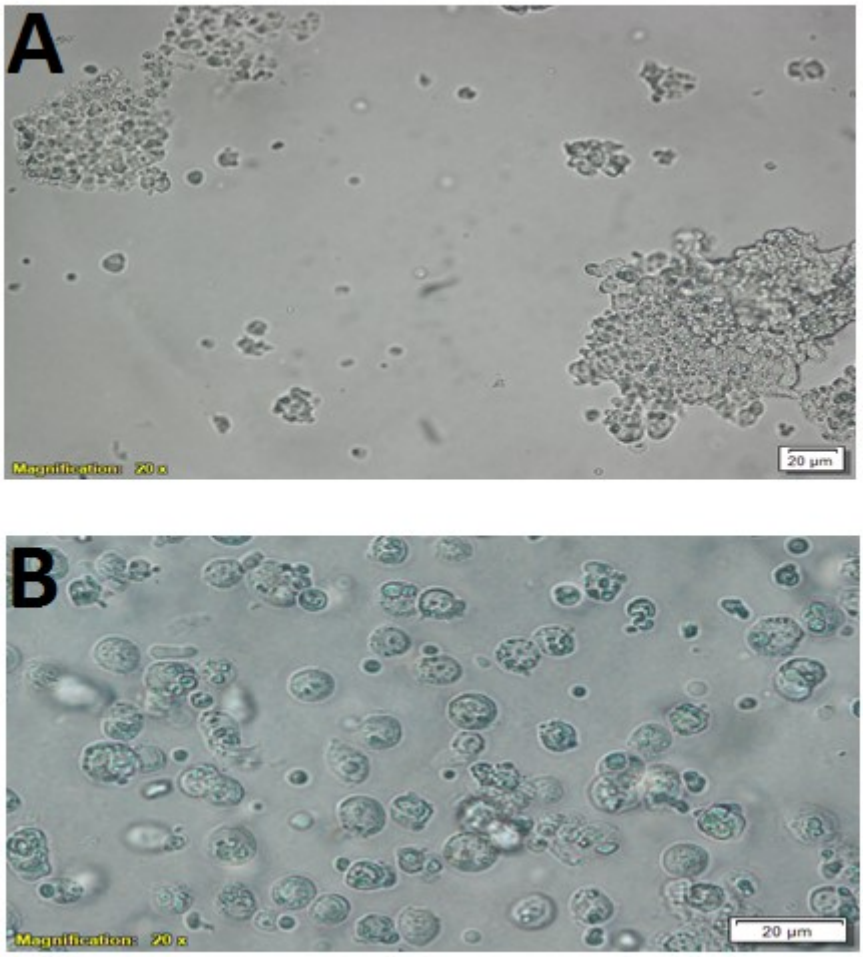


Figure 5.5 Comparing the passaging of human IPSCs as clusters vs single cells.
A) Human IPSCs after dissociation, as large aggregates or clumps. B) Human IPSCs after dissociation as singe cells in the presence of 10 µM of Y-27632 ROCK inhibitor. (Scale for both images: 20µm).

Single cell suspensions of human IPSCs proliferation were assayed by quantification of metabolically active cells using the MTS assay at 4 time points 12, 48, 72, and 96 hours and the four groups mentioned above. Interestingly, the inhibitor/hypoxia group showed a significantly higher number of cells in culture for all time points (Figure 5.6 A, B, C and D). After 12 hours, around $4x10^4$ cells out of the $5x10^4$ initially seeded survived in the condition inhibitor/hypoxia, a significant difference in comparison with the other conditions (Figure 5.6 A). At 48 hours, cells had doubled in number to $1x10^5$ in the inhibitor/hypoxia group whereas in inhibitor/normoxia they had reached less than $7x10^4$.

Likewise, at 72 hours, the proliferation rate continued exponentially in the inhibitor/hypoxia group and reached more than $2x10^5$ cells. Finally, after 4 days, cell numbers were significantly higher in presence of inhibitor and 5% O_2 compared to all other groups. The positive effects of the Y-27632 ROCK inhibitor on cell growth have been extensively studied (Watanabe et al., 2007). However, in this condition, where the low oxygen tension of 5% was combined with the use of the inhibitor, cell numbers increased drastically in comparison with Watanabe's observations (inhibitor/normoxia). Recently, Piltti et al. showed that exposing chondrocytes to 10 μM Y-27632 and only 5% oxygen resulted in the deregulation of cell cycle associated proteins, cellular growth and proliferation, and development of tissue-like morphology. In addition, increased production of extracellular matrix was also observed in chondrocytes under these conditions (Piltti et al., 2017). The observation of increased cellular attachment after 12 hours under hypoxic conditions (Figure 5.7 B) could provide an explanation for the increased cell proliferation in the rock/hypoxia group. Although there was no treatment with 10 μM Y-27632 in the no inhibitor/hypoxia group, proliferation was >2-fold higher when compared to the no inhibitor/normoxia group over the whole 96 hours, denoting the positive effect of the low oxygen tension in proliferation (Figure 5.6 C).

Previous studies have reported that hypoxia enhances adhesion, through enhanced production of ECM (extracellular matrix) proteins such as fibronectin and E-selectin, by inducing the expression of the integrin chains αV, α6, and β5 (INs). For instance, hypoxia has been shown to enhance the expression of β1 through a HIFα mediated transcriptional mechanism in breast carcinoma cells, human colon cancer cells, fibroblasts and ESCs (Berry et al., 2000; Pirone et al., 2006; Kim et al., 2010; LEE, 2011). The effects of the ECM are mediated mainly by surface receptors such as integrins, which trigger different cellular responses. From these studies, it is clear that altered reactive oxygen species (ROS) levels have an effect on IN-mediated signaling, and thereby also have an effect on cell adhesion, migration, and survival. In addition, hypoxia stimulates the production of galectin-1, a lactose-binding lectin, which enhances cell-to-ECM adhesion and has been shown to contribute through this mechanism to hypoxia-induced pulmonary hypertension in mice (Jean et al., 2011). These mechanisms may provide an explanation for the results seen in the conditions where low oxygen tension was present but no inhibitor was added, suggesting that hypoxia, on its own, plays an important role in IPSCs single-cell

survival. Moreover, the potential of Y-27632 to enhance cellular adhesion has also been observed in other cell types, for example, adhesion of human trabecular meshwork cells to fibronectin or collagen type I is increased by the addition of Y-27632. Recently, it has been reported that addition of ROCK inhibitor in Matrigel™ ® may increase plating efficiency by influencing ECM-integrin interactions. In contrast, it has been observed that ROCK-treated human ESCs are considerably more difficult to dissociate enzymatically, regardless of the type of enzymatic dissociation used, whether it be Trypsin, TripLE, Accutase, or Collagenase (Li et al., 2009). This observation implies that ROCK inhibitor treated cells display an increased cellular adhesion or "stickiness" of the plasma membrane(Krawetz, Li and Rancourt, 2009).

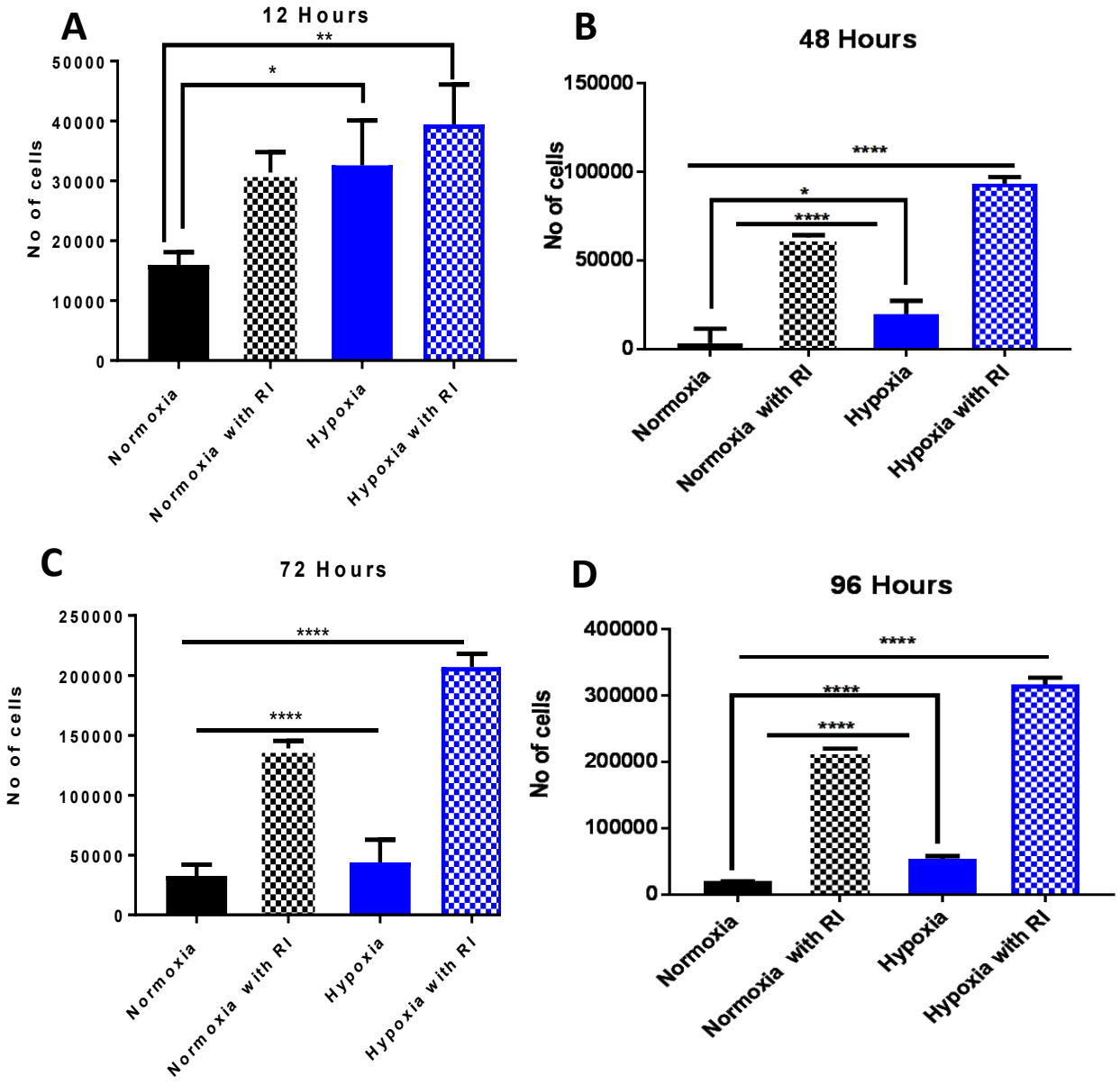


Figure 5.6. Cells proliferation of single human IPSCs in different conditions and different time points.

Cellular proliferation was evaluated with the MTS assay. A) After 12 hours, cell proliferation in both hypoxia groups was significantly higher in comparison to no inhibitor-normoxia B) ,C) after 48 and D) 96 hours, hypoxia with inhibitor was remarkably better in comparison to other groups; normoxia with inhibitor showed significantly higher cell proliferation compared to both groups without inhibitor; the no inhibitor/hypoxia showed improved survival and proliferation when compared to the no inhibitor/normoxia group. Data are expressed as mean ± SD of four independent experiments. (****P<0.0001, **P<0.1 and *P<0.5; p-values calculated from one-way ANOVA)

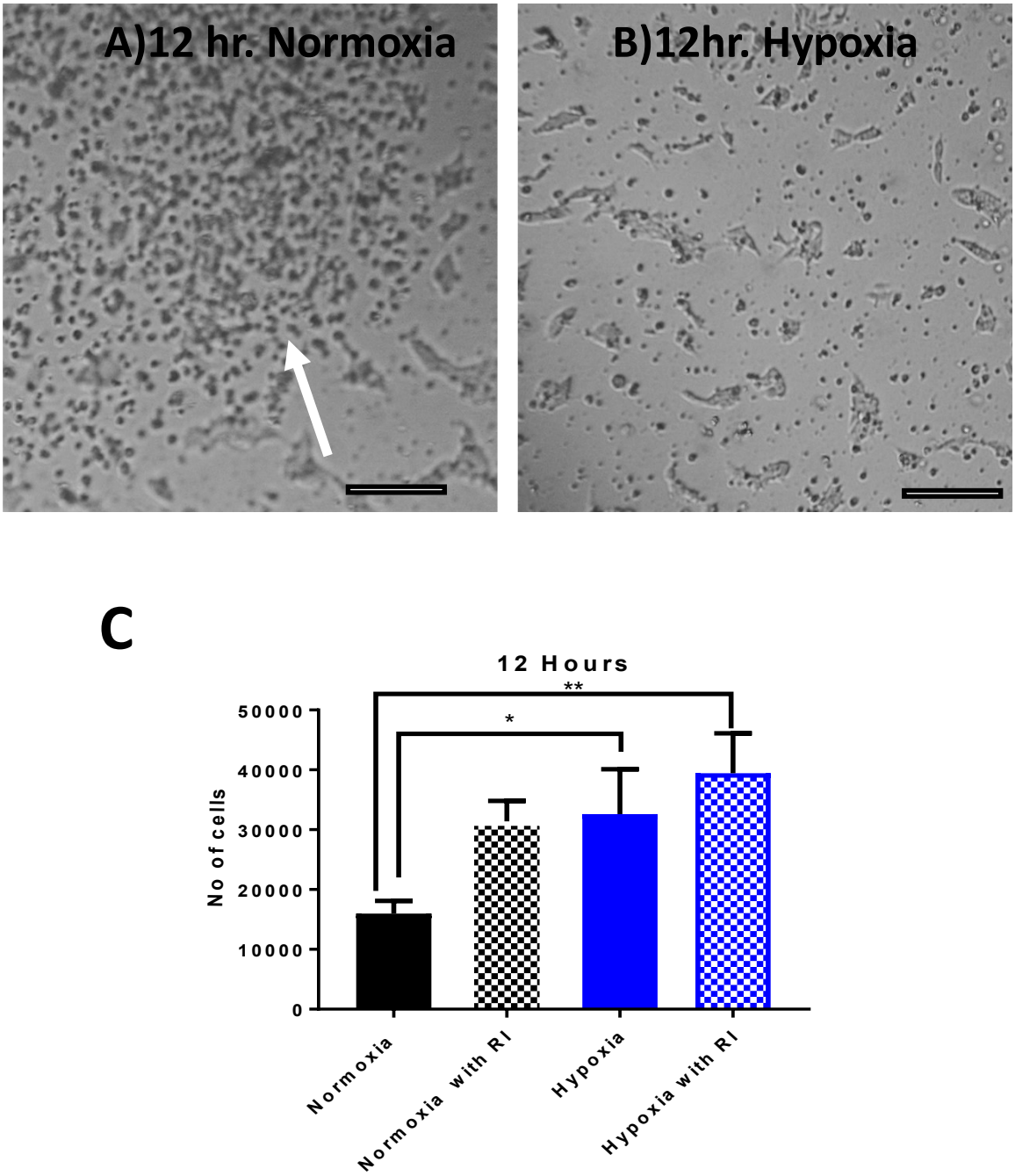


Figure 5. 7 Single human IPSCs after 12 of plating.

A) Cells are poorly adherent after 12 hours under normoxia in the absence of inhibitor. B) No floating cells observed in hypoxia in the absence of inhibitor. Scale bars, 50 μm. C) After 12 hours, cell numbers in the no inhibitor/hypoxia group were significantly higher compared to both normoxia groups and inhibitor/hypoxia group. Cellular proliferation was evaluated by MTS assay. Data are expressed as mean ± SD of four independent experiments. (**P<0.1 and *P<0.5; p-values calculated from one-way ANOVA)

Although, to the best of my knowledge no study has shown the combined effect of ROCK inhibitor and 5% oxygen, there have been previous evidences of their separate effects (Krawetz, Li and Rancourt, 2009). Many of the hypoxia-related effects include the activation of the HIF pathway, which plays many roles in several downstream-target genes. At 5% oxygen Catherine et al. 2010, demonstrated cell proliferation and attachment of human ESCs cells whether on MEFs or feeder-free on Matrigel™, and increased cell proliferation data, which is in agreement with the results of Ludwig et al. 2006 (Forristal et al., 2010a; Ludwig et al. 2006). This may be due to the increase in Nanog expression levels, since it has recently been shown that Nanog is involved in the regulation of S-phase entry in human ESCs and that overexpression of this gene results in a significant increase in proliferation, through binding to regulatory regions of CDK6 and CDC25A, as these are important cell cycle regulators (Neganova et al. 2009; Zhang et al. 2009). Similarly, increased proliferation rates have also been observed in many other primitive populations including mesenchymal stem cells and neural progenitor cells when cultured under low oxygen tensions (Grayson et al. 2007; Zhao et al. 2008). This indicates that there is accumulating evidence suggesting that ROCK inhibition may play an active role in cell cycle regulation (Chen et al., 2009; John et al., 2004; Yin and Yu, 2008; Zohourabian et al., 2009). In addition, inhibiting the ROCK pathway has a direct effect on cell proliferation in different type of cells, as for examples Nakashima et al. 2011 have shown it to enhance pancreatic cancer cell proliferation; Nakamura K et al. 2014 on maintenance of the multi-layered proliferation of confluent mouse ESCs; Horani A. et al. 2013 enhanced basal-cell proliferation in cultured human tracheobronchial and mouse tracheal epithelial cells and GSL Peh et al. 2015 on the propagation of primary human corneal endothelial cells. The inhibitor/normoxia group showed significantly higher cell numbers after 48 and 96 hours compared to groups without inhibitor (Figure 5.6 B and D). In agreement with Watanabe's observation, the no inhibitor/normoxia group showed poor survival of human IPSCs in single cell suspensions throughout 96 hours (Nakashima et al. 2011; Nakamura et al. 2014; Horani A. et al. 2013; Peh et al. 2015).

The question of whether the inhibitor/hypoxia group had an impact on the cellular self-renewal capacity remains unanswered. This finding would not be of use for the culture if it affected the quality of the cells. The expression of the pluripotency markers

Nanog, Oct3/4 and SSEA4 was assessed by flow cytometry, with cells in all conditions expressing >70% of all markers, without any statistical significance between the groups (Figure 5.8). The positive effect of hypoxia on pluripotency observed in many studies is likely explained in part by the demonstration that OCT-4, SOX-2 and Nango have all been shown to be regulated by HIF-2α (Covello et al., 2006; Forristal et al., 2010a). Moreover, recent papers by Kurosawa et al. and Gauthaman et al. have brought to light the important role of ROCK signalling for the maintenance of human ESCs pluripotency. Kurosawa et al. (Kurosawa, 2012) have demonstrated that Y-27632 treatment increased levels of Oct4 expression and according to Gauthaman et al. (Gauthaman, Fong and Bongso, 2010), human ESCs can be grown without the need for niche-forming feeder layers or animal-derived matrices with the addition of Y-27632 to a single synthetic matrix. Although further investigation is required, as there are many possible mechanisms for hypoxia and ROCK-inhibitor treatment, these results are quite promising and provide a first evidence of the combined effect of these two strategies in obtaining a viable pluripotent single-cell suspension of human IPSCs. Unstained human IPSCs cells and the manufacturer recommended isotype controls were used as controls to set the exclusion gates that generated these results please reviewed the plot at (Appendix III).

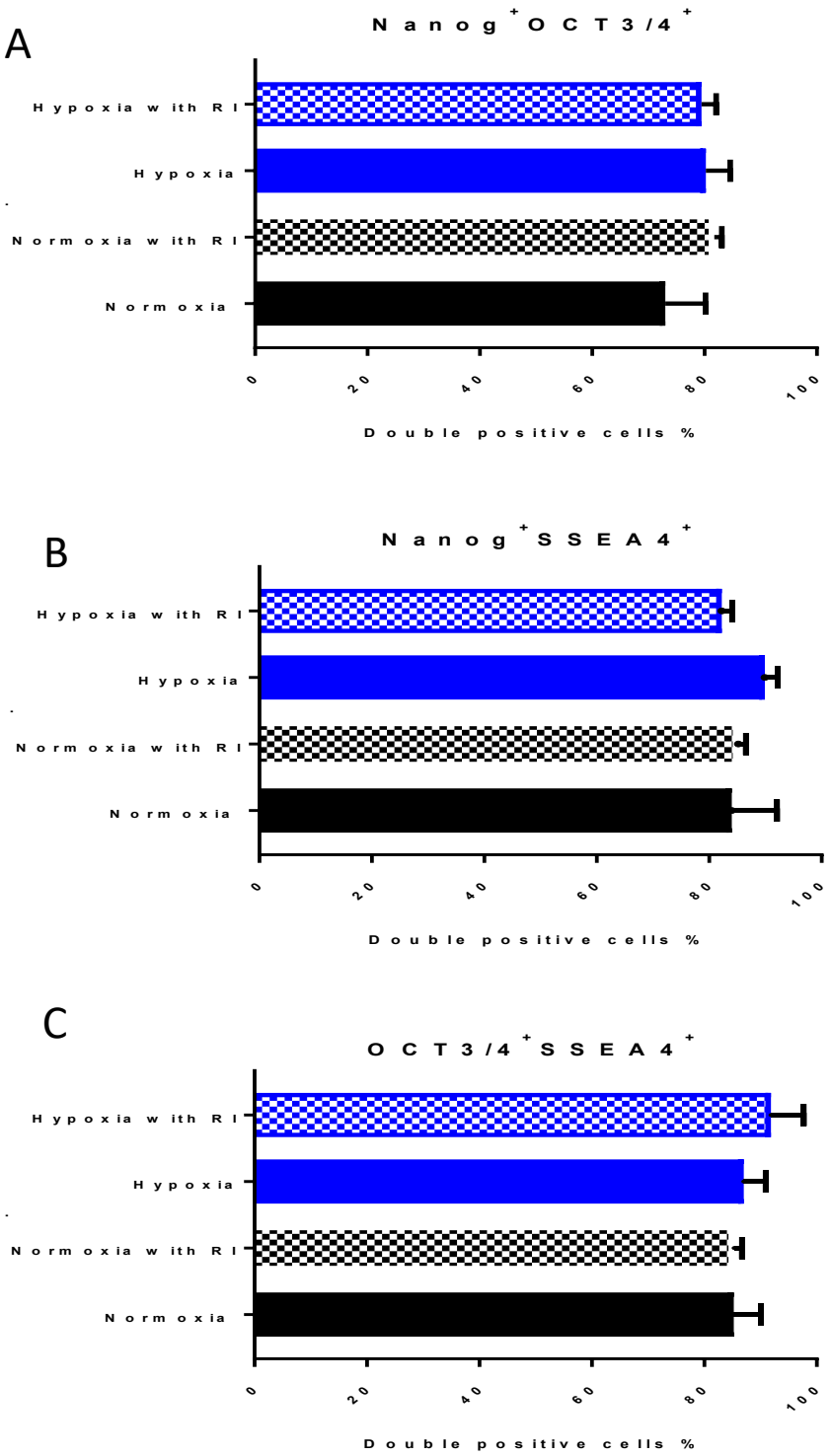


Figure 5. 8 Flow Cytometry Analysis of Pluripotency Marker Expression of human IPSCs dissociated to single cell suspensions in in different conditions at 96 hours.
The percentage of double positive cells of both nuclear markers OCT4/3 and Nanog positive was at comparable level within the groups B) and C) the same result was observed for the double positive of nuclear marker Nanog and surface mark SSEA4 and nuclear marker OCT4/3 and surface mark SSEA4. Unstained human IPSCs control and isotope control. (Appendix III).

Final, to confirm the robustness of these experiments, the same conditions were applied to the human ESCs 9H cell line and the same trend was observed for all the groups. In this section, human ESCs were used to evaluate the effect of ROCK present or absent and oxygen tension level and compare their effects with those observed on human IPSCs (Figure 5.9 B and C).

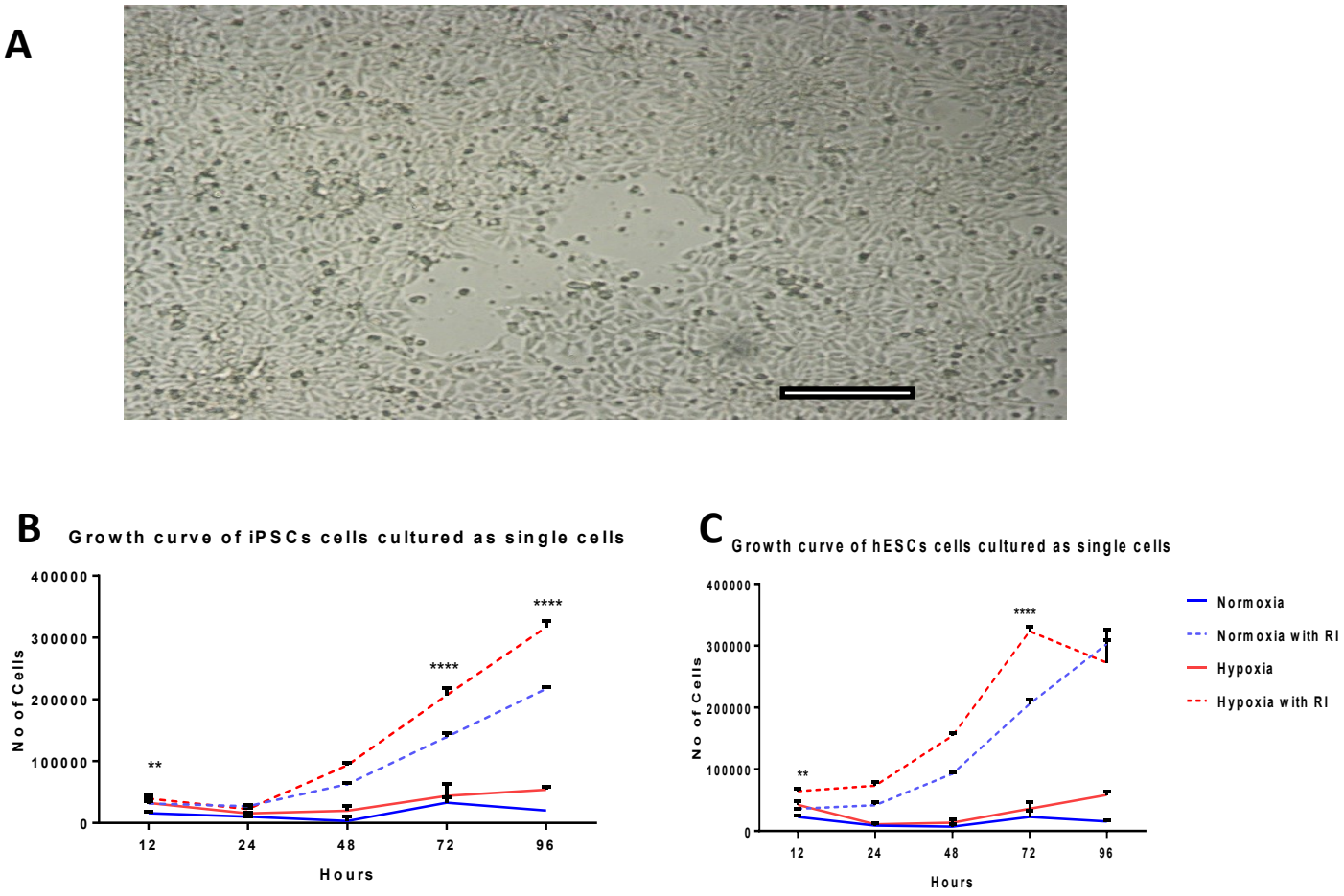


Figure 5. 9 Comparing cellular proliferation of human IPSCs and ESCs.
A) Human ESCs confluent after 96 hours (hypoxia with inhibitor). Scale bar, 50 µm; B) and C) Growth curve of IPSCs and human ESCs cultured as single cells within different time courses in different conditions of Y-27632 treatment and hypoxia. Both cell types show positive effects of hypoxia with RI in the first 12 hours until the end of the culture. Data is expressed as (mean ± SD) of four independent experiments. (**P<0.01, ****P<0.0001, two-way ANOVA, one-way analysis of variance).

5.5 CONCLUSION

Our findings supported previous evidence showing that culturing human IPSCs in mTeSR™1 medium and Matrigel-coated plates maintained stemness with high expansion rates (Lannon et al., 2008). As compared to the conventional protocols, this culture method is simple, straightforward, and reproducible. Using different self-renewal assays involving ICC, AP and flow-cytometry proved the ability to maintain undifferentiated human IPSCs in these experiments. Sustaining pure pluripotent colonies prior to the differentiation process is vital to enable the ease of lineage derivation and to reduce heterogenic cell populations. Therefore, self-renewal assessments should be a routine assay performed during different stages of differentiation to determine the presence or absence of pluripotency markers. Hypoxia combined with rock inhibition enhances proliferation of single human IPSCs. Additionally, pluripotency markers show a similar expression both in hypoxia and normoxia with or without ROCK inhibitor treatment conditions.

Single-cell cultures of human ESCs show a similar growth trend when compared to human IPSCs. In summary, the results presented in this chapter are extremely promising but need further experimentation to unveil the underlying mechanisms associated with the combined effect of low oxygen tension and an inhibitor of the ROCK pathway. This method allowed for a successful encapsulation of viable pluripotent human IPSCs, as described in the following chapters, improving the efficiency of the application of any differentiation protocol to these cells.

Chapter 6

Maintain of Human-induced pluripotent stem cells (human IPSCs) Proliferation and Pluripotency in Alginate Beads and Evaluate the Effect of Static and Dynamic Motion

Results presented in chapter 5 have shown that dissociation of colonies into single cells was proven to be successful by the addition of the Y-27632 ROCK inhibitor without reducing the pluripotency of the cells. The next goal was the optimization of the culture conditions in three-dimensional (3D) alginate beads and the HARV bioreactor. In this chapter, the testing of several conditions aimed at optimizing viability/ proliferation in the 3D environment is described: static vs. dynamic cultures, adhesion protein added to alginate (Matrigel™ vs. Gelatin) and the influence of the long-term addition of Y-27632 to the culture. All results will be assayed for proliferation using the MTS proliferation assay. Moreover, cells will be analysed all for the expression of pluripotency, hypoxia response, ECM and ectoderm markers.

6.1 Introduction

Human induced pluripotent stem cells (human IPSCs), have several promising biomedical applications, such as cell replacement therapies, tissue engineering, and high-throughput toxicological and pharmacological screenings (Lewitzky and Yamanaka, 2007). The use of these cells for any of the mentioned applications requires large numbers of cells of high quality. However, the scalable expansion and differentiation of these cells has proven to be very demanding and inefficient, particularly has it most commonly resorts to the use of two dimensional cultures (Lei and Schaffer, 2013). Most of our understanding of biological stem cell processes has been obtained largely from two dimensional monolayer cultures. Currently, 2D-based cell culture systems suffering from inherent heterogeneity and limited scalability have emerged as bottlenecks for producing sufficient numbers of high-quality cells for biomedical applications. In *vivo*, cells are incorporated in a complex

environment composed of the extracellular matrix (ECM), mechanical and chemical cues (such as cytokines and growth factors). The plastic surface used for tissue culture lacks the structural, mechanical and biochemical cues that provide human PSCs with the structure and support of their natural environment *in-vivo* (Kinney, Sargent and McDevitt, 2011). A recent strategy arose to circumvent this problem utilising various natural or synthetic biomaterials, or encapsulating 3D constructs. These approaches not only help avoiding extrinsic factors supplement but aim at mimicking as well an environment similar to the one found *in-vivo* (Chowdhury et al., 2010a; Randle et al., 2007; Hwang et al., 2009).

Cell encapsulation means the entrapment of living cells within the structure of semi-permeable membranes, forming a three-dimensional structure. These membranes allow for the exchange of nutrients, oxygen and stimuli between the culture environment and the cells, excluding antibodies from the host that are larger than the capsule pore size, striving to create products with low immunogenic response (Orive et al., 2003). Another advantage of cell encapsulation was shown in a study by Dean et al. (Dean et al., 2006) where encapsulated mouse embryonic stem cells (mouse ESCs) and human ESCs did not result in the formation of teratomas 4 weeks after transplantation into the immunodeficient SCID mice, an important breakthrough in the PSCs field, as teratoma generation is one of the problems to avoid when using this type of cells. Furthermore, this 3D configuration has been shown to promote better growth, differentiation, maturation and protein secretion of various cell types, particularly mesenchymal stem cells (Batorsky et al., 2005), mouse ESCs (Dean et al., 2006; Wang et al., 2006), human ESCs (Dang et al., 2004) and neural stem cells (X. Li et al., 2006).

Despite the numerous advantages of this approach, some studies have also highlighted significant challenges for 3D human PSC culture (Serra et al., 2012) one of them being the use of undefined human or animal derived components (e.g., Matrigel™ , serum, and/or albumin), which limits reproducibility and/or scalability and impairs the use of good manufacturing practice (GMP) for cell production (Unger et al., 2008) . Furthermore, there are two ways of seeding cells for human PSC-aggregated cultures: clump versus single-cell inoculation, which poses another problem. One of the major problems of inoculating cell aggregates is that it is difficult to control the size of human PSC clumps, which

may lead to increased apoptosis or spontaneous differentiation in the course of the culture. On the other hand, single-cell inoculation for suspension culture, using the inhibitor of the ROCK pathway Y-27632, has shown to be one way to control the size of human PSC aggregates (Watanabe et al., 2007). Mass transport is also raised as a limiting factor for 3D culture in static conditions, due to the difficulty of nutrients and gases to reach the centre of the construct. This limitation is reduced when encapsulated cells are cultured in "well mixed" dynamic bioreactors (Randle et al., 2007; Hwang et al., 2009). For instance, a rotary wall vessel (RWV) bioreactor has been shown to improve the mass transfer in alginate hydrogel beads, by providing a constant fall motion mimicking a micro gravity environment. This bioreactor is an example of a dynamic motion culture that aids mass transfer with minimal shear stress. The use of a high aspect ratio vessel (HARV) has also been shown to increase passive diffusion transport by 100 times in comparison with RWV and to improve cell densities to approximately $3x10^6$ cells/mL due to the combination of the absence of shear stress and the improved passive mass transport (Randle et al., 2007).

6.2 Aim and Hypothesis

6.2.1 Aim

The aim of this chapter is to assess the effects of 3D culture platforms on viability, proliferation, metabolic profiles, self-renewal, differentiation and morphology of human IPSCs.

6.2.2 Objectives

1. Assess the effects of cell adhesion protein added to alginate (Matrigel™ vs. Gelatin) on cell proliferation.
2. Assess the influence of the long-term addition of Y-27632 to the culture.
3. Determine the effects of 3D static/dynamic condition on the growth kinetics, pluripotency level, ECM production and oxygenation level effect.

6.3 Method

Undifferentiated human IPSCs (day 4 or 5 of culture) were incubated with fresh mTeSR™1 medium supplemented with 10 μM of Y-27632 and then resuspended in 1.1% (w/v) low viscosity alginic acid (Sigma–Aldrich, Dorset, UK) and 0.1% (v/v) bovine gelatin (Sigma-Aldrich) at room temperature (solution in PBS at pH 7.4). Using a peristaltic

pump from a drop height of 3 cm the cell-gel solution was passed through a 25-gauge needle into a sterile 100mM $CaCl_2$ solution at pH 7.4. Gelation was instantaneous on contact with the $CaCl_2$ solution resulting in the formation of spherical beads (approximately 2.5mm in diameter after swelling.

Several conditions were tested to optimize viability/proliferation in the 3D environment: static vs. dynamic cultures, adhesion protein added to alginate (Matrigel™ vs. Gelatin) and the influence of the long-term addition of Y-27632 to the culture. All results were assayed by using the MTS proliferation assay at days 1, 5, 10, and 20 respectively. Moreover, cells were assayed for their expression of pluripotency markers Nanog and Oct3/4, PAX6 an ectoderm differentiation marker as spontaneous differentiation marker, HIF1α and HIF2α, as it has been suggested that with time there will be the formation of a hypoxic niche in the core of the bead and laminin5 and fibronectin to verify the production of extracellular matrix (ECM), all by qRT-PCR on day 5 day and day 20 for 2D culture, 20 days for 3D static and 3D dynamic culture Sample collected at Day 5 for qRT-PCR, and light microscopic micrograph to compared 2D culture with 3D static and dynamic. In addition, qRT-PCR comparison between 3D static and dynamic culture was done at day 5 and 20 vs day 5 in 2D culture (Figure 6.1)

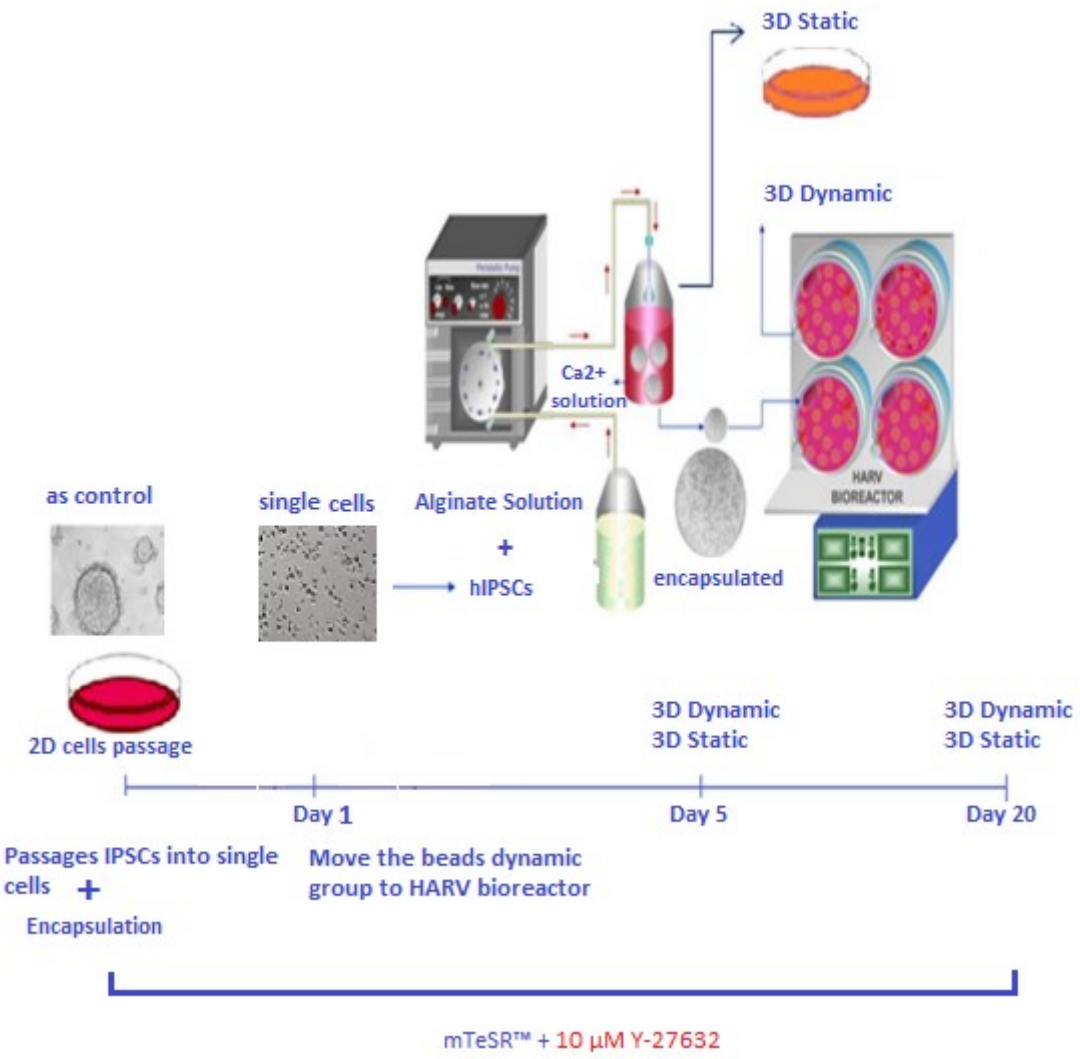


Figure 6.1: Summary of the experimental scheme used to culture cells in 3D platforms. (Modify Teo, Mantalaris and Lim, 2014).

6.4 Results and Discussion

6.4.1 Human IPSCs morphology in alginate hydrogels microbeads

The undifferentiated human IPSC cells encapsulated in alginate hydrogels and cultured for extended periods of time (20 days) without passaging, enzymatic or mechanical dissociation were evaluated morphologically. As a control, human IPSCs cells were cultured on feeder-free Matrigel™ and mTeSR™1 as monolayer (Figure 6.2 A). Each alginate bead contained approximately 20000 single cells (Figure 6.2 B) upon encapsulation. Cells tend

to aggregate over time and at day 5 the cells proliferate more in the dynamic group (Figure 6.2 F). These human IPSCs cell aggregates presented a spherical or oval shape with closely packed cells inside; showing no morphological indications of the formation of germ layers or of cystic cavities in culture. At day 5 in both 3D cultures aggregates were sectioned down the middle to investigate the morphological characteristics of the tightly packed cells. The cells were found to be tightly packed and very homogeneous (Figure 6.2 C, D). There was no formation of typical tissue-like structures such as the teratoma features that might indicate the formation of the three germ layers.

The encapsulated aggregates were originally small in size but increased as the culture progressed, but despite their size they remained intact and did not escape the hydrogel for the duration of the culture periods. The aggregates formed were tightly packed and defined spherical and homogeneous borders could be observed. These aggregates remained undifferentiated and pluripotent over prolonged periods of maintenance culture without any mechanical expansion or manipulation, as the following results confirm.

Previous work using alginate beads found they could enable pluripotency maintenance for up to 250 days without cell passaging (Siti-Ismail et al., 2008) There have been several reports of human ESCs cultured on scaffolds or hydrogels (Gerecht et al., 2007; Levenberg et al., 2003; Chung, Rodriguez and Healy, 2006; Mohour, de Pablo, & Palecek, 2006). In agreement with the observations made in this thesis, cultures in 3D appeared to maintain human ESCs in an undifferentiated state (Li et al., 2006) for several weeks without passaging (Mohour et al., 2006). Particularly, Gerecht and colleagues (2007) encapsulated human ESCs in hyaluronic acid hydrogels and proved that these remained undifferentiated, preserved their normal karyotype and maintained their differentiation capacity in EB formation (Gerecht et al., 2007).

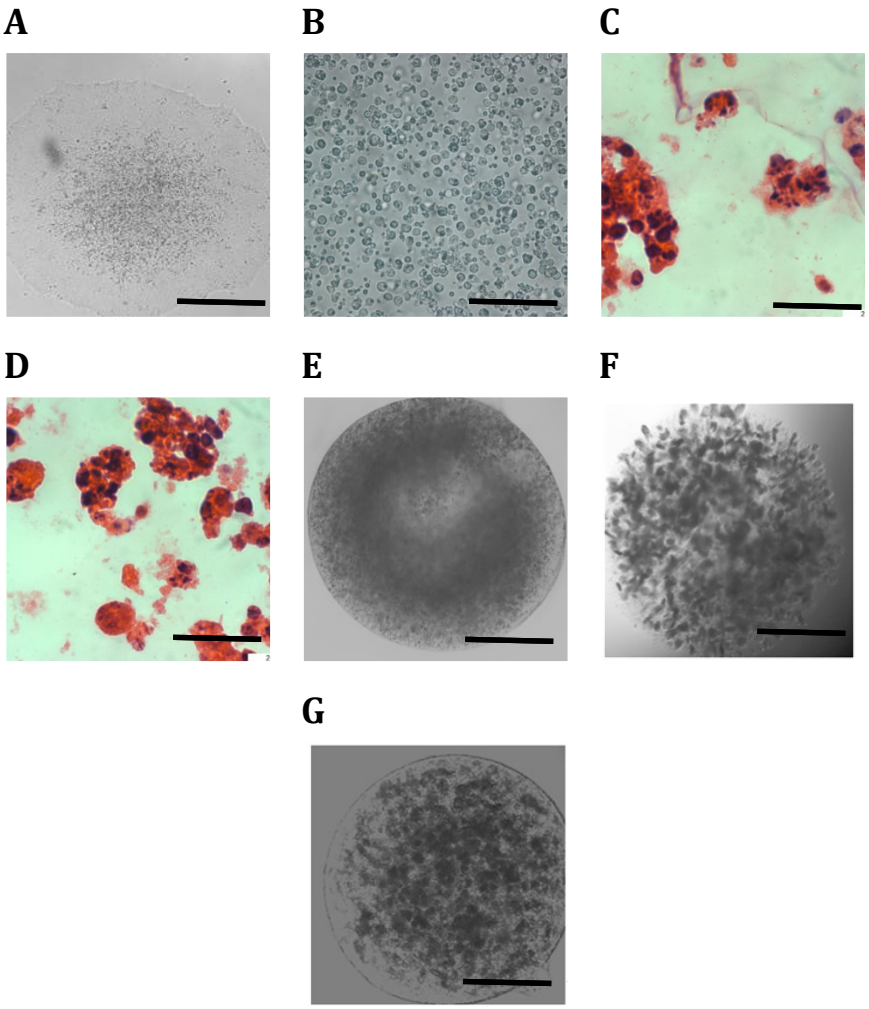


Figure 6.2: IPSCs morphology before and after encapsulation.
A) Image of Day 5 in 2D culture showing large and tightly packed human IPSCs multicellular colonies with distinct borders, which was the optimal time for passaging was used as control. B) Human IPSCs passaging as single cells were then incubated with fresh mTeSR™1 and 10 µM of Y-27632 for 2 hours to encapsulated cells be resuspended in 1.1% (w/v) low viscosity alginic acid to encapsulated. C) Image of Day 5 in 3D static culture staining with Hematoxylin – eosin (H&E) for cellular morphology and overall cell distribution within the hydrogel There was no formation of typical tissue-like structures such as the teratoma. D) Image of Day 5 in 3D dynamic culture staining with Hematoxylin – eosin (H&E) for cellular morphology and overall cell distribution within the hydrogel was no formation of typical tissue-like structures such as the teratoma. E) Human IPSCs after 24 hours of encapsulation before moved to HARV culture. F) Day 5 from 3D dynamic culture showed highly proliferative and packed viable cells without any sing of debris. G) Image of Day 5 from 3D static culture showed the aggregates of cells and smaller particules possibly debris from necrotic or dead cells. Scale: 200µm for figure A and 20 µm for figures B-G.

6.4.2 Optimization of proliferation of human IPSCs 3D cultures

Several conditions were tested to optimize viability and proliferation in 3D environments: static vs. dynamic cultures, adhesion protein added to alginate (Matrigel™ vs. Gelatin) and the influence of the long-term addition of Y-27632 to the culture.

6.4.2.1 Simulated dynamic motion and 3D culture promote the proliferation of human IPSCs

Proliferation was assessed at different time points to compare cells growing in 3D dynamic to cells in 3D static conditions. Cell proliferation was measured using MTS assay, where viable cells convert tetrazolium salts to a formazan product in metabolically active cells. After 24 hours from encapsulation, the first MTS measurements were performed before moving the beads onto the dynamic culture. This showed viable single cells as well as it allowed for the normalization of the other time points with first 24 hour. At day 5 the cellular proliferation increased more than 2-fold from day one and significantly more than cells cultured in 3D static mode (Figure 6.3). Moreover, the proliferation rate in dynamic cultures was higher, at all-time points, and was statistically significantly again at day 15 compared to static (Figure 6.3). Dynamic or microgravity culture conditions are also known to modulate cell proliferation and survival (Grimm et al., 2014; Jha et al., 2016). For example, simulated microgravity has been shown to increase the proliferation of bone marrow-derived human mesenchymal stem cells (Yuge et al., 2006). Therefore, by using the HARV bioreactor in a gentle, low-shear and low-turbulence environment, with sufficient oxygenation and effective mass transfer of nutrients and waste, it is able to promote cell proliferation (Jha et al., 2016). Surprisingly, qRT-PCR results at day 5 showed that, in dynamic cultures, FN1 and LAMA5 were upregulated significantly compared to static. FN1 has been linked to a number of signaling pathways essential for ESCs self-renewal and proliferation. For example, FN1 phosphorylates Akt and activate PI3K/Akt signaling and ncogenes such as C-Myc, associated with self-renewal (Park, Ryu and Han, 2011). Subsequently, it promotes cell survival and proliferation through the activation of caveolin-1 signaling and their interaction in the ECM network enhances cell adhesion and has an important impact in cell proliferation. (Yue, 2014).

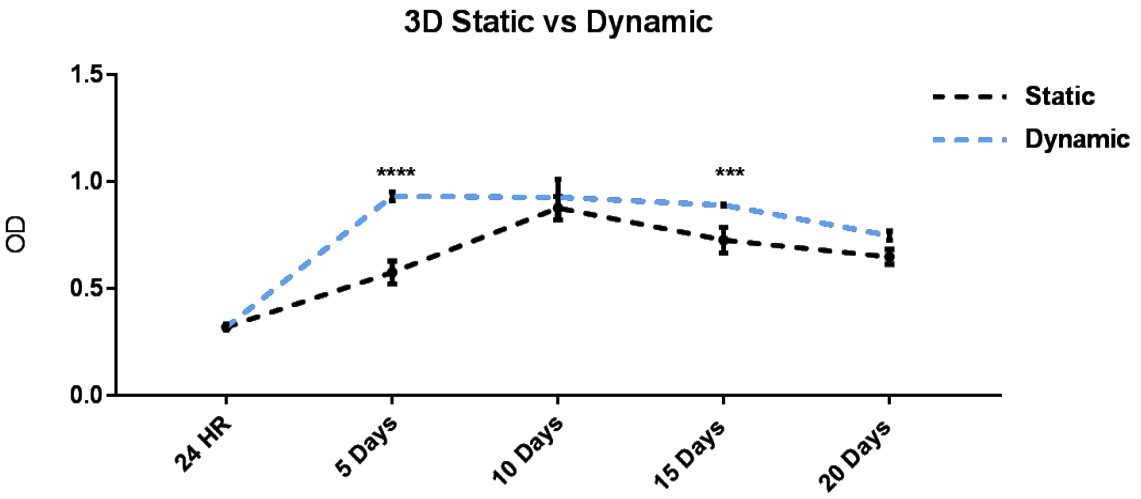


Figure 6.3 Comparison of cells proliferation between static and dynamic cultures of human induced pluripotent stem cells.

Proliferation plot were determined by MTS assay. Cells growth were applied to absorbance at 570 nm. Cells encapsulated in 1.1% alginic acid and 0.2% gelatin at dynamic show significantly different proliferation at day 5 and day 15 compere to static. Data shown as mean of three independent experiments. Error bars show one standard deviation. P-values obtained by two-way ANOVA (***P<0.001 and ****P<0.0001).

6.4.2.2 The effect of adhesion substrate on cells proliferation added to alginate solution (Matrigel™ vs. Gelatin)

From previous experiments it has been found that cellular proliferation was enhanced in dynamic 3D cultures. Consequently, further optimisation was carried out in this culture mode. To find an optimal adhesion substrate to improve cell adhesion and subsequent proliferation, alginate solution mixed with Matrigel™ and alginate solution mixed with Gelatin were compared. Cell proliferation assessed by MTS indicates that a good proliferation was maintained throughout the culture in both culture groups, with no significant differences between the two conditions, except at day 10 (Figure 6.4). Previous studies have demonstrated that improving cell adhesion to the scaffold enhances cells proliferation. Surface modification to increase the adhesion and proliferation of cells is an area of interest in biological and biomedical research for the use of various synthetic materials (Anselme and Bigerelle, 2006). Considering the various options available, alginate and gelatine were preferred it in term of cost and ease of preparation.

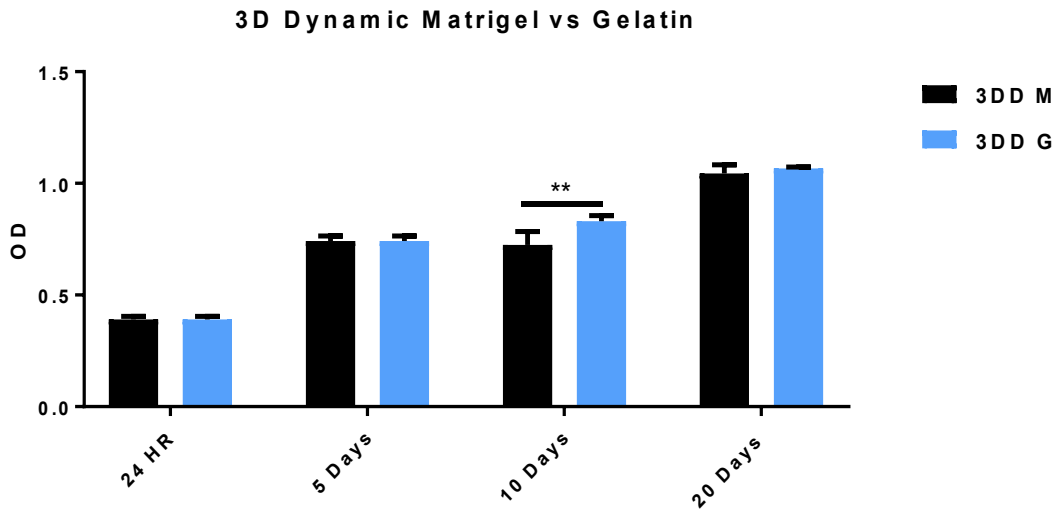


Figure 6.4 Comparison of cell proliferation of human IPSCs encapsulated in hydrogels of (alginate/gelatin - 3DD G) or (alginate/Matrigel™ - 3DD M) in 3D dynamic cultures.

Proliferation plot was obtained by MTS assay. No significant difference was seen in proliferation between cells encapsulated in 1.1% alginic acid and 0.1% gelatin and cells encapsulated in 1.1% alginic acid and Matrigel™ in dynamic motion, except at day 10. All data represents the mean of three independent experiments; error bars show one standard deviation. P-values obtained by two-way ANOVA**$p \leq 0.01$.

6.4.2.3 The stimulus of the long-term addition of 10 µM of Y-27632 to the culture

From chapter 5, the dissociation of colonies into single cells was proven to be successful by the addition of Y-27632 four days without reducing the pluripotency of the cells. According to our design of the 3D dynamic experiments, 10 µM of Y-27632 were added to the culture media 2 hours before passaging the cells into single cells and then cells were encapsulated and kept overnight in static condition with 10 µM of Y-27632. The first MTS measurements were performed before moving the beads to dynamic culture, showing viable single cells. The conditions were divided into two groups one with 10 µM of Y-27632 until day 20 and the other without it. Y-27632 treatment increased cells proliferation at days 5 and 20 of the 3D dynamic culture treated with 10 µM of Y-27632 compared with the non-treated group (Figure 6.5). The main purpose of this study was to investigate a way to enhance cellular proliferation and scale it up by using 3D dynamic cultures.

According to the literature, 10 μM of Y-27632 has a positive impact on human ESCs cultures, rendering them protected from apoptosis after dissociation from the colony, even in serum-free suspension cultures, allowing for the formation of floating aggregates (Watanabe et al., 2007). In addition, another study tested the ability of 10 μM Y-27632 to enhance extracellular matrix production in HCS-2/8 cells(Piltti et al., 2017), correlating with the qRT-PCR (Figure 6.12) . Moreover, Lee et al indicated that the ROCK inhibitor used purified chick embryo cells improved wound healing by promoting cell proliferation (Lee et al., 2016).

At days 5 and 20, the use of inhibitor showed a significant increase in proliferation for the condition with the continuous block of the ROCK pathway. This result suggests that by blocking this pathway, apoptosis in the long term culture is reduced, which has also been reported in David study (Claassen 2012; Chapman et al., 2014), who state the importance of the addition of this molecule even after colonies have been established. Finally, other research groups in 2014 demonstrated that the extension of keratinocytes in the presence of fibroblast feeders and a ROCK inhibitor within the time period of one month reverts cellular senescence and removing the inhibitor from the medium gradually has a negative effect on the lifespan of the same cells. Similarly, it was shown that the effect of ROCK inhibition on cellular proliferation is immediate and ROCK inhibited cells differentiation or stratification (Chapman et al., 2014).

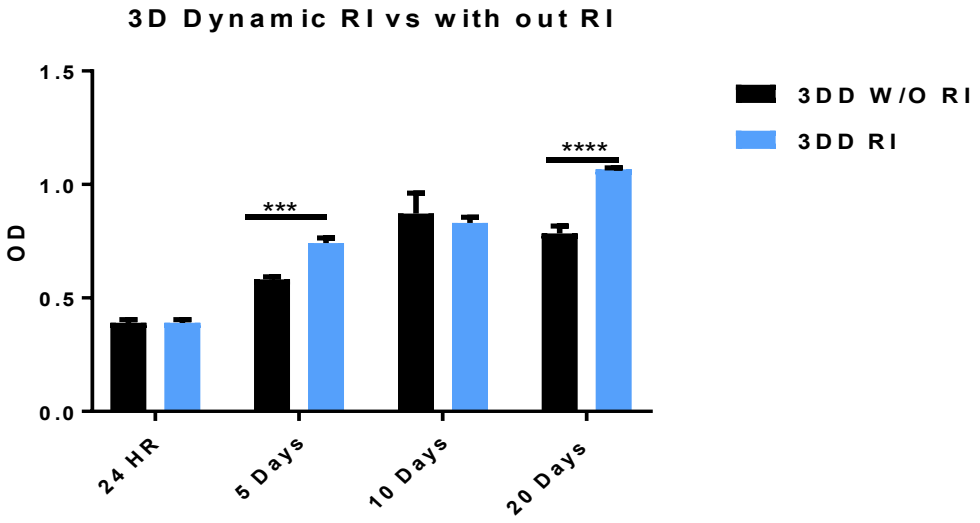


Figure 6.5 Comparison of cells proliferation of human IPSCs encapsulated within alginate hydrogel + gelatin and cultured with mTeSR™ medium with ROCK inhibitor (3DD RI) or without ROCK inhibitor (3DD W/O RI) in 3D dynamic culture.
Proliferation plot was obtained by MTS assay. Cells proliferated significantly more at day 5 and day 20 in 3D dynamic cultures with 10 µM ROCK inhibitor in comparison to those where no inhibition was used. All data represents the mean of three independent experiments; error bars show one standard deviation. P-values obtained by two-way ANOVA***p ≤ 0.001 and ****p ≤ 0.0001.

6.4.3 The gene expression profiles of self-renewal of human IPSCs and spontaneous differentiation markers

Encapsulation of stem cells in hydrogel capsules provides a defined microenvironment that can impact cell fate. In *vivo*, stem cells reside in a specific niche defined by a particular combination of soluble factors and cell–cell and matrix interactions required for self-renewal and, when necessary, differentiation and tissue regeneration (Morrison and Spradling, 2008; Scadden, 2006). In this chapter, we verified the gene expression of markers associated with pluripotency and spontaneous differentiation. We compared between the impact of dynamic and static conditions on the expression of pluripotency markers Nanog and OCT3/4 in two time points. First, this was done following a routine short-term culture for 5 days and following for a longer term for up to 20 days, without any enzymatic treatment or mechanical stress to passage the cells.

Oct4 and Nanog are two embryonic stem (ES) cell-specific transcription factors that play critical roles in the maintenance of ES cell pluripotency. 3D dynamic showed significant in Nanog and OCT3/4 endogenous expression in day 5 compared to 3D static (Figure 6.6).

However, in day 20, OCT 3/4 was significantly difference in 3D dynamic with no significant change in Nanog expression (Figure 6.6). The tested transcription factors OCT3/4, and Nanog act in the regulatory circuitry as mentioned before, where loss of OCT3/4 causes differentiation of the epiblast cells into trophectoderm derivatives (Niwa et al., 2000). Effectively, in *vivo* OCT3/4 is abundant in the inner cell mass (ICM) cells of the blastocyst and down-regulated in the trophectoderm, whereas in the primitive endoderm the level of expression increases (Palmieri et al., 1994). These findings highlight the fundamental function of OCT3/4 in preventing dedifferentiation of epiblast cells or of ESCs into trophectoderm lineage. Exogenous expression only of OCT3/4 is sufficient to generate pluripotent stem cells from mouse neural stem cells (Kim et al., 2009) and together with three other transcription factors it is essential in the reprogramming of somatic cells into the pluripotent state (Nakagawa et al., 2008; Takahashi and Yamanaka, 2006). While the other factors involved in reprogramming are replaceable by family members or other factors, without OCT3/4 no reprogramming occurs (Nakagawa et al., 2008). Although human ES and IPS cells can grow indefinitely in culture, they commonly undergo adaptive changes during prolonged passaging in vitro (Zweigerdt et al., 2011). These findings have supported the decision shown here to investigate the expression pattern in different culture time points.

Initially, 3D static presented no significant difference between day 5 and day 20 for both markers NANOG and OCT3/4 (Figure 6.8). Both these markers were significantly upregulated at day 20 compared with day 5 (Figure 6.7). It is hypothesised that the up-regulation of pluripotency master genes further along in the culture may be due to the presence of the free fall environment in the HARV bioreactor. Simulated microgravity has been found to be sufficient to sustain pluripotency in mouse ESCs in the absence of leukemia inhibitory factor (LIF) (Kawahara et al., 2009). Interestingly, Oct-4 expression was found to be at integrin-mediated focal adhesions, indicating that growing mouse

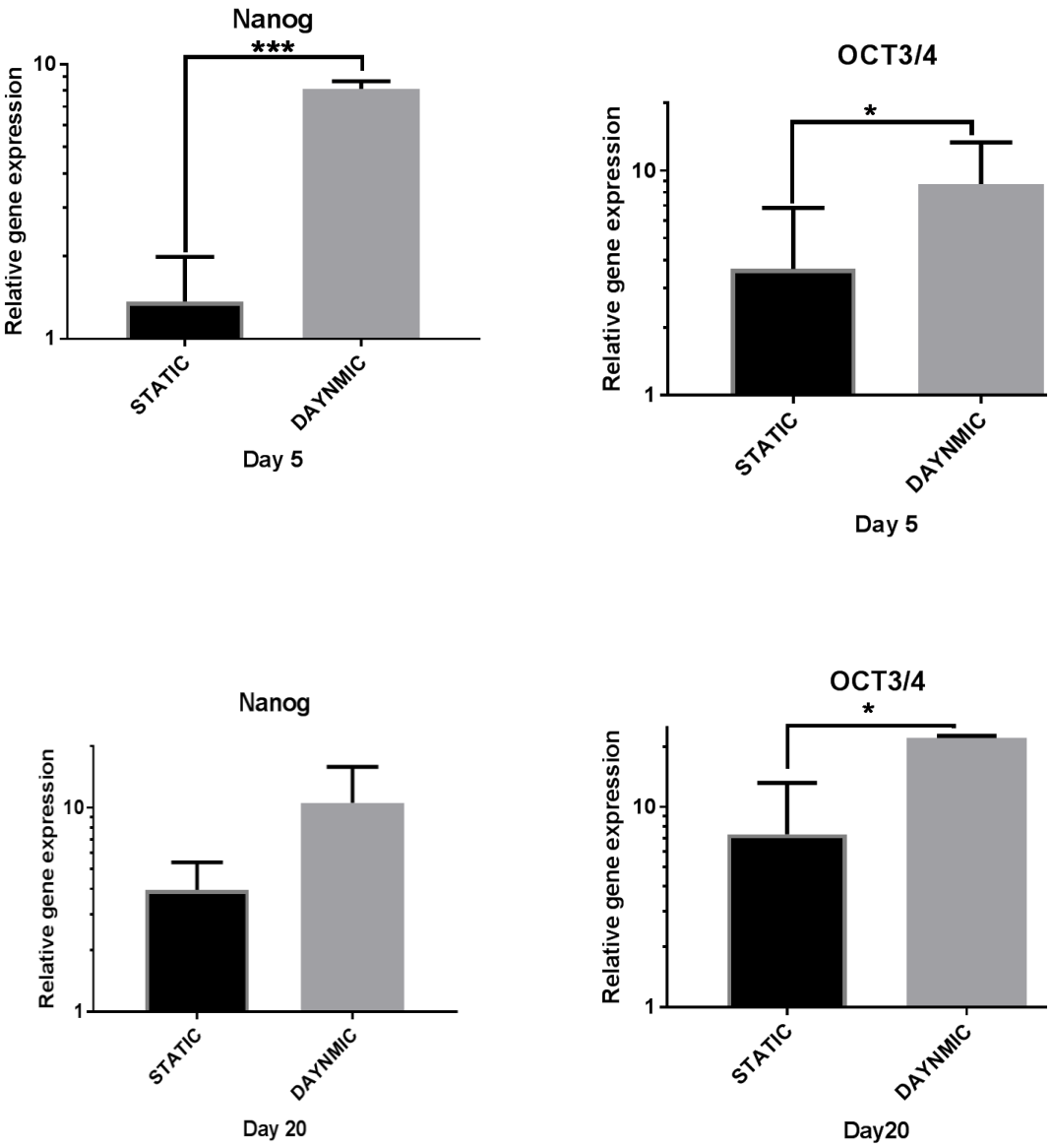


Figure 6.6: Comparing the expression of pluripotency markers OCT3/4 and Nanog in static condition vs dynamic at day 5 and 20.

qRT-PCR of ECM markers. Bars show the mean fold change at day 5 and day 20; error bars show one standard deviation; N=3 biological replicates, n=3 technical replicates. Data normalized to 2D Day 5 ($2^{\Delta\Delta Ct}$). P-values obtained by one way ANOVA *p ≤0.5, ***p ≤ 0.001

ESCs on rigid surfaces inhibits Oct-4 expression despite the presence of LIF (Moledina et al., 2012b). This is further supported by a recently published paper that showed that 3D

dynamic encapsulation aids fibroblast reprogramming and the acquisition of "stemness" without transcription factors (Han et al., 2013).

In contrast to this finding, it is possible that high cell density in dynamic 3D culture promotes higher Oct3/4 expression, compared to the early days of the culture where cell density is low, supporting the present data (Moledina et al., 2012b). This may be due to differences in cell growth, dimensions and morphology. In conventional monolayer culture, the cells are grown in the horizontal plane, not in a vertical dimension, allowing LIF to diffuse freely in the monolayer of cells and rapidly equilibrate in the medium, whereas the presence of 3D substrate and deposition of ECM slows down diffusion according to Moledina's observation. In addition, using a dynamic bioreactor was found to enhance LIF delivery to the cells and overcome the inheriting problem of cell density (Moledina et al., 2012b).

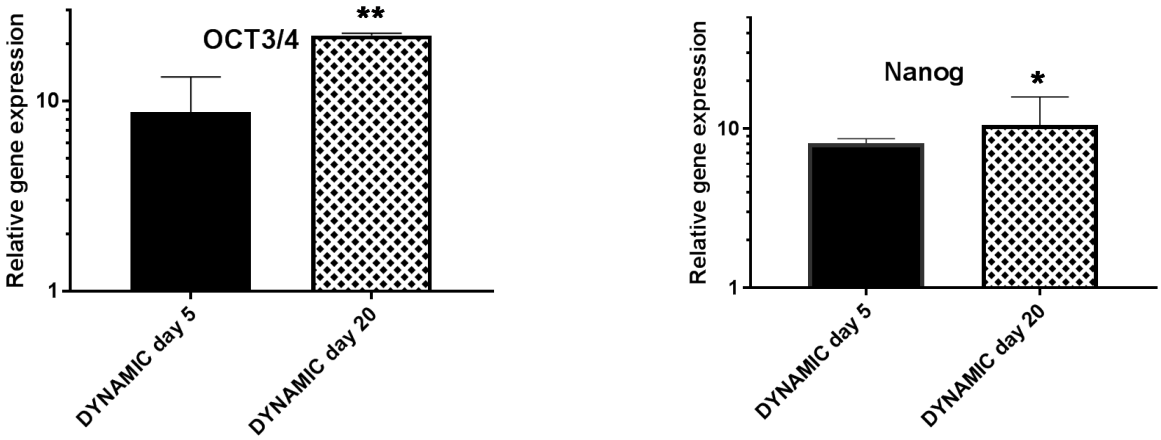


Figure 6.7 Comparing the expression of pluripotency markers OCT3/4 and Nanog in dynamic conditions at day 5 vs 20.

qRT-PCR of pluripotency markers. Bars show the mean fold change at day 5 and day 20; error bars show one standard deviation; N=3 biological replicates, n=3 technical replicates; data normalized to 2D Day 5 ($2^{\Delta\Delta Ct}$). P-values obtained by one way ANOVA**p ≤ 0.01 and *p ≤ 0.05.

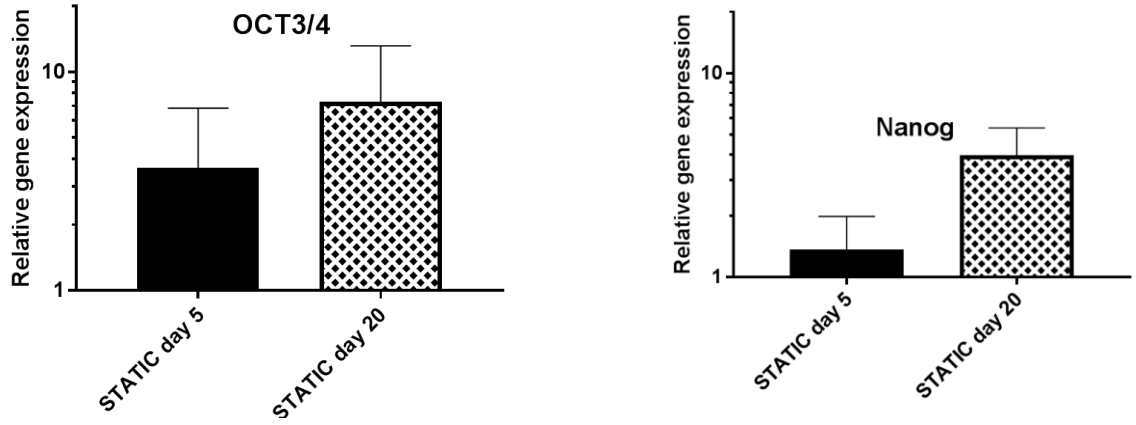


Figure 6.8 Comparing the expression of pluripotency markers OCT3/4 and Nanog in static condition day 5 vs 20.

qRT-PCR of pluripotency markers. Bars show the mean fold change at day 5 and day 20; error bars show one standard deviation; N=3 biological replicates n=3 technical replicates; data normalized to 2D Day 5 ($2^{\Delta\Delta Ct}$). P-values obtained by one way ANOVA.

PAX6 was used before as an indicator for the spontaneous expression of differentiation (Hu *et al.*, 2018) therefore we used it in this study to assess spontaneous differentiation in our cultures. All 3D conditions were able to completely suppress PAX6 mRNA expression at day 5 (Figure 6.9). Interestingly, until day 20, both static and dynamic cultures were capable of suppressing PAX6 in comparison with the 2D culture used as a normalization condition. Thus, it was concluded that 3D dynamic cultures can maintain human IPSCs in their pluripotent state without any passage for at least 20 days.

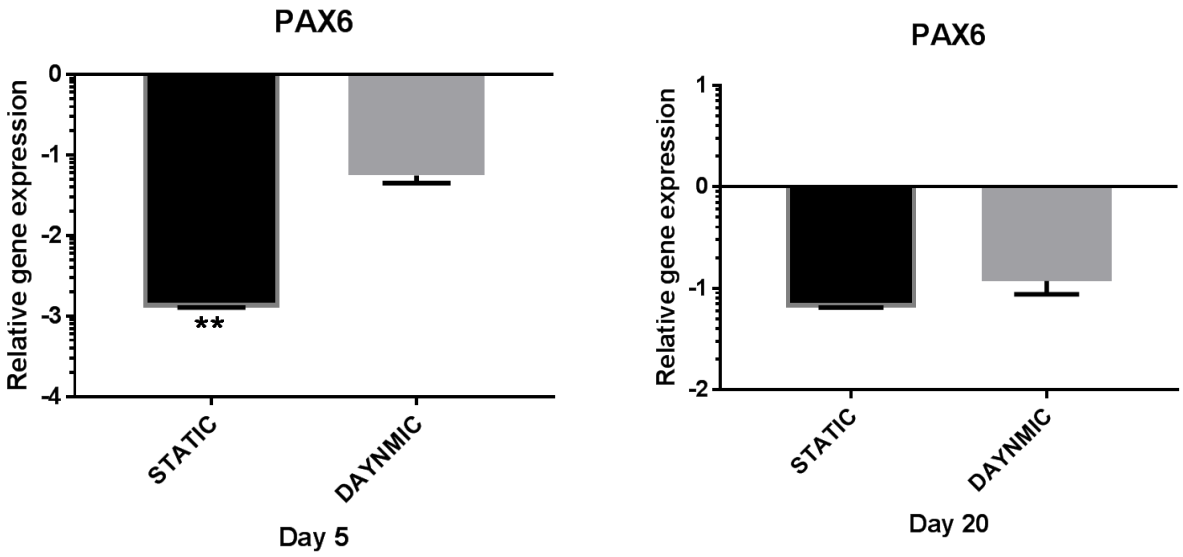


Figure 6.9 Comparing the expression of spontaneous differentiation marker PAX6 in static condition vs dynamic at day 5 and 20.

qRT-PCR of spontaneous differentiation marker. Bars show the mean fold change at day 5 and day 20; error bars show one standard deviation; N=3 biological replicates, n=3 technical replicates; data normalized to 2D Day 5 ($2^{\Delta\Delta Ct}$). P-values obtained by one way ANOVA **p ≤ 0.01.

6.4.4 The effect of hypoxia on prolonged adaption

As a general rule, it can be stated that the more cells proliferate, the more oxygen they consume. It has even been suggested that the oxygen consumption rate may be used as a monitoring tool to assess proliferation (Guarino et al., 2004). This knowledge is essential for the optimization of tissue-biomaterial interfaces in all tissue engineering applications and provides insight into tissue-specific cell guidance. To investigate if the dynamic culture platform herein developed and tested has formed a hypoxic environment, the gene expression of both HIF1α and HIF2α were measured as these genes can be used as oxygen sensors. Simultaneously, pluripotency and differentiation markers were also analysed. At day 5 differences exist between dynamic and static cultures in the expression of HIF1α. Indeed, most research has focused on the HIF1α subunit which is thought to be the master regulator of the hypoxic response (Mazure et al., 2004). HIF1α was expressed in human IPSCs cultured into both dynamic and static but, surprisingly, this gene was signifi-

cantly upregulated in cells cultured in 3D-dynamic cultures (Figure 6.10). It is hypothesised that this result corresponds to the upregulation of pluripotency markers OCT3/4 and Nanog, similar to many studies that observed that hypoxia enhanced the pluripotent population of human ESCs (Forristal et al., 2010b). Previous literature suggests that the hypoxic environment maintains the cell renewal potential and proliferation in embryonic stem cells (Forristal 2010). Similar results were found in this study, as the high hypoxic gene expression seen in the dynamic culture correlates with a higher cell number and a higher expression of pluripotency markers. In addition, at day 5 where high cell proliferation was observed (Figure 6.3), cells cultured in dynamic mode shown an increase in Nanog expression levels (Figure 6.6) which is linked to proliferation as it has recently been shown that Nanog regulates S-phase entry in human ESCs and that overexpression of Nanog significantly increases proliferation by binding to regulatory regions of CDK6 and CDC25A, two important cell cycle regulators (Neganova et al., 2008). However, we examined if a long term 3D-culture for both conditions has any impact on HIF1α expression. The expression of HIF1α was significantly higher in 3D dynamic cultures at day 20 which might be linked with the significant upregulation of OCT3/4 and Nanog (Figure 6.10). To explain these results, it is necessary to further consider proliferation previously shown. In fact, at day 20 of culture, increased proliferation was observed from the MTS assay, but several factors might have influenced this. A variety of methods have been used to solubilize, stabilize the colour, avoid evaporation and reduce phenol red interference in the detection of the formazan product measured in the MTS assay used for proliferation (Tada et al., 1986; Hansen, Nielsen and Berg, 1989). However, MTS offers the best available approach for encapsulated cells viability measurement. Nonetheless, comparing HIF1Aα expression at day 5 and at day 20 in each condition separately there were no significant upregulations compared to 2D, which was used as control in this chapter (Figure 6.10).

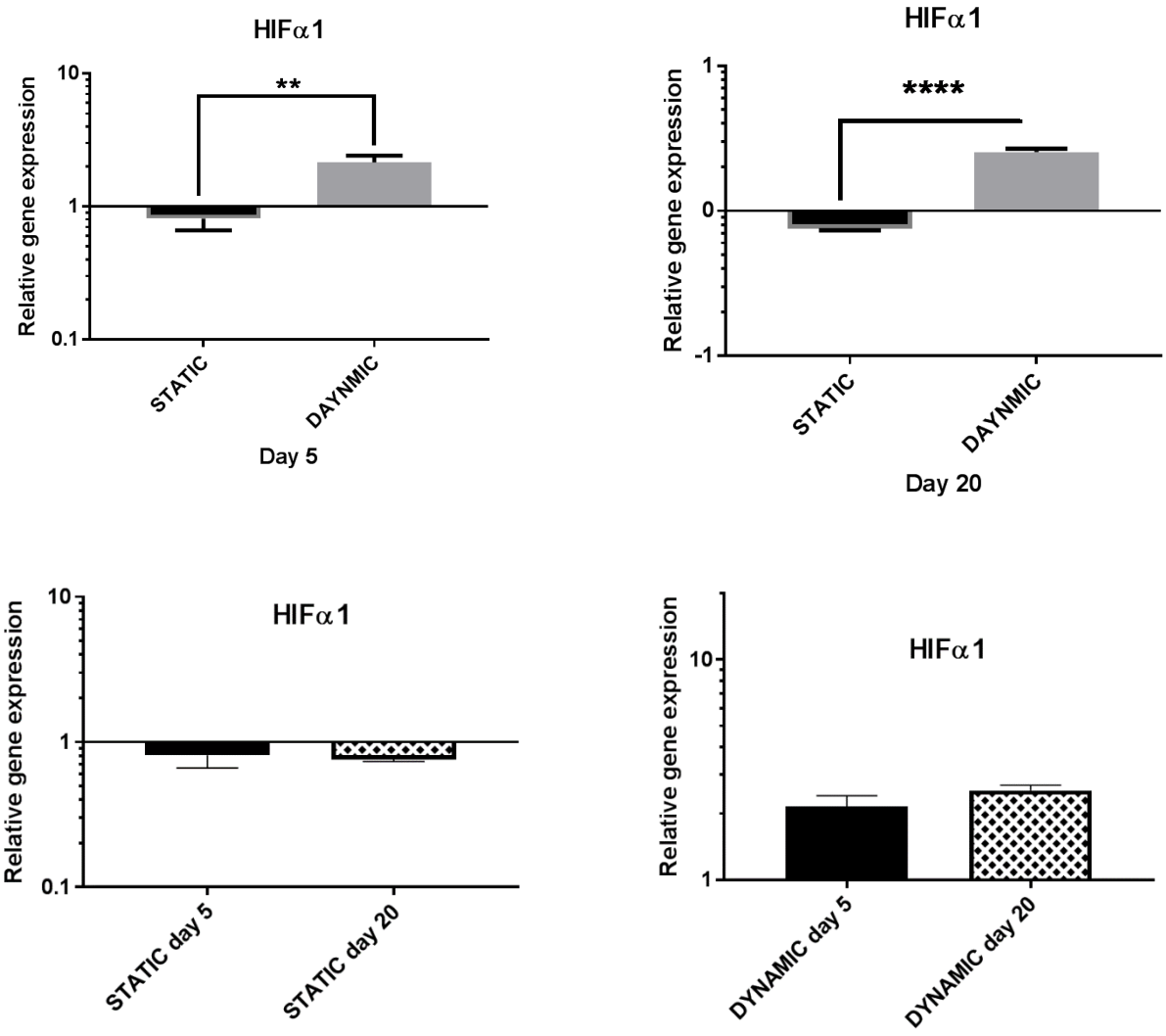


Figure 6.10 Comparing the expression of acute hypoxia associated marker HIFα in both dynamic and static 3D-conditions at different time points.

Bars show the mean fold change at day 5 and day 20; error bars show one standard deviation; N=3 biological replicates; data normalized to 2D Day 5 ($2^{\Delta\Delta Ct}$). P-values obtained by one way ANOVA**p ≤ 0.01 and ****p ≤ 0.0001.

In human ESCs HIF1α has been suggested to be key in the initial adaptation of human ESC to the hypoxic environment, but when this expression is lost after 48h in hypoxic conditions(Forristal et al., 2010a), other HIF units are upregulated, translocated to the nucleus where they are transcriptionally active, and take over from HIF1α in maintaining the

long-term response to hypoxia. Thus, HIF2α was tested in all conditions: 3D dynamic vs 3D static at day 5, 3D dynamic vs 3D static at day 20, 3D dynamic day 5 vs day 20 and 3D static day 5 vs day 20 (Figure 6.11). HIF2α was expressed in all comparison groups used, with no significant difference in the mRNA expression of the HIF2α with respect to the motion and elapsed time. As expected, only when comparing 3D static at day 5 vs day 20 HIF2α was significantly upregulated. This may be associated with the progressive impairment of oxygen with time in 3D static, as the cell number in this condition was higher and might have prevented oxygen from reaching the centre of the beads, therefore generation a hypoxic core.

This data indicates that a low oxygen tension for short term is preferential for the maintenance of a highly proliferative, pluripotent population of human IPSCs encapsulated in hydrogel beads. This is in agreement with several studies displaying the benefits of low oxygen tension in stem cell cultures (Forristal et al., 2010a;Forristal et al., 2010b; Hawkins, Sharp and McKay, 2013b; Pimton et al., 2015)

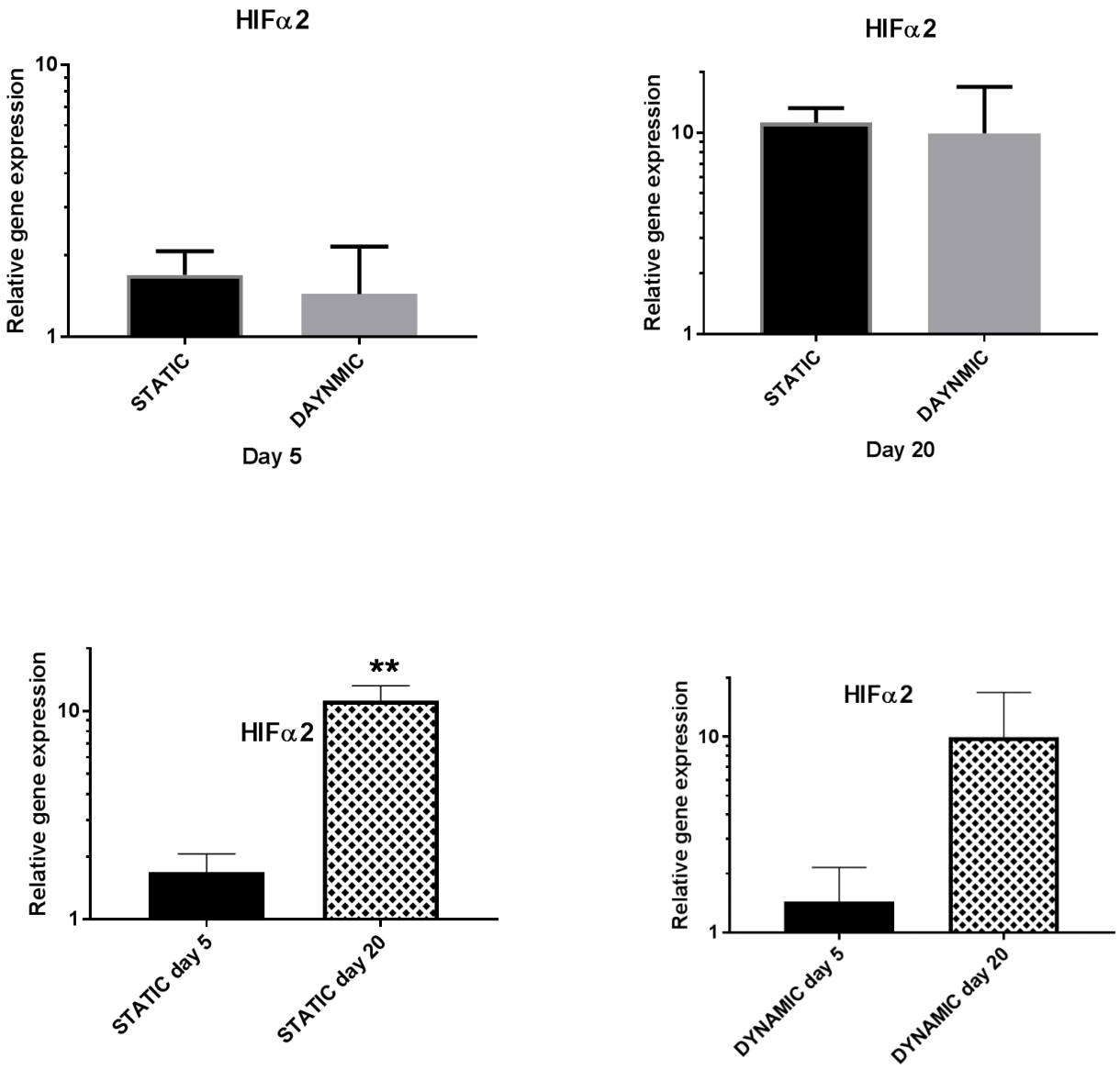


Figure 6.11 Comparing the expression of chronic hypoxia adaption associated marker HIF2α in both 3D conditions at different time points.

qRT-PCR of HIFα2. Bars show the mean fold change at day 5 and day 20; error bars show one standard deviation; N=3 biological replicates; data normalized to 2D Day 5 ($2^{-\Delta\Delta Ct}$). P-values obtained by one way ANOVA**$p \leq 0.01$.

6.4.5 Evaluate the ECM secretion by human IPSCs cultured in 3D environment

The protein composition of the ECM varies according to the type of tissue. The main fibrillary components of the ECM can be divided into two groups: collagens and cell adhesive glycoproteins (e.g. laminin and fibronectin) (Mecham, 2012). The same conditions tested in this chapter were assessed for the expression of ECM secreted proteins associated with embryonic development. Up-regulation of mRNA levels of two secreted ECM proteins like LAMA 5 and FN1 in both types of 3D culture compared to 2D may indicates that absence of adhesive in alginate beads increases their production. Cells grown in 3D dynamic show high expression of LAMA 5 gene at day 5 and day 20 compared to the cells in 2D or static conditions (Figure 6.12). Moreover, we investigated if cells were able to synthesise ECM throughout the period of a long-term culture. Results show that between day 5 and day 20 in dynamic LAMA 5 was expressed remarkably at day 20 (Figure 6.13). ECM proteins such laminin 511 and 521 have been shown to maintain human ESC pluripotency and self-renewal (Domogatskaya, Rodin and Tryggvason, 2012; Laperle et al., 2015). Therefore, it is hypothesised that the ability of the cells to synthesise LAMA5 in dynamic is correlated with the high expression of pluripotency markers shown before (Figure 6.6). In addition, Laperle et al., 2015 sugested that LAMA 5 plays a role in cellular proliferation due to the fact that human PSC cells had disruption in endogenous α-5 laminin assembly, which led to apoptosis possibly explaining the enhanced cell proliferation found under dynamic condition (Figure 6.3) in our study (Laperle et al., 2015).

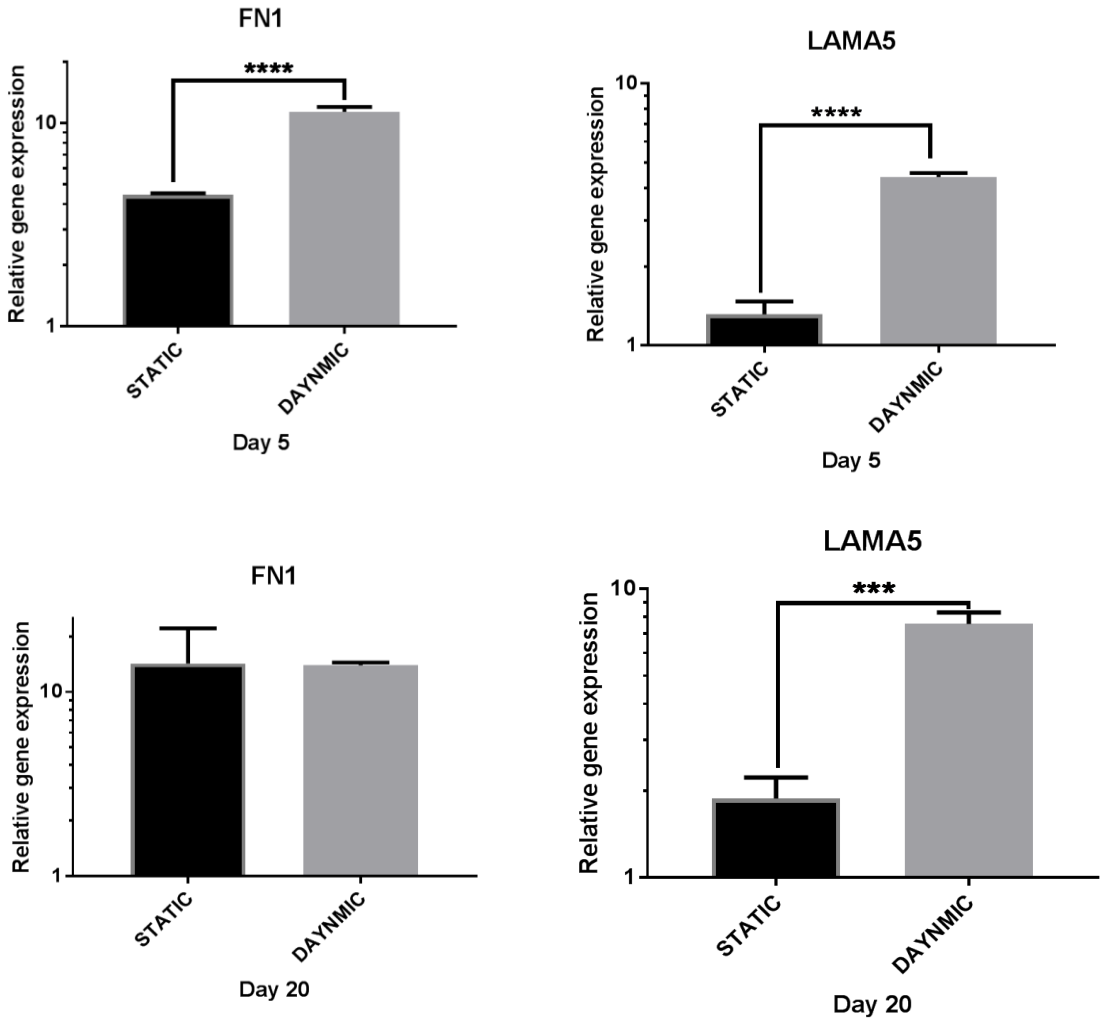


Figure 6.12 Comparing the expression of LAMA5 and FN1 genes in static vs dynamic condictions at days 5 and 20.

Bars show the mean fold change at day 5 and day 20; error bars show one standard deviation; N=3 biological replicates; data normalized to 2D Day 5 ($2^{-\Delta\Delta Ct}$). P-values obtained by one way ANOVA ****p ≤0.0001, ***p ≤ 0.001.

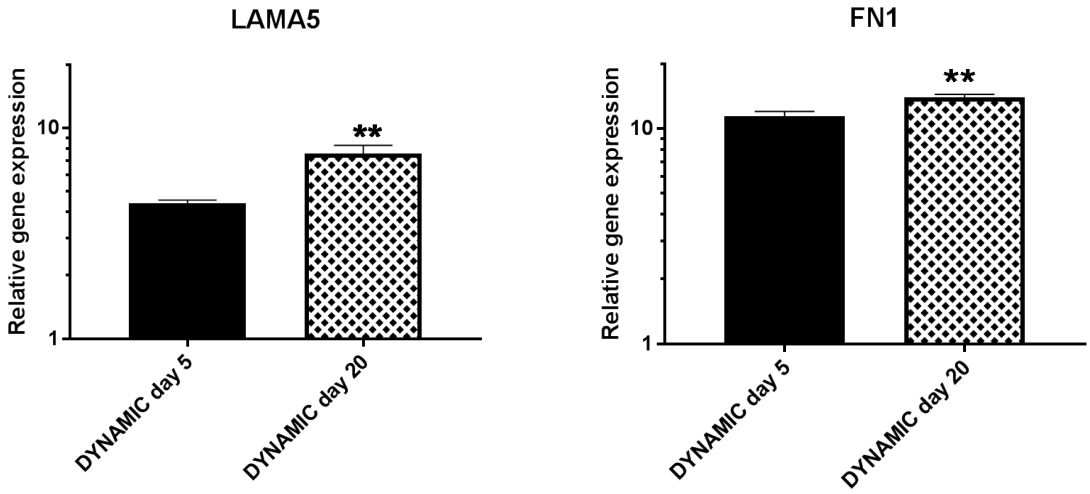


Figure 6.13 Comparing the gene expression of LAMA5 and FN1 in dynamic conditions at day 5 vs day 20.

Bars show the mean fold change at day 5 and day 20; error bars show one standard deviation; N=3 biological replicates; data normalized to 2D Day 5 ($2^{-\Delta\Delta Ct}$). P-values obtained by one way ANOVA **$p \leq 0.01$

Following this, the expression of fibronectin was assessed, an ubiquitous ECM component that has been the focus of many studies of ECM assembly, mechanical properties and cell–ECM interactions, and on chondrogenesis, a stem cell differentiation process that depends on changes in ECM protein expression and deposition (Singh and Schwarzbauer, 2012). qRT-PCR was performed in both 3D groups at days 5 and 20. FN1 was significant in day 5 for dynamic however at day 20 it was comparable between static and dynamic. Surprisingly at day 5 self-renewal markers were also upregulated in 3D dynamic cultures which is in agreement with the role of fibronectin to support the bind of α5β1 integrin and αVβ1 integrin, shown to stimulate human IPSCs to secret several proteins required for their attachment, proliferation, and self-renewal like laminin-332, -511, -521, and collagen IV (Nakashima and Omasa, 2016). Furthermore fibronectin can interact with α8β1 to increase cell survival through the PI3K pathway, by α8-mediated cell survival (Farias et al., 2005).

However, when comparing day 5 vs day 20 in static, fibronectin gene expression was significantly higher and similar to 3D dynamic cultures at day 5 vs day 20 (Figure 6.14). It is hypothesised that poor alginate adhesion may be responsible for the increase of ECM proteins production in both 3D dynamic and static cultures despite the presence of 1.1%

gelatin (attachment enhancer) in our alginate mixture. Conversely, the presence of the same concentration of gelatin used to coat 2D culture plates did not result in ECM secretion. This may be either because of the mechanical properties of the beads surfaces, the change in cell morphology or the cell-cell contacts that are responsible for differences in ECM production between 2D and 3D cultures (Alsobaie, 2015 Submitted et al., 2015). Proteins as laminin and fibronectin have recently been used to maintain and prolong self-renewing human ESCs and proliferation (Garcia, Vega and Boettiger, 1999; Sevilla, Dalecki and Hocking, 2013; Ahmed and ffrench-Constant, 2016). An enriched matrix containing both Lama5 and E-cadherin has recently been used to maintain and prolong self-renewing human ESCs without feeder cells in a serum-free environment (Rodin et al., 2014). Moreover, a combination of collagen IV, fibronectin, laminin, and vitronectin has be used to replace Matrigel™ for deriving and expanding human PSCs under defined culture conditions (Levenstein, et al., 2006). Interestingly, single or multiple ECM proteins successfully can control the fate of stem cells, as for example, fibronectin and laminin direct neural cell lineage commitment, and collagen promotes osteogenic differentiation (Hosseinkhani et al., 2008).

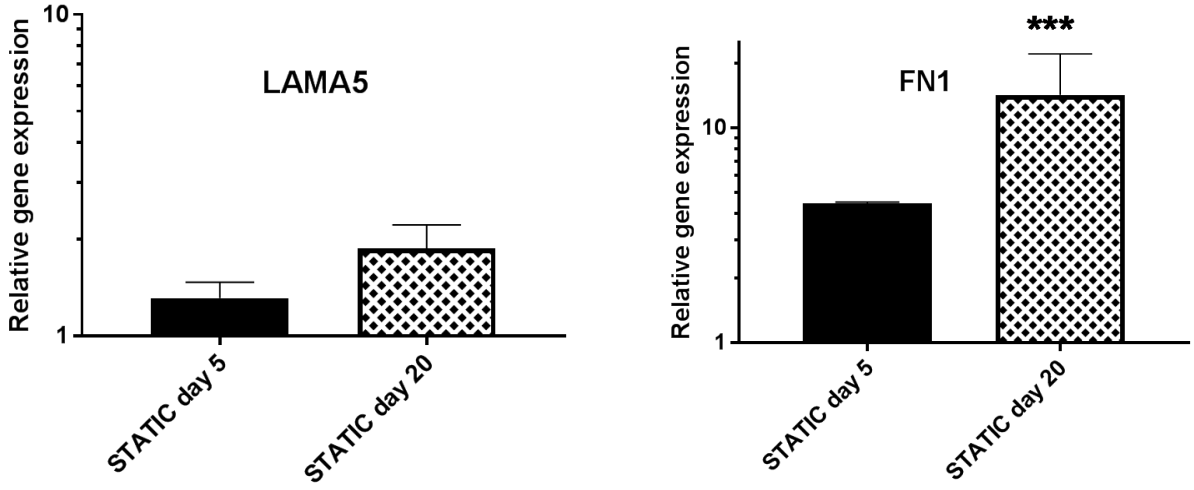


Figure 6.14 Comparing the gene expression of LAMA5 and FN1 in static conditions at days 5 vs 20.

Bars show the mean fold change at day 5 and day 20; error bars show one standard deviation; N=3 biological replicates; data normalized to 2D Day 5 ($2^{-\Delta\Delta Ct}$). P-values obtained by one way ANOVA ***$p \leq 0.001$.

6.5 Conclusion

In this chapter, the ability of human IPSCs encapsulated in alginate hydrogels to be maintained in their undifferentiated state for more than 20 days while still maintaining their pluripotent capabilities was demonstrated. This was achieved without any enzymatic treatment, mechanical expansion or manipulation in a feeder-free environment. Human IPSCs encapsulated into 1.1% (w/v) alginate and cultured in a HARV bioreactor to enhance the mass transport presented inhibited differentiation at the morula-like stage without cystic EB formation. Moreover, human IPSCs in 3D dynamic cultures were able to secrete the necessary ECM components required for their adhesion which in turn might play a role in maintaining the pluripotent state. Although enhanced cellular proliferation resulted in acute hypoxia in 3D dynamic, the low oxygen tension has impacted the culture positively, by allowing the maintenance of pluripotency. Finally, the addition of 10 μM of Y-27632 along the culture severely improved the proliferation rate, particularly in the 3D dynamic culture. Overall, these results suggested that 3D dynamic is desirable for large-scale expansion of undifferentiated human IPSCs.

Chapter 7

Optimizing the Differentiation of Human IPSCs towards Endoderm in 3D Dynamic Culture.

This chapter reports the application of the adaptation and optimisation of the successful protocol for the generation of lung epithelium published by Huang et al (Huang et al., 2013) in 2D to the dynamic 3D system developed in this work and reported in chapter 6. This system consists of human IPSCs encapsulated in alginate beads cultured in a HARV bioreactor. The importance of improving methods that use human IPSCs to derive endoderm cells is justified with the need to generate endodermal tissues including tissues of the pancreas, lung and hepatocyte. Thus, a better understanding and control of the definitive endoderm differentiation process in *vitro* should result in enhanced efficiency and higher fidelity in the resulting cells (Goessling and Stainier, 2016). Normally, four steps of induction are required in order to differentiate human or mouse PSCs into lung lineages. Before the stage of converting cells to a lung progenitor, endoderm lineages must be induced producing cells that express the endodermal transcription factors SOX16 and FOXA2 and *surf*ace markers CXCR4, c-KIT and EPCAM. This step is followed by differentiation into NKX2.1-expressing anterior foregut cells (Green, Huang and Snoeck, 2013). Several approaches have been used to induce definitive endoderm through the use of 2-dimensional (2D) monolayer cultures, with high variability of results. (Huang et al., 2013; Naujok, Diekmann and Lenzen, 2014). Therefore, certain factors should be taken into consideration while moving from a monolayer culture method to 3D cultures. For instance, the stability of 3D scaffolds, the combination of growth factors as well as signal transducers and cell viability must be considered.

The first experiments conducted in 3D towards the differentiation of the cells into type II lung epithelium were done to compare two previously established protocols in 2D (Huang et al., 2013; Naujok, Diekmann and Lenzen, 2014), as they presented two different ways to achieve endoderm differentiation. The main difference between the two approaches is the use of Wnt3a growth factor for the activation of Wnt or the addition by

Naujok of CHIR99021, a glycogen synthase kinase 3β (GSK3-β) inhibitor, as a specific activator of the canonical Wnt pathway. In addition, while studying differentiation protocols, another factor was notoriously important: the addition of 2% serum reported by Firth et al. in 2014 proved to be beneficial for long-term proliferation in culture when compared to serum-free and was chosen as it was a lower concentration than the 15% used by Naujok (Naujok, Diekmann and Lenzen, 2014; Firth et al., 2014). This was especially important due to the previous report that the addition of serum influences the activation of Wnt pathway via Wnt3a by Adrian K Teo (Naujok, Diekmann and Lenzen, 2014; Teo et al., 2014).

7.1 Introduction

The importance of developing efficient and reproducible conditions for the direct differentiation of pluripotent stem cells into specific cell types lies in the need for understanding early human development as well as enabling further practical applications such as in-*vitro* disease modelling, drug discovery, and cell therapies (Murry and Keller, 2008). In particular, the generation of surrogate cells for treatment of liver, lung and pancreas diseases (i.e. diabetes mellitus) is of great interest. (Kubo et al., 2004; D'Amour et al., 2005). These organs originate from the endoderm germ layer. Respectively, the definitive endoderm (DE) depicts a vital intermediate stage at the time of in-*vitro* differentiation towards the aforementioned tissues. The induction of DE can be achieved by inducing ESCs with high concentrations of Activin A, imitating nodal signalling during gastrulation. In addition, the activation of the transforming growth factor beta 1 (TGFβ1) pathway triggering DE differentiation is generally accepted. Nevertheless, the role of lineage specification of ESCs into the DE may not be solely attributed to TGF1 /Activin A (D'Amour et al., 2005).

Four distinctive events are required for in *vivo* DE formation. Changes from moving from the embryoblast stage to the epiblast stage are affected by the nidation of the blastula in the endometrium. Another migration from epiblast cells to the embryonic disk median line causes the formation of the primitive streak (PS). Moreover, ventral migration of primitive streak cells leads to the formation of the short-lived mesendoderm predecessor. (Rodaway and Patient, 2001) Finally, the mesendoderm is separated into mesoderm

and definitive endoderm germ layers. (Technau and Scholz, 2003). Human ESCs are regarded as derivatives of the epiblast (Hanna, Saha and Jaenisch, 2010). Hence, there is no necessity for the direct differentiation into epiblast cells. It is improbable that a single pathway controls well concerted events directing ESCs into the DE. Therefore, numerous research groups combine additional growth factors or small molecules with Activin A, e.g. Wnt3a (D'Amour et al., 2006; Kroon et al., 2008; Mfopou, Chen and Mateizel, 2010) PI3K-inhibitors (Cho et al., 2012) etc.

Encapsulation of stem cells in hydrogels, is an approach to challenge scalable bioprocessing to enable suspension culture and improve the control of microenvironmental cues. One of the methods used to protect enclosed cells from the immune system of the host during transplantation is encapsulation. Yet, it may shield cells from hydrodynamic shear forces found in bioreactor environments as well as prevent agglomeration of the aggregates of stem cells while leaving diffusion of nutrients and oxygen through the encapsulated material permissioned (Wilson and Mcdevitt, 2013)

7.2 Aims and Objectives

The focus of this chapter is to establish a new direct protocol that could enhance the induction of Endoderm differentiation from human IPSCs in (3D) culture system, optimized from previous protocols reported in the literature. Herein, it was hypothesized by using Chemical substance CHIR99021, as small molecule that mimics Wnt signaling, with Activin A can be more efficient in terms of cost, differentiation and stability in compared with Wnt3a.Moreover we assess the effect of serum addition in cells proliferation by comparing and no serum low (2%) concentration.

7.3 Methodology

For these experiments, 10 μM of Y-27632 were added to the culture media 2 hours before the dissociation of colonies into single cells. Then, the cells were encapsulated and left in static culture for 24 hours in MTeSR™1 media with 10 μM Y-27632. After 24 hours, primitive streak formation is induced for 1 day in basal differentiation media composed of RPMI 1640 media supplemented with N2 supplement, B27 supplement, ascorbic acid (50 μg/ml), Glutamax (2 mM), Monothioglycerol (0.4 μM), 10 μM Y-27632 and either with or without 2 % of FBS. To the basal media it was also added 1 ng/ml BMP-4. On days 2 to 5 we proceed to endoderm induction by adding to the basal differentiation media human 100 ng/ml Activin A and 3μM CHIR99021 or 25 ng/ml Wnt3a. The expression of endoderm surface marker CXCR4 and transcription factor FOXa2 was assessed after 5 days by q RT-PCR. The proliferation of the cultured cells was assayed by using the MTS proliferation assay to compare between serum and non-serum conditions. (Figure 7. 1)

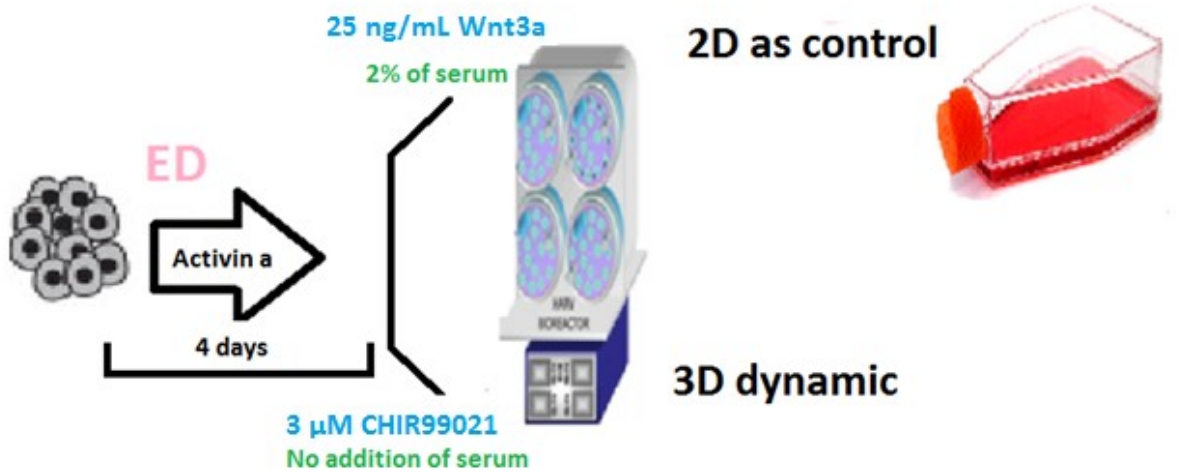


Figure 7.1: Schematic diagram of the direct differentiation of human IPSCs towards the endoderm lineage under 3D dynamic culture. (Modify Teo, Mantalaris and Lim, 2014).

7.4 RESULTS and DISCUSSION

7.4.1 Evaluating the effect of Wnt3a on endoderm differentiation by using qRT-PCR in both 2D and 3D dynamic cultures

The efficiency of DE cell induction from human IPSCs was the first factor examined. Activin A has been used to induce DE cells in most previous studies, and it has been reported that Activin A and Wnt3a can be used to differentiate DE cells from human PSCs (D'Amour et al., 2006; Kroon et al., 2008; Maehour et al., 2009). In this differentiation process, Wnt is known to participate in at least three pathways including β-catenin, PCP and Ca^{2+} signalling. Moreover, it has also been shown that the combination of Activin A with Wnt3a results in a more efficient induction of DE cells. Endoderm differentiation was assessed by endoderm surface marker CXCR4 and transcription factor FOXa2 associated markers. Samples of differentiated human IPSCs with the addition of 100 ng/mL Activin A, 25 ng/mL Wnt3a and 2% of serum of each culture group (2D and 3D cultures) were collected at day 4. Cells were only treated with Activin A for 4 days because any longer caused cell death (Takeuchi, Nakatsuji and Suemori, 2014) and this was compared to day 0 undifferentiated human IPSCs as the control sample.

Both CXCR4 and FOXa2 markers showed a significantly higher expression in 3D dynamic cultures, which is indicating high efficiency of the endoderm induction for this condition (Figure 7.2). Traditional 2D cultures have the advantage of cells being exposed homogeneously to factors added to the culture medium and that immunochemical assays can be performed easily. However, a 3D dynamic culture system in the presence of the two factors achieved further induction of human IPSCs into endoderm cells. Our findings agree with the observations of Teo et al., 2014 who reported activation of Nodal/Activin signalling and activation of β-catenin signalling by using 25 ng/mL Wnt3a and 2% serum (Teo et al., 2014). These results highlight the benefit of coupling the use of known chemical molecules with a 3D dynamic culture system that supports human PSC biology and provides both biochemical and mechanical contributions that aim to mimic the in *vivo* microenvironment. (Schmeichel, 2003; Yuge et al., 2006). Cells in *vivo* are in a three-dimensional environment having characteristic biophysical and biomechanical signals according to the type of tissue they are in, which influences cell functions like differentiation and gene expression (Souza et al., 2010). Thus, 3D culture has many advantages that support and enhance endoderm induction such as integration of flow, providing oxygen and other

essential nutrients to the right place, interaction between different types of cells, higher degree of structural complexity and retaining a "steady state" (homeostasis) for longer (Bonaventure et al., 1994; Chang and Hughes-Fulford, 2009).

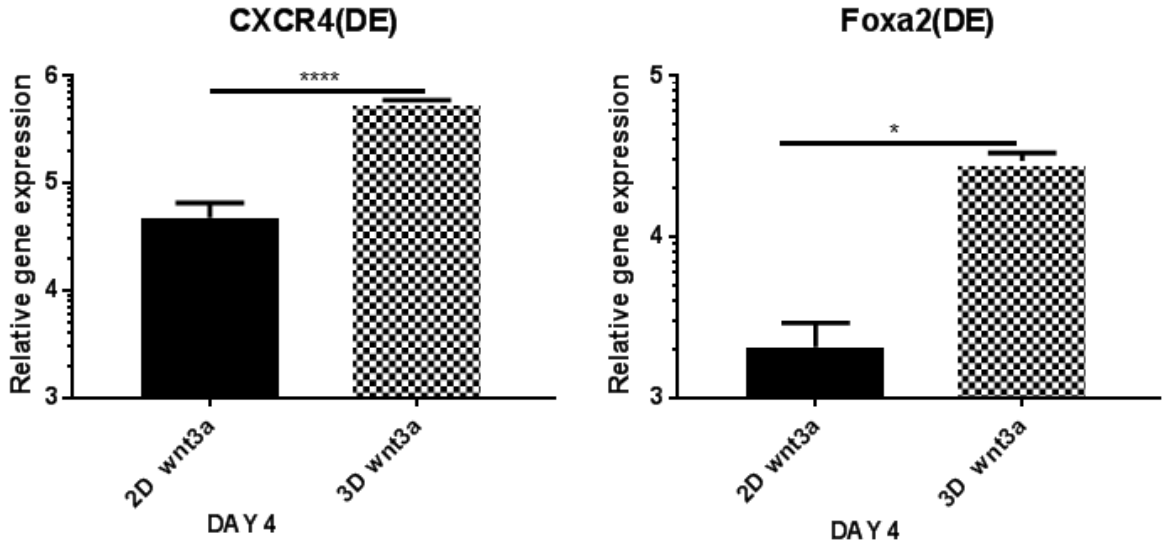


Figure7.2: Gene expression of CFCR4 and Foxa2.
qRT-PCR of endoderm surface marker CXCR4 and transcription factor FOXa2 shows a significant increase in both gene expressions is obtained in 3D cultures. Results reported as mean fold change at day 4 vs day 0 ($2^{-\Delta\Delta Ct}$); error bars show one standard deviation, N=3 biological replicates separated on day 4; ****$p \leq 0.0001$, and *$p \leq 0.05$ by one way ANOVA.

7.4.2 The effect of CHIR99021 on endoderm differentiation in 2D and 3D dynamic cultures

GSK3 is a serine/threonine kinase that plays a central role in the regulation of the Wnt/β-catenin signalling pathway, an important pathway for endoderm specification, proliferation and differentiation. Thus, pharmacologic inhibition of GSK3 activity can lead to the stabilization and activation of β-catenin and TCF/LEF-dependent gene transcription, which reflects the activity of Wnt signal transduction (Wu and Pan, 2010). Because small molecules provide a highly temporal and tuneable approach to modulate cellular fate and functions, they have

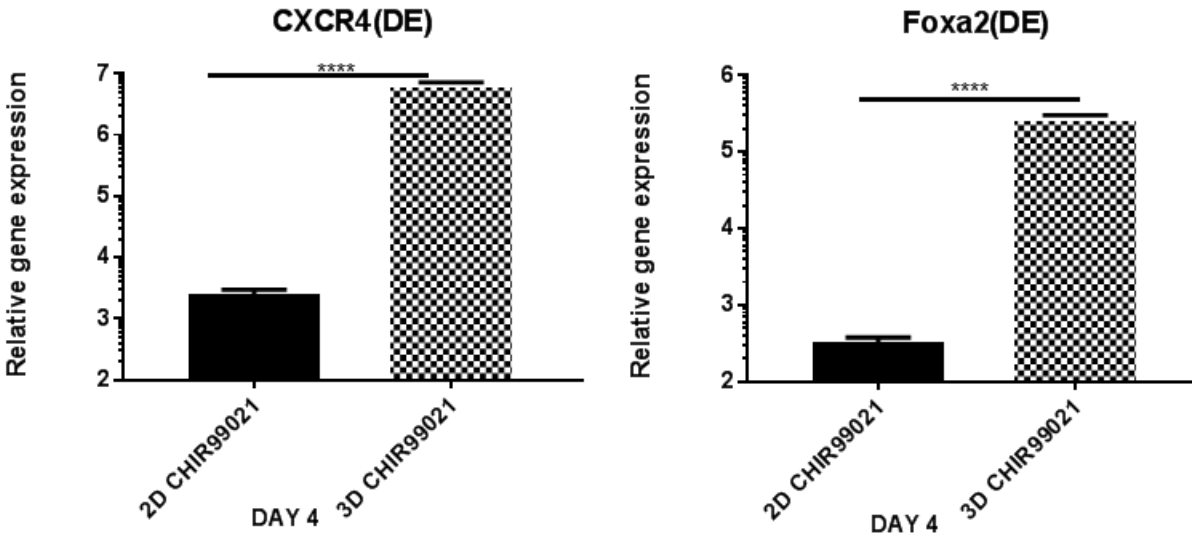


Figure 7.3: CHIR99021 effect on endoderm differentiation in 2D vs 3D dynamic. qRT-PCR analysis of endoderm surface marker CXCR4 and transcription factor FOXa2. Results reported as mean fold change at day 4 vs day 0 ($2^{-\Delta\Delta Ct}$); error bars show one standard deviation from N = 3 biological replicates separated on day 4; ****p ≤ 0.0001by one way ANOVA.

been identified to enhance and enable stem cell differentiation towards a faster, more efficient and directed process (Yu et al., 2014).

To further investigate this, the 3D dynamic culture system was used. To define the synergism between Wnt and Activin signaling in inducing DE without serum, we activated Wnt signaling by inhibiting the downstream signaling molecule GSK-3, using independent 3μM CHIR99021 instead of Wnta protein (Kunisada et al., 2012; Illing et al., 2013).

At day 4 we collected samples from both 2D and 3D dynamic and assessed the same markers CXCR4 and FOXa2 by qRT-PCR. The 3D dynamic increases significantly gene expression of endoderm markers compared with conventional 2D culture (Figure7.3).

These results indicate that 3D culture has an advantage for the induction of endoderm lineage. Although Kunisada et al. (2012) and Illing et al. (2013) used CHIR99021 to induce DE differentiation from human PSCs, they also included FBS in their protocol. Although we used another approach to induce the formation of endoderm, herein 3D dynamic showed again the ability to enhance the induction of endoderm significantly, which might be related to the advantage of 3D dynamic culture that was explained in previous observations. 3D dynamic could be an alternative strategy for effectively inducing DE

cells, particularly via the activation of Wnt signaling pathway (in addition to the indispensable Activin signaling pathway).

7.4.3 Wnt3a vs CHIR99021 towards endoderm induction in 3D dynamic culture

After concluding that 3D dynamic cultures up-regulated the endoderm markers FOXA2 and CXCR4 significantly it was decided to proceed with the activation of the Wnt pathway in comparison with 2D. Here, the question was posed whether the activation of Wnt/β-catenin signaling via GSK3 inhibitors within 3D dynamic will be more specific towards definitive endoderm than the specification of endoderm by just adding Wnt3a to activate the pathway. Consequently, we compared the both approaches used to induce endoderm in 3D dynamic only by adding to the culture media 100 ng/mL Activin A and 3μM CHIR99021 or 100 ng/mL Activin A and 25 ng/mL Wnt3a. At day 4 of culture samples were collected from both 3D dynamic cultures. Interestingly, the combination of 100 ng/mL Activin A and 3μM CHIR99021 resulted in the highest expression of endoderm markers CXCR4 and FOXA2 (Figure 7.4). This result is in agreement with several reports in the literature (Wu and Pan, 2010; Kempf et al., 2014; Naujok, Diekmann and Lenzen, 2014; Teo et al., 2014). Huang et al., 2017 found that GSK3 inhibitors increase the expression and nuclear distribution of β-catenin, which significantly increased the mRNA and protein levels of GATA4 and FOXA2 in human ASCs after 24 hours exposure. Furthermore, at day 5, more than 75% of the cells expressed the FOXA2 and CXCR4, the markers of definitive endoderm cells (Huang, 2017). Typically, the comparison and optimisation of endoderm induction by using growth factors or small molecules combined with Activin A has been attempted in 2D (Kunisada et al., 2012). In this study, we developed a simple protocol for inducing the differentiation of human IPSCs into definitive endoderm. By using 3D dynamic cultures and treatment with a combination of low molecular weight compounds, definitive endoderm cells were obtained with an increase of more than 2-fold. This protocol does not include complicated and extensive processes, such as embryoid body formation, cell sorting by FACS, and re-seeding into other plates making the differentiation process efficient, stable and easy to reproduce. In addition, comparing with (Kroon et al., 2008 and Teo, Valdez, Dirice, & Kulkarni, 2014) further demonstrated that the 3D dynamic culture optimized conditions induced DE comparably and efficiently, and might give rise to DE derivatives with equivalent potential. Taken together, these findings

suggest that CHIR99021 is the preferred choice, in combination with Activin A, to generating DE cells, whereas results suggest that the development of similar compounds may be useful for robust, potentially scalable and cost-effective generation of large numbers of other organs originating from endoderm Wnta3 is both expensive and requires a high dose to be effective. Finally, these for drug screening and predictive toxicology platforms.

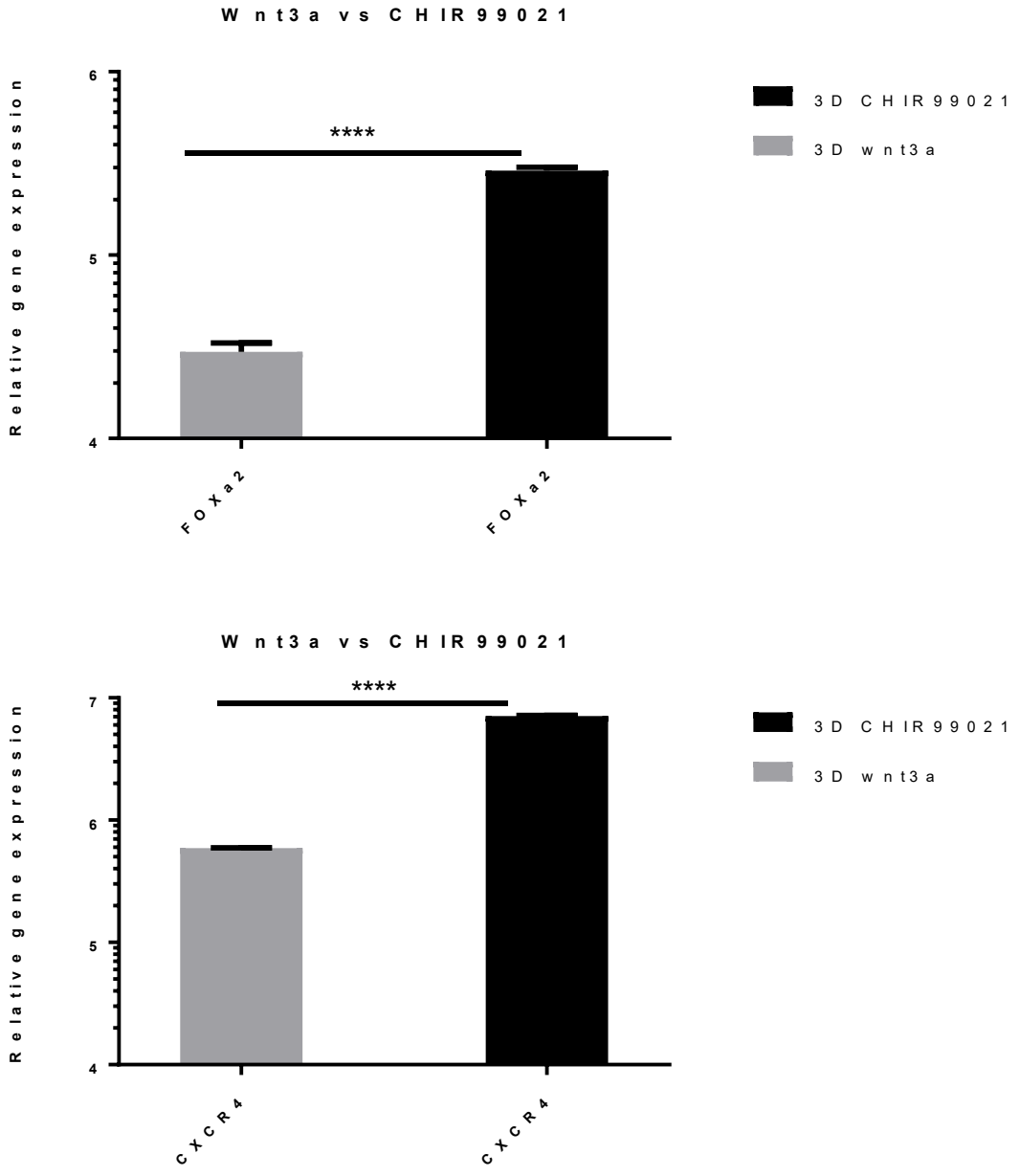


Figure 7.4: Wnta3 vs CHIR99021 effect on endoderm differentiation in 3D dynamic cultures.

qRT-PCR of endoderm surface marker CXCR4 and transcription factor FOXa2. Results reported as mean fold change at day 4 vs day 0 ($2^{-\Delta\Delta Ct}$); error bars show one standard deviation from N = 3 biological replicates separated on day 4; ****p ≤ 0.0001by one way ANOVA.

7.4.4 Presence of serum promotes proliferation throughout 3D cultures

Cellular proliferation along 20 days of culture was evaluated at different time points in both 3D culture adapted in presence of serum or without it groups. In order to evaluate the growth kinetics of human IPSCs differentiated in both conditions we used the MTS proliferation assay. However, MTS might not be the most appropriate assay to evaluate the cells proliferation in alginate beads throughout a culture. It is known that the MTS assay is based on the reduction of the MTS tetrazolium compound by viable cells to generate a coloured formazan dye that is soluble in cell culture media (Berridge, Herst and Tan, 2005). In this case, due to a high cell concentration achieved inside the beads, the transport of the formazan dye from the inside of the beads to the medium can vary and might have a negative impact on the sensitivity of the MTS assay (Appendix IV). It was observed that beads cultured in 2% serum, 100 ng/ml Activin A and 25 ng/ml Wnt3a showed a significantly higher cell proliferation at day 15 and day 20 when compared with beads cultured with Activin A and CHIR99021 but no serum (Figure7.5). There are a number of cues that are able to encourage the growth of human IPSCs including medium components and ECM. *Serum* is vitally important as a source of growth and adhesion factors. It is a rich source of often unidentified components such as growth factors, hormones, attachment factors, micronutrients, trace elements, proteases, and protective elements (antitoxins, antioxidants, antiproteases), not provided by the basal medium and that can promote rapid cell growth (Yao and Asayama, 2017). Furthermore, the high albumin content of serum ensures that the cells are well-protected from potentially adverse conditions such as acidification of the media or shear stress, which may occur particularly in large-scale cultures. Nonetheless, the supplementation of culture media with serum has many inherent disadvantages, such as the introduction of animal derived products into human cell cultures, rendering it difficult to use for medical applications and the fact that serum does not have a defined composition. This suggests the need for further optimisation to grow cells in 3D dynamic culture without serum (van der Valk et al., 2010).

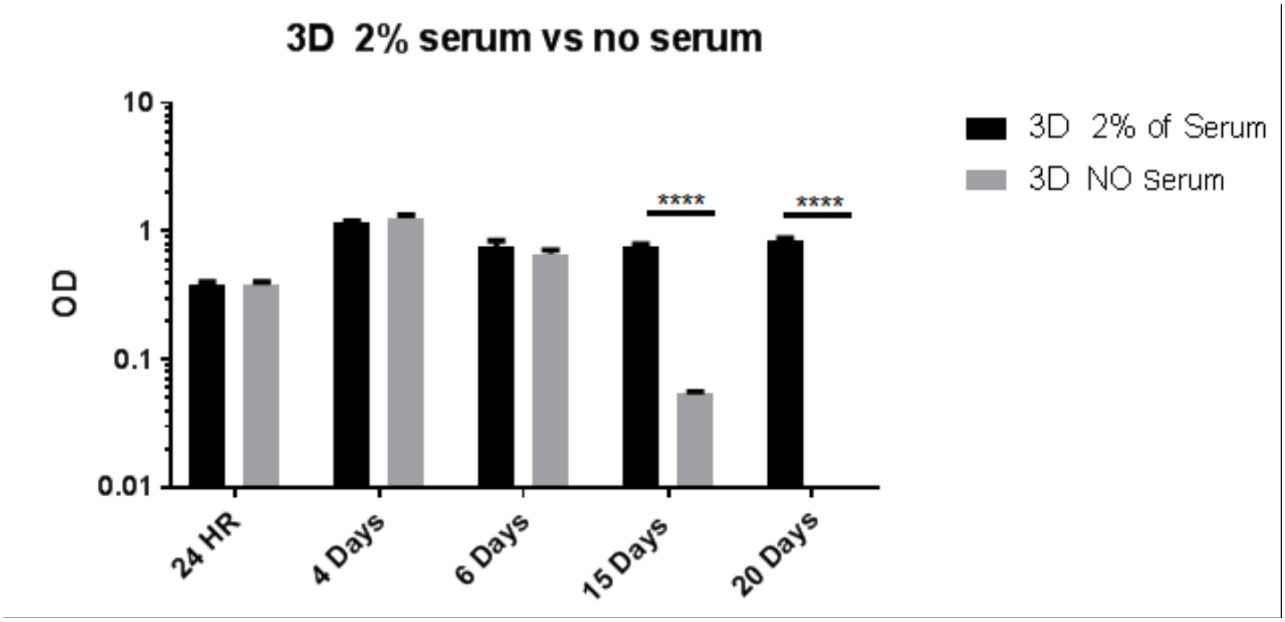


Figure 7.5: Human IPSCs proliferation within encapsulated alginate beads.
Direct correlation of formazan absorbance (570nm) with cell number. Results reported as mean fold change in growth at day 4 vs day 1,day 6 vs day 1, day 15 vs day 1 and day 20 vs day1; error bars show one standard deviation from N=3 biological replicates; ****p ≤ 0.0001by one way ANOVA.

7.4.5 Effect of RPMI 1640 medium on the stability of alginate beads in 3D dynamic culture

Several reports have demonstrated that directed induction towards endoderm can be performed from human PSCs, both ESCs and IPSCs have used RPMI 1640 media (Chouristodoulou et al., 2011; D'Amour et al., 2005; Dutt et al., 2003; Kadzik & Morrisey, 2012; Naujok et al., 2014; Yasunaga et al., 2005) . In this work, it was observed that beads cultured in RPMI 1640 showed a remarkable diameter increase in the centre of capsules (Figure 7.6). Diameter and stability of alginate beads during long-term culture in RPMI 1640 decreased compared with culturing in DMEM F12. Therefore, the use of RPMI 1640 media was damaging the beads due to its high sodium concentration which was replaced calcium ions in the crosslinking structure of the beads, causing disintegration, an effect reported earlier in literature for alginate beads exposed to high-sodium media formulation (Gaumann et al., 2000). By changing the culture media to DMEM F12, mechanical

resistance stabilized. This was determinant for the success of future experiments and change medium from RPMI 1640 to DMEM F12.

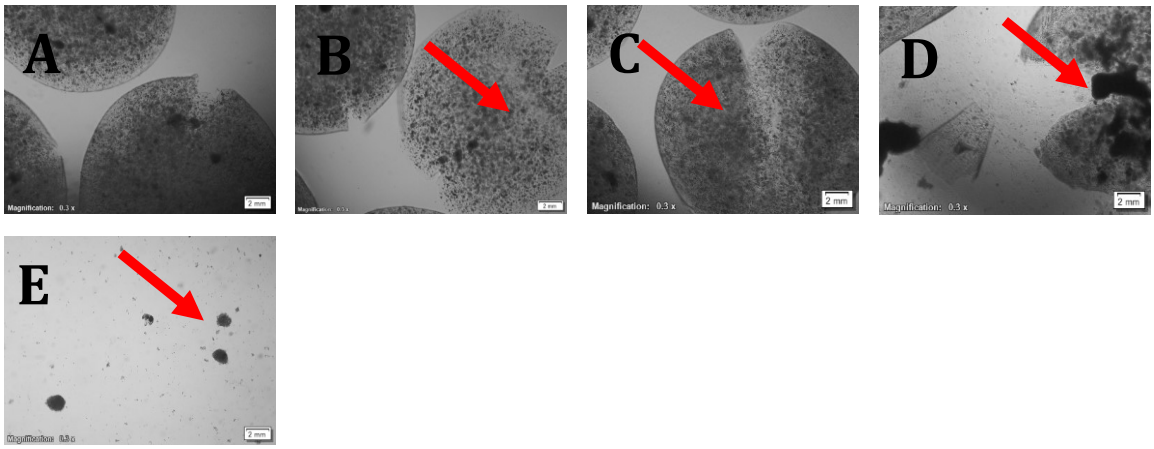


Figure 7.6: Calcium alginate beads were cultured in RPMI 1640 leading to membrane rupture.
A, B and C images showed the swelling of the beads in the centre and the diameter increase, leading to membrane rupture. D and E images show alginate beads ruptured causing cells to be released into the medium. Scale bars, 2µm.

7.5 Conclusion

This chapter describes an efficient and scalable method to generate endoderm cells from human IPSCs in 4 days. 3D dynamic culture in both conditions studied in this chapter displayed the capability to enhance the differentiation towards endoderm significantly when compared to the traditional 2D monolayer culture. Particularly, the treatment with Activin (100 ng/mL) and CHIR99021 (3µM) for 4 days showed the best results. Long term proliferation of human IPSCs in alginate beads and dynamic motion was improved when cultured in medium containing 2% serum. Moreover, it was found in this chapter that the use of RPMI 1640 media was damaging the beads due to its high sodium concentration, as suggested earlier (Gaumann et al., 2000). The stability of alginate beads was affected by RPMI 1640, which resulted in the inability to perform more assays to confirm the efficiency of differentiation into endoderm. This realization was determinant for the success of the following experiments. In addition, it was considered that MTS is not the

most suitable assay to evaluate the cell proliferation within the beads. Indeed, all the information obtained in this chapter contributed to the optimisation and improvement of the protocol to derive alveolar *type II cells* in 3D dynamic culture.

Chapter 8

Differentiation of Human Induced Pluripotent Stem Cells into Functional Lung Alveolar Epithelial Cells in 3D Dynamic Culture

The ability to efficiently generate lung epithelium type 2 cells from human induced pluripotent stem cells has been observed for regenerative medicine applications (Green, Huang and Snoeck, 2013). As stated in Chapter 7, dynamic motion and 3D cultures are able to enhance cell proliferation and survival. Furthermore, cell proliferation was significantly stimulated, as shown in the previous chapter by the addition of 10 μM Y-27632 in a 20 day culture period. The results in Chapter 7 prove that encapsulated human IPSCs grown in dynamic conditions were able to be induced towards endoderm more successfully when the combination of 3μM CHIR99021 and human Activin A was used, in comparison with the combination of Wnt3a and Activin A. These successful results suggest that the inclusion of 10 μM Y-27632 may potentially be added to optimise the Huang protocol in 2D (Huang et al., 2013), coupled with the following use of 3μM CHIR99021 and human Activin A to induce the endoderm stage, as suggested by Huang et al. (2013).

8.1 Introduction

It is estimated that about 60 million people worldwide are living with a type of lung disease and 4 million die from it every year (Ghaedi 2015). Currently, the only definitive treatment for terminal lung disease is lung transplantation, a procedure that brings several problems, namely, the shortage of donors, the risk of graft rejection and the life-long administration of immunosuppressive drugs to the patients (Ahmad 2011). Recent studies suggest that a very promising alternative would be to use the patient's own cells as they could be used to produce an engineered lung to be implanted into the patient or used externally as support (Ott et al., 2010). However, the application of lung tissue engineering has been compromised by the low abundance of lung epithelial cells in the body and their difficult isolation and expansion in *vitro* (Wagner 2010). Lung epithelial cells differentiated from human Induced Pluripotent Stem Cells (human IPSCs) have the potential

to be a patient-specific source of cells with the potential advantage of minimizing the graft rejection issues and the need for immunosuppressive drugs post transplantation (Ghaedi 2015).

The lung has a complex three-dimensional structure with major relevant epithelial differences along the proximo-distal axis. The most distal region of the lung is organized within a complex system of alveoli, which are lined by two primary epithelial cells types: type I and type II pneumocytes. The majority of the alveolar surface area (up to 95%) is composed of type I pneumocytes which are primarily responsible for gas-exchange, while Type II pneumocytes secrete alveolar surfactants (such as protein C) and are organised in a cube-like structure (Rawlins 2006). Lung epithelia remains one of the least studied lineages derived from embryonic stem cells in *vitro* (Siti-Ismail 2012). As mentioned above, an alternative strategy is the use of human IPSCs which can be obtained by genetically reprogramming adult cells (Takahashi 2006). These cells can be further differentiated into different lineages including lung epithelium (Siti-Ismail 2012; Ghaedia 2014). It has been proven that reprogramming cells resets their epigenetic fate map, which then allows extracellular cues such as cell culture conditions to direct phenotypic changes in these cells. Despite its technical feasibility, generation of lung progenitors from human IPSCs is yet to be done at an appreciable scale so as to satisfy the need for large numbers of fully differentiated cells. This could be accomplished by moving from traditional 2D cultures into 3D geometries such as scaffolds or bioreactors (Tsuchiya 2014). A three-dimensional culture requires a matrix suitable for the culture of anchorage-dependent cells whose size and structural properties allow for efficient supply of gas and nutrients to all cells and for the removal of waste products. Semi-permeable alginate beads have been successfully used for this application (Miranda 2010). In particular, the generation of lung epithelium may benefit from state of microgravity whereby cells are not exposed to turbulence and high shear stress, improving cell to cell interaction while agitation required to provide enhanced diffusion of gases and nutrients can still be present (Hammond 2001).

8.2 Aims and Objectives

The aim of the present study was to develop a strategy for the culture and differentiation of human IPSCs into alveolar type II cells in an *in-vitro* system that mimics the *in-vivo* environment. It was hypothesized that hydrogel beads offer a suitable matrix for 3D cultures and the HARV bioreactor can be used to mimic dynamic microgravity conditions. This is expected to increase the differentiation of human IPSCs cells to a similar, or possibly greater, degree to that obtained with traditional monolayer cultures.

8.3 Methodology

Human IPSCs were encapsulated and cultured in static mode for 24 hours in MTeSR™1 media with 10 μM Y-27632. After 24 hours primitive streak formation is induced for 1 day in basal differentiation media composed of DMEM F12 media supplemented with N2 supplement, B27 supplement, ascorbic acid (50 μg/ml), Glutamax (2 mM), Monothioglycerol (0.4 μM), 2 % of FBS and 10 μM Y-27632. Additionally, 1 ng/ml BMP-4 was added to the basal medium. On days 2 to 5, endoderm was induced by adding 3μM CHIR99021 and human Activin A to a final concentration of 100 ng/ml. On days 5 to 7, 200 ng/ml human Noggin and 10 μM SB-431542 were added to the basal media for anterior foregut endoderm induction and, from days 7 to 15, lung progenitor formation was induced with 3μM CHIR99021, 10 ng/ml human FGF10, 10 ng/ml human FGF7, 20 ng/ml murine EGF and 500 μM all-trans retinoic acid. Finally, for the maturation stage (days 15 to 20) 3μM CHIR99021, 10 ng/ml human FGF10, 10 ng/ml human, 50 nM Dexamethasone, 0.1 mM 8-Bromo-cAMP and 0.1 mM IB were added.

This protocol, illustrated in (Figure 8.1) has been followed for 3D static and dynamic cultures and 2D cultures were run in parallel as control as the original protocol (Huang et al., 2013) had been established for 2D cultures.

The viability and proliferation of cells inside the beads were assayed through fluorescence by incorporation of Calcein AM and Ethidium homodimer and using proliferation assay the Cell Titer Glo 3D assay, which measures ATP inside the bead. This assay was applied in this chapter as it is a highly powerful lytic assay, which resulted in a higher degree of sensitivity at all the stages of the protocol, as this was a problem found in the

previous chapter with the use of the MTS assay. Immunostaining, qRT-PCR and western blot were used to evaluate the differentiation, and the effect of culture conditions and component, such as hypoxia and the presence of extracellular matrix (ECM) in early and late stages of the protocol. In addition, transmission electron microscopy (TEM) was performed on the differentiated beads to confirm morphological and functional characteristics of the cells, such as lamellar bodies and micro filaments.

Finally, to confirmation of the positive impact of hypoxia on the differentiation a small experiment in 2D was conducted. The optimised protocol was applied on two group of cells: one cultured and differentiated under 20% O2 and the other under 5% O2 to create a hypoxic environment and these cells were analysed at day 20 by using qRT-PCR.

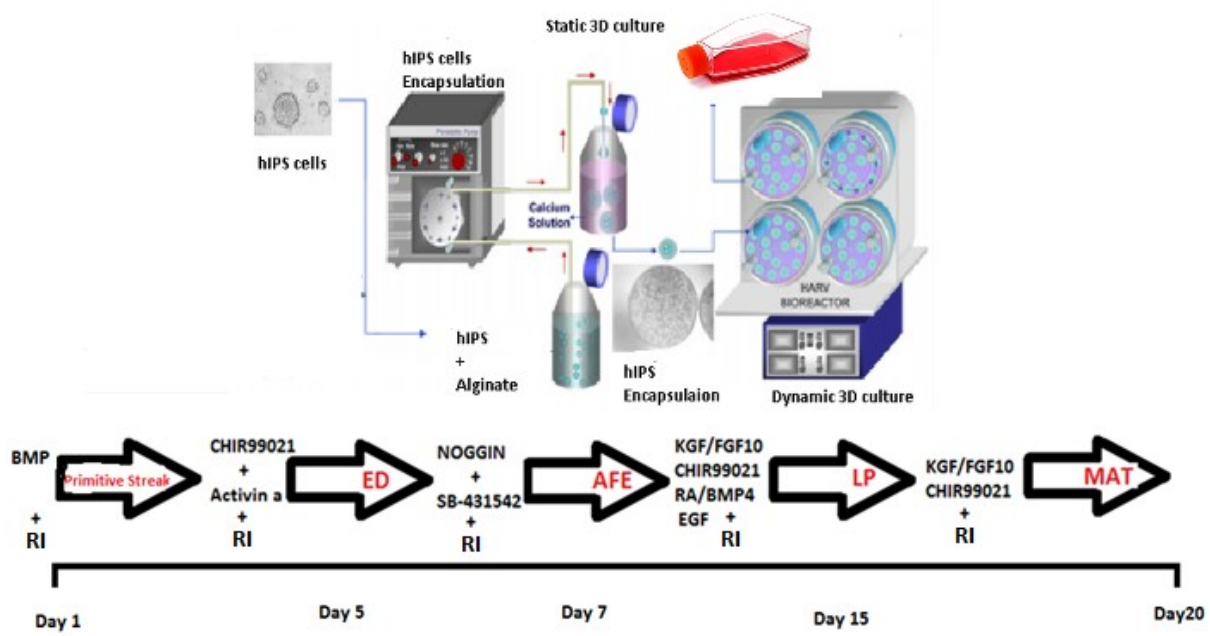


Figure 8.1 Differentiation protocol followed for the induction of lung epithelium from human IPSCs. After 24 in static cultures, cells were differentiated in 4 stages during the days of culture. (Modify Teo, Mantalaris and Lim, 2014).

8.4 RESULTS and DISCUSSION

8.4.1 Cell proliferation and viability in static and dynamic 3D cultures

Cell viability was evaluated at different time points by live/dead staining with Calcein AM and an Ethidium homodimer and observation was conducted by fluorescence microscopy, using the appropriate filters. The results for days 1, 6, 15 and 20 shown in (Figure 8.2 A) show that viability of the dynamic 3D cultures was high, without any evidence of a necrotic core at these time points (Figure 8.2A). The difference between the two conditions was analysed using the Cell Titer Glo 3D assay which allowed to confirm that the viability in dynamic cultures was higher than that in static cultures for all time points as shown in (Figure 8.2 B) ($p < 0.0001$). In addition, TEM analysis at days 15 showed the presence of necrotic and apoptotic bodies in static but not in dynamic cultures (Figure 8.2 C). Lastly, at day 20, huge cell aggregates were formed like a tissue around the beads (Figure 8.15 B). In contrast with the static culture, the aggregates accumulated around the periphery of the beads, allowing the formation of interactions between neighbouring cells and ECM as it would occur in normal tissue. It is hypothesised that this is due to the agitation of the system supporting enhanced mass transport within the culture, which in turn allows them the cells to proliferate more. This is also supported by the greater production of ECM in dynamic cultures, which is noticeable from the pictures of the beads in H&E staining and from the expression of fibronectin and laminin assessed by qRT-PCR (Figure 8.15). This suggests that the rotating movement of the vessel maintained adequate levels of gas and nutrient exchange inside and outside the beads.

Results from both live/ dead imaging and ATP, provide evidence that both static and dynamic 3D cultures enhance cells proliferation. Previously published studies have showed that 3D cultures provide a suitable environment for differentiation, cell-cell interaction, ECM production, and cell-medium contact (Chen, Reuveny and Oh, 2013; Kempf et al., 2014; Otsuji et al., 2014). The differences in cell proliferation observed between 3D static and dynamic cultures amount to an 8-fold higher yield of cells and were found statistically significant. The dynamic culture environment allows for a reduction of the stress caused by waste products accumulation and improves cell oxygenation (Unsworth and Lelkes, 1998; Yuge et al., 2006; Zhang et al., 2015) which may support our findings. The TEM data showed necrotic cells and apoptotic bodies in static compared to dynamic conditions. Additionally, live/dead assay showed increase cell density on the bead edge on

static and reduction in the centre of the beads, possibly due to oxygen transport limitations within the microcapsules, that might have led to cellular necrosis in the core (Huang et al., 2012). Furthermore, an "O-ring"-like growth pattern was observed in 3D static possibly due to nutrient limitation occurring in the centre (Figure 8.2 A). This phenomenon was demonstrated by De Vos et al., 1997 and related to the size of the beads (Vos, Haan and Van Schilfgaarde, 1997). Therefore, reducing the size of microcapsules or using agitation motion might be useful strategies to overcome this issue.

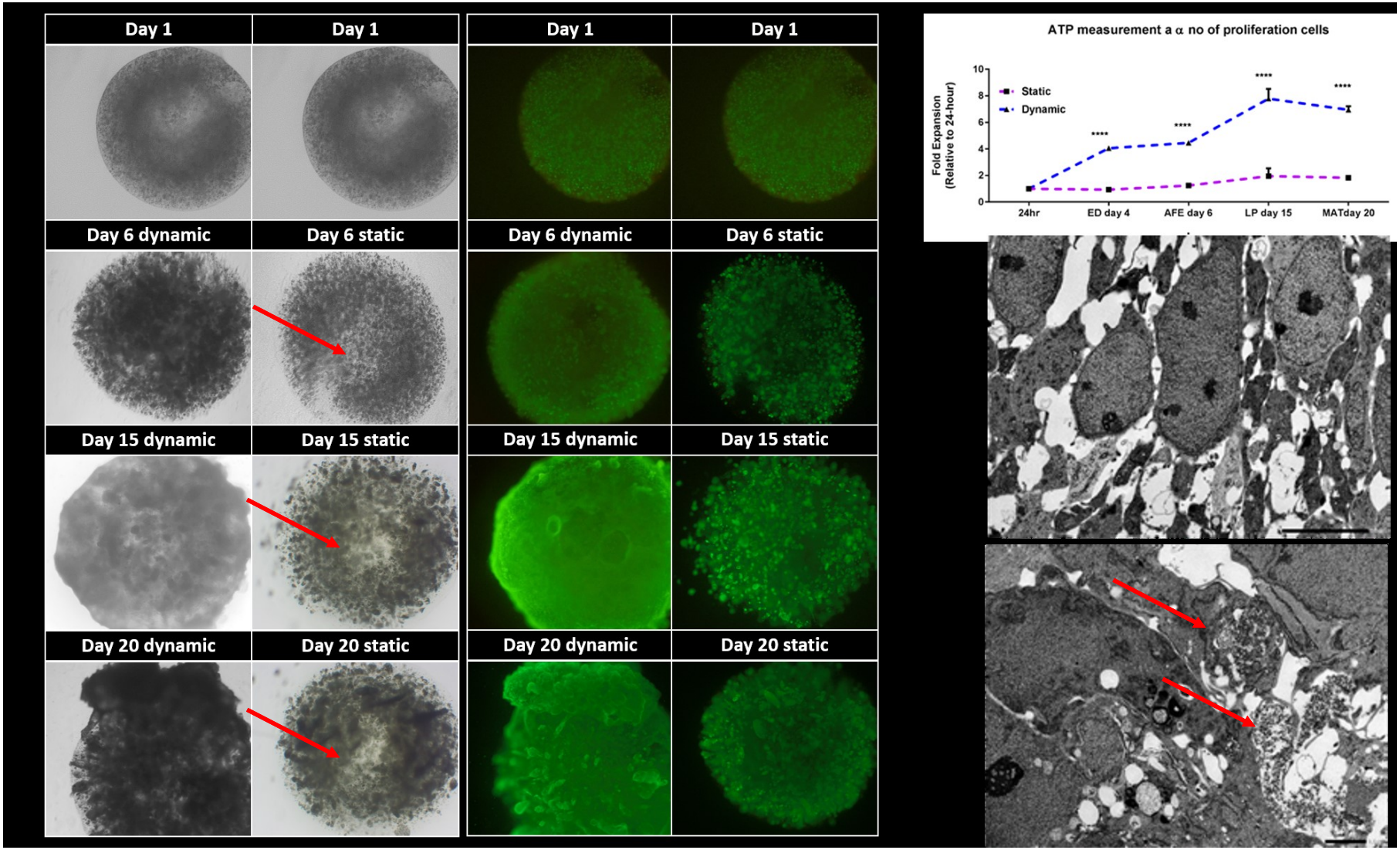


Figure 8.2 Comparison of static and dynamic 3D cultures in cells proliferation.

A) Images of live/dead staining showed increased cell growth throughout the differentiation process and the red arrows show the necrotic core in static. Scale bars, 2 mm for Images; B) Cell Titre Glo profile of encapsulated human IPSCs. Proliferation (normalized to day one, error bars show one standard deviation, n = 3 biological replicates. **** = $p < 0.0001$; C) TEM of dynamic cultures at day 15 revealed the presence of necrotic cells or apoptotic bodies and a heterogeneous population in static condition whereas no necrotic or apoptotic structures were found in the homogenous dynamically cultured cells. Scale bars, 5.0 μm for images.

8.4.2 Induction of human IPSCs differentiation into type II alveolar cells

To examine the effect of static and dynamic 3D cultures on the induction of type II alveolar cells, we analyzed the expression of markers associated with type II alveolar cells at various time points during the differentiation process, namely days 4, 6, 15 and 20. The genetic markers analysed were CXCR4, an endoderm marker, FOXa2, the endodermal trascription factor and distal epithelia marker, OCT3/4, a pluripotency marker, Nkx2.1 a lung progenitor, SFTPS as a marker type 2 cells, CFTR as a marker of proximal epithelia finaly for Type 1 cells AQ5a was used.

On day 4, both CXCR4 and FOXa2 markers were significantly upregulated in dynamic cultures compared to static cultures and to the control 2D cultures (Figure 8.3). The pluripotency marker expression was not significanly changed at this time between the control and the dynamic culture (Figure 8.3)(Kubo et al., 2004; D'Amour et al., 2005; Sturgeon et al., 2014). On day 6, the expression of CXCR4 was reduced compared to day 4, and this reduction was seen for both static and dynamic cultures with significant differences between the two 3D culture modes and between those and the control (2D) suggesting the induction towards anterior foregut endoderm was effective (Figure 8.4 A). This was confirmed by immunohistochemistry, which allowed to detect the TTF-1/Nkx2.1 protein in both dynamic and static cultures at this point (Figure 8.4 B) (Green et al., 2011).

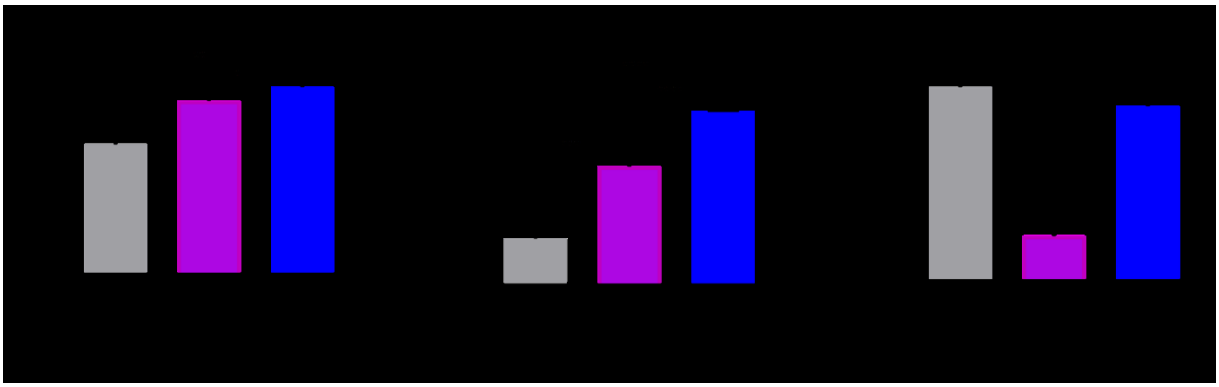


Figure 8.3 Characterization of endoderm induction at day 4.
qRT-PCR of endoderm associated markers: Cxcr4, Foxa2 and pluripotency marker OCT3/4. Bars show mean fold change on day 4, error bars show 1 standard deviation, n=3 biological replicates. Gene expression normalized to day 0 ($2-\Delta\Delta Ct$). P-values were obtained by one-way ANOVA where ****$p \leq 0.0001$, ***$p \leq 0.001$, **$p \leq 0.01$.

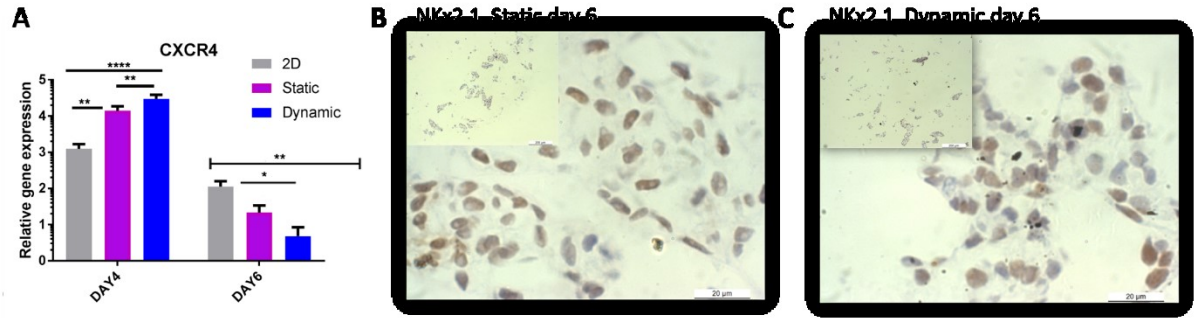


Figure 8.4 Gene expression and immunohistochemistry analyses conducted on day 6.

A) qRT-PCR of endoderm associated marker Cxcr4. Bars shown the mean fold change at day 4 and day 6; error bars show one standard deviation; n=3 biological replicates; data normalized to day 0 ($2^{-\Delta\Delta Ct}$). P-values obtained by one way ANOVA *p ≤0.0001, **p ≤ 0.01 and *p ≤ 0.05. B and C) Representative immunohistochemistry images with antibodies against NKX2.1, on day 6 in both static (B) and dynamic (C) cultures. Scale bars, 20 μm.

By day 15, the stage of differentiation towards distal lung bud progenitor was confirmed by the analysis of gene expression of the FOXa2, Nkx2.1, moreover we sought CFTR for proximal epithelium. All markers were found significantly up-regulated in dynamic cultures compared to both static cultures and 2D controls (Figure 8.5 A, B, D) especially the markers for distal epithelium. In addition, we looked if there was early differentiation for cells that expressed SFTPC because functional AEC2s derive from cells SFTPC+ distal lung. The expression of SFTPC was significantly upregulated in the dynamic condition compared to static and 2D control (Figure 8. 5 C). Type 1 cells were assessed by the expression of AQ5a, to see the ability of the dynamic culture to enhance alveolar differentiation, however there was no significant upregulation detected (Figure 8.5 E). The expression of the corresponding proteins for type 2 cells Nkx2.1, proSFTPC and proSFTPB were observed by immunohistochemistry at this stage. Both 3D cultures expressed all proteins qualitatively (Figure 8. 6). Surpsingly the results displayed proteins markers of mature type 2 which go against the findings of the publication from which this protocol was adapted (Huang et al., 2013) that Huang et al., 2013 claimed no mRNA expression of lung and airway markers were detected at d15 of the culture .In addition, the proSFTPC protein was detected strongly in dynamic by using western blot for the same time point to confirm the maturation of type 2 cells in an early stage of the protocol (Figure 8. 9).

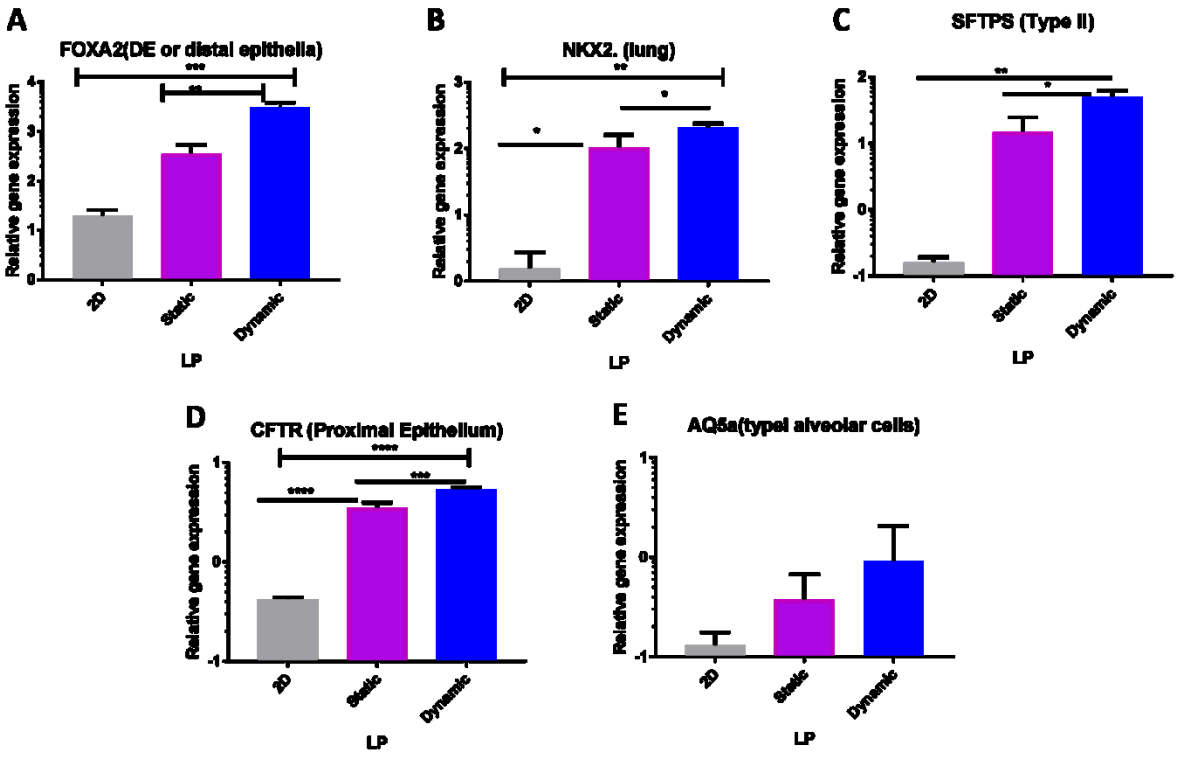


Figure 8.5 Gene expression conducted on day 15.

qRT-PCR of lung progenitor markers. Bars shown the mean fold change at day 15; error bars show one standard deviation; n=3 biological replicates; data normalized to day 0 (2−ΔΔCt). P-values obtained by one way ANOVA ****p ≤0.0001, ***p ≤ 0.001, **p≤ 0.01 and *p ≤ 0.05.

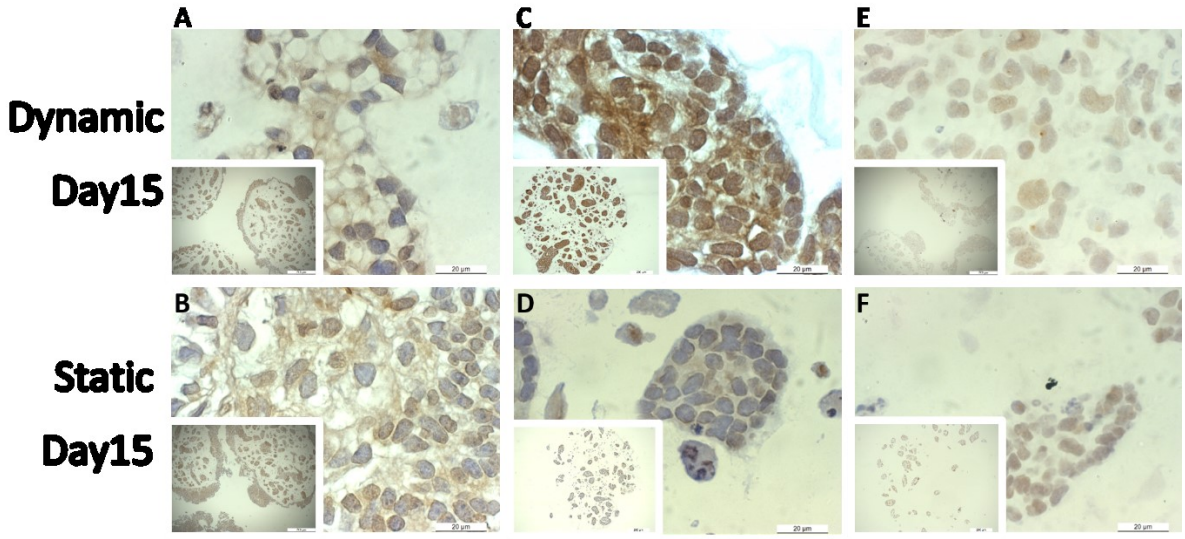


Figure 8.6 Immunohistochemistry analyses conducted on day 15.

Representative Immunohistochemistry images with (Evans & Cabral, 1975) antibodies against proSFTPB (A and B), proSFTPC (C and D) and NKX2-1 (E and F) on day 15 in both static and dynamic cultures. Scale bars, 20 µm.

Finally, at day 20 we sought the same genes used at the previous stage to determine the maturation of type 2 cells. Nkx2.1 and proSFTPC were downregulated in 3D dynamic compared to day 15 and AQ5a was upregulated significantly, suggesting the possibility of mature type II to transdifferentiate into ATI cells (Evans and Cabral, 1975; Kawanami, Ferrans and Crystal, 1982; Barkauskas et al., 2013) (Figure 8.7). The genes expression profile of the static culture at day 20 was not enough to draw a conclusion. It is possible that the transport of nutrient and gas caused different populations of cells to co-exist within the beads or that cells were in varied stages, for example quiescent cells, trans-differentiation cells, etc. (Lin and Chang, 2008). In 2D, cells expressed markers related to early lung progenitor stage (Figure 8.7). Immunohistochemistry analyses were also performed, where cells extracted from dynamic and static showed results corresponding with the genes expression (Figure 8.8).

To summarise, gene expression analysis showed significant upregulation of the genes of interest in the cultures conducted in the HARV bioreactor. Despite this, both 3D cultures expressed distal lung alveolar epithelial markers. On days 6, 15 and 20 we performed immunohistochemistry staining on the beads in static and HARV. The cells were stained with antibodies against TTF-1/Nkx2.1, on day 6 to confirm the AFE and lung bud specification (Figure 8.4 B). To test for type II pneumocyte differentiation, the beads grown in both conditions were immunostained with antibodies anti-TTF-1/Nkx2.1, proSPC and proSPB. All the aggregates showed immunoreactivity for all the markers at day 15 and 20 (Figure 8. 6 and Figure 8.8). At both time points, immunohistochemistry results show that the cells are positive for proteins proSPB, proSPC, and NKx2.1 although the expression seems to be higher in dynamic, probably due to the higher number of cells observed. In addition, the expression of protein C was also confirmed by Western Blot, where both 3D conditions show higher expression than 2D (Figure 8.9).

The proteins and genes of proSPC, proSPB, and Nkx2.1 specific markers of type II pneumocystis of lung epithelium were detected as early as day 15 of the differentiation. Huang et al., have not identified any such markers at these stages (Huang et al., 2013). The early development of type II epithelium in our protocol indicates the role of 3D alginate beads on lung induction (Anton, Burckel, Josset, & Noel, 2015; Jha et al., 2016; Chandrasekaran et al., 2017).

At the maturation stage (day 20) both static and dynamic cultures showed more potential to produce type II cells compared to the control group (2D culture) based on gene expression. The increase on type I gene expression and decrease of type II marker is evidence of the ability of mature type II to give rise to their progenitor (Jacob et al., 2017).All controls of immunohistostaining presented in (Appendix V)

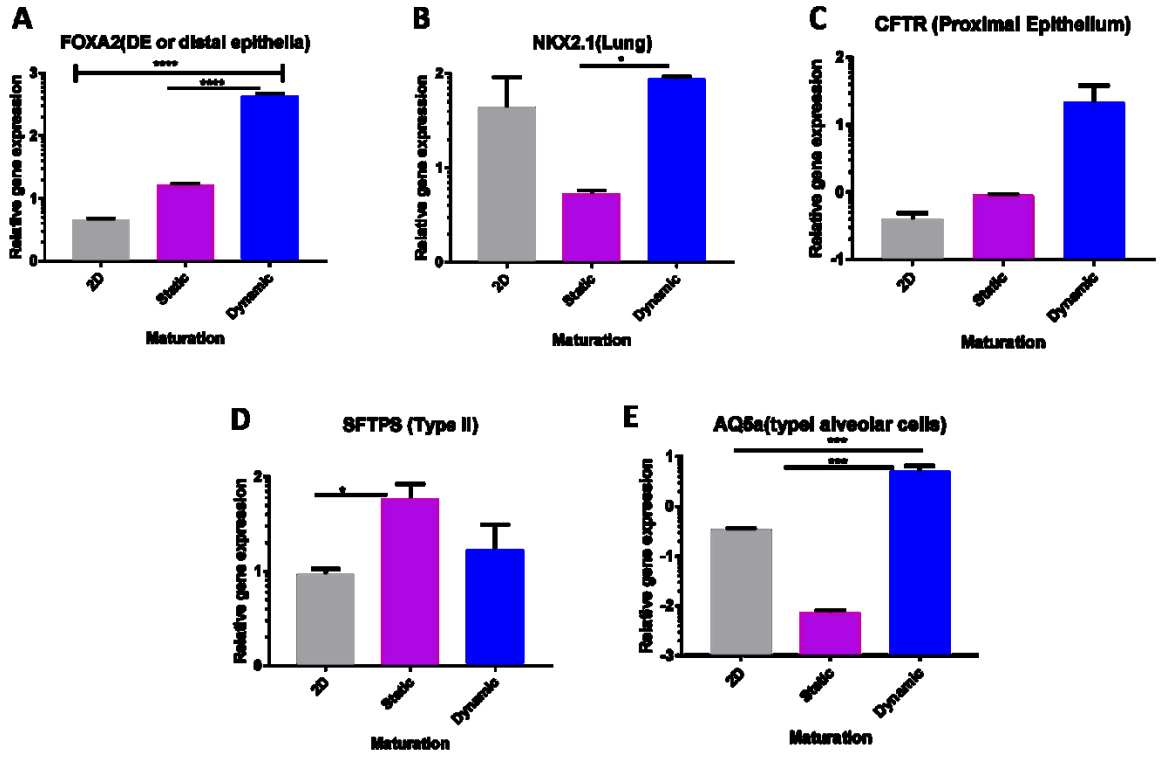


Figure 8.7 Gene expression conducted on day 20.

qRT-PCR of lung progenitor markers: with mean fold change day 20 vs day 0 (2−ΔΔCt) ± SD, n = 3 biological replicates separated on day15; ****p ≤ 0.0001, ***p ≤ 0.001, **p ≤ 0.01 and *p % 0.05 by one way ANOVA.

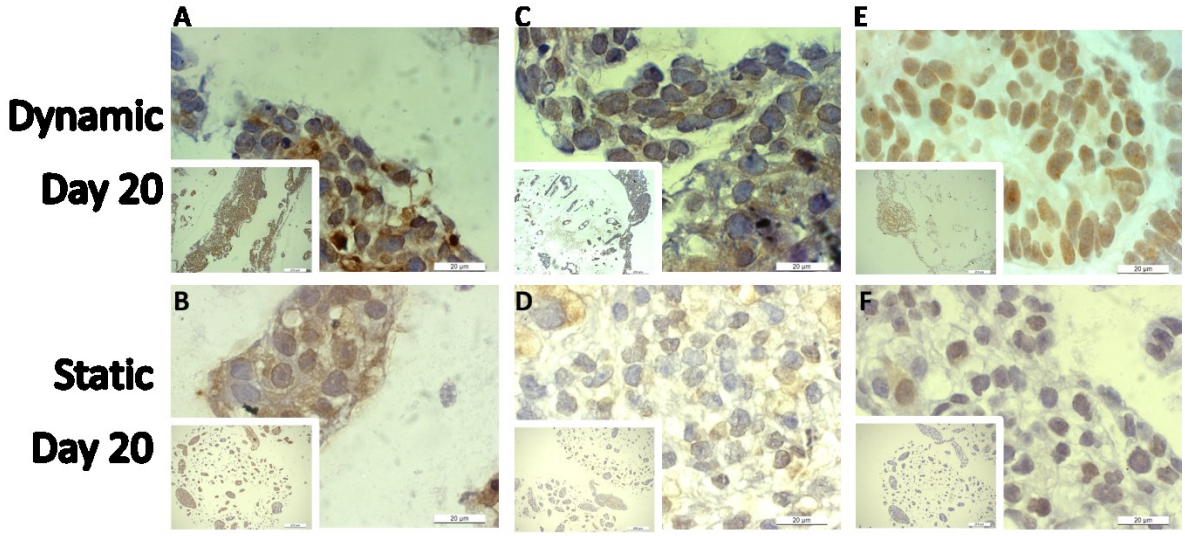


Figure 8.8 Immunohistochemistry analyses conducted on day 20.
Representative Immunohistochemistry microscopy images with antibodies against proSFTPB (A and B), proSFTPC (C and D) and NKX2-1 (E and F) on day 20 in both conditions. Scale bars, 20 µm.

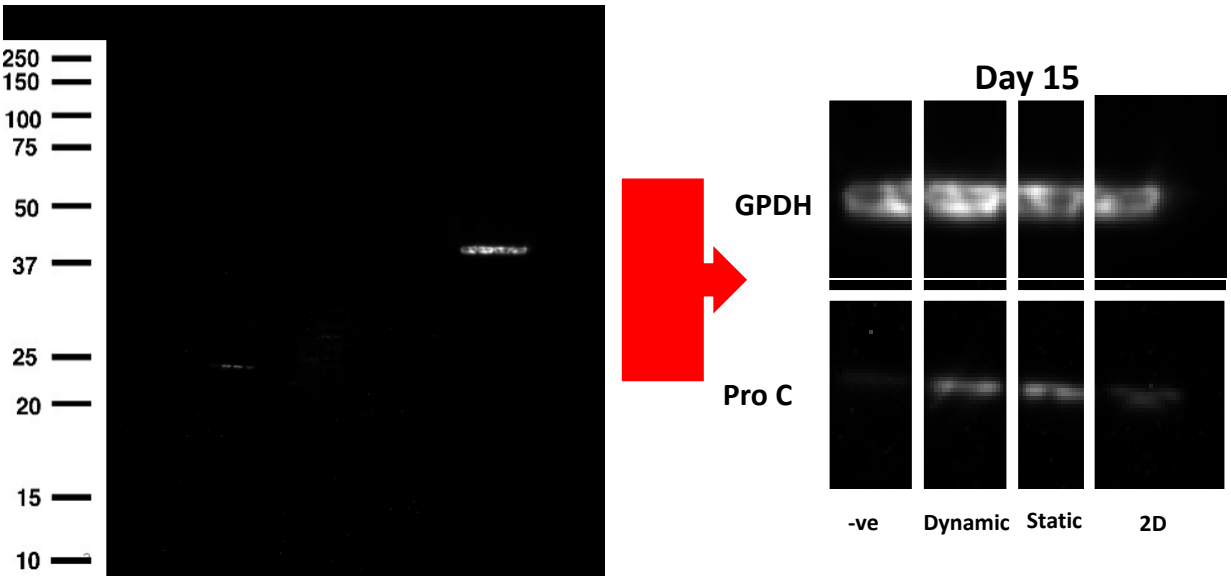


Figure 8.9 Western blot for Pro C of day 15 for 3D dynamic, static and 2D

8.4.3 Differentiated lung epithelium cells produced in 3D cultures are functional

Despite the early expression of in *vivo* SFTPC or other surfactant markers in alveolar progenitors in week 12-15 of human gestation (Khoor et al., 1994), the maturity of functional lamellar bodies becomes significant after week 24 in type 2. We assessed by (TEM)

whether cells grown in 3D cultures express these highly specialized organelles of type 2 like functional lamellar bodies, microvascular and microfilament (Fehourenbach et al., 2001).

At day 15 cells cultured in 3D dynamic environment had loosely organized membranes ,Glycogen particles trapped inside an immature lamellar body, surface microvilli, and multivesicular bodies which is consider as identity of typical immature lamellar bodies as Ridsdale and Post have identified (Ridsdale and Post, 2004)(Figure 8.10). In static cultures, lamellar bodies appeared to be immature and no microvilli nor any of multivesicular bodies, showing some debris and typical apoptotic morphology (Figure 8.11).

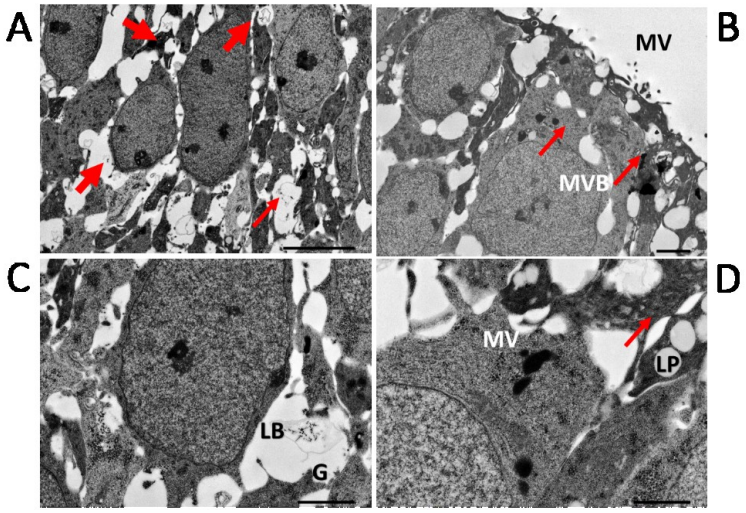


Figure 8.10 TEM of a dynamic culture at day 15.
This technique has revealed the presence of loosely organized membranes of an immature lamellar body (red arrows) as visibly seen in A) image and all following figures; .Scale bars, 5 µm. B) MV = the surface of the epithelial layer or the surface microvilli, MVB multivesicular bodies and the red arrows show electron-dense bodies for lamellar body. Scale bars, 1 µm; C) LB = formation of lamellar bodies and G= Glycogen particles trapped inside an immature lamellar body. Scale bars, 2 µm. D) LP= Lipid droplets and microvilli (MV) and some of an immature lamellar body (red arrows). Scale bars, 2 µm.

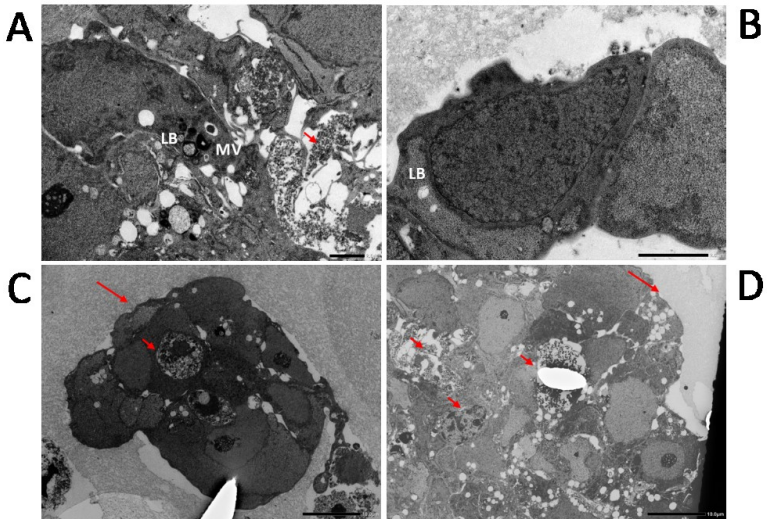


Figure 8.11 TEM of a static culture at day 15.
This technique revealed A) MV = microvilli and LP = Lipid droplets were also seen. Scale bars, 5 µm; B) LB = an immature lamellar body, MV= microvilli, and small red arrow = the extracellular space shows little debris, a typical apoptotic cell. Scale bars, 2 µm; C) LB = an immature lamellar; D) Cells form the aggregates inside the beads and there is heterogeneous between the cells shaped a typical apoptotic cell Scale bars, 10 µm ; D) Long arrow= the surface of the epithelial layer or the surface of cells sheet no microvilli and small arrow = the extracellular space shows little debris, a typical apoptotic cell. Scale bars, 10 µm.

At day 20, functional lamellar bodies, the classic marker of AEC2 maturity, were found as were other highly specialized organelles, namely, multivesicular bodies and no microvilli in 3D dynamic cultures (Figure 8.12) (Castranova et al., 1988). However, at day 20 static cells derived alveolosphere structures like multivesicular bodies, corroborating the formation of matured lamellar bodies with microvilli (Figure 8.13).

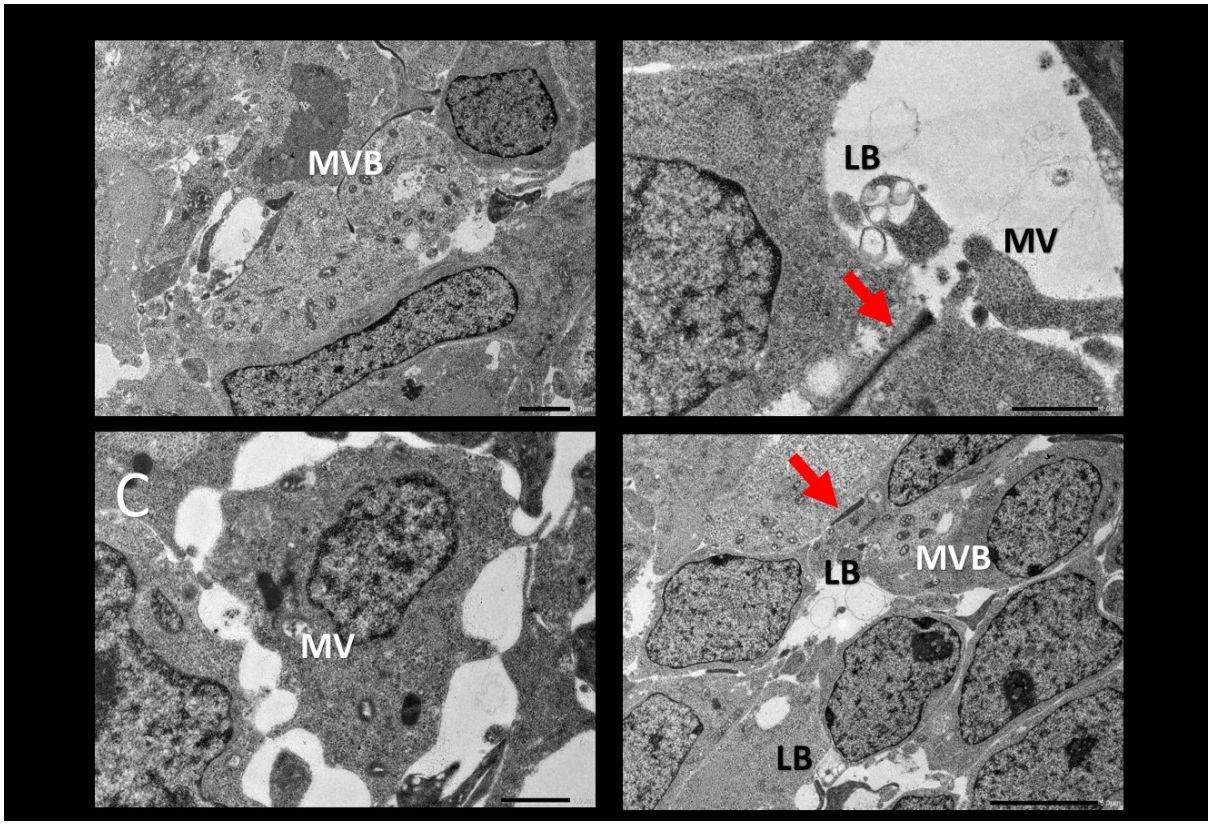


Figure 8.12 Representative TEM microscopy images of day 20 dynamic.
Cells derived alveolospheres. MVB= multivesicular bodies, the black arrow= tight junction, LB = formation of lamellar bodies and) MV = microvilli. Scale bars, 6 µm for images A and D. Scale bars, 2 µm for images B and C.

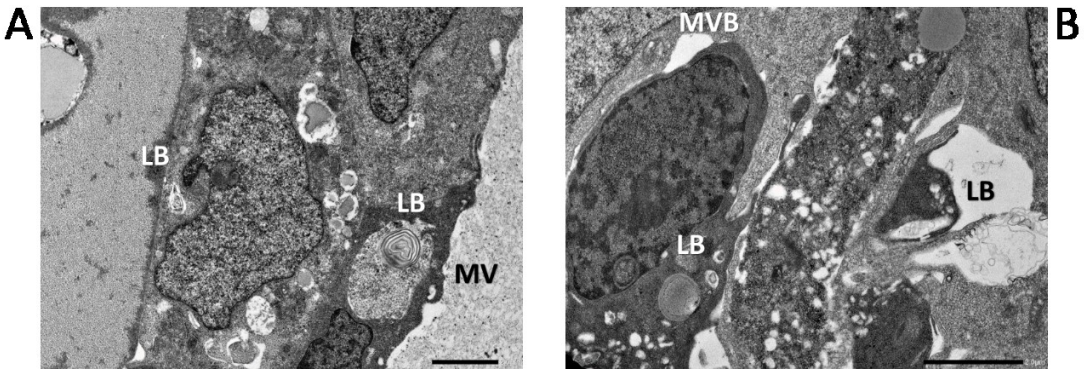


Figure 8.13Representative TEM microscopy images of day 20 static.
Cells derived alveolospheres. MVB= multivesicular bodies, LB = formation of lamellar bodies and) MV = microvilli. Scale bars, 2 µm for images A and B.

8.4.4 The interaction of the microenvironment and the encapsulated cells.

Monolayer 2D cultures ensure a uniform oxygenation and nutrient transport to the entire cell population whereas 3D cultures tend to be more structurally heterogeneous which impacts the transport of gases and nutrients. To some extent, 3D geometries mimic the physiological environment better than 2D cultures but a 3D culture environment may affect cell behaviour (Barthes et al., 2014; Edmondson et al., 2014).

As a consequence of uneven gas distribution in 3D cultures, a hypoxic niche may be formed (Duval et al., 2017) which may compromise the viability and proliferation (Majmundar, Wong, & Simon, 2010). However, it has been reported that hypoxia may play a positive role in the induction of lung epithelium differentiation and proliferation (Garreta, Melo, Navajas, & Farre, 2014; Huang et al., 2013; Pimton et al., 2015). The response of cells when oxygen changes are arbitrated through the family of transcriptional regulators which are called hypoxia-inducible factors (HIF). Under normoxic conditions, HIF is rapidly degraded. On the other hand, under hypoxia, HIF is stable and accumulates in the nucleus and works as a promoter of many hypoxia-responsive target genes involved in the control of cellular proliferation, glucose metabolism, and angiogenesis (Groenman et al. 2007).

The presence of hypoxic niches has been evaluated by measuring the expression of HIF-1α for acute low oxygen tension and HIF-2α gene expression for long term adaption of hypoxia. The two genes are co-expressed (Yu et al., 1998). These analyses were conducted on days 4 and 20 of the culture corresponding to early time of the culture protocol and late time of culture. Hypoxic niches are possibly important for lung differentiation as HIF-2α has been reported to correlate with enhanced differentiation of lung epithelium. On day four, the expression patterns of HIF2α and HIF-1α were starting to increase on both 3D cultures without any significant demonstration. On day 20 the gene expression was significantly different between the control 2D culture and both 3D culture geometries tested in terms of HIF2α expression. The HIF-1α expression was further statistically significant between dynamic and static cultures (Figure 8.14 A). This observation could be correlated with high proliferation of cells at day 20, upregulation of differentiation markers and notable ECM production in dynamic culture. Hypoxia inducible factor, a key

transcriptional factor in response to hypoxia, is involved in stimulation of excessive ECM like fibronectin (Ho et al., 2014; Xiong and Liu, 2017) and promotes extracellular matrix remodelling which showed by Gilkes (Gilkes et al., 2013). Additionally, one factor known to organise the development of lung epithelium and vasculature is VEGF, a main down-stream target gene of HIF-1a (Van Tuyl et al. 2005; Zhao et al. 2005). Zhao et al. (2005) presented that inhibition of VEGF activity resulted in reduced epithelial proliferation in a lung renal capsule allograft model that mimics lung development. Also, Lee et al. (2012) have confirmed that mouse embryoid bodies (EBs) cultured in hypoxic and exogenous growth factors-deprived conditions upregulated HIF-1-mediated VEGF and led to the efficient differentiation of mouse ESC. Therefore, VEGF is involved in endothelial cell differentiation from ESC in *vitro* as well as lung epithelium proliferation in *vivo* (Zhao et al. 2005) and in (Lee et al. 2012).

In order to confirm the positive effect of hypoxia on the differentiation of human IPSCs, the latter were cultured in 2D under two levels of oxygen (5% and 20%) and differentiated by using a step-wise differentiation protocol which was used previously in 3D comparison experiments (Figure 8.14B). On day 20 of the differentiation method, gene expression analysis of differentiated human IPSCs showed that Nkx2.1 and SFTPC and AQ5A were up-regulated at 5% compared to 20% oxygen tension (Figure 8.14C). The effect of hypoxia in the in *vitro* culture has been extensively studied in stem cell research (reprogramming, differentiation, maintaining, etc.). Moreover, many studies reported the beneficial effect of low pO2 in stem cell specification lineage e.g. heart, lung and lung from pluripotent stem cells (Huang et al., 2013; Garreta et al., 2014). Although, as previously stated in literature, the mechanism behind low-oxygen-induced lung epithelium differentiation is not yet fully understood, this study supports earlier findings suggesting that hypoxia does enhance human IPSCs differentiation into lung epithelium cells (Garreta et al., 2014).

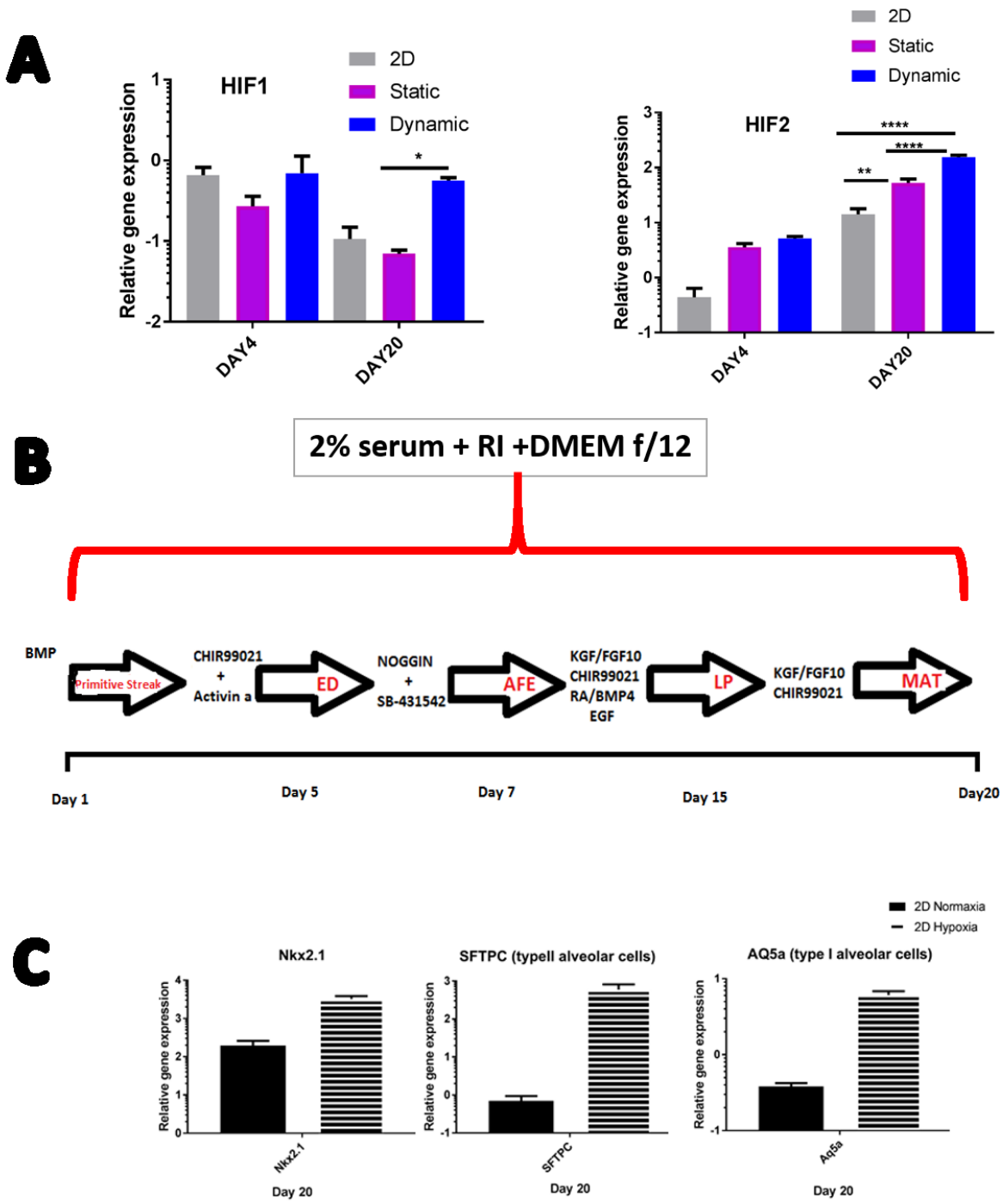


Figure 8.14 The impact of hypoxia in cells differentiation.
(A). The expression of HIF-1a and HIF-2a has significantly increased between geometries at day 20 suggesting that hypoxia plays a role in differentiation (B) This has been confirmed by a step-wise differentiation protocol (C). At the day 20 the expression of Nkx2.1, SFTPC and AQ5a were up-regulated confirming increased differentiation in hypoxia in compression with normoxia group.

8.4.5 Extracellular matrix production in 3D dynamic enhancing cells proliferation and differentiation

The development of multicellular organs requires the assembly of ECM that serves to spatially organize cells as per their function in *vivo*. Maintaining and mediating lung function relies on the ECM role. Numerous reports suggest that the phenotypic behaviour of cells can be influenced by the 3D matrix structure and organization (Salgado, Coutinho and Reis, 2004). Lung ECM proteins have been implicated in lung branching morphogenesis, vasculogenesis, and alveolar maturation during development. Fibronectin (FN) plays a role in processes of lung development like proliferation and differentiation (Roman, 1997).

The effects of 3D dynamic culture on the mRNA expression of FN1 and LAMA5 were evaluated by real-time RT-qPCR. Cells cultured in 3D dynamic showed significantly up-regulated levels of fibronectin (FN1) mRNA expression on day 20 ($p<0.05$). The same was observed for (LAMA5) ($p<0.05$) on day 4 and day 20 ($P<0.05$) compared to 2D cultures (Figure 8. 15A) which is crucial for distal lung epithelial cell differentiation and normal late lung development (Nguyen and Senior, 2006).

Hornberger et al., 2000 showed that the proliferation of human Fetal Ventricular Myocyte cells (HFVMs) depended on the abilty of cells to secrete collagen and fibronectin (Hornberger *et al.*, 2000). In agreement with Hornberger et al., 2000, cells in the 3D dynamic condition exhibited higher proliferation in day 20 correlated with significant expression of FN. Induction of a dynamic state for cells by using bioreactors combined with three dimensional scaffolds have proved their role in cellular proliferation and ECM production, in comparison with static culture (Freed *et al.*, 1994; Bueno, Bilgen and Barabino, 2005). In summary, synthesis of extracellular matrix in 3D dynamic culture enhanced cellular proliferation and differentiation into type 2 lung epithelium.

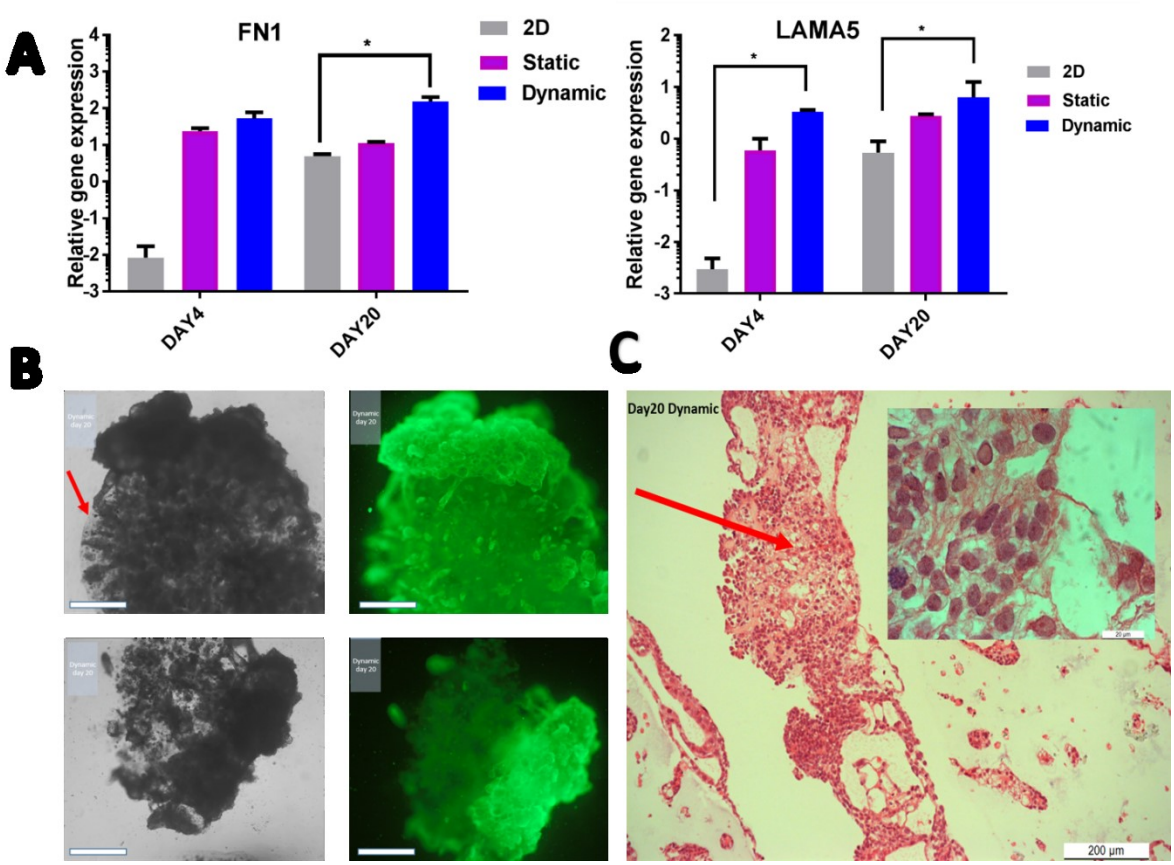


Figure 8.15 ECM gene expression in static and rotary environment.
A) Expression of FN1 (fibronectin) and LAMA5 (laminin) genes on days 4 and 20 of culture. Results show significant differences at day 20 between 3D dynamic dultures and the control culture (2D). B) formation of tissues-like which include ensemble of similar cells and their extracellular matrix at 3D daynmic by day 20. C) Representative images of hematoxylin & eosin (HE) stained showed cells and their extracellular matrix fromed tissues-like and how the cells proliferate more in 3D daynmic by day 20. Scale for images, 2mm. Scale for images, 200µm.

8.5 Conclusion

In this chapter, we have studied whether 3D tissue engineering of type II pneumocytes. In combination with alginate beads and dynamic motion could improve the efficiency of the differentiation of human pulmonary type II cells from human IPSCs. Human IPSCs were encapsulated inside alginate hydrogel beads and dynamic movement was simulated by using the HARV bioreactor. In addition, the impact of 3D culture dynamics was examined for induction of differentiation, proliferation, survival, molecular changes and functionality of type II pneumocytes. To the best of our knowledge, to date, no study has been

performed testing the direct differentiation of human IPSCs towards lung epithelium using alginate encapsulation and a HARV bioreactor. This technique promises to differentiate and expand high numbers of mature lung progenitors as a future autologous therapy for diseases incurring damage to the lung alveolar epithelium.

The differentiation conditions used in this work prove the ability of both static and dynamic 3D cultures to deliver mature lung epithelium cells from human IPSCs differentiation. However, in terms of scaling up cell production, dynamic cultures provide a better environment for cell growth and proliferation. Our method provides the best available approach combining suitable biomaterials and bioprocess conditions for future production of cells to be used for transplants.

Chapter 9

Conclusion and Future Work

This chapter provides an overview to the contributions of the present thesis as well as propose future research directions.

9.1 The contribution and general conclusion

Diseases such as idiopathic fibrosis and lung cancer could be treated by the use of alveolopheres which is derived from human PSCs and the primary tissue (Dye, Miller and Spence, 2016; Barkauskas et al., 2017).This research has emphasized on type II alveolar epithelial cells since they have been proven to act as a self-renewal cell as well as a generator to type I cells under-injury circumstances (Barkauskas et al., 2013; Gotoh et al., 2014; Dye, Miller and Spence, 2016; Barkauskas et al., 2017). In an attempt to form alveolopheres from the primary tissue, researchers found that fetal lung fibroblast cell line and Matrigal droplet were necessary in terms of support. As a result, AECI and AECII were found within the Matrigel droplet (Barkauskas et al., 2013).

In another attempt, researchers purified lung epithelial progenitors using flow cytometry which was further cultured with human fetal lung fibroblast cell line and given particular biochemical factors via a specific medium. The results of this attempt were similar to the earlier attempt and formations of the thin cysts were found within the Matrigel droplet (Huang et al., 2013; Firth et al., 2014; Gotoh et al., 2014). Although the previous attempts were made using 2D and 3D lung models from primary human lung tissues and human PSCs, certain limitations were found (Barkauskas et al., 2013; Rock et al., 2009; Gotoh et al., 2014; Konishi et al., 2016; Dye et al., 2015; Firth et al., 2014; Mou et al., 2016; Wong et al., 2012; Huang et al., 2013). The robustness of both approaches were not clear and whether this would yield to a degree of organization (Dye et al., 2016). The major limitation within the previous trials was that the tissue organization cannot be generated in *vitro*. This is because the alveolar structure is unique within its capacity and couldn't be formed instantly in *vitro*. Therefore, there is a need for in *vivo* transportation and com-

plete differentiation (Mathieu et al., 2013). In order to provide a fully mature and functional tissue, the need of supporting mesenchyme and vascular supply is required (Dye, Miller and Spence, 2016).

One of the most crucial factors of moving from in *vitro* to in *vivo* is immune response, which impacts both organoid growth and maturation. In addition, the role of the immune system under organ development is not clear. It is also crucial to know that the transplantation into adult animals may be affected by the host immune system. Transplantation is also correlated with surgical injury and the consequential inflammatory response that can impact progenitor cell differentiation (Dye et al., 2017). In order to support in *vivo* transplantation, biomaterials can be used the assist in handling the immune system response and in order to minimize the impact of the injury and inflammatory response on the organoid engraftment (Dye et al., 2017).

Matrigel has been used as one of the main biomaterials for coating alveolopheres. However, Matrigel is comprised from undefined matrix and is derived from mouse tumors. Additionally, the physical and chemical priorities of Matrigel cannot be easily altered (Gjorevski et al., 2016). Therefore, the required material must be fully defined in matrix from either natural or synthetic materials. Furthermore, both matrix and stiffness that define the native airway environment are vital to derive airway structures whether it is in *vitro* or in *vivo* (Czerwinski and Spence, 2017). The native organ can be recapitulated in terms of physical and chemical properties and biomaterials have the potential to do so and maintain the growth and maturity of the respiratory system in *vivo* or in *vitro* (Finkbeiner et al., 2015).

The contribution of this research lies in filling a gap where a fully defined and functional natural material is needed for in *vivo* transplantation. In this thesis, we presented a protocol integrating the fundamentals of cell biology and engineering as a successful example of a multidisciplinary approach. The production of functional type II pneumocyte cells from human IPSCs was achieved within 20 days in a novel, direct, low serum, feeder-free, 3D dynamic culture, avoiding the EB formation stage, the co-culture needs and the use of Matrigel™. Slight manipulation of the concentrations and combinations of cytokines and the additive of chemical supplements from a previously suggested protocol (Huang et al., 2013) assisted reproducible and directed differentiation into type II pneumocytes cells.

Exploiting the 3D dynamic culture condition as a key differentiation enhancer, improved the maturation of type II pneumocytes, functionality and cell culture scale-up.

The experimental design used in this work combined analytical techniques and assays as presented in chapter 5. The protocol herein developed allowed to maintain and sustain pluripotent states of human IPSCs. In addition, the use of low oxygen tensions in combination with the Y-27632 RHO/ROCK pathway inhibitor enhanced proliferation and pluripotency of after passaging human IPSCs to a single cell. The study of micro environmental effects in cell proliferation of encapsulated human IPSCs in alginate hydrogel (chapter 6) resulted in the identification of significant factors which allowed for the optimisation of existing differentiation protocols as successfully shown in the differentiation of human IPSCs to airway epithelium cells (chapters 7-8).

Several significant conclusions can be drawn from the findings of this work:

- Hypoxia alone without inhibiting the RHO/ROCK pathway has a positive impact in proliferation when human IPSCs are passaged as single cells. However, combined with the Y-27632 RHO/ROCK pathway inhibitor hypoxia increases the rate of human IPSC and human ESC cells proliferation far more significantly.

- 3D dynamic cultures maintain and sustain pluripotent states of human IPSCs within 20 days without passaging cells enzymatically or mechanically. In addition, human IPSCs were able to produce their own ECM into 3D dynamic cultures which might be correlated with the increase of the rate of cell growth and upregulates the expression of associated pluripotency markers.

- 3μM CHIR99021 having previously been shown to suppress pluripotency, effectively generating DE from human PSCs in traditional 2D monolayer cultures, in this thesis its combination with 100 ng/mL Activin A in 3D dynamic culture maximally and significantly induced DE differentiation.

Using natural biomaterials (alginate) which are renewable, cost effective and biocompatible has allowed to develop a highly efficient protocol to produce type-II alveolar epithelial cells. This protocol is herein presented for the first time. This approach can be further refined and used to meet the need for transplantation of type-II-like alveolar epithelial

into animals to reach maturity (blood flow, immune factors, neural innervation, or mechanical strain of the local environment).

9.2 Future work

Although the main aims of this thesis have been achieved, many challenges and questions remain to be overcome in the lung cell bioprocessing field. In order to move research nearer to clinical applications, further studies will have to be carried out following up on the promising results of this work. The next points discuss the crucial areas that need further investigation.

9.2.1 2D culture

Cell cultivation needs further optimization to find effective matrix alternatives for adherent 2D cultures. In our human IPSCs culture protocols, both maintenance medium mTeSR™1 and cell-substrate adherence Corning® Matrigel® human ESC-qualified Matrix contains either animal products or undefined components (please refer to chapter 5). The mTeSR™1 medium contains bovine serum albumin (BSA) while Corning® Matrigel® has several unidentified components (Osiecka-Iwan et al., 2008, Rodin et al., 2014). The presence of animal products on growth medium can cause cross-species contamination (Choumerianou et al., 2008). Replacing mTeSR™1 with formulations like TeSR™2 and TeSR™-E8™ will provide fully-defined, serum- and feeder-free medium retaining the self-renewal capabilities of the cells (Chen et al., 2011). Also, this formulation allows for an easy transition to stem cells clinical and research applications. In the case of Matrigel™, there is a number of fully characterized alternatives such as xeno-free adherent matrix Vitronectin XF™ (Braam et al., 2008, Prowse et al., 2010) and a chemically defined Laminin-521 (Lu et al., 2014, Rodin et al., 2014).

9.2.2 3D culture

Alginate is a non-toxic, non-immunogenic and biocompatible material but did not promote mammalian cells-adhesion to hydrogels. Coating with gelatin overcomes this limitation but it is not optimal for therapeutic applications. Gelatin may trigger an immune response because it is animal derived. Another issue related to the use of gelatin is its batch-to-batch variability. Finding appropriate ligands is crucial to promote and regulate cellular interactions such as peptides including the sequence arginine-glycine-aspartic

acid (RGD). RGD is widely used as adhesion ligand owing to the presence of integrin receptors (e.g., αvβ3, α5β1) on various cell types. Therefore, covalently modified alginate with RGD was effective on promoting self-renewal, differentiation, as well as to substitute exogenous soluble factors. Substituting gelatin with more defined cell-adhesive peptides could be one of the approaches in future experiments (Hoffman, 2012; Lee & Mooney, 2012).

9.2.3 Further assays to validate type II pneumocytes maturation

9.2.3.1 Mature SFTPB and SFTPC protein forms localize to lamellar bodies (LBLs), multivesicular bodies (MVBs)

As was reported for mature II pneumocytes, the processing of pro-SP-B (pro surfactant protein B) to mature SP-B in alveolar type 2 cells requires a series of post-translational modifications and proteolytic cleavages. Through the course of SP-B processing, the mature protein must be transported to the (LBLs) where it is concentrated with SP-C and surfactant-specific phospholipids. The mechanisms controlling the process of LBL formation and the aggregation of these diverse surfactant components are poorly understood. To elucidate these events, it is important to examine the intracellular localization of SP-B processing (Korimilli et al., 2000; Brasch et al., 2004).

We suggest to detect mature SFTPB (pro surfactant protein B) and SFTPC (pro surfactant protein C) protein forms in human IPSC-derived type II pneumocytes-like cells in alginate beads by using immunogold labelling based on a method described in this paper (Ridsdale et al., 2011).

9.2.3.2 Lipid profile analysis to determine whether putative II pneumocytes synthesize and secrete surfactant-specific 32:0 dipalmitoyl phosphatidylcholine (DPPC)

Using gas chromatography to measure in particular, 32:0 dipalmitoyl phosphatidylcholine would be important. DPPC is the most abundant class of phospholipids in pulmonary surfactant (Jacob *et al.*, 2017).

9.2.3.3 Define more related genes for both of II pneumocytes and I pneumocytes

Next, we are going to sought and define more related genes for types I and II pneumocytes. In terms of II pneumocytes, markers such as Surfactant protein D (SFTPD), Pulmonary surfactant-associated protein A1 (SFTPA1), Pulmonary surfactant-associated protein A2 (SFTPA2), ABCA3, Lysosome-associated membrane glycoprotein 3 (LAMP3), LPCAT (Lysophosphatidylcholine acyltransferase), PGC, cathepsin H (CTSH) and Napsin A Aspartic Peptidase (NAPSA) could be looked at whereas for type-I pneumocytes PDPN, AGER, and CAV1 could be suitable markers (Jacob *et al.*, 2017). We suggest to analyse 3 different time points in iPSC-derived type 2 like cells in alginate beads differentiation: day 0 undifferentiated cells, day 15 lung progenitors and day 20 lung maturation. For a control we suggest to do comparison with 2 primary cells, 1-primary fetal distal alveolar epithelial progenitors (21week gestation) and second adult human II pneumocytes.

9.2.3.4 Display Transdifferentiation Capacities

As has been published for primary adult human AEC2s maintained in 3D sphere cultures (Barkauskas et al., 2013), PSC-derived SFTPC+ cells do not detectably transdifferentiate into AEC1 in 3D cultures. Therefore, we are going to decapsuled the cells and culture them on 2D based on the protocol was published by Dobbs et al., 1988; (Dobbs et al., 1988; Borok et al., 1998). To observe the morphology of AEC1 flat and senescent squamous cells and see if their upregulation of AEC1 marker genes—PDPN, AGER, QA5A and CAV1 and downregulation of SFTPC type AEC2 marker. In addition we are going to see the ability of product cells in forming an epithelial barrier with ZO-1-positive tight junctions (Zhao, Yee and O'Reilly, 2013).

9.2.3.5 Validate the protocol on other cell stem cell lines

Testing the AEC2 induction protocol on other cell line such as embryonic or adult stem cells will assets its reproducibility, competence, and the therapeutic readiness to animal studies and in future clinical trials.

Bibliography

A Grapin-Botton. 2008. Endoderm Specification. SourceStemBook [Internet] - Google Scholar. https://scholar.google.com/scholar_lookup?title=Endoderm specification. SourceStemBook %5BInternet%5D&author=A. Grapin-Botton&publication_year=2008.

Abujarour, Ramzey, Bahram Valamehr, Megan Robinson, Betsy Rezner, Florin Vranceanu, and Peter Flynn. 2013. "Optimized Surface Markers for the Prospective Isolation of High-Quality Hipscs Using Flow Cytometry Selection." Scientific Reports 3. https://doi.org/10.1038/srep01179.

Ahmed, Maqsood, and Charles ffrench-Constant. 2016. "Extracellular Matrix Regulation of Stem Cell Behavior." Current Stem Cell Reports 2 (3): 197–206. https://doi.org/10.1007/s40778-016-0056-2.

Ali, Nadire N., Alasdair J. Edgar, Ali Samadikuchaksaraei, Catherine M. Timson, Hanna M. Romanska, Julia M. Polak, and Anne E. Bishop. 2002. "Derivation of Type II Alveolar Epithelial Cells from Murine Embryonic Stem Cells." Tissue Engineering 8 (4): 541–50. https://doi.org/10.1089/107632702760240463.

Alvarez-Tejado, M, S Naranjo-Suarez, C Jiménez, A C Carrera, M O Landázuri, and L del Peso. 2001. "Hypoxia Induces the Activation of the Phosphatidylinositol 3-Kinase/Akt Cell Survival Pathway in PC12 Cells: Protective Role in Apoptosis." The Journal of Biological Chemistry 276 (25): 22368–74. https://doi.org/10.1074/jbc.M011688200.

Ameri, Jacqueline, Anders Ståhlberg, Jesper Pedersen, Jenny K. Johansson, Martina M. Johannesson, Isabella Artner, and Henrik Semb. 2009. "FGF2 Specifies HESC-Derived Definitive Endoderm into Foregut/Midgut Cell Lineages in a Concentration-Dependent Manner." Stem Cells 28 (1): N/A-N/A. https://doi.org/10.1002/stem.249.

Amit, M, M K Carpenter, M S Inokuma, C P Chiu, C P Harris, M A Waknitz, J Itskovitz-Eldor, and J A Thomson. 2000. "Clonally Derived Human Embryonic Stem Cell Lines Maintain Pluripotency and Proliferative Potential for Prolonged Periods of Culture." Developmental Biology 227 (2): 271–78. https://doi.org/10.1006/dbio.2000.9912.

Andrade, C. F., A. P. Wong, T. K. Waddell, S. Keshavjee, and M. Liu. 2006. "Cell-Based Tissue Engineering for Lung Regeneration." AJP: Lung Cellular and Molecular Physiology 292 (2): L510–18. https://doi.org/10.1152/ajplung.00175.2006.

Anselme, Karine, and Maxence Bigerelle. 2006. "Effect of a Gold-Palladium Coating on the Long-Term Adhesion of Human Osteoblasts on Biocompatible Metallic Materials." Surface and Coatings Technology 200 (22–23 SPEC. ISS.): 6325–30. https://doi.org/10.1016/j.surfcoat.2005.11.001.

Anton, Delphine, Hélène Burckel, Elodie Josset, and Georges Noel. 2015. "Three-Dimensional Cell Culture: A Breakthrough in Vivo." International Journal of Molecular Sciences. https://doi.org/10.3390/ijms16035517.

Athanazio, R. 2012. “Airway Disease: Similarities and Differences between Asthma, COPD and Bronchiectasis.” Clinics 67 (11): 1335–43. https://doi.org/10.6061/clinics/2012(11)19.

Badger, J L, M L Byrne, F S Veraitch, C Mason, I B Wall, and M A Caldwell. 2012. “Hypoxic Culture of Human Pluripotent Stem Cell Lines Is Permissible Using Mouse Embryonic Fibroblasts.” Regenerative Medicine 7 (5): 675–83. https://doi.org/Doi 10.2217/Rme.12.55.

Banerjee, Ena Ray, Michael A. Laflamme, Thalia Papayannopoulou, Michael Kahn, Charles E. Murry, and William R. Henderson. 2012. “No Title.” Edited by Mauricio Rojas. PLoS ONE 7 (3): e33165. https://doi.org/10.1371/journal.pone.0033165.

Barkauskas, Christina E, Michael J Cronce, Craig R Rackley, Emily J Bowie, Douglas R Keene, Barry R Stripp, Scott H Randell, Paul W Noble, and Brigid L M Hogan. 2013. “Type 2 Alveolar Cells Are Stem Cells in Adult Lung.” The Journal of Clinical Investigation 123 (7): 3025–36. https://doi.org/10.1172/JCI68782.

Barthes, Julien, Hayriye Özçelik, Mathilde Hindié, Albana Ndreu-Halili, Anwarul Hasan, and Nihal Engin Vrana. 2014. “Cell Microenvironment Engineering and Monitoring for Tissue Engineering and Regenerative Medicine: The Recent Advances.” BioMed Research International. https://doi.org/10.1155/2014/921905.

Batorsky, Anna, Jiehong Liao, Amanda W Lund, George E Plopper, and Jan P Stegemann. 2005. “Encapsulation of Adult Human Mesenchymal Stem Cells within Collagen-Agarose Microenvironments.” Biotechnology and Bioengineering 92 (4): 492–500. https://doi.org/10.1002/bit.20614.

Bean, Allison C., and Rocky S. Tuan. 2013. “Stem Cells and Nanotechnology in Tissue Engineering and Regenerative Medicine.” In Micro and Nanotechnologies in Engineering Stem Cells and Tissues, 1–26. Hoboken, New Jersey: John Wiley & Sons, Inc. https://doi.org/10.1002/9781118574775.ch1.

Ben-Haim, Nadav, Cindy Lu, Marcela Guzman-Ayala, Luca Pescatore, Daniel Mesnard, Mirko Bischofberger, Felix Naef, Elizabeth J. Robertson, and Daniel B. Constam. 2006. “The Nodal Precursor Acting via Activin Receptors Induces Mesoderm by Maintaining a Source of Its Convertases and BMP4.” Developmental Cell 11 (3): 313–23. https://doi.org/10.1016/j.devcel.2006.07.005.

Berridge, Michael V., Patries M. Herst, and An S. Tan. 2005. “Tetrazolium Dyes as Tools in Cell Biology: New Insights into Their Cellular Reduction.” Biotechnology Annual Review. https://doi.org/10.1016/S1387-2656(05)11004-7.

Bienaimé, Christophe, Jean-Noël Barbotin, and José-Edmundo Nava-Saucedo. 2003. “How to Build an Adapted and Bioactive Cell Microenvironment? A Chemical Interaction Study of the Structure of Ca-Alginate Matrices and Their Repercussion on Confined Cells.” Journal of Biomedical Materials Research Part A 67A (2): 376–88. https://doi.org/10.1002/jbm.a.10487.

Bonaventure, J., N. Kadhom, L. Cohen-Solal, K. H. Ng, J. Bourguignon, C. Lasselin, and P. Freisinger. 1994. “Reexpression of Cartilage-Specific Genes by Dedifferentiated Human Articular Chondrocytes Cultured in Alginate Beads.” Experimental Cell Research 212 (1): 97–104. https://doi.org/10.1006/excr.1994.1123.

Braam, S R, L Zeinstra, S Litjens, D Ward-van Oostwaard, S van den Brink, L van Laake, F Lebrin, et al. 2008. “Recombinant Vitronectin Is a Functionally Defined Substrate That Supports Human Embryonic Stem Cell Self-Renewal via Alpha V Beta 5 Integrin.” Stem Cells 26 (9): 2257–65. https://doi.org/10.1634/stemcells.2008-0291.

Bueno, Ericka M, Bahar Bilgen, and Gilda a Barabino. 2005. “Wavy-Walled Bioreactor Supports Increased Cell Proliferation and Matrix Deposition in Engineered Cartilage Constructs.” Tissue Engineering 11 (11): 1699–1709. https://doi.org/10.1089/ten.2005.11.1699.

Buschmann, M D, Y A Gluzband, A J Grodzinsky, and E B Hunziker. 1995. “Mechanical Compression Modulates Matrix Biosynthesis in Chondrocyte/Agarose Culture.” Journal of Cell Science, April, 1497–1508. http://www.ncbi.nlm.nih.gov/pubmed/7615670.

Buschmann, M D, Y A Gluzband, A J Grodzinsky, J H Kimura, and E B Hunziker. 1992. “Chondrocytes in Agarose Culture Synthesize a Mechanically Functional Extracellular Matrix.” Journal of Orthopaedic Research : Official Publication of the Orthopaedic Research Society 10 (6): 745–58. https://doi.org/10.1002/jor.1100100602.

Busslinger, Meinrad, Stephen L. Nutt, Barry Heavey, and Antonius G. Rolink. 1999. “Commitment to the B-Lymphoid Lineage Depends on the Transcription Factor Pax5.” Nature 401 (6753): 556–62. https://doi.org/10.1038/44076.

Calle, Elizabeth A., Mahboobe Ghaedi, Sumati Sundaram, Amogh Sivarapatna, Michelle K. Tseng, and Laura E. Niklason. 2014. “Strategies for Whole Lung Tissue Engineering.” IEEE Transactions on Biomedical Engineering 61 (5): 1482–96. https://doi.org/10.1109/TBME.2014.2314261.

Cardoso, W. V., and Jining Lü. 2006. “Regulation of Early Lung Morphogenesis: Questions, Facts and Controversies.” Development 133 (9): 1611–24. https://doi.org/10.1242/dev.02310.

Cardoso, W V. 2001. “Molecular Regulation of Lung Development.” Annu Rev Physiol 63: 471–94. https://doi.org/10.1146/annurev.physiol.63.1.471.

Castranova, V., J. Rabovsky, J. H. Tucker, and P. R. Miles. 1988. “The Alveolar Type II Epithelial Cell: A Multifunctional Pneumocyte.” Toxicology and Applied Pharmacology 93 (3): 472–83. https://doi.org/10.1016/0041-008X(88)90051-8.

Chai, Chou, and Kam W Leong. 2007. “Biomaterials Approach to Expand and Direct Differentiation of Stem Cells.” Molecular Therapy 15 (3): 467–80. https://doi.org/10.1038/sj.mt.6300084.

Chang, S C, J A Rowley, G Tobias, N G Genes, A K Roy, D J Mooney, C A Vacanti, and L J Bonassar. 2001. “Injection Molding of Chondrocyte/Alginate Constructs in the Shape of Facial Implants.” Journal of Biomedical Materials Research 55 (4): 503–11. http://www.ncbi.nlm.nih.gov/pubmed/11288078.

Chang, Tammy T., and Millie Hughes-Fulford. 2009. “Monolayer and Spheroid Culture of Human Liver Hepatocellular Carcinoma Cell Line Cells Demonstrate Distinct Global Gene Expression Patterns and Functional Phenotypes.” Tissue Engineering Part A 15 (3): 559–67. https://doi.org/10.1089/ten.tea.2007.0434.

Chapman, Sandra, David H. McDermott, Kui Shen, Moon Kyoo Jang, and Alison A. McBride. 2014. "The Effect of Rho Kinase Inhibition on Long-Term Keratinocyte Proliferation Is Rapid and Conditional." Stem Cell Research and Therapy 5 (2): 60. https://doi.org/10.1186/scrt449.

Chen, Allen, Shaul Reuveny, and Steve Oh. 2013. "Application of Human Mesenchymal and Pluripotent Stem Cell Microcarrier Cultures in Cellular Therapy: Achievements and Future Direction." Biotechnology Advances. https://doi.org/10.1016/j.biotechadv.2013.03.006.

Chen, Guokai, Zhonggang Hou, Daniel R. Gulbranson, and James A. Thomson. 2010. "Actin-Myosin Contractility Is Responsible for the Reduced Viability of Dissociated Human Embryonic Stem Cells." Cell Stem Cell 7 (2): 240–48. https://doi.org/10.1016/j.stem.2010.06.017.

Chen, Kevin G., Barbara S. Mallon, Ronald D.G. McKay, and Pamela G. Robey. 2014. "Human Pluripotent Stem Cell Culture: Considerations for Maintenance, Expansion, and Therapeutics." Cell Stem Cell 14 (1): 13–26. https://doi.org/10.1016/j.stem.2013.12.005.

Chen, Patty, Erika Marsilio, Ronald H. Goldstein, Ioannis V. Yannas, and Myron Spector. 2005. "Formation of Lung Alveolar-Like Structures in Collagen–Glycosaminoglycan Scaffolds in Vitro." Tissue Engineering 11 (9–10): 1436–48. https://doi.org/10.1089/ten.2005.11.1436.

Cho, C. H, N. R F Hannan, F. M. Docherty, H. M. Docherty, M. João Lima, M. W B Trotter, K. Docherty, and L. Vallier. 2012. "Inhibition of Activin/Nodal Signalling Is Necessary for Pancreatic Differentiation of Human Pluripotent Stem Cells." Diabetologia 55 (12): 3284–95. https://doi.org/10.1007/s00125-012-2687-x.

Christodoulou, C, T A Longmire, S Shen, A Bourdon, C A Sommer, P Gadue, A Spira, et al. 2011. "Mouse ES and IPS Cells Can Form Similar Definitive Endoderm despite Differences in Imprinted Genes." J Clin Invest 121 (6): 2313–25. https://doi.org/10.1172/JCI43853.

Claassen, David A., Michelle M. Desler, and Angie Rizzino. 2009. "ROCK Inhibition Enhances the Recovery and Growth of Cryopreserved Human Embryonic Stem Cells and Human Induced Pluripotent Stem Cells." Molecular Reproduction and Development 76 (8): 722–32. https://doi.org/10.1002/mrd.21021.

Constam, D B, and E J Robertson. 2000. "SPC4/PACE4 Regulates a TGFbeta Signaling Network during Axis Formation." Genes & Development 14 (9): 1146–55. http://www.ncbi.nlm.nih.gov/pubmed/10809672.

Covello, Kelly L, James Kehler, Hongwei Yu, John D Gordan, Andrew M Arsham, Cheng-Jun Hu, Patricia A Labosky, M Celeste Simon, and Brian Keith. 2006. "HIF-2alpha Regulates Oct-4: Effects of Hypoxia on Stem Cell Function, Embryonic Development, and Tumor Growth." Genes & Development 20 (5): 557–70. https://doi.org/10.1101/gad.1399906.

CSETE, MARIE. 2005. "Oxygen in the Cultivation of Stem Cells." Annals of the New York Academy of Sciences 1049 (1): 1–8. https://doi.org/10.1196/annals.1334.001.

Cypel, Marcelo, Bronwyn Levvey, Dirk Van Raemdonck, Michiel Erasmus, John Dark, Robert Love, David Mason, et al. 2015. "International Society for Heart and Lung Transplantation Donation After Circulatory Death Registry Report." The Journal of Heart and Lung Transplantation 34 (10): 1278–82. https://doi.org/10.1016/j.healun.2015.08.015.

D'Amour, Kevin A., Anne G. Bang, Susan Eliazer, Olivia G. Kelly, Alan D. Agulnick, Nora G. Smart, Mark A. Moorman, Evert Kroon, Melissa K. Carpenter, and Emmanuel E. Baetge. 2006. "Production of Pancreatic Hormone-Expressing Endocrine Cells from Human Embryonic Stem Cells." Nature Biotechnology 24 (11): 1392–1401. https://doi.org/10.1038/nbt1259.

D'Amour, Kevin A, Alan D Agulnick, Susan Eliazer, Olivia G Kelly, Evert Kroon, and Emmanuel E Baetge. 2005. "Efficient Differentiation of Human Embryonic Stem Cells to Definitive Endoderm." Nat Biotechnol 23 (12): 1534–41. https://doi.org/10.1038/nbt1163.

Dang, S. M., Sharon Gerecht-Nir, Jinny Chen, Joseph Itskovitz-Eldor, and Peter W Zandstra. 2004. "Controlled, Scalable Embryonic Stem Cell Differentiation Culture." Stem Cells 22 (3): 275–82. https://doi.org/10.1634/stemcells.22-3-275.

Darling, Eric M., and Kyriacos A. Athanasiou. 2003. "Articular Cartilage Bioreactors and Bioprocesses." Tissue Engineering 9 (1): 9–26. https://doi.org/10.1089/107632703762687492.

Davis, R L, H Weintraub, and A B Lassar. 1987. "Expression of a Single Transfected CDNA Converts Fibroblasts to Myoblasts." Cell 51 (6): 987–1000. http://www.ncbi.nlm.nih.gov/pubmed/3690668.

Dean, Sophia K, Yulyana, Georgia Williams, Kuldip S Sidhu, and Bernard E Tuch. 2006. "Differentiation of Encapsulated Embryonic Stem Cells after Transplantation." Transplantation 82 (9): 1175–84. https://doi.org/10.1097/01.tp.0000239518.23354.64.

Desai, Tushar J., Felicia Chen, Jining Lü, Jun Qian, Karen Niederreither, Pascal Dollé, Pierre Chambon, and Wellington V. Cardoso. 2006. "Distinct Roles for Retinoic Acid Receptors Alpha and Beta in Early Lung Morphogenesis." Developmental Biology 291 (1): 12–24. https://doi.org/10.1016/j.ydbio.2005.10.045.

Domogatskaya, Anna, Sergey Rodin, and Karl Tryggvason. 2012. "Functional Diversity of Laminins." Annual Review of Cell and Developmental Biology 28 (1): 523–53. https://doi.org/10.1146/annurev-cellbio-101011-155750.

Douglas, William H.J., Gary W. Moorman, and Robert W. Teel. 1976. "The Formation of Histotypic Structures from Monodisperse Fetal Rat Lung Cells Cultured on a Three-Dimensional Substrate." In Vitro 12 (5): 373–81. https://doi.org/10.1007/BF02796315.

Dutt, Kamla, Gary Sanford, Sandra Harris-Hooker, Lawrence Brako, Ravindra Kumar, Angela Sroufe, and Caroline Melhado. 2003. "Three-Dimensional Model of Angiogenesis: Coculture of Human Retinal Cells with Bovine Aortic Endothelial Cells in the NASA Bioreactor." Tissue Engineering 9 (5): 893–908. https://doi.org/10.1089/107632703322495547.

Duval, Kayla, Hannah Grover, Li-Hsin Han, Yongchao Mou, Adrian F. Pegoraro, Jeffery Fredberg, and Zi Chen. 2017. "Modeling Physiological Events in 2D vs. 3D Cell Culture." Physiology 32 (4): 266–77. https://doi.org/10.1152/physiol.00036.2016.

Dye, Briana R., Priya H. Dedhia, Alyssa J. Miller, Melinda S. Nagy, Eric S. White, Lonnie D. Shea, and Jason R. Spence. 2016. "A Bioengineered Niche Promotes in Vivo Engraftment and Maturation of Pluripotent Stem Cell Derived Human Lung Organoids." ELife 5 (September2016). https://doi.org/10.7554/eLife.19732.

Edmondson, Rasheena, Jessica Jenkins Broglie, Audrey F Adcock, and Liju Yang. 2014. "Three-Dimensional Cell Culture Systems and Their Applications in Drug Discovery and Cell-Based Biosensors." Assay and Drug Development Technologies 12 (4): 207–18. https://doi.org/10.1089/adt.2014.573.

Emre, Nil, Jason G. Vidal, Jeanne Elia, Eric D. O'Connor, Rosanto I. Paramban, Michael P. Hefferan, Roman Navarro, et al. 2010. "The ROCK Inhibitor Y-27632 Improves Recovery of Human Embryonic Stem Cells after Fluorescence-Activated Cell Sorting with Multiple Cell Surface Markers." Edited by Catherine M. Verfaillie. PLoS ONE 5 (8): e12148. https://doi.org/10.1371/journal.pone.0012148.

Evans, M. J., and M. H. Kaufman. 1981. "Establishment in Culture of Pluripotential Cells from Mouse Embryos." Nature 292 (5819): 154–56. https://doi.org/10.1038/292154a0.

Evans, M J, L J Cabral, R J Stephens, and G Freeman. 1973. "Renewal of Alveolar Epithelium in the Rat Following Exposure to NO2." The American Journal of Pathology 70 (2): 175–98. http://www.pubmedcentral.nih.gov/articlerender.fcgi?artid=1903972&tool=pmcentrez&rendertype=abstract.

Ezashi, Toshihiko, Padmalaya Das, and R Michael Roberts. 2005. "Low O2 Tensions and the Prevention of Differentiation of HES Cells." Proceedings of the National Academy of Sciences of the United States of America 102 (13): 4783–88. https://doi.org/10.1073/pnas.0501283102.

Farias, E, M Lu, X Li, and L M Schnapp. 2005. "Integrin Alpha8beta1-Fibronectin Interactions Promote Cell Survival via PI3 Kinase Pathway." Biochem Biophys Res Commun 329 (1): 305–11. https://doi.org/10.1016/j.bbrc.2005.01.125.

Fehrenbach, Heinz, MJ Scott, MM Reza, PD Killen, D Brubacher, M Chiquet, JS Stamler, et al. 2001. "No Title" 2 (1). http://www.ncbi.nlm.nih.gov/pubmed/11686863.

Fernandes, Tiago G., Maria Margarida Diogo, Ana Fernandes-Platzgummer, Cláudia Lobato da Silva, and Joaquim M.S. S Cabral. 2010. "No Title" 5 (1): 76–89. https://doi.org/10.1016/j.scr.2010.04.003.

Firth, A. L., C. T. Dargitz, S. J. Qualls, T. Menon, R. Wright, O. Singer, F. H. Gage, A. Khanna, and I. M. Verma. 2014. "Generation of Multiciliated Cells in Functional Airway Epithelia from Human Induced Pluripotent Stem Cells." Proceedings of the National Academy of Sciences 111 (17): E1723–30. https://doi.org/10.1073/pnas.1403470111.

Forristal, C E, D R Christensen, F E Chinnery, R Petruzzelli, K L Parry, T Sanchez-Elsner, and F D Houghton. 2013. "Environmental Oxygen Tension Regulates the Energy Metabolism and Self-Renewal of Human Embryonic Stem Cells." PLoS One 8 (5): e62507. https://doi.org/10.1371/journal.pone.0062507.

Forristal, Catherine E, Kate L Wright, Neil A Hanley, Richard O C Oreffo, and Franchesca D Houghton. 2010. "No Title" 139 (1): 85–97. https://doi.org/10.1530/REP-09-0300.

Forsyth, Nicholas R., Antonio Musio, Paolo Vezzoni, A. Hamish R.W. Simpson, Brendon S. Noble, and Jim McWhir. 2006. “Physiologic Oxygen Enhances Human Embryonic Stem Cell Clonal Recovery and Reduces Chromosomal Abnormalities.” Cloning and Stem Cells 8 (1): 16–23. https://doi.org/10.1089/clo.2006.8.16.

Foxler, Daniel E., Katherine S. Bridge, Victoria James, Thomas M. Webb, Maureen Mee, Sybil C. K. Wong, Yunfeng Feng, et al. 2012. “No Title” 14 (2). https://doi.org/10.1038/ncb2424.

Fragonas, E, M Valente, M Pozzi-Mucelli, R Toffanin, R Rizzo, F Silvestri, and F Vittur. 2000. “Articular Cartilage Repair in Rabbits by Using Suspensions of Allogenic Chondrocytes in Alginate.” Biomaterials 21 (8): 795–801. http://www.ncbi.nlm.nih.gov/pubmed/10721748.

Francis, K R, and L Wei. 2010. “No Title” 1 (2): e22. https://doi.org/10.1038/cddis.2009.22.

Franzdóttir, Sigrídur R., Ivar T. Axelsson, Ari J. Arason, Ólafur Baldursson, Thorarinn Gudjonsson, and Magnus K. Magnusson. 2010. “Airway Branching Morphogenesis in Three Dimensional Culture.” Respiratory Research 11. https://doi.org/10.1186/1465-9921-11-162.

Freed, L. E., J. C. Marquis, R. Langer, G. Vunjak-Novakovic, and J. Emmanual. 1994. “Composition of Cell-polymer Cartilage Implants.” Biotechnology and Bioengineering 43 (7): 605–14. https://doi.org/10.1002/bit.260430710.

Fuller, Julia, and Andrew J. Fisher. 2013. “An Update on Lung Transplantation.” Breathe 9 (3): 189–200. https://doi.org/10.1183/20734735.001913.

Funa, Nina S., Karen A. Schachter, Mads Lerdrup, Jenny Ekberg, Katja Hess, Nikolaj Dietrich, Christian Honoré, Klaus Hansen, and Henrik Semb. 2015. “β-Catenin Regulates Primitive Streak Induction through Collaborative Interactions with SMAD2/SMAD3 and OCT4.” Cell Stem Cell 16 (6): 639–52. https://doi.org/10.1016/j.stem.2015.03.008.

Gao, H, P S Ayyaswamy, P Ducheyne, and S Radin. 2001. “Surface Transformation of Bioactive Glass in Bioreactors Simulating Microgravity Conditions. Part II: Numerical Simulations.” Biotechnology and Bioengineering 75 (3): 379–85. http://www.ncbi.nlm.nih.gov/pubmed/11590611.

Garcia, A. J., M. D. Vega, and D. Boettiger. 1999. “Modulation of Cell Proliferation and Differentiation through Substrate-Dependent Changes in Fibronectin Conformation.” Molecular Biology of the Cell 10 (3): 785–98. https://doi.org/10.1091/mbc.10.3.785.

Garreta, Elena, Esther Melo, Daniel Navajas, and R. Farre. 2014. “Low Oxygen Tension Enhances the Generation of Lung Progenitor Cells from Mouse Embryonic and Induced Pluripotent Stem Cells.” Physiological Reports 2 (7): e12075–e12075. https://doi.org/10.14814/phy2.12075.

Gaumann, A., M. Laudes, B. Jacob, R. Pommersheim, C. Laue, W. Vogt, and J. Schrezenmeir. 2000. “Effect of Media Composition on Long-Term in Vitro Stability of Barium Alginate and Polyacrylic Acid Multilayer Microcapsules.” Biomaterials 21 (18): 1911–17. https://doi.org/10.1016/S0142-9612(00)00071-5.

Gauthaman, Kalamegam, Chui-Yee Fong, and Ariff Bongso. 2010. “Effect of ROCK Inhibitor Y-27632 on Normal and Variant Human Embryonic Stem Cells (HESCs) In Vitro: Its Benefits in

HESC Expansion." Stem Cell Reviews and Reports 6 (1): 86–95. https://doi.org/10.1007/s12015-009-9107-8.

Gerecht-Nir, Sharon, Smadar Cohen, Anna Ziskind, and Joseph Itskovitz-Eldor. 2004. "Three-Dimensional Porous Alginate Scaffolds Provide a Conducive Environment for Generation of Well-Vascularized Embryoid Bodies from Human Embryonic Stem Cells." Biotechnology and Bioengineering 88 (3): 313–20. https://doi.org/10.1002/bit.20248.

Gerecht, Sharon, Jason A Burdick, Lino S Ferreira, Seth A Townsend, Robert Langer, and Gordana Vunjak-Novakovic. 2007. "Hyaluronic Acid Hydrogel for Controlled Self-Renewal and Differentiation of Human Embryonic Stem Cells." Proceedings of the National Academy of Sciences of the United States of America 104 (27): 11298–303. https://doi.org/10.1073/pnas.0703723104.

Ghaedi, M, EA Calle, and JJ Mendez. 2013. "Human IPS Cell–derived Alveolar Epithelium Repopulates Lung Extracellular Matrix." The Journal Of. https://www.jci.org/articles/view/68793?utm_campaign=impact_2013_november&utm_content=short_url&utm_medium=pdf&utm_source=impact.

Ghaedi, Mahboobe, Julio J. Mendez, Peter F. Bove, Amogh Sivarapatna, Micha Sam B. Raredon, and Laura E. Niklason. 2014. "Alveolar Epithelial Differentiation of Human Induced Pluripotent Stem Cells in a Rotating Bioreactor." Biomaterials 35 (2): 699–710. https://doi.org/10.1016/j.biomaterials.2013.10.018.

Ghaedi, Mahboobe, Laura E. LE Niklason, and Jordana C. JC Williams. 2015. "Development of Lung Epithelium from Induced Pluripotent Stem Cells" 2 (1): 81–89. https://doi.org/10.1007/s40472-014-0039-0.

Gilkes, Daniele M., Saumendra Bajpai, Pallavi Chaturvedi, Denis Wirtz, and Gregg L. Semenza. 2013. "Hypoxia-Inducible F0actor 1 (HIF-1) Promotes Extracellular Matrix Remodeling under Hypoxic Conditions by Inducing P4HA1, P4HA2, and PLOD2 Expression in Fibroblasts." Journal of Biological Chemistry 288 (15): 10819–29. https://doi.org/10.1074/jbc.M112.442939.

Goessling, W., and D. Y. Stainier. 2016. "Endoderm Specification and Liver Development." In Methods in Cell Biology, 134:463–83. https://doi.org/10.1016/bs.mcb.2016.03.042.

Goss, Ashley M., Ying Tian, Tadasuke Tsukiyama, Ethan David Cohen, Diane Zhou, Min Lu, Terry P. Yamaguchi, and Edward E. Morrisey. 2009. "Wnt2/2b and β-Catenin Signaling Are Necessary and Sufficient to Specify Lung Progenitors in the Foregut." Developmental Cell 17 (2): 290–98. https://doi.org/10.1016/j.devcel.2009.06.005.

Govan, J R, J A Fyfe, and T R Jarman. 1981. "Isolation of Alginate-Producing Mutants of Pseudomonas Fluorescens, Pseudomonas Putida and Pseudomonas Mendocina." Journal of General Microbiology 125 (1): 217–20. https://doi.org/10.1099/00221287-125-1-217.

Grant, Gregor T., Edwin R. Morris, David A. Rees, Peter J.C. Smith, and David Thom. 1973. "Biological Interactions between Polysaccharides and Divalent Cations: The Egg-Box Model." FEBS Letters 32 (1): 195–98. https://doi.org/10.1016/0014-5793(73)80770-7.

Green, Michael D., Sarah X.L. Huang, and Hans-Willem Snoeck. 2013. “Stem Cells of the Respiratory System: From Identification to Differentiation into Functional Epithelium.” BioEssays 35 (3): 261–70. https://doi.org/10.1002/bies.201200090.

Green, Michael D, Antonia Chen, Maria-Cristina C Nostro, Sunita L d’Souza, Christoph Schaniel, Ihor R Lemischka, Valerie Gouon-Evans, Gordon Keller, and Hans-Willem W Snoeck. 2011. “Generation of Anterior Foregut Endoderm from Human Embryonic and Induced Pluripotent Stem Cells.” Nat Biotechnol 29 (3): 267–72. https://doi.org/10.1038/nbt.1788.

Grimm, Daniela, Markus Wehland, Jessica Pietsch, Ganna Aleshcheva, Petra Wise, Jack van Loon, Claudia Ulbrich, Nils E. Magnusson, Manfred Infanger, and Johann Bauer. 2014. “Growing Tissues in Real and Simulated Microgravity: New Methods for Tissue Engineering.” Tissue Engineering Part B: Reviews 20 (6): 555–66. https://doi.org/10.1089/ten.teb.2013.0704.

Guarino, Richard D., Laura E. Dike, Tariq A. Haq, Jon A. Rowley, J. Bruce Pitner, and Mark R. Timmins. 2004. “Method for Determining Oxygen Consumption Rates of Static Cultures from Microplate Measurements of Pericellular Dissolved Oxygen Concentration.” Biotechnology and Bioengineering 86 (7): 775–87. https://doi.org/10.1002/bit.20072.

Guenther, Matthew G., Garrett M. Frampton, Frank Soldner, Dirk Hockemeyer, Maya Mitalipova, Rudolf Jaenisch, and Richard A. Young. 2010. “Chromatin Structure and Gene Expression Programs of Human Embryonic and Induced Pluripotent Stem Cells.” Cell Stem Cell 7 (2): 249–57. https://doi.org/10.1016/j.stem.2010.06.015.

Hagos, Engda G, and Scott T Dougan. 2007. “Time-Dependent Patterning of the Mesoderm and Endoderm by Nodal Signals in Zebrafish.” BMC Developmental Biology 7 (1): 22. https://doi.org/10.1186/1471-213X-7-22.

Hanna, Jacob H., Krishanu Saha, and Rudolf Jaenisch. 2010. “Pluripotency and Cellular Reprogramming: Facts, Hypotheses, Unresolved Issues.” Cell. https://doi.org/10.1016/j.cell.2010.10.008.

Hansen, Morten Bagge, Svend Erik Nielsen, and Kurt Berg. 1989. “Re-Examination and Further Development of a Precise and Rapid Dye Method for Measuring Cell Growth/Cell Kill.” Journal of Immunological Methods 119 (2): 203–10. https://doi.org/10.1016/0022-1759(89)90397-9.

Hasegawa, Kouichi, Tsuyoshi Fujioka, Yukio Nakamura, Norio Nakatsuji, and Hirofumi Suemori. 2006. “A Method for the Selection of Human Embryonic Stem Cell Sub-Lines with High Replating Efficiency after Single Cell Dissociation.” Stem Cells 24 (12): DOI: 10.1634/stemcells.2005-0657. https://doi.org/10.1634/stemcells.2005-0657.

Haute, Lindsey Van, Gert De Block, Inge Liebaers, Karen Sermon, and Martine De Rycke. 2009. “Generation of Lung Epithelial-like Tissue from Human Embryonic Stem Cells.” Respir Res 10 (1): 105. https://doi.org/10.1186/1465-9921-10-105.

Hawkins, Kate E, Tyson V Sharp, and Tristan R McKay. 2013. “The Role of Hypoxia in Stem Cell Potency and Differentiation.” Regenerative Medicine 8 (6): 771–82. https://doi.org/10.2217/rme.13.71.

Haycock, J W. 2011. “3D Cell Culture: A Review of Current Approaches and Techniques.” Methods Mol Biol 695: 1–15. https://doi.org/10.1007/978-1-60761-984-0_1.

Heikkilä, Minna, Annika Pasanen, Kari I. Kivirikko, and Johanna Myllyharju. 2011. “Roles of the Human Hypoxia-Inducible Factor (HIF)-3α Variants in the Hypoxia Response.” Cellular and Molecular Life Sciences 68 (23): 3885–3901. https://doi.org/10.1007/s00018-011-0679-5.

Ho, Yuen Yee, David Lagares, Andrew M. Tager, and Mohit Kapoor. 2014. “Fibrosis - A Lethal Component of Systemic Sclerosis.” Nature Reviews Rheumatology. https://doi.org/10.1038/nrrheum.2014.53.

Hoffman, Allan S. 2012. “Hydrogels for Biomedical Applications.” Advanced Drug Delivery Reviews. https://doi.org/10.1016/j.addr.2012.09.010.

Hoffman, Lisa M., and Melissa K. Carpenter. 2005. “Characterization and Culture of Human Embryonic Stem Cells.” Nature Biotechnology. https://doi.org/10.1038/nbt1102.

Høidal, H K, H Ertesvåg, G Skjåk-Braek, B T Stokke, and S Valla. 1999. “The Recombinant Azotobacter Vinelandii Mannuronan C-5-Epimerase AlgE4 Epimerizes Alginate by a Nonrandom Attack Mechanism.” The Journal of Biological Chemistry 274 (18): 12316–22. http://www.ncbi.nlm.nih.gov/pubmed/10212201.

Hornberger, L. K., S. Singhroy, T. Cavalle-Garrido, W. Tsang, F. Keeley, and M. Rabinovitch. 2000. “Synthesis of Extracellular Matrix and Adhesion Through B1 Integrins Are Critical for Fetal Ventricular Myocyte Proliferation.” Circulation Research 87 (6): 508–15. https://doi.org/10.1161/01.RES.87.6.508.

Hosseinkhani, Hossein, Mohsen Hosseinkhani, Nathan P. Gabrielson, Daniel W. Pack, Ali Khademhosseini, and Hisatoshi Kobayashi. 2008. “DNA Nanoparticles Encapsulated in 3D Tissue-Engineered Scaffolds Enhance Osteogenic Differentiation of Mesenchymal Stem Cells.” Journal of Biomedical Materials Research - Part A 85 (1): 47–60. https://doi.org/10.1002/jbm.a.31327.

Hu, Qidong, Puja Khanna, Belinda Shu Ee Wong, Zealyn Shi Lin Heng, Charannya Sozheesvari Subhramanyam, Lal Zo Thanga, Sharon Wui Sing Tan, and Gyeong Hun Baeg. 2018. “Oxidative Stress Promotes Exit from the Stem Cell State and Spontaneous Neuronal Differentiation.” Oncotarget 9 (3): 4223–38. https://doi.org/10.18632/oncotarget.23786.

Huang, Jieqiong. 2016. “Design Research on Self-Service Medical Apparatus and Instruments Aiming at Elderly Users.” In Lecture Notes in Computer Science (Including Subseries Lecture Notes in Artificial Intelligence and Lecture Notes in Bioinformatics), 9755:3–15. https://doi.org/10.1007/978-3-319-39949-2_1.

Huang, Sarah X L, Mohammad Naimul Islam, John O’Neill, Zheng Hu, Yong-Guang Yang, Ya-Wen Chen, Melanie Mumau, et al. 2013. “Efficient Generation of Lung and Airway Epithelial Cells from Human Pluripotent Stem Cells.” Nature Biotechnology 32 (1): 84–91. https://doi.org/10.1038/nbt.2754.

Huang, Xiaobo, Xiangyu Zhang, Xiaoguang Wang, Chan Wang, and Bin Tang. 2012. “Microenvironment of Alginate-Based Microcapsules for Cell Culture and Tissue Engineering.” Journal of Bioscience and Bioengineering. https://doi.org/10.1016/j.jbiosc.2012.02.024.

Huang, Yadi, Joshua Kapere Ochieng, Marjon Buscop-van Kempen, Anne Boerema-de Munck, Sigrid Swagemakers, Wilfred van IJcken, Frank Grosveld, Dick Tibboel, and Robbert J. Rottier. 2013. “Hypoxia Inducible Factor 3α Plays a Critical Role in Alveolarization and Distal Epithelial Cell Differentiation during Mouse Lung Development.” PLoS ONE 8 (2): e57695. https://doi.org/10.1371/journal.pone.0057695.

Huelsken, J, R Vogel, V Brinkmann, B Erdmann, C Birchmeier, and W Birchmeier. 2000. “Requirement for Beta-Catenin in Anterior-Posterior Axis Formation in Mice.” The Journal of Cell Biology 148 (3): 567–78. http://www.ncbi.nlm.nih.gov/pubmed/10662781.

Hwang, Yu Shik, Johann Cho, Feng Tay, Jerry Y Heng, Raimundo Ho, Sergei G. Kazarian, Daryl R. Williams, Aldo R. Boccaccini, Julia M. Polak, and Athanasios Mantalaris. 2009. “The Use of Murine Embryonic Stem Cells, Alginate Encapsulation, and Rotary Microgravity Bioreactor in Bone Tissue Engineering.” Biomaterials 30 (4): 499–507. https://doi.org/10.1016/j.biomaterials.2008.07.028.

Illing, Anett, Marianne Stockmann, Narasimha Swamy Telugu, Leonhard Linta, Ronan Russell, Martin Müller, Thomas Seufferlein, Stefan Liebau, and Alexander Kleger. 2013. “Definitive Endoderm Formation from Plucked Human Hair-Derived Induced Pluripotent Stem Cells and SK Channel Regulation.” Stem Cells International. https://doi.org/10.1155/2013/360573.

Jacob, Anjali, Michael Morley, Finn Hawkins, Katherine B. McCauley, J. C. Jean, Hillary Heins, Cheng Lun Na, et al. 2017. “Differentiation of Human Pluripotent Stem Cells into Functional Lung Alveolar Epithelial Cells.” Cell Stem Cell 21 (4): 472–488.e10. https://doi.org/10.1016/j.stem.2017.08.014.

Jean, C, P Gravelle, J-J Fournie, and G Laurent. 2011. “Influence of Stress on Extracellular Matrix and Integrin Biology.” Oncogene 30 (24): 2697–2706. https://doi.org/10.1038/onc.2011.27.

Jensen, Todd, Blair Roszell, Fan Zang, Eric Girard, Adam Matson, Roger Thrall, Diane M Jaworski, Cayla Hatton, Daniel J Weiss, and Christine Finck. 2012. “A Rapid Lung De-Cellularization Protocol Supports Embryonic Stem Cell Differentiation in Vitro and Following Implantation.” Tissue Engineering. Part C, Methods 18 (8): 632–46. https://doi.org/10.1089/ten.TEC.2011.0584.

Jeong, Chul-Ho, Hyo-Jong Lee, Jong-Ho Cha, Jeong Hun Kim, Kwang Rok Kim, Ji-Hye Kim, Dae-Kwan Yoon, and Kyu-Won Kim. 2007. “Hypoxia-Inducible Factor-1 Alpha Inhibits Self-Renewal of Mouse Embryonic Stem Cells in Vitro via Negative Regulation of the Leukemia Inhibitory Factor-STAT3 Pathway.” The Journal of Biological Chemistry 282 (18): 13672–79. https://doi.org/10.1074/jbc.M700534200.

Jha, Rajneesh, Qingling Wu, Monalisa Singh, Marcela K. Preininger, Pengcheng Han, Gouliang Ding, Hee Cheol Cho, et al. 2016. “Simulated Microgravity and 3D Culture Enhance Induction, Viability, Proliferation and Differentiation of Cardiac Progenitors from Human Pluripotent Stem Cells.” Scientific Reports 6 (August): 30956. https://doi.org/10.1038/srep30956.

Ji, Lei, Yu-xiao Liu, Chao Yang, Wen Yue, Shuang-shuang Shi, Ci-xian Bai, Jia-fei Xi, Xue Nan, and Xue-Tao Pei. 2009. “No Title” 221 (1): 54–66. https://doi.org/10.1002/jcp.21826.

Kadzik, R S, and E Morrisey. 2012. “Directing Lung Endoderm Differentiation in Pluripotent Stem Cells.” Cell Stem Cell 10 (4): 355–61. https://doi.org/10.1016/j.stem.2012.03.013.

Kawanami, O, V J Ferrans, and R G Crystal. 1982. “Structure of Alveolar Epithelial Cells in Patients with Fibrotic Lung Disorders.” Lab Invest 46 (1): 39–53. http://www.ncbi.nlm.nih.gov/entrez/query.fcgi?cmd=Retrieve&db=PubMed&dopt=Citation&list_uids=7054589.

Kaza, Aditya K, Irving L Kron, Shari M Leuwerke, Curtis G Tribble, and Victor E Laubach. 2002. “Keratinocyte Growth Factor Enhances Post-Pneumonectomy Lung Growth by Alveolar Proliferation.” Circulation 106 (12 Suppl 1): I120-4. http://www.ncbi.nlm.nih.gov/pubmed/12354720.

Kempf, Henning, Ruth Olmer, Christina Kropp, Michael Rückert, Monica Jara-Avaca, Diana Robles-Diaz, Annika Franke, et al. 2014. “Controlling Expansion and Cardiomyogenic Differentiation of Human Pluripotent Stem Cells in Scalable Suspension Culture.” Stem Cell Reports 3 (6): 1132–46. https://doi.org/10.1016/j.stemcr.2014.09.017.

Kim, Tae-Sun, Sachiyo Misumi, Cha-Gyun Jung, Tadashi Masuda, Yoshiaki Isobe, Fujiya Furuyama, Hitoo Nishino, and Hideki Hida. 2008. “No Title” 86 (11). https://doi.org/10.1002/jnr.21687.

Kinney, Melissa A., Carolyn Y. Sargent, and Todd C. McDevitt. 2011. “The Multiparametric Effects of Hydrodynamic Environments on Stem Cell Culture.” Tissue Engineering Part B: Reviews 17 (4): 249–62. https://doi.org/10.1089/ten.teb.2011.0040.

Koay, E J, and K A Athanasiou. 2008. “Hypoxic Chondrogenic Differentiation of Human Embryonic Stem Cells Enhances Cartilage Protein Synthesis and Biomechanical Functionality.” Osteoarthritis and Cartilage 16 (12): 1450–56. https://doi.org/10.1016/j.joca.2008.04.007.

Krawetz, Roman J., Xiangyun Li, and Derrick E. Rancourt. 2009. “Human Embryonic Stem Cells: Caught between a ROCK Inhibitor and a Hard Place.” BioEssays 31 (3): 336–43. https://doi.org/10.1002/bies.200800157.

Kroon, Evert, Laura A. Martinson, Kuniko Kadoya, Anne G. Bang, Olivia G. Kelly, Susan Eliazer, Holly Young, et al. 2008. “Pancreatic Endoderm Derived from Human Embryonic Stem Cells Generates Glucose-Responsive Insulin-Secreting Cells in Vivo.” Nature Biotechnology 26 (4): 443–52. https://doi.org/10.1038/nbt1393.

Kubo, A., Katsunori Shinozaki, John M Shannon, Valerie Kouskoff, Marion Kennedy, Savio Woo, Hans Joerg Fehling, and Gordon Keller. 2004. “Development of Definitive Endoderm from Embryonic Stem Cells in Culture.” Development 131 (7): 1651–62. https://doi.org/10.1242/dev.01044.

Kunisada, Yuya, Noriko Tsubooka-Yamazoe, Masanobu Shoji, and Masaki Hosoya. 2012. “Small Molecules Induce Efficient Differentiation into Insulin-Producing Cells from Human Induced Pluripotent Stem Cells.” Stem Cell Research 8 (2): 274–84. https://doi.org/10.1016/j.scr.2011.10.002.

Kurosawa, Hiroshi. 2012. “Application of Rho-Associated Protein Kinase (ROCK) Inhibitor to Human Pluripotent Stem Cells.” Journal of Bioscience and Bioengineering. https://doi.org/10.1016/j.jbiosc.2012.07.013.

Lam, Mai T., and Michael T. Longaker. 2012. “Comparison of Several Attachment Methods for Human IPS, Embryonic and Adipose-Derived Stem Cells for Tissue Engineering.” Journal of Tissue Engineering and Regenerative Medicine 6 (SUPPL. 3). https://doi.org/10.1002/term.1499.

Lannon, C., J. Moody, D. King, T. Thomas, A. Eaves, and C. Miller. 2008. “A Defined, Feeder-Independent Medium for Human Embryonic Stem Cell Culture.” Cell Research 18: 34. https://doi.org/10.1038/cr.2008.124.

Laperle, Alex, Cheston Hsiao, Michael Lampe, Jaime Mortier, Krishanu Saha, Sean P. Palecek, and Kristyn S. Masters. 2015. “α-5 Laminin Synthesized by Human Pluripotent Stem Cells Promotes Self-Renewal.” Stem Cell Reports 5 (2): 195–206. https://doi.org/10.1016/j.stemcr.2015.06.009.

Lee, K Y, and D J Mooney. 2001. “Hydrogels for Tissue Engineering.” Chemical Reviews 101 (7): 1869–79. http://www.ncbi.nlm.nih.gov/pubmed/11710233.

Lee, Kuen Yong, and David J. Mooney. 2012. “Alginate: Properties and Biomedical Applications.” Prog Polym Sci 37 (1): 106–26. https://doi.org/10.1016/j.progpolymsci.2011.06.003.

Lee, Sae-Won, Han-Kyul Jeong, Ji-Young Jaewon Lee, Jimin Yang, Eun Ju Lee, Su-Yeon Kim, Seock-Won Youn, et al. 2012. “No Title” 4 (9). https://doi.org/10.1002/emmm.201101107.

Lee, Sang Hun, Yu Jin Lee, and Ho Jae Han. 2011. “Role of Hypoxia-Induced Fibronectin-Integrin B1 Expression in Embryonic Stem Cell Proliferation and Migration: Involvement of PI3K/Akt and FAK.” Journal of Cellular Physiology 226 (2): 484–93. https://doi.org/10.1002/jcp.22358.

Lee, Whayoung, Yuko Miyagawa, Cassandra Long, Matthew Zhang, David K.C. Cooper, and Hidetaka Hara. 2016. “Effect of Rho-Kinase Inhibitor, Y27632, on Porcine Corneal Endothelial Cell Culture, Inflammation and Immune Regulation.” Ocular Immunology and Inflammation 24 (5): 579–93. https://doi.org/10.3109/09273948.2015.1056534.

Lei, Y., and D. V. Schaffer. 2013. “A Fully Defined and Scalable 3D Culture System for Human Pluripotent Stem Cell Expansion and Differentiation.” Proceedings of the National Academy of Sciences 110 (52): E5039–48. https://doi.org/10.1073/pnas.1309408110.

Leor, J, S Aboulafia-Etzion, A Dar, L Shapiro, I M Barbash, A Battler, Y Granot, and S Cohen. 2000. “Bioengineered Cardiac Grafts: A New Approach to Repair the Infarcted Myocardium?” Circulation 102 (19 Suppl 3): III56-61. http://www.ncbi.nlm.nih.gov/pubmed/11082363.

Levenberg, S, N F Huang, E Lavik, A B Rogers, J Itskovitz-Eldor, and R Langer. 2003. “Differentiation of Human Embryonic Stem Cells on Three-Dimensional Polymer Scaffolds.” Proc Natl Acad Sci U S A 15 (22): 15. https://doi.org/10.1073/pnas.1735463100.

Levy, A P, N S Levy, S Wegner, and M A Goldberg. 1995. “Transcriptional Regulation of the Rat Vascular Endothelial Growth Factor Gene by Hypoxia.” The Journal of Biological Chemistry 270 (22): 13333–40. http://www.ncbi.nlm.nih.gov/pubmed/7768934.

Lewitzky, M, and S Yamanaka. 2007. “Reprogramming Somatic Cells towards Pluripotency by Defined Factors.” Curr Opin Biotechnol 18 (5): 467–73. https://doi.org/10.1016/j.copbio.2007.09.007.

Li, Xiangqin, Tianqing Liu, Kedong Song, Lisong Yao, Dan Ge, Chunyu Bao, Xuehu Ma, and Zhanfeng Cui. 2006. “Culture of Neural Stem Cells in Calcium Alginate Beads.” Biotechnology Progress 22 (6): 1683–89. https://doi.org/10.1021/bp060185z.

Li, Xiangyun, Roman Krawetz, Shiying Liu, Guoliang Meng, and Derrick E Rancourt. 2009. “ROCK Inhibitor Improves Survival of Cryopreserved Serum/Feeder-Free Single Human Embryonic Stem Cells.” Human Reproduction (Oxford, England) 24 (3): 580–89. https://doi.org/10.1093/humrep/den404.

Li, Ying J., Eugene H. Chung, Ryan T. Rodriguez, Meri T. Firpo, and Kevin E. Healy. 2006. “Hydrogels as Artificial Matrices for Human Embryonic Stem Cell Self-Renewal.” Journal of Biomedical Materials Research - Part A 79 (1): 1–5. https://doi.org/10.1002/jbm.a.30732.

Lim, F, and A M Sun. 1980. “Microencapsulated Islets as Bioartificial Endocrine Pancreas.” Science (New York, N.Y.) 210 (4472): 908–10. http://www.ncbi.nlm.nih.gov/pubmed/6776628.

Lin, Ruei Zhen, and Hwan You Chang. 2008. “Recent Advances in Three-Dimensional Multicellular Spheroid Culture for Biomedical Research.” Biotechnology Journal. https://doi.org/10.1002/biot.200700228.

Longmire, Tyler A, Laertis Ikonomou, Finn Hawkins, Constantina Christodoulou, Yuxia Cao, J C Jean, Letty W Kwok, et al. 2012. “Efficient Derivation of Purified Lung and Thyroid Progenitors from Embryonic Stem Cells.” Cell Stem Cell 10 (4): 398–411. https://doi.org/10.1016/j.stem.2012.01.019.

Ludwig, Tenneille E., Veit Bergendahl, Mark E. Levenstein, Junying Yu, Mitchell D. Probasco, and James A. Thomson. 2006. “Feeder-Independent Culture of Human Embryonic Stem Cells.” Nature Methods 3 (8): 637–46. https://doi.org/10.1038/nmeth902.

Ludwig, Tenneille E., Mark E. Levenstein, Jeffrey M. Jones, W. Travis Berggren, Erika R. Mitchen, Jennifer L. Frane, Leann J. Crandall, et al. 2006. “Derivation of Human Embryonic Stem Cells in Defined Conditions.” Nature Biotechnology 24 (2): 185–87. https://doi.org/10.1038/nbt1177.

Maehr, René, Shuibing Chen, Melinda Snitow, Thomas Ludwig, Lisa Yagasaki, Robin Goland, Rudolph L Leibel, and Douglas A Melton. 2009. “Generation of Pluripotent Stem Cells from Patients with Type 1 Diabetes.” Proceedings of the National Academy of Sciences of the United States of America 106 (37): 15768–73. https://doi.org/10.1073/pnas.0906894106.

Magyar, J P, M Nemir, E Ehler, N Suter, J C Perriard, and H M Eppenberger. 2001. “Mass Production of Embryoid Bodies in Microbeads.” Annals of the New York Academy of Sciences 944 (November): 135–43. http://www.ncbi.nlm.nih.gov/pubmed/11797664.

Maherali, Nimet, and Konrad Hochedlinger. 2008. “Guidelines and Techniques for the Generation of Induced Pluripotent Stem Cells.” Cell Stem Cell. https://doi.org/10.1016/j.stem.2008.11.008.

Malpel, S, C Mendelsohn, and W V Cardoso. 2000. “Regulation of Retinoic Acid Signaling during Lung Morphogenesis.” Development (Cambridge, England) 127 (14): 3057–67. http://www.ncbi.nlm.nih.gov/pubmed/10862743.

Mauck, R L, M A Soltz, C Wang, D Wong, P H Chao, W B Valhmu, C T Hung, and G A Ateshian. 2000. “Functional Tissue Engineering of Articular Cartilage through Dynamic Loading of Chondrocyte-Seeded Agarose Gels.” Journal of Biomechanical Engineering 122 (3): 252–60. http://www.ncbi.nlm.nih.gov/pubmed/10923293.

Mazure, Nathalie M., M. Christiane Brahimi-Horn, Mélanie A. Berta, Emmanuel Benizri, Rebecca L. Bilton, Frédéric Dayan, Amandine Ginouvès, Edurne Berra, and Jacques Pouysségur. 2004. “HIF-1: Master and Commander of the Hypoxic World: A Pharmacological Approach to Its Regulation by SiRNAs.” In Biochemical Pharmacology, 68:971–80. https://doi.org/10.1016/j.bcp.2004.04.022.

McLean, Amanda B., Kevin A. D’Amour, Karen L. Jones, Malini Krishnamoorthy, Michael J. Kulik, David M. Reynolds, Alan M. Sheppard, et al. 2007. “Activin A Efficiently Specifies Definitive Endoderm from Human Embryonic Stem Cells Only When Phosphatidylinositol 3-Kinase Signaling Is Suppressed.” STEM CELLS 25 (1): 29–38. https://doi.org/10.1634/stemcells.2006-0219.

Mecham, Robert P. 2012. “Overview of Extracellular Matrix.” Current Protocols in Cell Biology, no. SUPPL.57. https://doi.org/10.1002/0471143030.cb1001s57.

Mfopou, J. K., B. Chen, and I. Mateizel. 2010. “Erratum: Noggin, Retinoids, and Fibroblast Growth Factor Regulate Hepatic or Pancreatic Fate of Human Embryonic Stem Cells (Gastroenterology (2010) 138 (2233-2245)).” Gastroenterology. https://doi.org/10.1053/j.gastro.2010.11.008.

Miyazaki, Takamichi, Sugiko Futaki, Hirofumi Suemori, Yukimasa Taniguchi, Masashi Yamada, Miwa Kawasaki, Maria Hayashi, et al. 2012. “Laminin E8 Fragments Support Efficient Adhesion and Expansion of Dissociated Human Pluripotent Stem Cells.” Nature Communications 3. https://doi.org/10.1038/ncomms2231.

Mohr, Jeffrey C., Juan J. de Pablo, and Sean P. Palecek. 2006. “3-D Microwell Culture of Human Embryonic Stem Cells.” Biomaterials 27 (36): 6032–42. https://doi.org/10.1016/j.biomaterials.2006.07.012.

Mollamohammadi, Sepideh, Adeleh Taei, Mohammad Pakzad, Mehdi Totonchi, Ali Seifinejad, Najmehsadat Masoudi, and Hossein Baharvand. 2009. “A Simple and Efficient Cryopreservation Method for Feeder-Free Dissociated Human Induced Pluripotent Stem Cells and Human Embryonic Stem Cells.” Human Reproduction (Oxford, England) 24 (10): 2468–76. https://doi.org/10.1093/humrep/dep244.

Mondrinos, Mark J., Sirma Koutzaki, Eugean Jiwanmall, Mengyan Li, Jean-Pierre Dechadarevian, Peter I. Lelkes, and Christine M. Finck. 2006. “Engineering Three-Dimensional Pulmonary Tissue Constructs.” Tissue Engineering 12 (4): 717–28. https://doi.org/10.1089/ten.2006.12.717.

Moreno-Manzano, Victoria, Francisco J Rodríguez-Jiménez, Jose L Aceña-Bonilla, Santos Fustero-Lardíes, Slaven Erceg, Joaquin Dopazo, David Montaner, et al. 2010. “No Title” 285 (2). https://doi.org/10.1074/jbc.M109.008326.

Morrisey, Edward E., and Brigid L.M. Hogan. 2010. “Preparing for the First Breath: Genetic and Cellular Mechanisms in Lung Development.” Dev Cell 18 (1): 8–23. https://doi.org/10.1016/j.devcel.2009.12.010.

Mou, Hongmei, Rui Zhao, Richard Sherwood, Tim Ahfeldt, Allen Lapey, John Wain, Leonard Sicilian, et al. 2012. “Generation of Multipotent Lung and Airway Progenitors from Mouse ESCs and Patient-Specific Cystic Fibrosis IPSCs.” Cell Stem Cell 10 (4): 385–97. https://doi.org/10.1016/j.stem.2012.01.018.

Murry, Charles E., and Gordon Keller. 2008. “Differentiation of Embryonic Stem Cells to??Clinically Relevant Populations: Lessons from Embryonic Development.” Cell 132 (4): 661–80. https://doi.org/10.1016/j.cell.2008.02.008.

Nakagawa, Masato, Yukimasa Taniguchi, Sho Senda, Nanako Takizawa, Tomoko Ichisaka, Kanako Asano, Asuka Morizane, et al. 2014. “A Novel Efficient Feeder-Free Culture System for the Derivation of Human Induced Pluripotent Stem Cells.” Scientific Reports 4. https://doi.org/10.1038/srep03594.

Nakashima, Yoshiki, and Takeshi Omasa. 2016. “What Kind of Signaling Maintains Pluripotency and Viability in Human-Induced Pluripotent Stem Cells Cultured on Laminin-511 with Serum-Free Medium?” BioResearch Open Access 5 (1): 84–93. https://doi.org/10.1089/bores.2016.0001.

Naujok, Ortwin, Ulf Diekmann, and Sigurd Lenzen. 2014. “The Generation of Definitive Endoderm from Human Embryonic Stem Cells Is Initially Independent from Activin A but Requires Canonical Wnt-Signaling.” Stem Cell Reviews and Reports 10 (4): 480–93. https://doi.org/10.1007/s12015-014-9509-0.

Neganova, I., X. Zhang, S. Atkinson, and M. Lako. 2008. “Expression and Functional Analysis of G1 to S Regulatory Components Reveals an Important Role for CDK2 in Cell Cycle Regulation in Human Embryonic Stem Cells.” Oncogene 28 (1): 20–30. https://doi.org/10.1038/onc.2008.358.

Nguyen, Nguyet M., and Robert M. Senior. 2006. “Laminin Isoforms and Lung Development: All Isoforms Are Not Equal.” Developmental Biology. https://doi.org/10.1016/j.ydbio.2006.03.032.

Niebruegge, Sylvia, Céline L. Bauwens, Raheem Peerani, Nimalan Thavandiran, Stephane Masse, Elias Sevaptisidis, Kumar Nanthakumar, et al. 2009. “No Title” 102 (2): 493–507. https://doi.org/10.1002/bit.22065.

Ninomiya, Naoto, Tatsuo Michiue, Makoto Asashima, and Akira Kurisaki. 2013. “BMP Signaling Regulates the Differentiation of Mouse Embryonic Stem Cells into Lung Epithelial Cell Lineages.” In Vitro Cellular & Developmental Biology - Animal 49 (3): 230–37. https://doi.org/10.1007/s11626-013-9589-1.

O’Connor, Michael D., Melanie D. Kardel, Ioulia Iosfina, David Youssef, Min Lu, Michael M. Li, Suzanne Vercauteren, Andras Nagy, and Connie J. Eaves. 2008. “Alkaline Phosphatase-Positive Colony Formation Is a Sensitive, Specific, and Quantitative Indicator of Undifferentiated Human Embryonic Stem Cells.” Stem Cells 26 (5): 1109–16. https://doi.org/10.1634/stemcells.2007-0801.

Ohgushi, Masatoshi, Michiru Matsumura, Mototsugu Eiraku, Kazuhiro Murakami, Toshihiro Aramaki, Ayaka Nishiyama, Keiko Muguruma, et al. 2010. “Molecular Pathway and Cell State Responsible for Dissociation-Induced Apoptosis in Human Pluripotent Stem Cells.” Cell Stem Cell 7 (2): 225–39. https://doi.org/10.1016/j.stem.2010.06.018.

Orive, Gorka, Rosa Maria Hernandez, Alicia R Gascon, Riccardo Calafiore, Thomas M S Chang, Paul De Vos, Gonzalo Hortelano, et al. 2003. “Cell Encapsulation: Promise and Progress.” Nature Medicine 9 (1): 104–7. https://doi.org/10.1038/nm0103-104.

Otsuji, Tomomi G., Jiang Bin, Azumi Yoshimura, Misayo Tomura, Daiki Tateyama, Itsunari Minami, Yoshihiro Yoshikawa, et al. 2014. “A 3D Sphere Culture System Containing Functional Polymers for Large-Scale Human Pluripotent Stem Cell Production.” Stem Cell Reports 2 (5): 734–45. https://doi.org/10.1016/j.stemcr.2014.03.012.

Ott, Harald C., Ben Clippinger, Claudius Conrad, Christian Schuetz, Irina Pomerantseva, Laertis Ikonomou, Darrell Kotton, and Joseph P. Vacanti. 2010. “Regeneration and Orthotopic Transplantation of a Bioartificial Lung.” Nature Medicine 16 (8): 927–33. https://doi.org/10.1038/nm.2193.

Paige, K T, L G Cima, M J Yaremchuk, B L Schloo, J P Vacanti, and C A Vacanti. 1996. “De Novo Cartilage Generation Using Calcium Alginate-Chondrocyte Constructs.” Plastic and Reconstructive Surgery 97 (1): 168-78; discussion 179-80. http://www.ncbi.nlm.nih.gov/pubmed/8532775.

Park, Jae Hong, Jung Min Ryu, and Ho Jae Han. 2011. “Involvement of Caveolin-1 in Fibronectin-Induced Mouse Embryonic Stem Cell Proliferation: Role of FAK, RhoA, PI3K/Akt, and ERK 1/2 Pathways.” Journal of Cellular Physiology 226 (1): 267–75. https://doi.org/10.1002/jcp.22338.

Petersen, Thomas H., Elizabeth A. Calle, Liping Zhao, Eun Jung Lee, Liqiong Gui, Micha Sam B. Raredon, Kseniya Gavrilov, et al. 2010. “Tissue-Engineered Lungs for in Vivo Implantation.” Science 329 (5991): 538–41. https://doi.org/10.1126/science.1189345.

Piltti, Juha, Joakim Bygdell, Cecilia Fernández-Echevarría, Daniel Marcellino, and Mikko J. Lammi. 2017. “Rho-Kinase Inhibitor Y-27632 and Hypoxia Synergistically Enhance Chondrocytic Phenotype and Modify S100 Protein Profiles in Human Chondrosarcoma Cells.” Scientific Reports 7 (1). https://doi.org/10.1038/s41598-017-03958-5.

Pimton, Pimchanok, Shimon Lecht, Collin T. Stabler, Gregg Johannes, Edward S. Schulman, and Peter I. Lelkes. 2015. “Hypoxia Enhances Differentiation of Mouse Embryonic Stem Cells into Definitive Endoderm and Distal Lung Cells.” Stem Cells and Development 24 (5): 663–76. https://doi.org/10.1089/scd.2014.0343.

Prado-Lopez, Sonia, Ana Conesa, Ana ArmiÃ±Ã¡n, Magdalena MartÃ-nez-Losa, Carmen Escobedo-Lucea, Carolina Gandia, Sonia Tarazona, et al. 2010. “Hypoxia Promotes Efficient Differentiation of Human Embryonic Stem Cells to Functional Endothelium.” Stem Cells 28 (3): 407–18. https://doi.org/10.1002/stem.295.

Prigione, A, and J Adjaye. 2010. “Modulation of Mitochondrial Biogenesis and Bioenergetic Metabolism upon in Vitro and in Vivo Differentiation of Human ES and IPS Cells.” Int J Dev Biol 54 (11–12): 1729–41. https://doi.org/10.1387/ijdb.103198ap.

Qin, M, G Tai, P Collas, J M Polak, and A E Bishop. 2005. “Cell Extract-Derived Differentiation of Embryonic Stem Cells.” Stem Cells 23 (6): 712–18. https://doi.org/10.1634/stemcells.2004-0195.

Ramírez-Bergeron, Diana L, Anja Runge, Karen D Cowden Dahl, Hans Joerg Fehling, Gordon Keller, and M Celeste Simon. 2004. “Hypoxia Affects Mesoderm and Enhances Hemangioblast Specification during Early Development.” Development (Cambridge, England) 131 (18): 4623–34. https://doi.org/10.1242/dev.01310.

Randle, Wesley L, Jae Min Cha, Yu-Shik Hwang, K L Andrew Chan, Sergei G Kazarian, Julia M Polak, and Athanasios Mantalaris. 2007. “Integrated 3-Dimensional Expansion and Osteogenic Differentiation of Murine Embryonic Stem Cells.” Tissue Engineering 13 (12): 2957–70. https://doi.org/10.1089/ten.2007.0072.

Raval, Raju R, Kah Weng Lau, Maxine G B Tran, Heidi M Sowter, Stefano J Mandriota, Ji-Liang Li, Christopher W Pugh, Patrick H Maxwell, Adrian L Harris, and Peter J Ratcliffe. 2005. “Contrasting Properties of Hypoxia-Inducible Factor 1 (HIF-1) and HIF-2 in von Hippel-Lindau-Associated Renal Cell Carcinoma.” Molecular and Cellular Biology 25 (13): 5675–86. https://doi.org/10.1128/MCB.25.13.5675-5686.2005.

Ridsdale, Ross, and Martin Post. 2004. “Surfactant Lipid Synthesis and Lamellar Body Formation in Glycogen-Laden Type II Cells.” American Journal of Physiology. Lung Cellular and Molecular Physiology 287 (4): L743–51. https://doi.org/10.1152/ajplung.00146.2004.

Rodaway, Adam, and Roger Patient. 2001. “Mesendoderm: An Ancient Germ Layer?” Cell. https://doi.org/10.1016/S0092-8674(01)00307-5.

Rodrigues, Carlos A.V., Maria Margarida Diogo, Cláudia Lobato da Silva, and Joaquim M.S. Cabral. 2010. “Hypoxia Enhances Proliferation of Mouse Embryonic Stem Cell-Derived Neural Stem Cells.” Biotechnology and Bioengineering 106 (2): n/a-n/a. https://doi.org/10.1002/bit.22648.

Roman, Jesse. 1997. “Fibronectin and Fibronectin Receptors in Lung Development.” Experimental Lung Research. https://doi.org/10.3109/01902149709074027.

Romero-Moya, Damia, Clara Bueno, Rosa Montes, Oscar Navarro-Montero, Francisco J. Iborra, L. C. Lopez, Miguel Martin, et al. 2013. “No Title.” Haematologica 98 (7). https://doi.org/10.3324/haematol.2012.079244.

Sahara, Makoto, Emil M. Hansson, Oliver Wernet, Kathy O. Lui, Daniela Sp??ter, and Kenneth R. Chien. 2014. “Manipulation of a VEGF-Notch Signaling Circuit Drives Formation of Functional Vascular Endothelial Progenitors from Human Pluripotent Stem Cells.” Cell Research 24 (7): 820–41. https://doi.org/10.1038/cr.2014.59.

Salgado, António J., Olga P. Coutinho, and Rui L. Reis. 2004. “Bone Tissue Engineering: State of the Art and Future Trends.” Macromolecular Bioscience. https://doi.org/10.1002/mabi.200400026.

Schittny, Johannes C. 2017. “Development of the Lung.” Cell and Tissue Research. https://doi.org/10.1007/s00441-016-2545-0.

Schmeichel, K. L. 2003. “Modeling Tissue-Specific Signaling and Organ Function in Three Dimensions.” Journal of Cell Science 116 (12): 2377–88. https://doi.org/10.1242/jcs.00503.

Schnerch, Angelique, Chantal Cerdan, and Mickie Bhatia. 2010. “Distinguishing between Mouse and Human Pluripotent Stem Cell Regulation: The Best Laid Plans of Mice and Men.” Stem Cells. https://doi.org/10.1002/stem.298.

Semenza, G L, and G L Wang. 1992. “A Nuclear Factor Induced by Hypoxia via de Novo Protein Synthesis Binds to the Human Erythropoietin Gene Enhancer at a Site Required for Transcriptional Activation.” Molecular and Cellular Biology 12 (12): 5447–54. http://www.ncbi.nlm.nih.gov/pubmed/1448077.

Sevilla, Carlos A., Diane Dalecki, and Denise C. Hocking. 2013. “Regional Fibronectin and Collagen Fibril Co-Assembly Directs Cell Proliferation and Microtissue Morphology.” PLoS ONE 8 (10). https://doi.org/10.1371/journal.pone.0077316.

Shapiro, L, and S Cohen. 1997. “Novel Alginate Sponges for Cell Culture and Transplantation.” Biomaterials 18 (8): 583–90. http://www.ncbi.nlm.nih.gov/pubmed/9134157.

Shi, Jianjian, and Lei Wei. 2007. “Rho Kinase in the Regulation of Cell Death and Survival.” Archivum Immunologiae et Therapiae Experimentalis 55 (2): 61–75. https://doi.org/10.1007/s00005-007-0009-7.

Shimada, Hidenori, Yoshiya Hashimoto, Akira Nakada, Keiji Shigeno, and Tatsuo Nakamura. 2012. “No Title” 417 (2). https://doi.org/10.1016/j.bbrc.2011.11.111.

Shu, Weiguo, Susan Guttentag, Zhishan Wang, Thomas Andl, Philip Ballard, Min Lu, Stefano Piccolo, et al. 2005. “Wnt/β-Catenin Signaling Acts Upstream of N-Myc, BMP4, and FGF Signaling to Regulate Proximal–distal Patterning in the Lung.” Developmental Biology 283 (1): 226–39. https://doi.org/10.1016/j.ydbio.2005.04.014.

Simon, M. Celeste, and Brian Keith. 2008. “The Role of Oxygen Availability in Embryonic Development and Stem Cell Function.” Nature Reviews Molecular Cell Biology 9 (4): 285–96. https://doi.org/10.1038/nrm2354.

Singh, Purva, and Jean E. Schwarzbauer. 2012. “Fibronectin and Stem Cell Differentiation - Lessons from Chondrogenesis.” Journal of Cell Science 125 (16): 3703–12. https://doi.org/10.1242/jcs.095786.

Song, Jeremy J., Sam S. Kim, Zhilin Liu, Joren C. Madsen, Douglas J. Mathisen, Joseph P. Vacanti, and Harald C. Ott. 2011. “Enhanced in Vivo Function of Bioartificial Lungs in Rats.” Annals of Thoracic Surgery 92 (3): 998–1006. https://doi.org/10.1016/j.athoracsur.2011.05.018.

Souza, Glauco R., Jennifer R. Molina, Robert M. Raphael, Michael G. Ozawa, Daniel J. Stark, Carly S. Levin, Lawrence F. Bronk, et al. 2010. “Three-Dimensional Tissue Culture Based on Magnetic Cell Levitation.” Nature Nanotechnology 5 (4): 291–96. https://doi.org/10.1038/nnano.2010.23.

Strand, Berit L, Yrr A Mørch, Kjersti R Syvertsen, Terje Espevik, and Gudmund Skjåk-Braek. 2003. “Microcapsules Made by Enzymatically Tailored Alginate.” Journal of Biomedical Materials Research. Part A 64 (3): 540–50. https://doi.org/10.1002/jbm.a.10337.

Studer, L, M Csete, S H Lee, N Kabbani, J Walikonis, B Wold, and R McKay. 2000. “Enhanced Proliferation, Survival, and Dopaminergic Differentiation of CNS Precursors in Lowered Oxygen.” The Journal of Neuroscience : The Official Journal of the Society for Neuroscience 20 (19): 7377–83. http://www.ncbi.nlm.nih.gov/pubmed/11007896.

Sturgeon, Christopher M., Andrea Ditadi, Geneve Awong, Marion Kennedy, and Gordon Keller. 2014. “Wnt Signaling Controls the Specification of Definitive and Primitive Hematopoiesis from Human Pluripotent Stem Cells.” Nature Biotechnology 32 (6): 554–61. https://doi.org/10.1038/nbt.2915.

Submitted, A Thesis, I N Partial, Fulfillment Of, T H E Requirements, F O R The, Degree Of, Doctor Of, Diploma O F Imperial, Faculty Of, and Natural Sciences. 2015. “CHARACTERISATION OF ENCAPSULATED EMBRYONIC STEM CELLS USING SILAC-BASED PROTEOMICS A THESIS SUBMITTED IN PARTIAL FULFILLMENT OF THE REQUIREMENTS.”

Sueblinvong, V, and D J Weiss. 2009. “Cell Therapy Approaches for Lung Diseases: Current Status.” Curr Opin Pharmacol 9 (3): 268–73. https://doi.org/10.1016/j.coph.2009.03.002.

Sun, A M. 1997. “Microencapsulation of Cells. Medical Applications.” Annals of the New York Academy of Sciences 831 (December): 271–79. http://www.ncbi.nlm.nih.gov/pubmed/9616719.

Tada, Hiroko, Osamu Shiho, Ken ichi Kuroshima, Masaru Koyama, and Kyozo Tsukamoto. 1986. “An Improved Colorimetric Assay for Interleukin 2.” Journal of Immunological Methods 93 (2): 157–65. https://doi.org/10.1016/0022-1759(86)90183-3.

Takahashi, K, and S Yamanaka. 2006. “Induction of Pluripotent Stem Cells from Mouse Embryonic and Adult Fibroblast Cultures by Defined Factors.” Cell 126 (4): 663–76. https://doi.org/10.1016/j.cell.2006.07.024.

Takahashi, Kazutoshi, Koji Tanabe, Mari Ohnuki, Megumi Narita, Tomoko Ichisaka, Kiichiro Tomoda, and Shinya Yamanaka. 2007. “Induction of Pluripotent Stem Cells from Adult Human Fibroblasts by Defined Factors.” Cell 131 (5): 861–72. https://doi.org/10.1016/j.cell.2007.11.019.

Takeuchi, Hiroki, Norio Nakatsuji, and Hirofumi Suemori. 2014. “Endodermal Differentiation of Human Pluripotent Stem Cells to Insulin-Producing Cells in 3D Culture.” Scientific Reports 4. https://doi.org/10.1038/srep04488.

Tapias, Luis F., and Harald C. Ott. 2014. “Decellularized Scaffolds as a Platform for Bioengineered Organs.” Current Opinion in Organ Transplantation. https://doi.org/10.1097/MOT.0000000000000051.

Technau, Ulrich, and Corinna B. Scholz. 2003. “Origin and Evolution of Endoderm and Mesoderm.” International Journal of Developmental Biology.

Teo, Adrian Kee Keong, Sebastian J. Arnold, Matthew W.B. Trotter, Stephanie Brown, Lay Teng Ang, Zhenzhi Chng, Elizabeth J. Robertson, N. Ray Dunn, and Ludovic Vallier. 2011. "Pluripotency Factors Regulate Definitive Endoderm Specification through Eomesodermin." Genes and Development 25 (3): 238–50. https://doi.org/10.1101/gad.607311.

Teo, Adrian Kee Keong, Ivan Achel Valdez, Ercument Dirice, and Rohit N. Kulkarni. 2014. "Comparable Generation of Activin-Induced Definitive Endoderm via Additive Wnt or BMP Signaling in Absence of Serum." Stem Cell Reports 3 (1): 5–14. https://doi.org/10.1016/j.stemcr.2014.05.007.

Thisse, Bernard, Christopher V. E. Wright, and Christine Thisse. 2000. "Activin- and Nodal-Related Factors Control Antero-Posterior Patterning of the Zebrafish Embryo." Nature 403 (6768): 425–28. https://doi.org/10.1038/35000200.

Thomson, J A, J Itskovitz-Eldor, S Shapiro, M A Waknitz, J Swiergiel, V S Marshall, and J M Jones. 1998. "Embryonic Stem Cell Lines Derived from Human Blastocysts." Science (New York, N.Y.) 282 (5391): 1145–47. http://www.ncbi.nlm.nih.gov/pubmed/9804556.

Totonchi, Mehdi, Adeleh Taei, Ali Seifinejad, Mohammadsharif Tabebordbar, Hassan Rassouli, Ali Farrokhi, Hamid Gourabi, Nasser Aghdami, Ghasem Hosseini-Salekdeh, and Hossein Baharvand. 2010. "Feeder- and Serum-Free Establishment and Expansion of Human Induced Pluripotent Stem Cells." The International Journal of Developmental Biology 54 (5): 877–86. https://doi.org/10.1387/ijdb.092903mt.

Tyler, J E. 1990. "Microencapsulation of Mammalian Cells." Bioprocess Technology 10: 343–61. http://www.ncbi.nlm.nih.gov/pubmed/1367064.

Unger, Christian, Heli Skottman, Pontus Blomberg, M Sirac Dilber, and Outi Hovatta. 2008. "Good Manufacturing Practice and Clinical-Grade Human Embryonic Stem Cell Lines." Human Molecular Genetics 17 (R1): R48-53. https://doi.org/10.1093/hmg/ddn079.

Unsworth, Brian R., and Peter I. Lelkes. 1998. "Growing Tissues in Microgravity." Nature Medicine. https://doi.org/10.1038/nm0898-901.

Valk, J. van der, D. Brunner, K. De Smet, Å Fex Svenningsen, P. Honegger, L. E. Knudsen, T. Lindl, et al. 2010. "Optimization of Chemically Defined Cell Culture Media - Replacing Fetal Bovine Serum in Mammalian in Vitro Methods." Toxicology in Vitro. https://doi.org/10.1016/j.tiv.2010.03.016.

Volckaert, Thomas, and Stijn P. De Langhe. 2015. "Wnt and FGF Mediated Epithelial-Mesenchymal Crosstalk during Lung Development." Developmental Dynamics 244 (3): 342–66. https://doi.org/10.1002/dvdy.24234.

Vos, Paul De, Bart De Haan, and Reinout Van Schilfgaarde. 1997. "Effect of the Alginate Composition on the Biocompatibility of Alginate-Polylysine Microcapsules." Biomaterials 18 (3): 273–78. https://doi.org/10.1016/S0142-9612(96)00135-4.

Walker, Andrea, Hua Su, Mary Anne Conti, Nicole Harb, Robert S. Adelstein, and Noboru Sato. 2010. "Non-Muscle Myosin II Regulates Survival Threshold of Pluripotent Stem Cells." Nature Communications 1 (6). https://doi.org/10.1038/ncomms1074.

Wang, D., D. L. Haviland, A. R. Burns, E. Zsigmond, and R. A. Wetsel. 2007. “A Pure Population of Lung Alveolar Epithelial Type II Cells Derived from Human Embryonic Stem Cells.” Proceedings of the National Academy of Sciences 104 (11): 4449–54. https://doi.org/10.1073/pnas.0700052104.

Wang, Xiuli, Wei Wang, Juan Ma, Xin Guo, Xingju Yu, and Xiaojun Ma. 2006. “Proliferation and Differentiation of Mouse Embryonic Stem Cells in APA Microcapsule: A Model for Studying the Interaction between Stem Cells and Their Niche.” Biotechnology Progress 22 (3): 791–800. https://doi.org/10.1021/bp050386n.

Warburton, David, Ahmed El-Hashash, Gianni Carraro, Caterina Tiozzo, Frederic Sala, Orquidea Rogers, Stijn De Langhe, et al. 2010. “Lung Organogenesis.” Current Topics in Developmental Biology 90 (C): 73–158. https://doi.org/10.1016/S0070-2153(10)90003-3.

Watanabe, Kiichi, Morio Ueno, Daisuke Kamiya, Ayaka Nishiyama, Michiru Matsumura, Takafumi Wataya, Jun B Takahashi, et al. 2007. “A ROCK Inhibitor Permits Survival of Dissociated Human Embryonic Stem Cells.” Nat Biotechnol 25 (6): 681–86. https://doi.org/10.1038/nbt1310.

Wilson, Jenna L., and Todd C. Mcdevitt. 2013. “Stem Cell Microencapsulation for Phenotypic Control, Bioprocessing, and Transplantation.” Biotechnology and Bioengineering. https://doi.org/10.1002/bit.24802.

Wong, Amy P, Christine E Bear, Stephanie Chin, Peter Pasceri, Tadeo O Thompson, Ling-Jun Huan, Felix Ratjen, James Ellis, and Janet Rossant. 2012. “Directed Differentiation of Human Pluripotent Stem Cells into Mature Airway Epithelia Expressing Functional CFTR Protein.” Nature Biotechnology 30 (9): 876–82. https://doi.org/10.1038/nbt.2328.

Wu, Dianqing, and Weijun Pan. 2010. “GSK3: A Multifaceted Kinase in Wnt Signaling.” Trends in Biochemical Sciences. https://doi.org/10.1016/j.tibs.2009.10.002.

Xiong, Anji, and Yi Liu. 2017. “Targeting Hypoxia Inducible Factors-1α as a Novel Therapy in Fibrosis.” Frontiers in Pharmacology. https://doi.org/10.3389/fphar.2017.00326.

Xu, Ren-He, Xin Chen, Dong S. Li, Rui Li, Gregory C. Addicks, Clay Glennon, Thomas P. Zwaka, and James A. Thomson. 2002. “BMP4 Initiates Human Embryonic Stem Cell Differentiation to Trophoblast.” Nature Biotechnology 20 (12): 1261–64. https://doi.org/10.1038/nbt761.

Xu, Zhiyun, Yanghui Gao, Yuanyuan Hao, Encheng Li, Yan Wang, Jianing Zhang, Wenxin Wang, Zhancheng Gao, and Qi Wang. 2013. “Application of a Microfluidic Chip-Based 3D Co-Culture to Test Drug Sensitivity for Individualized Treatment of Lung Cancer.” Biomaterials 34 (16): 4109–17. https://doi.org/10.1016/j.biomaterials.2013.02.045.

Yao, Tatsuma, and Yuta Asayama. 2017. “Animal-Cell Culture Media: History, Characteristics, and Current Issues.” Reproductive Medicine and Biology. https://doi.org/10.1002/rmb2.12024.

Yasunaga, Masahiro, Shinsuke Tada, Satomi Torikai-Nishikawa, Yoko Nakano, Mitsuhiro Okada, Lars Martin Jakt, Satomi Nishikawa, Tsutomu Chiba, Takumi Era, and Shin-Ichi Nishikawa. 2005. “Induction and Monitoring of Definitive and Visceral Endoderm Differentiation of Mouse ES Cells.” Nature Biotechnology 23 (12): 1542–50. https://doi.org/10.1038/nbt1167.

Yoshida, Yoshinori, Kazutoshi Takahashi, Keisuke Okita, Tomoko Ichisaka, and Shinya Yamanaka. 2009. “Hypoxia Enhances the Generation of Induced Pluripotent Stem Cells.” Cell Stem Cell 5 (3): 237–41. https://doi.org/10.1016/j.stem.2009.08.001.

Yu, A Y, M G Frid, L A Shimoda, C M Wiener, K Stenmark, and G L Semenza. 1998. “Temporal, Spatial, and Oxygen-Regulated Expression of Hypoxia-Inducible Factor-1 in the Lung.” American Journal of Physiology 275 (4 Pt 1): L818–26.

Yu, Chen, Kai Liu, Shibing Tang, and Sheng Ding. 2014. “Chemical Approaches to Cell Reprogramming.” Current Opinion in Genetics & Development 28: 50–56. https://doi.org/10.1016/j.gde.2014.09.006.

Yu, J., M. A. Vodyanik, K. Smuga-Otto, J. Antosiewicz-Bourget, J. L. Frane, S. Tian, J. Nie, et al. 2007. “Induced Pluripotent Stem Cell Lines Derived from Human Somatic Cells.” Science 318 (5858): 1917–20. https://doi.org/10.1126/science.1151526.

Yu, Junying, Maxim A Vodyanik, Ping He, Igor I Slukvin, and James A Thomson. 2006. “Human Embryonic Stem Cells Reprogram Myeloid Precursors Following Cell-Cell Fusion.” Stem Cells (Dayton, Ohio) 24 (1): 168–76. https://doi.org/10.1634/stemcells.2005-0292.

Yue, Beatrice. 2014. “Biology of the Extracellular Matrix: An Overview.” Journal of Glaucoma. https://doi.org/10.1097/IJG.0000000000000108.

Yuge, Louis, Teruyuki Kajiume, Hidetoshi Tahara, Yumi Kawahara, Chika Umeda, Reiko Yoshimoto, Shu-Liang Wu, et al. 2006. “Microgravity Potentiates Stem Cell Proliferation While Sustaining the Capability of Differentiation.” Stem Cells and Development 15 (6): 921–29. https://doi.org/10.1089/scd.2006.15.921.

Yun, Zhong, Heather L Maecker, Randall S Johnson, and Amato J Giaccia. 2002. “Inhibition of PPAR Gamma 2 Gene Expression by the HIF-1-Regulated Gene DEC1/Stra13: A Mechanism for Regulation of Adipogenesis by Hypoxia.” Developmental Cell 2 (3): 331–41. http://www.ncbi.nlm.nih.gov/pubmed/11879638.

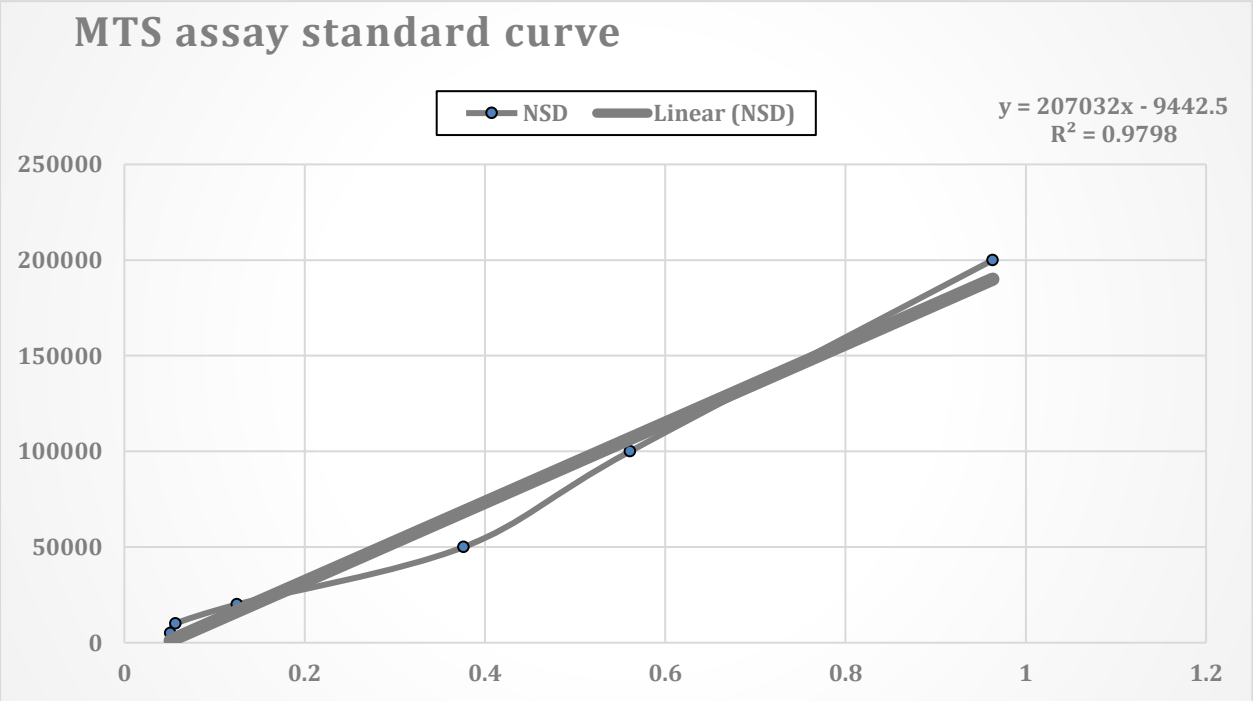
Yusen, R. D., T. H. Shearon, Y. Qian, R. Kotloff, M. L. Barr, S. Sweet, D. B. Dyke, and S. Murray. 2010. “Lung Transplantation in the United States, 1999-2008.” American Journal of Transplantation 10 (4p2): 1047–68. https://doi.org/10.1111/j.1600-6143.2010.03055.x.

Zhang, Li, Joseph M. Valdez, Boyu Zhang, Lei Wei, Jiang Chang, and Li Xin. 2011. “ROCK Inhibitor Y-27632 Suppresses Dissociation-Induced Apoptosis of Murine Prostate Stem/Progenitor Cells and Increases Their Cloning Efficiency.” PLoS ONE 6 (3). https://doi.org/10.1371/journal.pone.0018271.

Appendices

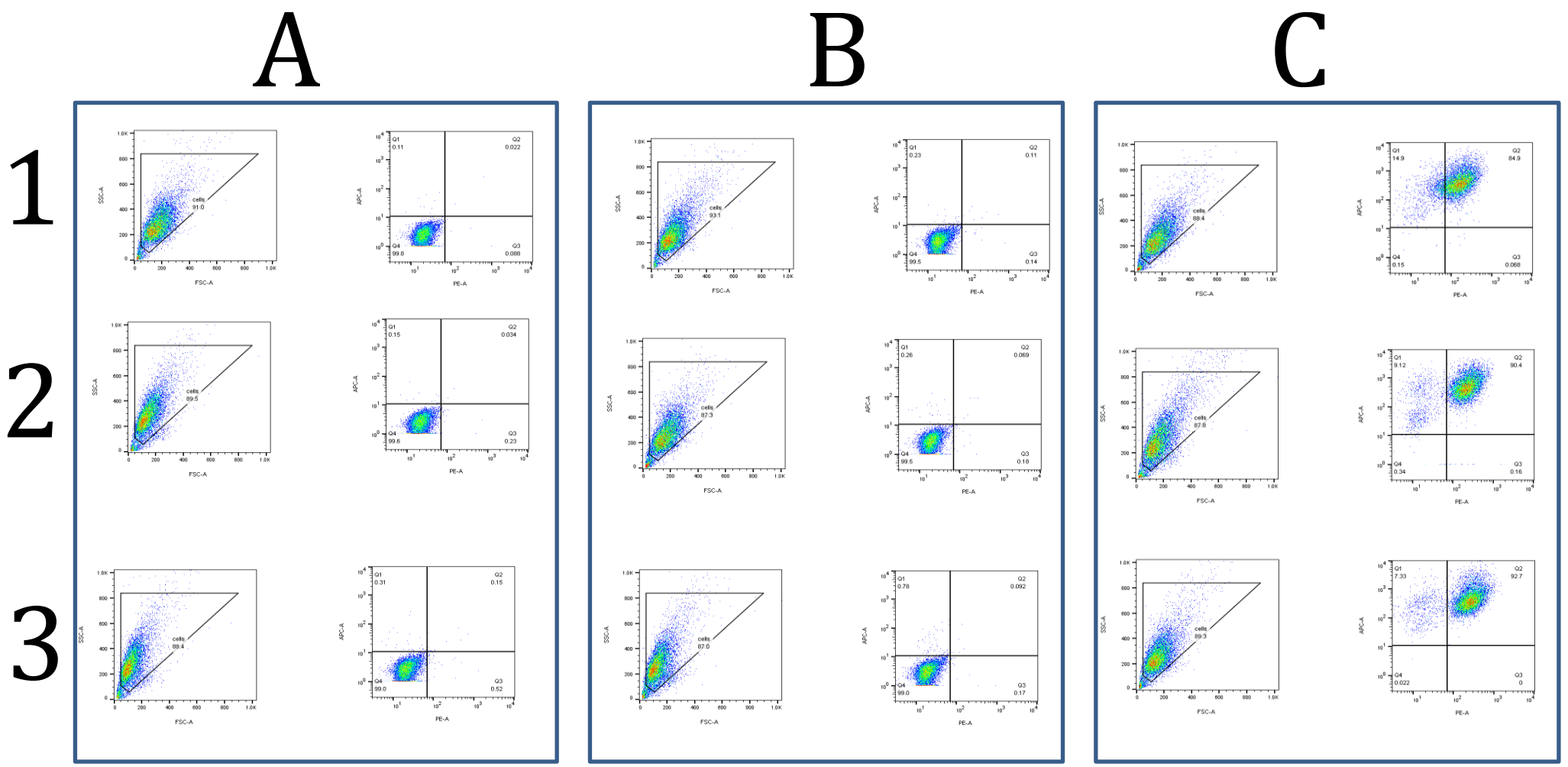
Appendix I

Effect of cell number on absorbance at 490 nm .Various number of human IPSCs were cultured in 96 well plate in final number 50000 cell per well ,cells inubating at 37C .MTS regaent was added and absorbence at 490 nm was recored using ELISA reder . y-axis presented cell number and x-axis presentd OD value, each point represents a mean of 3 replicayes .Assay perform according to the kit protocol.

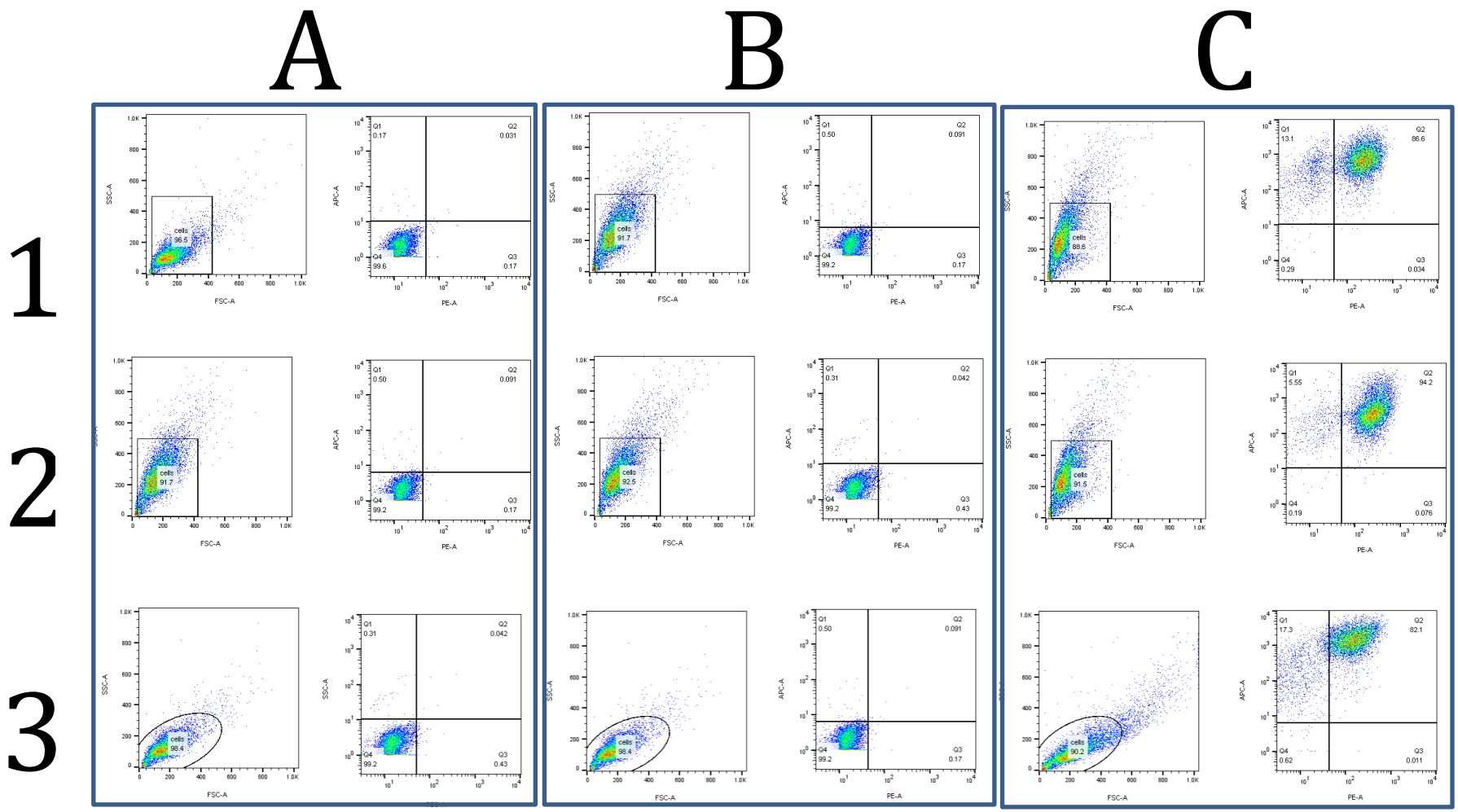


Appendix II

The Flow Cytometry Analysis Profile of the Cultured Human IPS Cells passages 34: (A) Flow cytometry plots of unstained human iPS cells; (B) Flow cytometry plots of the isotope control; (C) The plot shows the percentage of double positive cells stained with internal protein Nanog-PE and cell surface protein SSEA4-APC.



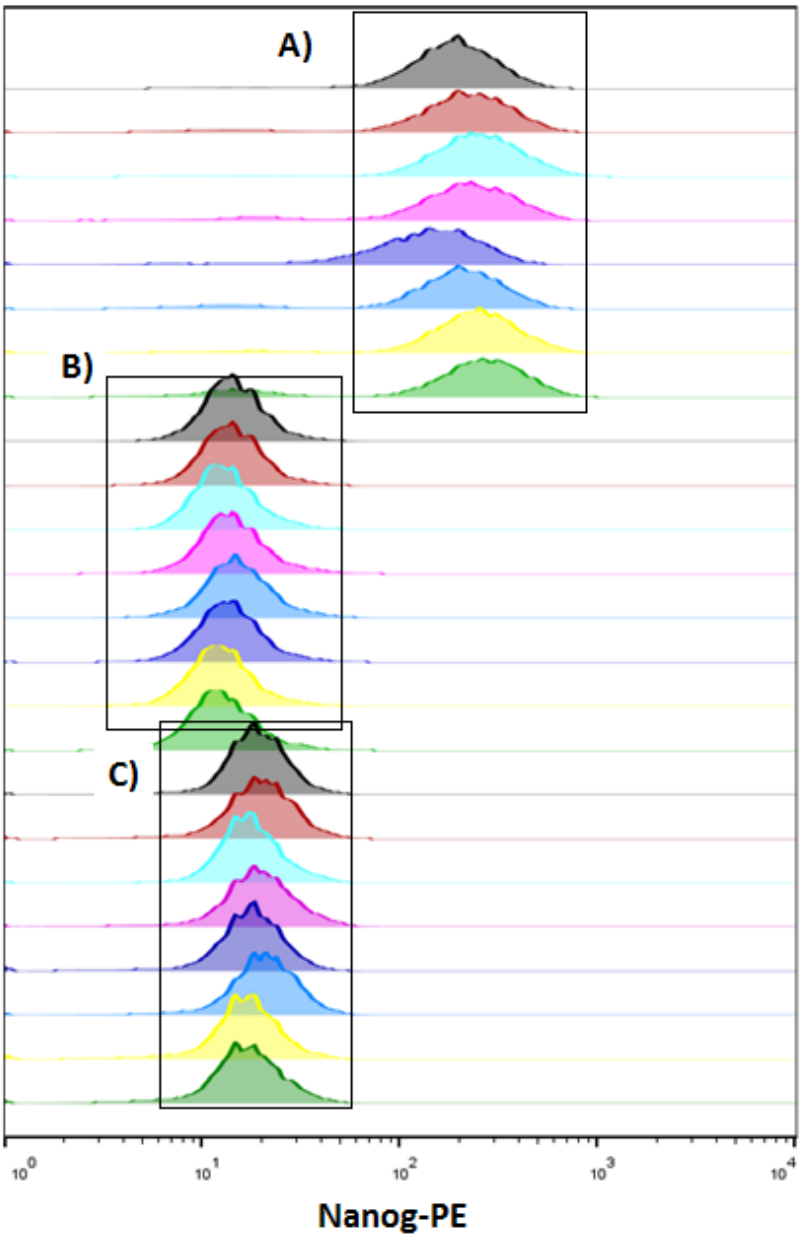
The Flow Cytometry Analysis Profile of the Cultured Human IPS Cells passages 39: (A) Flow cytometry plots of unstained human IPSCs (B) Flow cytometry plots of the isotope control; (C) The plot shows the percentage of double positive cells stained with internal protein Nanog-PE and cell surface protein SSEA4-APC.



Appendix III

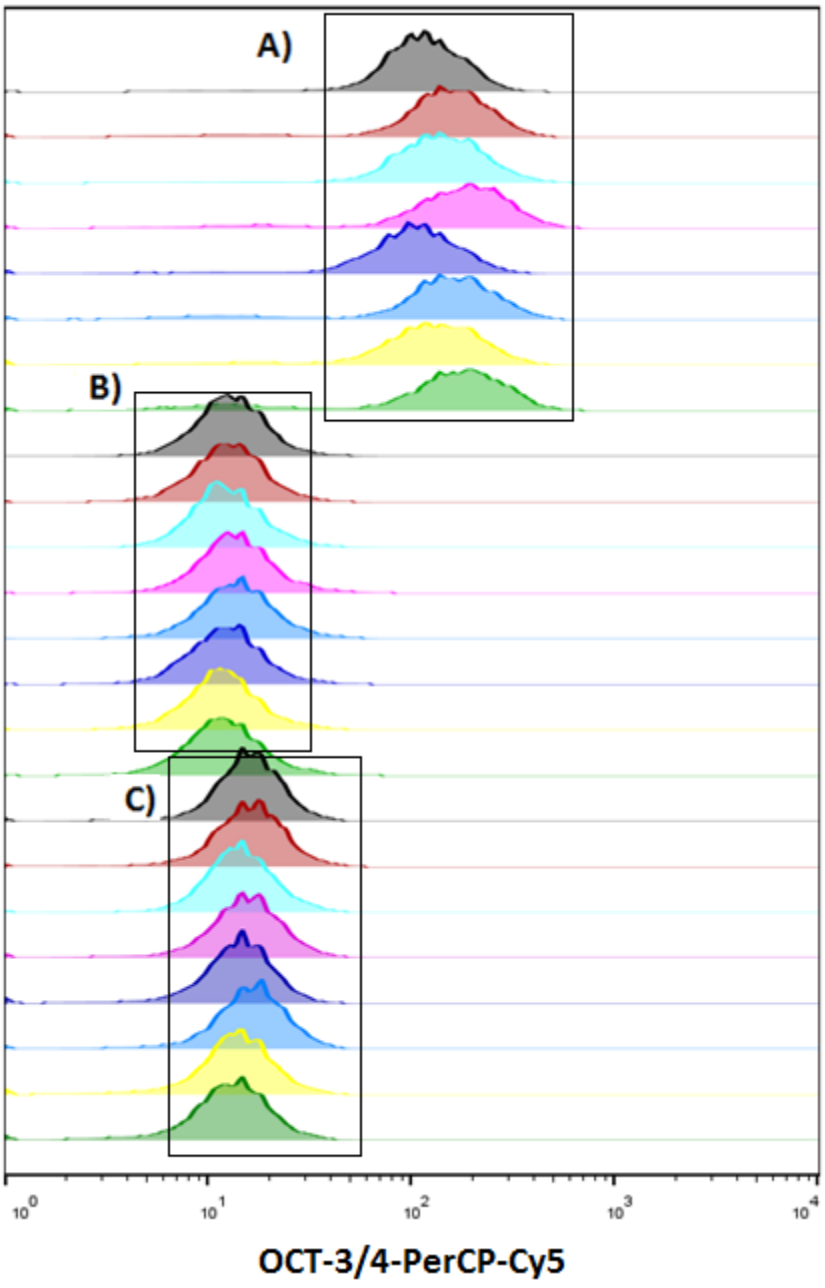
Flow Cytometry Analysis of Pluripotency Marker Expression of human IPSCs dissociated to single cell suspensions in in different conditions at 96 hour: NO ROCK/NORMOXIA, ROCK/NORMOXIA, NO ROCK/HYPOXIA and ROCK/HYPOXIA.

A) A histogram plot shows a positive peak of cells (NO ROCK/NORMOXIA, ROCK/NORMOXIA, NO ROCK/HYPOXIA and ROCK/HYPOXIA) stained with internal protein Nanog-PE shift in the histogram overlay with unstained and the isotope control) The histogram shows the negative peak of cells stained with unstained human IPSCs (NO ROCK/NORMOXIA, ROCK/NORMOXIA, NO ROCK/HYPOXIA and ROCK/HYPOXIA).C) The histogram shows the negative peak of cells (NO ROCK/NORMOXIA, ROCK/NORMOXIA, NO ROCK/HYPOXIA and ROCK/HYPOXIA) stained with the isotope control. (Offset because the isotope control and unstained overlaid)



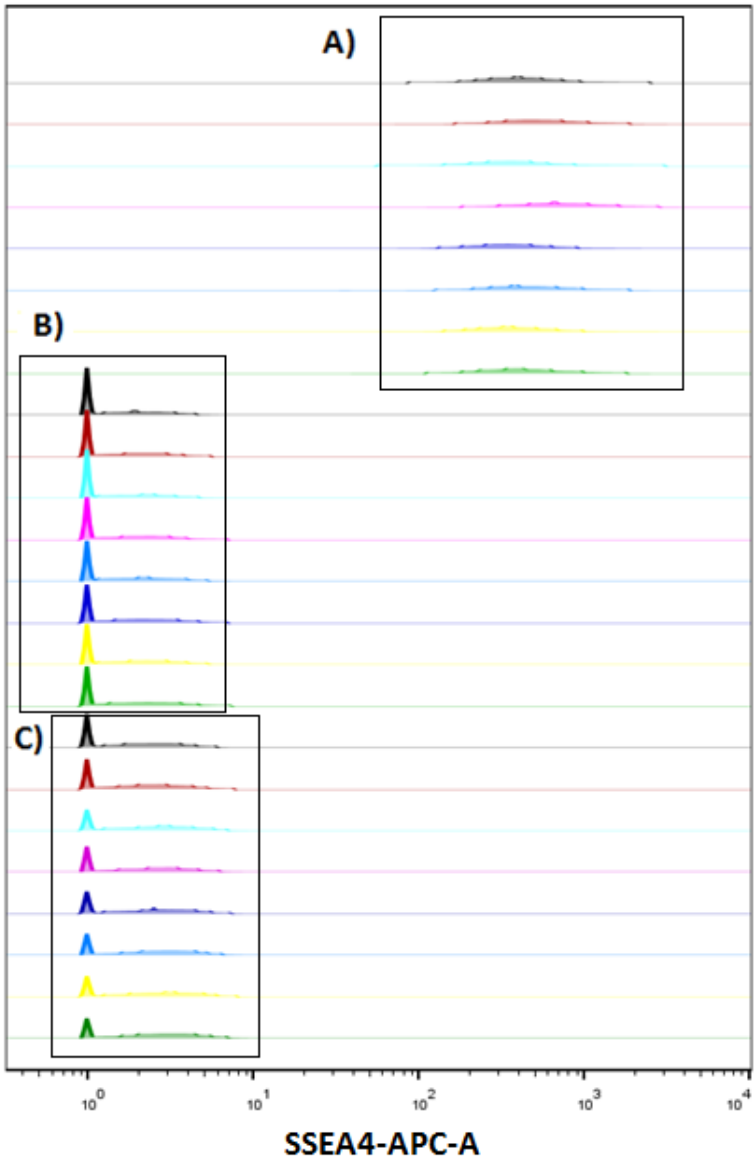
Flow Cytometry Analysis of Pluripotency Marker Expression of human IPSCs dissociated to single cell suspensions in in different conditions at 96 hour: NO ROCK/NORMOXIA, ROCK/NORMOXIA, NO ROCK/HYPOXIA and ROCK/HYPOXIA.

A) A histogram plot shows a positive peak of cells (NO ROCK/NORMOXIA, ROCK/NORMOXIA, NO ROCK/HYPOXIA and ROCK/HYPOXIA) stained with internal protein OCT3/4-percp-cy5 shift in the histogram overlay with unstained and the isotope control) The histogram shows the negative peak of cells stained with unstained human IPSCs (NO ROCK/NORMOXIA, ROCK/NORMOXIA, NO ROCK/HYPOXIA and ROCK/HYPOXIA).C) The histogram shows the negative peak of cells (NO ROCK/NORMOXIA, ROCK/NORMOXIA, NO ROCK/HYPOXIA and ROCK/HYPOXIA) stained with the isotope control. (Offset because the isotope control and unstained overlaid)



Flow Cytometry Analysis of Pluripotency Marker Expression of human IPSCs dissociated to single cell suspensions in in different conditions at 96 hour: NO ROCK/NORMOXIA, ROCK/NORMOXIA, NO ROCK/HYPOXIA and ROCK/HYPOXIA.

A) A histogram plot shows a positive peak of cells (NO ROCK/NORMOXIA, ROCK/NORMOXIA, NO ROCK/HYPOXIA and ROCK/HYPOXIA) stained with internal protein surface protein SSEA4-APC-A.shift in the histogram overlay with unstained and the isotope control) The histogram shows the negative peak of cells stained with unstained human IPSCs (NO ROCK/NORMOXIA, ROCK/NORMOXIA, NO ROCK/HY-POXIA and ROCK/HYPOXIA).C) The histogram shows the negative peak of cells (NO ROCK/NORMOXIA, ROCK/NORMOXIA, NO ROCK/HYPOXIA and ROCK/HYPOXIA) stained with the isotope control. (Offset because the isotope control and unstained overlaid)



Appendix IV

The sensitivity and specificity of the MTS tetrazolium assay: This images showed, high cell concentration inside the beads might have a negative impact on the sensitivity of the MTS assay, (The transport of the formazan dye from the inside of the beads to the medium can vary).

A

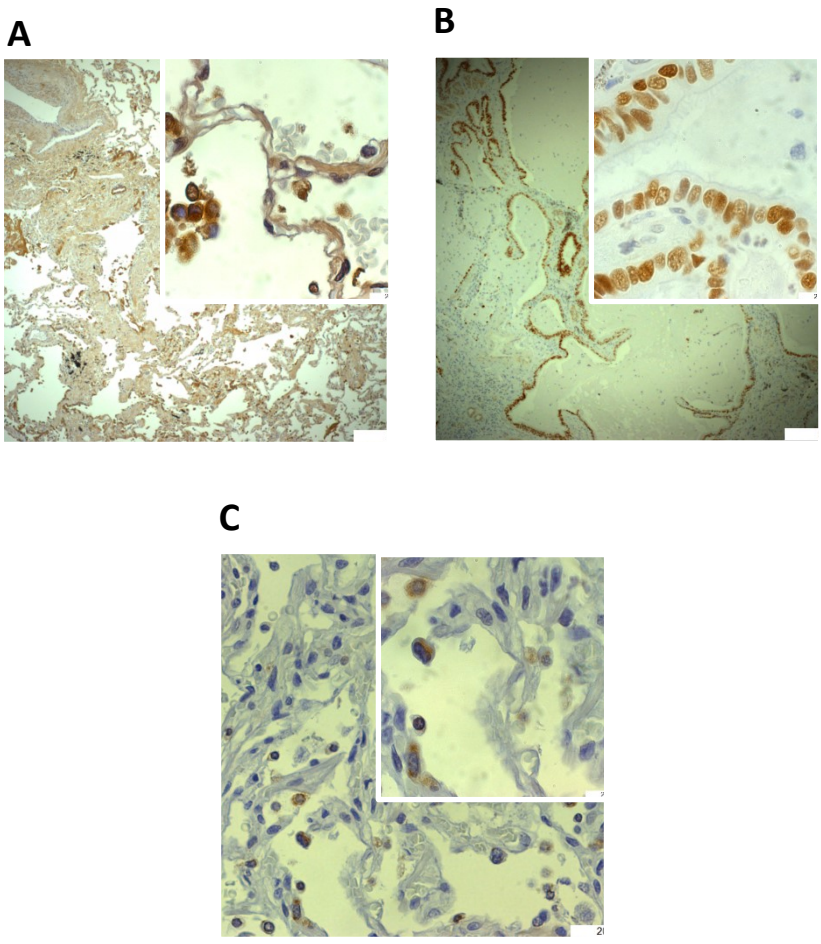


B



Appendix V

Positive tissue controls Immunohistochemistry (IHC) experiments: A) Immunohistochemical analysis of PROSP-B using anti- PROSP-B Polyclonal Antibody (AB3786-Millpore) in Sections of normal human lung the dilution for this antibody in immunohistochemistry applications was 1:4000-1:8000. B) Immunohistochemical analysis of ANTI-TTF using anti- ANTI-TTF Rabbit monoclonal IgG (AB76013-Abcam) in sections of human lung adenocarcinoma the dilution for this antibody in immunohistochemistry applications was 1:100-1:1000. C) Immunohistochemical analysis of PROSP-C using anti- PROSP-C Polyclonal antibody Rabbit (AB3786-Millpore) in Sections of normal human lungt he dilution for this antibody in immunohistochemistry applications was 1:1000-1:2000. Scale bars, 500 µm and 20 µm. (the tissues were provide by (National Heart & Lung Institute Faculty of Medicine Imperial College London)



Negative tissue controls Immunohistochemistry (IHC) experiments: A) Immunohistochemical analysis of ANTI-TTF using anti- ANTI-TTF Rabbit monoclonal IgG (AB76013-Abcam) in sections alginent beasds mantained in mTeSR™1 the dilution for this antibody in immunohistochemistry applications was 1:100-1:1000. B) Immunohistochemical analysis of PROSP-B using anti- PROSP-B Polyclonal Antibody (AB3786-Millpore) in Sections of alginent beasds mantained in mTeSR™1the dilution for this antibody in immunohistochemistry applications was 1:4000-1:8000. C) Immunohistochemical analysis of PROSP-C using anti- PROSP-C Polyclonal antibody Rabbit (AB3786-Millpore) in Sections of alginent beasds mantained in mTeSR™1he dilution for this antibody in immunohistochemistry applications was 1:1000-1:2000. Scale bars, 50 μm.

